ECOTOXICITY OF SILVER NANOPARTICLES ON ESTUARINE AND COASTAL BACTERIAL COMMUNITIES

Submitted by

Virginia Echavarri-Bravo

for the degree of Doctor of Philosophy

HERIOT-WATT UNIVERSITY
SCHOOL OF LIFE SCIENCES
MAY 2015

Abstract

The increasing use of silver nanoparticles (AgNPs) as a biocidal agent and their potential accumulation in coastal environments may threaten non-target natural environmental bacterial communities. For this reason the main aim of this PhD project was to examine the effects of AgNPs on the functioning of natural bacterial assemblages that inhabit estuaries and coastal areas including the mechanisms behind the recovery and resistance to AgNPs. The susceptibility of pure bacterial cultures to three different AgNP types, two standard reference materials (Sigma Aldrich AgNPs and the Organisation for Economic Co-operation and Development (OECD) NM-300 AgNPs) and a cleaning product purchased from Mesosilver containing AgNPs was examined. The Mesosilver AgNPs product exhibited the highest antibacterial activity followed by the NM-300 AgNPs. The higher toxicity exhibited by the Mesosilver AgNPs was associated with their smaller particle size and initially higher concentration of silver in ionic form. For all the AgNPs types tested, the toxicity was bacterial species-specific, Gram negative bacteria being more resistant than the Gram positive species. This initial work informed the design of the microcosm experiments established with sediments and water samples collected from the estuary to develop the exposure to AgNPs under more realistic environmental conditions. The results showed that a single pulse of NM-300 AgNPs (1 mg L^{-1}) that led to sediment concentrations below 6 mg Ag kg dry $weight^{-1}$ decreased the bacterial carbon utilization rate of environmentally relevant carbon substrates. Following a 24 hr exposure the functional diversity changed, but recovered after 120 hr. This recovery may be explained by a number of possible factors, such as the formation of compounds less toxic than AgNPs, or by the complexation of AgNPs with natural organic matter and sediments reducing their bioavailability, or also due to the presence of silver resistance genes or groups of organisms more resistant to silver. AgNPs did not affect the bacterial community

structure based on the phospholipid fatty acids (PLFAs) analysis. The microcosm experiments suggested that AgNPs under environmentally relevant conditions can negatively affect bacterial function and provides an insight into the understanding of the bacterial community response and resilience to AgNPs. The results of this research project have improved the current knowledge about the toxicity of different silver nanoparticles and the bacterial response under more realistic environmental conditions and will support future risk assessments and regulation process of products containing silver nanoparticles.

Dedication

I would like to dedicate this work to my grannies, Visi and Maria, and my parents, Marian and Victor.

Acknowledgments

This PhD thesis would not have been possible without the support of my supervisor Dr. Mark Hartl. Thank you very much Mark for all the time you have dedicated to me, your advice and your patience. I am also very grateful to my second supervisor Dr. Lynn Paterson for her support with the characterization of nanoparticles, her encouragement and helpful comments and revisions on my work.

I would like to say thanks to all the researchers from the School of Life Sciences. I am especially grateful to Dr. Joe Porter, Dr. Mike Winson, and Dr. Thomas Aspray and all the members from the Nanosafety group for their help with diverse techniques and inspiration. A big thank to Hugh, Sean, Margaret, Paul, Vicky, Gina, Dawn, Jim, Collin a Rob. The help and support of the technicians was crucial for the achievement of the present work.

I am also grateful to Dr. Andreas Pommerening-Röser (University of Hamburg) for providing me with his *Nitrosomonas* spp. cultures, to Dr. Christine Elgy (FENAC) for her advice with the nanoparticle characterization work, and Dr. Barry Thornton (James Hutton Institute) for his help with the PLFAs analysis.

Thanks to my mates at Heriot-Watt University, especially to Cristina, Majed, and Monica, and to my friends from out the uni, Fran and Yolanda, who encouraged me to keep going but also to stay calm.

This work was funded by Heriot-Watt University Environment and Climate Change Theme and the grant NERC-FENAC/2012/11/004.

ACADEMIC REGISTRY
Research Thesis Submission

Name*:*	Virginia Echavarri-Bravo		
School/PGI:	School of Life Sciences		
Version: *(i.e. First, Resubmission, Final)*	Final	Degree Sought (Award **and** Subject area)	Ph.D Microbiology & Nanotoxicology

Declaration

In accordance with the appropriate regulations I hereby submit my thesis and I declare that:

1) the thesis embodies the results of my own work and has been composed by myself
2) where appropriate, I have made acknowledgement of the work of others and have made reference to work carried out in collaboration with other persons
3) the thesis is the correct version of the thesis for submission and is the same version as any electronic versions submitted*.
4) my thesis for the award referred to, deposited in the Heriot-Watt University Library, should be made available for loan or photocopying and be available via the Institutional Repository, subject to such conditions as the Librarian may require
5) I understand that as a student of the University I am required to abide by the Regulations of the University and to conform to its discipline.

* *Please note that it is the responsibility of the candidate to ensure that the correct version of the thesis is submitted.*

Signature of Candidate*:*		Date:	

Submission

Submitted By *(name in capitals):*	
Signature of Individual Submitting:	
Date Submitted:	

For Completion in the Student Service Centre (SSC)

Received in the SSC by *(name in capitals):*			
Method of Submission *(Handed in to SSC; posted through internal/external mail):*			
*E-thesis Submitted (**mandatory for final theses)***			
Signature:		Date:	

TABLE OF CONTENTS

List of abbreviations

Acronym	Definition
AAS	Atomic Absorption Spectroscopy
AgNPs	Silver Nanoparticles
AFM	Atomic Force Microscopy
AMP	Antimicrobial Peptide
BSA	Bovine Serum Albumin
AWCD	Average Well Colour Development
CAT	Catalase
CLPP	Community Level Physiological Profile
COD	Chemical Oxygen Demand
ENMs	engineered nanomaterials
FENAC	Facility for Environmental Nanoscience Analysis and Characterisation
GC-FID	gas chromatography flame ionisation detection
GST	Glutathione-S-transferase
ICP-MS	Inductively coupled plasma mass spectrometry
LPS	Lipopolysaccharide
NADH	Nicotinamide adenine dinucleotide reduced form
OECD	Organisation for Economic Co-operation and Development
OM	Outer membrane
PCR	Polymerase chain reaction
qPCR	quantitative PCR
PLFA	Phospholipid fatty acids
PVP	polyvinylpyrrolidone
ROS	reactive oxygen species
TEM	Transmission electron microscopy
SCENIHR	Scientific Committee on Emerging and Newly Identified Health Risks
SEM	Scanning electron microscope
SRHA	Suwannee River humic acid
SOD	superoxide dismutase
WWTP	Waste water treatment plant
USEPA	United States Environmental Protection Agency

List of tables

Chapter 2

Chapter 3

Appendices

List of equations

List of figures

Chapter 1

Chapter 2

Chapter 3

Appendices

Output

Papers

Conference presentations

Chapter 1 Introduction and Aims

1. Introduction

The rise of nanotechnology has led to an increase in the manufacturing and use of new materials that, at the nano-scale, exhibit different characteristics to their respective bulk material. Silver nanoparticles (AgNPs) are one of these materials, and due to their physicochemical properties are incorporated in a wide variety of applications, such as conductive ink solution in the electronics industry and as active ingredients in biocides and pesticides (Kah and Hofmann, 2014). In addition, AgNPs are used as broad spectrum antimicrobial agents (Lansdown, 2010) and for this reason they are incorporated in food packaging (Echegoyen and Nerín, 2013), textiles (Benn and Westerhoff, 2008), toiletries and health care products (Chao *et al.*, 2011). Hitherto, the products containing nanosilver are the most numerous within all the products containing nanomaterials. Up to 434 items that incorporate nanosilver have been identified in the nanotechproject.org (Project on Emerging Nanotechnologies the Woodrow Wilson International Centre for Scholars) catalogue available on line[1](*accession date 08/09/2014)*.

As much of the silver is disposed of through domestic waste water (Blaser *et al.*, 2008), the question arises whether accumulation in the receiving estuarine environment could negatively affect the functioning of resident bacterial communities that play an important role in biogeochemical processes, such as nutrient recycling and bioremediation, a crucial ecosystem service. In addition, silver is a toxic and persistent heavy metal that can be bio-accumulated at different trophic levels. For all these reasons the fate of AgNPs and their impact on natural ecosystems is an important topic of research. The present study covers the effects of AgNPs on the functioning of natural bacterial assemblages that inhabit estuaries and coastal areas. Thus the present introductory section provides a review of the existing knowledge of antibacterial mechanisms of AgNPs. The physicochemical properties that confer the antimicrobial activity to this nanomaterial, together with the most relevant features of the bacterial cell biology are described first. Next, several issues associated with the implementation of the risk assessment and regulations of products that contain nanomaterials are discussed. The current knowledge about the emissions and fate of AgNPs in the marine environment based on the experimental and *in silico* studies developed to date is also

[1] http://www.nanotechproject.org/cpi/browse/nanomaterials/silver-nanoparticle/

covered. Finally, a rationale covering the main aims and objectives of the present project is included at the end of this introductory section.

1.1. AgNPs review: Properties, risk assessment and fate

1.1.1. Physicochemical properties of AgNPs

A nanoparticle is defined as a nano-object with at least one external dimension in the nanoscale range between 1 and 100 nm (Figure 1.1), and Ag-NP has been defined by the Scientific Committee on Emerging and Newly Identified Health Risks (SCENIHR) in a recent report (Epstein *et al.*, 2014) as: *"single particle, aggregate or agglomerate having one or more external dimensions in the size range 1 - 100 nm. Silver materials with a particle size larger than 100 nm are indicated as bulk silver"*. In the same report there is also a specific definition for nanosilver: "*Silver material with at least one size in the range between 1 and 100 nm. Examples are: thin films (one dimension smaller than 100 nm), fibres/wires (two dimensions smaller than 100 nm), particles (three dimensions smaller than 100 nm*. In the particular case of AgNPs, a wide variety of nanoparticle types have been produced to date according to their size and coating or capping agent used during their manufacturing process. These two main properties together with the shape influence other physicochemical properties as surface area, surface charge and solubility. These physicochemical properties condition the reactivity and toxicity of AgNPs. In the next subsections the most relevant physicochemical properties of AgNPs regarding their ecotoxicity are discussed.

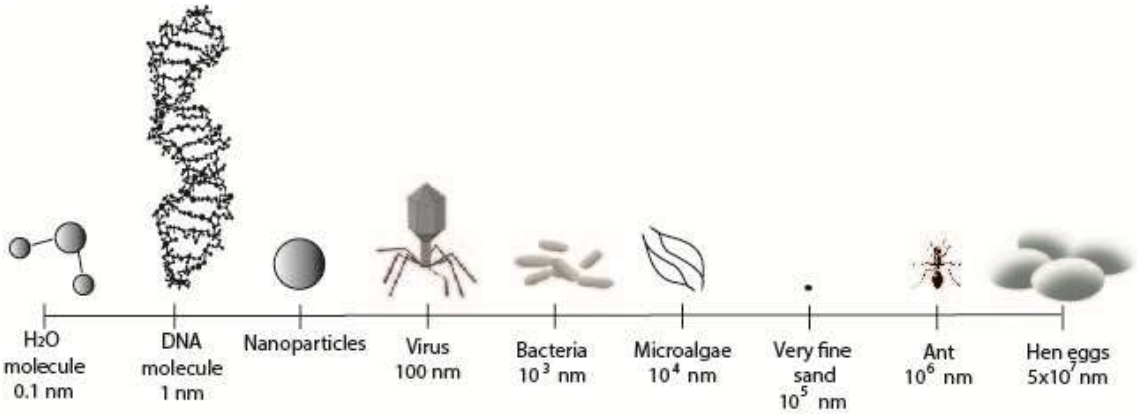

Figure 1.1 Scale diagram displaying the relative position of nanoparticles with other elements according to their size.

1.1.1.1. Size

The small size of nanoparticles that range between 1 and 100 nm is the most relevant characteristic of nanoparticles, and it is responsible for their surface charge and high surface area. If the particle is spherical, the ratio obtained from dividing the surface

area (SA) by the volume (V) is inversely proportional to the diameter of the particle. In other words, smaller particles exhibit a greater SA/ V ratio, and this means that the surface exchange with the surrounding environment is greater. Therefore, in an oxidizing environment as the estuarine water column and superficial sediments (the environments under study in the present PhD thesis), the smaller the particle, the higher is the potential to release ionic silver (Smetana *et al.*, 2008, Xiu *et al.*, 2012). AgNPs dissolution may occur due to oxidation by the dissolved O_2 in the suspension, thereby releasing Ag^+ ions (Liu and Hurt et al., 2010). Several studies confirmed that the smallest particles used in the AgNPs exposures caused the highest toxicity owing to higher release of silver ions (Xiu *et al.*, 2012), but also owing to their higher degree of direct interaction between the particle and the cell membrane that can lead to membrane disruption (Choi and Hu, 2008, Morones *et al.*, 2005).

1.1.1.2. Shape

To date, AgNPs with numerous different shapes have been synthesized for research purposes in different fields including biological applications (Ashkarran *et al.*, 2013). Pal *et al.*, (2007) observed that truncated triangular particles (40 nm edge length) exhibited higher bactericidal activity than spherical nanoparticles (39 nm diameter) with an initial cell number or colony forming units (CFU) of 10^7 CFU/ml . As mentioned previously, the surface area depends on the particle size in addition to their shape. Sadeghi *et al.*, (2012) measured the surface area of different nanosilver shapes with BET (Brunauer, Emmitt and Teller) technique (based on measuring the adsorption of gas on the nanoparticle surface). They demonstrated that surface area is dependent on the particle shape, and that the nanoparticles shape influences nanoparticle toxicity. Tetrahedral particles composed of four triangular faces of length "α", exhibit a higher SA/ V ratio than spherical particles with diameter "α". As discussed previously, at higher surface area the toxicity of AgNPs also increases. This would explain why Pal *et al.*, (2007) observed that truncated triangular nanoparticles exhibited higher toxicity.

1.1.1.3. Surface charge and capping agent

The surface charge of AgNPs determines their interaction with bacterial membranes which are generally negatively charged due to the presence of lipopolysaccharides (LPS) in Gram negative bacteria and the peptidoglycan wall in Gram positive bacteria, described in greater detail in section 1.1.2. The surface charge of uncoated AgNPs depends also on the pH of the media (see section 1.1.5.) but it can be modified by agents conferring electrostatic or steric stabilization (Badawy *et al.*, 2010). These agents can be coating or capping compounds used during the synthesis of

the nanoparticles to prevent agglomeration and to control the particle size. To date the most common stabilizing agents used are sodium citrate, sodium borohydride ($NaBH_4$), polyvinylpyrrolidone (PVP) and amines, followed by fatty acids, polyvinyl alcohol (PVA), Cetyltrimethylammonium bromide (CTAB), sugars and amides (Tolaymat *et al.*, 2010). Their respective properties on AgNPs stabilization and toxicity have been investigated during the past years. There is a higher attraction between positively charged AgNPs and negatively charged bacterial membranes, increasing the interaction between both, and causing physical damage by creating pits in the membrane (Sondi and Salopek-Sondi, 2004) and indirectly by inducing the production of reactive oxidative species (ROS), as observed in mammalian cells (Carlson *et al.*, 2008). The relevance of particle surface charge on AgNPs toxicity was comprehensively examined by Badaway *et al.*, (2010) who demonstrated that AgNPs with high positive surface charge due to the coating agent branched polyethylenemine (BPEI-AgNPs), were more reactive with the negatively charged bacterial membranes than negatively charged AgNPs coated with citrate or polyvinylpyrrolidone (PVP). Currently, new emerging nano-composites such as the combination of AgNPs and antimicrobial peptides (AMPs) have enhanced their antimicrobial properties, broadening their spectrum against Gram positive, Gram negative bacteria, yeast organisms (Lihong Liu *et al.*, 2013) and mycobacteria (Mohanty *et al.*, 2013). Lihong Liu *et al.*,(2013) functionalized AgNPs with the penetrating peptide GGGRRRRRRYGRKKRRQRR and observed that the minimum inhibitory concentrations (MIC) of AgNPs decreased in combination with the AMPs. However the effects of the peptide on its own were not investigated. On the other hand, Mohanty *et al.*, (2013) investigated the effects of cationic peptides (NK-2 and LLKKK-18) in combination with biogenic AgNPs. There was an additive antibacterial effect by the combination between the NK2 and the AgNPs. AgNPs functionalized with AMPs exhibit higher antimicrobial activity. This is possibly due to AMPs that enhance cell permeabilization facilitating the access of AgNPs inside the cell. Once inside the cell there are several target sites for silver ions such as DNA, respiratory chain and ribosomes. Nowadays the most widely used technique to analyze the surface charge of AgNPs in liquid suspensions is the zeta potential analysis, described in the methods section 2.2.2.

1.1.2. Bacterial cell

Bacteria are unicellular organisms classified within the group of prokaryotes. Bacteria lack a defined nucleus and other organelles typically found in eukaryotic cells, such as the mitochondria and the Golgi apparatus. In the absence of these organelles, it

is in the inner membrane, also known as the cytoplasmic membrane, where functions such as the electron chain transport takes place. Furthermore bacteria exhibit highly developed outer membranes (cell envelope) that confer to these microorganisms resistance against adverse environmental factors and antibiotic compounds. According to the characteristics of the cell envelope, bacteria have been divided in two main groups, Gram negative and Gram positive which are described next.

1.1.2.1. Bacterial cell envelope

One of the major functions of the bacterial cell envelope is the protection from external factors. For this reason, their structure and composition are diverse and species specific, playing a crucial role in the resistance of these organisms to silver ions and AgNPs. As mentioned previously, on the basis of the structure of the cell envelope, bacteria are classified in two broad groups, Gram positive and Gram negative bacteria. The cell envelope of the Gram positive bacteria is formed by a thick (30-100 nm) hydrophilic wall of peptidoglycan, named murein, that incorporates teichoic and teichuronic acids. In contrast, Gram negative bacteria have a more complex cell envelop formed by an outer membrane (OM) made up of lipopolysaccharides (LPS). The inner part of the OM is formed by a phospholipid bilayer. Thus the OM can exclude hydrophobic and hydrophilic compounds. Here the presence of porins, proteins that act as channels, allow the passive diffusion of hydrophilic compounds (sugars, aminoacids, some ions) smaller than 600-700 daltons, (6 – 10 Å in size; (Schulz, 2002). Other proteins are specialized in the transport of bigger compounds such the btuB and FhuA, transporters of the vitamin B12 and siderophore complexes respectively (Nikaido, 2003). Below the OM there is a thin (5-10 nm) murein layer (Figure 1. 2) that confers rigidity to the cell.

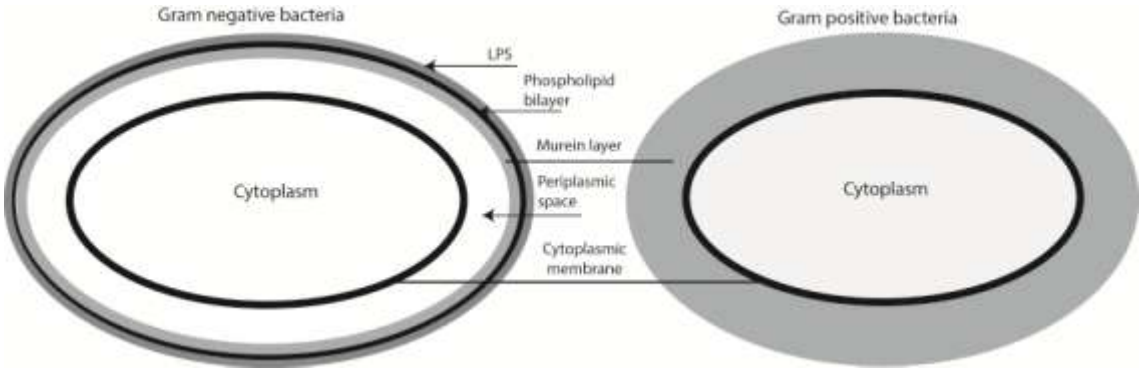

Figure 1. 2 Structure of the bacterial envelope in Gram negative (left) and Gram positive (right) bacteria.

The composition and structure of the bacterial envelope determines the permeability to different antibiotics and also the efflux properties of the cell. These

properties explain the differences between both bacterial groups in terms of their resistance to antibiotics. Gram positive bacteria are generally more susceptible to antibiotics as they are permeable to compounds of higher molecular weight and less efficient in terms of efflux pumps (O'Shea and Moser, 2008).

1.1.3. Bactericidal mechanism of AgNPs

As mentioned previously, the antibacterial activity of AgNPs depends on their physicochemical characteristics. These antibacterial properties have been attributed mainly to the release of silver ions, however, the particle interaction with biological membranes and the production of reactive oxygen species are other mechanisms that may explain the toxicity observed by AgNPs that cannot be exclusively linked to the release of ionic silver. These antibacterial mechanisms are described in greater detail next.

1.1.3.1. Release of ionic silver

The bactericidal properties of ionic silver (Ag^+) have been known for centuries (Just and Szniolis, 1936) cited by Flemming (1987). Silver ions exhibit numerous and diverse antibacterial mechanisms that have been described in several studies using *Escherichia coli* as a model species. For example Ag^+ can penetrate the cell membrane easily though the ion channel, and interact with the ribosomes disrupting the enzymatic activity and protein expression essential for ATP production (Yamanaka *et al.*, 2005). Ag^+ can also react with different sites in the respiratory chain, between the b cytochrome and a2 cytochrome, and less seriously in the site where the interaction of the substratum with the NADH and the flavoproteins take place (Bragg and Rainnie, 1974). Ag^+ modifies the redox state of these sites, interfering with the reduction of flavoprotein and cytochrome a1, a2, b1. At the cytoplasmic membrane level ionic silver disrupts the phosphate exchange and uptake that may cause efflux of internal phosphate (Schreurs and Rosenberg, 1982). Ag^+ once inside the cytoplasm causes DNA condensation suppressing cell replication (Feng *et al.*, 2000). Studies with other species such as *Vibrio cholerae*, revealed that Ag^+ may interact with membrane proteins in the phospholipid bilayer causing proton leakage followed by cell death (Dibrov *et al.*, 2002). One of the most recent studies in this field reported that the main antibacterial mechanism of AgNPs takes place by the time-dependent release of silver ions and that the nanoparticle effect is negligible (Xiu *et al.*, 2012).

1.1.3.2. Nanoparticle-bacterial membrane direct interaction

As discussed previously (1.1.1.3), the relatively high surface area of AgNPs compared to their small size, and their surface charge, enhances the interaction of AgNPs with biological membranes. To date several studies aimed to distinguish NP-specific effects from ionic effects. The nanoparticle-effect of AgNPs, the effect observed when the toxicity of AgNPs cannot be explained solely by the release of ionic silver, has been reported in former studies (Joshi *et al.*, 2012, Fabrega *et al.*, 2009a). This nanoparticle-effect may be due to the mechanical interaction between the nanoparticle and the bacterial membranes (Taglietti *et al.*, 2012). The nanoparticle-cell membrane interaction may also enhance the uptake of silver ions leading to an increase in the toxicity of AgNPs (Bondarenko *et al.*, 2013). The use of modified strains to act as a bioreporter of ionic silver concentration, together with other modified strains lacking ionic silver efflux systems and antioxidants mechanisms, showed that oxidative stress is one of the main antibacterial mechanisms of AgNPs. The surface of the AgNPs can catalyze the formation of ROS, and these ROS may oxidize AgNPs and consequently increase the release of ionic silver (Joshi *et al.*, 2015). On the other hand the addition of the Suwannee River humic acid (SRHA) decreases the toxicity of AgNPs (Fabrega *et al.*, 2009a). This may be explained by the fact that SRHA modifies the surface charge or nanomaterials but also may act as a physical barrier between AgNPs and bacterial membranes (Fabrega *et al.*, 2009a). Nowadays studies with models of biological membranes (artificial membranes) are being developed to mimic the real membrane behaviour in order to elucidate the membrane-nanoparticles interaction. These studies aim to have a better understanding of the NPs mechanism of toxicity involved, such as attachment/adhesion, deformation and disruption mode if any. However, the work involved is complex due to the high heterogeneity and dynamic properties of biological membranes that varies across organisms and bacterial species in particular, together with the numerous types of AgNP that have been produced to date. The lipid bilayer has been the most common type of model membrane used to date and future work aims to incorporate into this lipid bilayer a coat of peptidoglycan or bacterial lipids to model the bacterial envelop (Chen and Bothun, 2013). Microscopy techniques such as Transmission Electron Microscopy (TEM), Scanning Electron Microscopy (SEM) and Atomic Force Microscopy (AFM) have been used to examine bacterial-NPs interaction. These techniques have been applied to examine the effects of AgNPs on bacteria, as changes in the morphology and structure of the bacterial cell. TEM also enables the study of AgNPs inside the bacterial cell (Morones *et al.*, 2005, Joshi *et al.*, 2012,

Fabrega *et al.*, 2009b) while AFM (Suresh *et al.*, 2010) and SEM (Sondi and Salopek-Sondi, 2004) provide a three dimensional image of the bacterial surface. Moreover, AFM offers the possibility to analyze the adhesion forces of the molecules in the outer membrane (Stukalov *et al.*, 2008).

1.1.3.3. Reactive oxygen species (ROS) production

The ROS exhibit strong oxidizing properties and are responsible for causing cytotoxicity due to oxidative stress. This is because ROS may react with the biological membranes, causing lipid peroxidation that may lead to the destabilization and disruption of the bacterial membranes. The production of internal ROS is part of the normal metabolism of aerobic organisms that require oxygen as the terminal acceptor in the electron chain. The ROS produced are quenched by antioxidant enzymes such as superoxide dismutase (SOD), catalase (CAT) and glutathione-S-transferase (GST). The SOD catalyzes the reaction that transforms as $O_2^{\cdot -}$ into H_2O_2, and the catalase breaks down the H_2O_2 into H_2O and O_2, similar to the GSH that also scavenges ROS (Di Giulio *et al.*, 1995). Su *et al.*, (2009) proposed a theory to explain an increase in the concentration of the internal ROS based on hypothesis that AgNPs may damage the function of the transmembrane proteins by direct interaction of the NPs with the bacterial membrane. As a result of this, the proton exchange associated with the respiratory chain process may be disrupted. This may lead to the accumulation of electrons resulting in an increase in the concentration of ROS as $O_2^{\cdot -}$ and H_2O_2. The toxicity of AgNPs on bacteria has been associated with the production of extracellular ROS as the hydroxyl radical $OH^{\cdot}$ compound (Kim *et al.*, 2007) than can be produced by UV-radiation (Miyoshi *et al.*, 2010). AgNPs antibacterial activity due to the production of intracellular ROS has also been reported (Choi and Hu, 2008). The production of reactive nitrogen species (RNS), also responsible for causing oxidative stress, was investigated by Mohanty *et al.*, (2013). They observed that in presence of AgNPs, macrophages did not increase the production of nitric oxide (NO) to kill intracellular mycobacteria, but the concentration of NO decreased at increasing concentrations of AgNPs.

1.1.4. Bacterial resistance to AgNPs

Silver nanoparticles are regarded as antimicrobial agents of broad-spectrum owing to their multiple antibacterial mechanisms or bacterial target sites. Moreover it has been observed that the inhibitory activity of broad spectrum antibiotics such as Ampicillin has been enhanced in combination with AgNPs against both Gram positive and Gram negative bacteria (Fayaz *et al.*, 2010).

The bacterial resistance to silver ions have been investigated with a few bacterial species. Nowadays it is known that plasmids encoding metal resistance is one of the most common ways in which bacteria acquire resistance to ionic silver. For example, in the bacterial species *Salmonella typhimurium* the group of genes *sil* are known to confer resistance to silver. This group of genes is located in the pMG101 plasmid and are responsible for encoding a metal-binding protein and two different biochemical efflux mechanisms. The gene *silE* encodes a periplasmic protein that binds silver ions. This gene is next to a two component gene pair, *silRS*, encoding a transcriptional regulatory responder protein and membrane sensor kinase. The other genes responsible for the silver resistance are transcribed separately from the *silRSE* group. These are 1) the *silA* geneA encode a proton/cation antiporter located in the inner membrane, 2) the *silB* gene encodes a membrane fusion protein that spans the inner and outer membrane in Gram negative bacteria and 3) the gene *silC* encodes a protein in the outer membrane and 4) the gene *silP* is responsible for encoding the P-type ATPase. The plasmid R476b, isolated initially from *E.coli*, is also known for conferring resistance to silver, although lower degree of resistance compared to the pMG101. The metal resistance genes can also be included in the chromosomes such as the *copA* gene that is believed to be responsible for the efflux of Ag^{+}. In *E.coli*, the group of chromosomal genes *agr*, have been found to exhibit a similar role to the *sil* genes. In addition genes similar to the *sil* group have been identified in other members of the *Enterobacteriaceae* family (Gupta *et al.*, 2001).

Apart from the gene encoding resistance there are other mechanisms that confer silver resistance to bacteria such as the production of exopolysaccharides (EPS) by some bacterial species, such as *Pseudoalteromonas sp*. (Gutierrez *et al.*, 2008). EPS can sequester metals and as a result of this the resistance of the bacterial community to AgNPs increases (Gutierrez *et al.*, 2012). EPS also enhance cell aggregation thus the cell surface area exposed to nanoparticles is reduced (Joshi *et al.*, 2012). In addition some EPS containing sugars with aldehydes that can be oxidized into carboxyl groups by Ag^{+}. Thus, reduced Ag is immobilized by EPS resulting in a reduction of the bioavailability/toxicity of the ionic silver released from AgNPs (Kang *et al.*, 2013). Other organics rich in thiol groups (–SH) present in some amino acids such as cysteine, bind strongly to metallic ions such as Ag^{+} that enhance nanoparticle aggregation (Gondikas *et al.*, 2012) and reduce AgNPs toxicity (He *et al.*, 2012). To date there is not a general agreement about which bacterial group, Gram negative or Gram positive, is more resistant to AgNPs. Suresh (2010) and Ojha (2013) observed that Gram negative

bacterial species were more resistant than the Gram positive species examined. However, the method used by Ojha *et al.*, (2013) known as "Kirby-Bauer disk diffusion" may not be the most appropriate to investigate the antimicrobial properties of AgNPs, as only the effects of the ionic silver released and diffused in the agar can be evaluated, overlooking any existing antibacterial effect due to the nanoparticle-membrane interaction or "particle" effect. Other studies reported the opposite, that Gram positive species were more resistant to AgNPs than Gram negative species (Kim *et al.*, 2007, Amato *et al.*, 2011) and to silver ions (Jung *et al.*, 2008). The higher resistance to silver exhibited by some Gram positive species may be acquired by the thick peptidoglycan layer present in the cell envelope that may prevent the penetration of AgNPs inside the bacterial cell as observed by Taglietti *et al.*, (2012). The AgNPs used by this research group were previously functionalized with glutathione (GSH), and internalized by the Gram negative bacterium *E.coli*, whereas nanoparticle internalization did not occur in the Gram positive species (*Staphylococcus aureus*).

Most of the work performed to date to investigate the antibacterial mechanisms of AgNPs employed *E.coli* as species model for Gram negative bacteria and *S. aureus* as a model for Gram positive. For this reason there is not enough evidence to say that Gram negative bacteria are more resistant than the Gram positive bacteria, or *vice versa*, but there is a general agreement that the toxicity of AgNPs is bacterial species-specific. The fact that toxicity data of silver nanoparticles has been generated using a variety of particle types and target organisms (e.g. different bacterial species) comparison across multiple studies is difficult. In addition, the physicochemical properties of AgNPs can be affected by the environmental conditions (salinity of the medium, organic matter, temperature, pH, inorganic components such as clays) and as a result of this their antimicrobial properties may be also affected as discussed in the section 1.1.5. In a report published recently by the SCENIHR it was emphasized that there is a gap in knowledge relating to the dissemination of bacterial resistance associated to the use of AgNPs (Epstein *et al.*, 2014).

1.1.4.1. Ionic silver vs. AgNPs

Studies developed with natural bacterial communities showed that silver is more toxic against bacteria in the ionic than in the nano form (Doiron *et al.*, 2012, Colman *et al.*, 2012) contrary to former studies (Lok *et al.*, 2006, Choi and Hu, 2008, Choi *et al.*, 2009). These contradictions between studies may be explained by differences in bacterial species and the physicochemical properties of each AgNPs as observed by (Suresh *et al.*, 2010) and discussed previously.

1.1.5. Marine environmental factors that affect the physicochemical characteristics of AgNPs

The marine ecosystems are highly diverse due to several factors such as depth, geology, tidal regime, climatology and biology. In the present section, the environmental factors that will affect the physicochemical properties of AgNPs, such as salinity, pH, organic matter and UV-radiation are discussed. Temperature can affect the physicochemical properties of AgNPs as it has been observed that increasing temperature favoured AgNPs aggregation and surface charge (measured as zeta potential) became more negative (Oukarroum *et al.*, 2012). At higher temperatures an increase in the ROS formation and antibacterial activity of AgNPs has also been reported (Xu *et al.*, 2012). The influence of the redox conditions is discussed next along with the other environmental factors.

1.1.5.1. pH

The pH is a very important factor governing the physicochemical properties of AgNPs as it may affect their surface charge (zeta potential). Badawy and co-workers (2010) observed that uncoated AgNPs were stabilized electrostatically by the OH^- groups distributed around the particle surface achieving a zeta potential value of – 22 mV (at pH 8.9) that became less negative when the pH decreased, close to 0.0 mV at pH 2. The reason for this is that at lower pH, the surface of uncoated AgNPs may have a lower concentration of OH^-, but by increasing the pH, molecules such as OH^- and H_2O can donate a pair of electrons. As a result, in alkaline environments the OH^- concentration increases and can bond to the uncoated AgNPs surface and turn the surface charge negative . AgNPs stabilized electrostatically (with a capping agent that consisted of $NaBH_4$ and citrate) were not as stable as AgNPs stabilized sterically with PVP exposed to different pH range (between pH 3 and pH 9). In the marine environment differences within this range of pH are not expected as conditions are predominantly alkaline; the average estimated pH value oscillates between 8.08 to 8.33 (at S. 35 ‰ and 25ºC) although pH values can range from 7.4 to 9.6 (Marion *et al.*, 2011). The pH not only affects the surface charge of AgNPs but also their dissolution. Yu *et al.*, (2013) showed that dissolution of AgNPs was higher at pH 5 than at pH 8.3 and all metals in general exhibit higher dissolution rates at lower pH (López *et al.*, 2010). For this reason, the acidification of the marine environment as a consequence of climate change (predictions estimate a decrease in pH from 8.1 to 7.8 by 2100 (Hennige *et al.*, 2014)), could enhance the dissolution of metallic ENMs including AgNPs,

increasing their toxicity, and together with other anthropogenic stressors may also have a detrimental effect on the health and status of the marine ecosystems.

1.1.5.2. Ionic strength

The average salinity or ionic strength in the ocean is approximately 35‰ with sodium chloride (NaCl) the most abundant salt. The most abundant anion/cations in the marine environment are (in ‰) Cl^- 19.35 and Na^+ 10.78 followed by SO_4^{2-} 2.71, Mg^{2+} 1.28, Ca^{2+} 0.41, K^+ 0.40, and HCO_3^- 0.10 (Millero *et al.*, 2008). Salinity strongly affects the physicochemical properties of AgNPs as it will be explained next. For this reason, the fluctuations of the environmental factor is caused by the tidal regime in estuaries must be considered when studying the effects and fate of AgNPs in this environmental compartment. The charge of the double electric layer surrounding the AgNPs (Figure 1. 3) depends on the ionic strength of the aqueous suspension. At higher ionic strength there is a reduction in the electrical double layer surrounding the AgNPs, and as a result the absolute value of the surface charge (measured as zeta potential) also decreases.

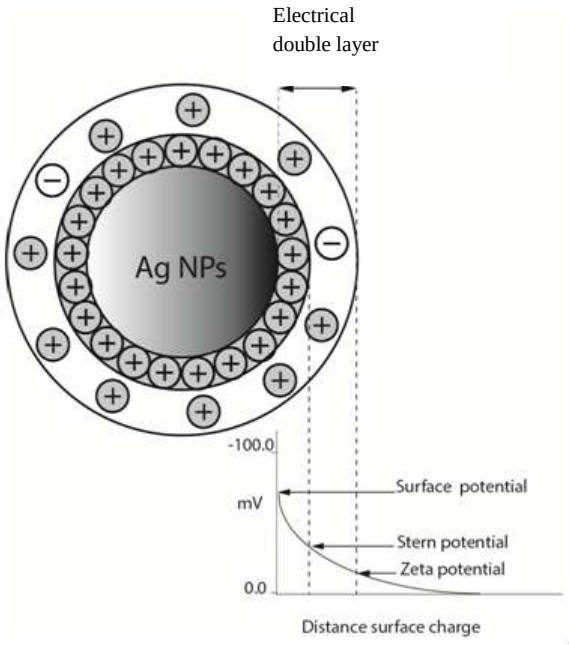

Figure 1. 3 Particle surface charge of AgNPs negatively charged. Diagram modified from Malvern Instruments. http://www.malvern.com/labeng/technology/zeta_potential/zeta_potential_lde.htm

A reduction in the electrical double layer favours nanoparticle interaction followed by agglomeration/aggregation (Chinnapongse *et al.*, 2011). Nanoparticles stabilized through steric repulsion are less susceptible to changes in the ionic strength although some capping agents such as PVP are more efficient than others as for example polyethylene glycol (PEG) or citrate (Tejamaya *et al.*, 2012). A reduction in the particle the electric double layer or surface charge owing to the ionic strength will enhance nanoparticle surface interaction, normally leading to particle agglomeration

reflected in an increase in the hydrodynamic diameter, which can lead to particle settling (Badawy *et al.*, 2010) and a shift in the peak absorbance of the UV-vis spectrum towards longer wavelengths (Chinnapongse *et al.*, 2011). Similar to the agglomeration/aggregation processes, some ionic species contained in the seawater such as Cl^- enhance the AgNPs dissolution (Kent and Vikesland, 2011, Zook *et al.*, 2011). AgNPs are together with ZnO NPs the most soluble metallic nanoparticles (Baker *et al.*, 2014). Special attention has been given to the effects of chloride on different AgNPs types as several studies have shown that under aerobic conditions (positive redox potential), AgNPs will be oxidized and ionic silver released (Xiu *et al.*, 2012, Liu *et al.*, 2010). Chloride exhibits a high affinity for Ag^+, and the formation of the low solubility silver chloride (AgCl) salt is very likely to occur. Depending on the Cl/Ag ratio, the formation of soluble forms of silver chloro-complexes such as AgCl, $AgCl_2^-$, $AgCl_3^{2-}$ and $AgCl_4^{3-}$ will be favoured (Levard *et al.*, 2012, Levard *et al.*, 2013, Liu *et al.*, 2010, Angel *et al.*, 2013). These ionic forms of silver are bioavailable (able to cross bacterial cell membranes) and studies carried out with the Gram negative bacterium Escherichia coli (Gupta *et al.*, 1998) have shown that at high concentrations they can decrease the bacterial resistance to ionic silver.

1.1.5.3. Organic matter and clays

The natural organic matter (NOM) in the aquatic environment can be regarded as dissolved organic matter (DOM) (< 0.45 µm). This includes solutes (< 0.001 µm) and colloids (0.001 to 0.45 µm), and particulate organic matter (POM), greater in size than 0.45 µm (Rand *et al.*, 1995) The interactions between the DOM fraction and AgNPs can lead to diverse physicochemical processes (complexation/chelation, photodegradation, aggregation, flocculation and redox reactions affecting dissolution and interaction with inorganic species such as sulphide and chloride) depending on the physicochemical characteristics of AgNPs and on the different composition of the natural organic colloids (which include proteins, carbohydrates, clays and humic acids produced during the microbial degradation of organic matter). AgNPs-DOM interactions are determined to a great extent by the pH and ionic strength of the surroundings. In the marine environment alginic acid can be a relevant organic colloid, as it is abundant and able to tame the toxicity of AgNPs. This polymer can decrease the toxicity of metals by reducing their solubility/bioavailability and adsorption in the intestine (Haye *et al.*, 2006). In addition, alginic acid exhibited stabilizing properties similar to the SRHA and has been used to investigate the fate and effects of ENMs (Loosli *et al.*, 2013, Fairbairn *et al.*, 2011). AgNPs-clays interactions are also of interest, as clays may enhance the

flocculation of ENMs. However, AgNPs-clay flocculation will only occur if they exhibit different surface charge as observed by Zhou *et al.,* such as TiO_2 and AgNPs (2012) . Under typically marine pH (7.5-8.5) most of the clays and uncoated AgNPs will be negatively charged thus flocculation will not take place. However positively charged AgNPs could react with negatively charged clays, and favour their accumulation in sediments.

1.1.5.4. UV-radiation

The photocatalytic activity of AgNPs can increase their reactivity and as a result, also increase their toxicity. Bare-AgNPs and citrate-coated AgNPs also produce ROS ($O_2^{\cdot -}$) if exposed to UV (365nm) radiation whereas the production of ROS by PVP-coated AgNPs has not been detected possibly because the coating acts as a donor-acceptor of electrons during the exposure to UV (Li *et al.*, 2013). UV-light can also degrade the PVP coating agent and as a result of this AgNPs dissolution is enhanced. On the other hand it has been reported that the photoreduction of the ionic silver may form nanobridges, small bridges between AgNPs and cause AgNPs aggregation (Yu *et al.,* 2013). Thus UV light is another factor that can influence the fate of AgNPs in shallow-intertidal areas and in the first metres of the water column.

1.1.6. Risk assessment of products containing AgNPs

As discussed in the previous sections, there are different types of AgNPs with different physicochemical properties. Moreover these physicochemical properties and their associated toxicity are influenced by the environmental conditions. For this reason the identification of the hazards associated to AgNPs and the routes of exposure are key factors to take into account during the risk assessment and regulation of products containing AgNPs (Stone *et al.*, 2014). For the regulation of ENMs, including AgNPs, it has been necessary to establish an unambiguous definition of nanomaterial, as well as identifying the accepted analytical techniques that can be applied to characterize the ENMs and the use of the particular reference materials to verify the measurements. A detailed and comprehensive revision related to the definition of nanomaterials has been provided by the Joint Research Centre, European Commission (Rauscher *et al.*, 2014) where major discrepancies between the different definitions include: 1) whether natural occurring particles in the nano scale should be regarded as nanomaterials; 2) the number size distribution threshold in % differs between some countries or organizations ; 3) if it exhibits nanoscale unique properties. In the next subsections a summary about the current state about the regulation of products containing ENMs is in the EU is

presented, together with a review relating to the emissions and fate of AgNPs in the marine environment.

1.1.6.1. Regulation of products containing nanomaterials

Nanomaterials are not included under this denomination explicitly in the OSPAR Co-ordinated Environmental Monitoring Programme (CEMP) or under the Water Framework Directive (2000/60/EC). However the European Union regulation concerning the **R**egistration, **E**valuation, **A**uthorisation & restriction of **Ch**emicals (REACH) and the Classification, Labelling and Packaging (CLP) regulation cover nanomaterials based on the regulation's substance definition indicated next: Substance definition: *"means a chemical element and its compounds in the natural state or obtained by any manufacturing process, including any additive necessary to preserve its stability and any impurity deriving from the process used, but excluding any solvent which may be separated without affecting the stability of the substance or changing its composition"*. Under the REACH regulation companies established in the EU must identify and manage the risks associated to the products they produce or/and commercialized in the EU during their whole life cycle. The CLP regulation aims to ensure an adequate classification and labelling of the substances with the aim to inform consumers and workers about any associated hazard in a clear way.

In addition the products containing nanomaterials are considered explicitly in the biocidal product regulation (BPR) under Regulation (EU) No 528/2012 (http://echa.europa.eu/regulations/nanomaterials). Thus the environmental impact assessment relating to ENMs-containing biocidal product is required. This implies that biocidal products containing ENMs must include the word "nano" in the label of the product and that the authorisation process is not simplified. In addition the risk to the environment associated to the ENMs included in the biocidal product must be assessed separately. In this context the use of reference nanomaterials is needed as they can be used for different purposes as instrument calibration, methodology development and validation and toxicity testing (Stefaniak *et al.*, 2012). As the number of different ENMs, including different AgNPs types is continuously increasing it is necessary to prioritize the ENMs toxicity testing work (Stone *et al.*, 2014). Highlight that AgNPs has been always included in the group of ENMs that require high priority (Stefaniak *et al.*, 2012, Stone *et al.*, 2010).

1.1.6.2. Emissions of AgNPs in the natural environment

A few studies have evidenced the release of AgNPs that had been incorporated in textiles and washing machines (Benn and Westerhoff, 2008, Farkas *et al.*, 2011). The

discharge of treated effluents containing ENMs is the main source of ENMs in the aquatic ecosystems (Sun *et al.*, 2014). Several studies showed that more than > 95% AgNPs contained in the sewage were removed and accumulated in the solid sludge (Kaegi *et al.*, 2013, Impellitteri *et al.*, 2013, Blaser *et al.*, 2008). Other critical routes for the release of AgNPs in the aquatic environment derive from the treatment of the solid sludge. The incineration and landfill application of biosolids that contain AgNPs are a source of emissions of these compounds via atmospheric deposition and runoff water respectively (Keller *et al.*, 2013, Sun *et al.*, 2014, Liu and Cohen, 2014). The diagram depicted in the Figure 1. 4 displays the most relevant emission routes of ENMs in the marine environment, placing the waste treatment process, identified as the waste water treatment plant (WWTP), as the main origin of the emissions (the use and manufacturing process as other possible sources of AgNPs release have been omitted). Associated fluxes connecting different environmental compartments such as the atmosphere, fresh water environment (rivers) and terrestrial (landfill applications and the use of biosolids as organic and mineral amendments in agriculture) were also considered. The major physicochemical processes affecting the fate of AgNPs in the marine environment described earlier in section 1.1.5 (dissolution, precipitation and heteroaggregation with organics and clays) are also depicted in Figure 1. 4.

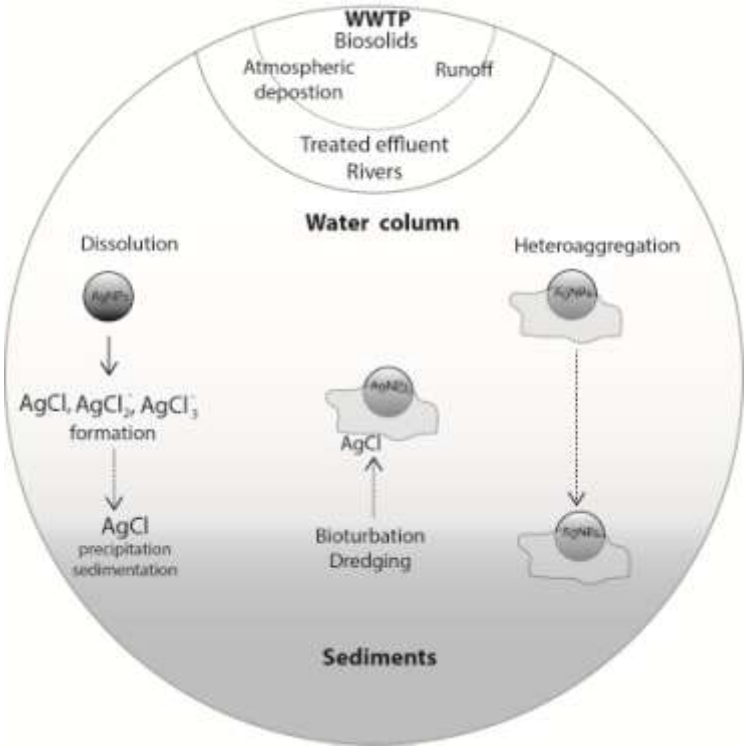

Figure 1. 4 Emission routes and fate of AgNPs in the marine environment, having the waste processing route as the main emission source of AgNPs in the marine environment based on the emission models (Keller *et al.*, 2013, Sun *et al.*, 2014, Liu and Cohen, 2014).

1.1.6.2.1. AgNPs transformation in waste water treatment plants (WWTPs)

In order to effectively assess the risks associated to AgNPs, it is necessary to understand the physicochemical transformations of AgNPs taking place in the WWTPs. The number of scientific reports available regarding the physicochemical transformations of AgNPs in WWTPs is higher than the information available for other ENMs. This is justified by the potential toxicity of AgNPs against the microbial communities that play a crucial role in the biological treatment of sewage in WWTPs. In general the studies related to the fate of AgNPs in WWTPs were in agreement, independently of the AgNPs coating type, or of the interaction of AgNPs with sulphide lead in the formation of Ag_2S under anaerobic conditions (Kaegi *et al.*, 2011, Doolette *et al.*, 2013, Lombi *et al.*, 2013, Kaegi *et al.*, 2013). The fact that the sulfidation process depends on the O_2 availability and is also pH-dependent (Ze-hua Liu *et al.*, 2013) , indicates that other silver compounds can be generated during the treatment of the sewage in the WWTPs. For this reason further investigation is needed related to the effects of the WWTPs process on the physicochemical properties of AgNPs (as these can be discharged directly into the aquatic environment if they are present in the treated effluent). The AgNPs contained in the solid sewage are likely to be released in landfills directly or after incineration. Impellitteri (2013) observed that the incineration of biosolids containing AgNPs transformed the nanoparticles into bulk silver, Ag associated with sulphydryl groups, Ag_2S and Ag_2SO_4. Like the AgNPs, the compounds derived from their physicochemical transformation, can reach the aquatic environment via runoff water or atmospheric deposition, and can release ionic silver through the oxidation process and dissolution of Ag_2SO_4. To date most of the studies related to the fate and toxicity of nanosilver have been developed using pristine AgNPs. The use of pristine NPs may not set a realistic exposure scenario but it allows the investigation of the mechanisms of toxicity and also poses one of the worst-case scenarios if the AgNPs are more toxic under this form (required by legislation, e.g. Regulation (EU) No 528/2012). The study of the physicochemical transformations and ecotoxicity of non-pristine AgNPs (such as aged nanoparticles in relevant WWTP media or in simulating transformation processes (life cycle) that take place during the use of products containing nanosilver), may provide a more realistic knowledge about the fate and potential toxicity of AgNPs. This information will support the development of the ecological risk assessment of these materials in a more efficient way (Nowack *et al.*, 2012).

1.1.6.2.2. Fate of AgNPs in the marine environment and analytical challenges

The understanding of the effects of different environmental factors on the physicochemical properties of AgNPs may support the identification and study of AgNPs that are present in environmental samples. However the analysis of AgNPs and other ENMs in these samples can be challenging due to the interference with other natural nanoparticles or colloids, even under controlled conditions as in mesocosm experiments (Cleveland *et al.*, 2012, Ferry *et al.*, 2009). The study of ENMs in sediments is particularly complex due to some of the widely accepted techniques used for the analysis of ENMs (these include UV-vis spectroscopy (Chinnapongse *et al.*, 2011), Dynamic Light Scattering (DLS) (Ciacci *et al.*, 2012, Al-Subiai *et al.*, 2012), field-flow fractionation (FFF) (Stolpe and Hassellöv, 2010) and single particle Inductively Coupled Plasma Mass Spectrometry or (spICP-MS)) require that the sample is in an aqueous phase, which means that the characteristics of the ENMs contained in solid samples such as sediments can be altered during the sample preparation process (von der Kammer *et al.*, 2012). The analytical techniques that have been used to date to identify and to examine ENMs in marine sediments, and which minimize the sample perturbation, can be expensive and time consuming. Two of these techniques are field emission scanning electron microscope- electron dispersive X-ray microanalysis (SEM–EDX) (Luo *et al.*, 2011) which was used to analyze TiO_2 NPs in coastal sediments and X-ray Absorption Spectroscopy (XAS) utilized to examine the fate of AgNPs in WWTP (Kaegi *et al.*, 2011). These techniques, (SEM–EDX) and (XAS), were also employed to investigate the fate of immobilized AgNPs embedded in films and exposed afterwards to real marine environmental conditions *in situ* (Sekine *et al.*, 2013). Even though the study of the effects of heteroaggregation was not feasible (this being a crucial process that determines the dissolution and surface modification of AgNPs (Gondikas *et al.*, 2012)) the approach developed by Sekine *et al.*, (2013) enabled the study of ENMs reactions and transformations processes in different ecological compartments such as the water column and sediments.

Marine vs. freshwater environment

The analysis of the fate of AgNPs in the marine environment includes the challenges already encountered in freshwater environments, in addition to the interferences caused by the high concentration of salts. For example, the technique named as single particle ICP-MS (spICP-MS) allows to distinguish between dissolved ENMs and small nanoparticles (10 nm) in liquid samples, and can also be used for the

analysis of environmental samples, even when the density of nanoparticles is expected to be low, in the order of ng L^{-1} (Mitrano *et al.*, 2014). The spICP-MS technique has been used successfully to identify ENMs in WWTP (Tuoriniemi *et al.*, 2012), however seawater samples may need to be pre-treated for salts removal or diluted prior to IPC-MS to prevent the deterioration of the instrument due to the seawater composition (Stolpe and Hassellöv, 2007), and these processes may also alter the environmental sample. Another issue encountered in the presence of high concentrations of salts (conductivity > 5 mS cm^{-2}) is that they can interfere with the analysis of the zeta potential (surface charge) of ENMs (Macken *et al.*, 2012). For this reason computational model simulation also known as *in silico* studies can support the research relating to the environmental fate of ENMs, including AgNPs as discussed in the next section.

1.1.6.3. In silico studies

The *in silico* studies, developed with computational analysis techniques, aim to predict the toxicity and fate of ENMs on the basis of their physicochemical characteristics. In this context, the quantitative structure-activity relationships (QSARs) models are very useful. QSARs are used in toxicology to relate the structure of a molecule or a compound with a specific effect of event (Cronin and Madden, 2010), and the same approach, denominated as QNTR (quantitative nanostructure–toxicity relationship) by some authors (Winkler *et al.*, 2013) has been adopted in the field of nanotoxicology to predict ENMs toxicity. This approach reduces the animal testing, time and experimental costs, although it requires experimental toxicity data to create and to validate the models. The combination of experimental data and *in silico* studies supports the study of the fate and effects of ENMs required for the environmental risk assessment of products containing ENMs (Cohen *et al.*, 2012). Software modelling such as Medusa (Puigdomenech, 2004) has been used by Levard *et al.*, (2012) to compute and depict chemical equilibrium diagrams relating to silver speciation in natural waters in the presence of different concentrations of chloride and thiol groups by applying thermodynamic stability constants and as a function for example of the pH and redox potential. MINEQL + (http://www.mineql.com/) and Visual MINTEQ (http://vminteq.lwr.kth.se/) are other software products developed for chemical equilibrium modelling, similar to Medusa. MINEQL + has been used for example to model the speciation of the silver ions released from poly(vinyl alcohol) (PVA)-coated AgNPs in order to investigate the toxicity exhibited against nitrifying bacteria in

presence of different ligands (PO_4^{3-}, SO_4^{2-}, Cl^-, S^{2-}, EDTA) usually present in wastewater (Choi *et al.*, 2009).

1.1.6.4. Predicted environmental concentrations

To date several studies aimed to predict the environmental concentration (PEC) of ENMs using probabilistic models as PEC information is required to assess their environmental risk (Gottschalk *et al.*, 2013). AgNPs have been included in all the studies developed to date due to their toxicity and the increasing number of products that incorporate AgNPs as a biocidal agent (Blaser *et al.*, 2008, Gottschalk *et al.*, 2009, Sun *et al.*, 2014, Keller *et al.*, 2013). The most recent study (Sun *et al.*, 2014) estimated that the PECs values for AgNPs (upper percentile Q_{85} in the EU) in surface water and sediments are 0.94 ng L^{-1} and 3.3 µg $kg^{-1} \cdot year^{-1}$, respectively. It should be kept in mind that the estimated PEC values per year in sediments (Sun *et al.*, 2014) can have an accumulative value; thus in 10 years' time the PECs value may increase progressively. These PEC values were modelled using the following estimated values: 1) manufacturing volume of products containing ENMs, 2) release during their consumption and disposal, 3) the transport of ENMs between different environmental compartments in European Union (EU). This model considers the assumption that sediments will ultimately serve as a sink for the ENMs discharged in surface waters, and that river flows will discharge into the sea. However, as it is usual in similar studies, the predicted environmental concentration in the marine and coastal areas has not been provided specifically, possibly due to the vast extension involved as discussed by (Whiteley *et al.*, 2013). Therefore the PEC values estimated in superficial waters and river sediments could be applied to estuaries and coastal areas as these are areas of discharge for WWTPs and tributary rivers.

The study of the life cycle and fate of ENMs is challenging and models must deal with uncertainty as often some input data is not available, for example the actual concentration of AgNPs in biocidal products is not always provided (Blaser *et al.*, 2008) and some products do not contain nanosilver, contrary to their manufacturers' claim (Chao *et al.*, 2011). The development of reliable models needs information about the production volumes, emissions and environmental fate of AgNPs. Nowadays it is crucial to address several critical points such as the uncertainty associated to the input values and the current difficulties to validate these models with real environmental data (Hendren *et al.*, 2011,Hendren *et al.*, 2013, Eckelman *et al.*, 2012). Nevertheless information relating to the environmental fate and effects of AgNPs and other metallic

anoparticles such as TiO_2 and ZnO NPs has increased in the recent years compared for instance to carbon base ENMs.

1.2. Aims

The main aim of my PhD study was to investigate the effects of AgNPs on the functioning of estuarine and coastal bacteria that play an important role in biogeochemical processes, such as nutrient recycling and bioremediation (Gao *et al.*, 2011). This question was addressed using a series of microcosm experiments established with sediment and water samples collected from the Firth of Forth estuary as there is an urgent need for studies that model environmentally relevant and realistic conditions (Stone *et al.*, 2014, Epstein *et al.*, 2014). Prior to these experiments with microcosms, exhaustive work was carried out with pure bacterial cultures isolated from the estuary with the aim to examine their susceptibility to AgNPs. The information obtained from the experiments carried out with pure bacterial cultures, and the analysis of the fate of AgNPs in relevant media established the foundations for the design of the microcosm experiments. The output of this research project will support the risk assessment and regulation of products containing silver nanoparticles, increasing the current knowledge about the toxicity of different silver nanoparticles and the bacterial response under more realistic environmental conditions. In addition, the experimental data obtained in the present work relating for example to the persistence of AgNPs in relevant media and bacterial response to AgNPs may contribute to the validation of *in silico* models. In the next subsections the aims are described in greater detail together with a brief introduction to the most relevant techniques used.

1.2.1. Characterization of the physiochemical properties of AgNPs

The toxicity of AgNPs depends on their physicochemical characteristics that are also influenced by the environmental factors, thus the characterization of AgNPs is compulsory in ENMs toxicity testing. In the present project the physicochemical properties and antibacterial activity of three different AgNPs types were examined, two standard reference materials, the NM-300 AgNPs purchased from the JCR standards and AgNPs purchased from Sigma Aldrich. In addition, the antibacterial activity of a biocidal product containing colloidal AgNPs commercialized by Mesosilver® was investigated to compare the antibacterial properties of AgNPs standard reference material with the toxicity of consumer products. The characterization of the physicochemical properties of the three different AgNPs types was needed to explain the antibacterial properties of AgNPs. On the basis of former studies it was hypothesized that the smallest NPs would exhibit the highest toxicity in the absence of coating or capping agent. The two standard reference AgNP were not coated but this information is not available for the AgNPs contained in the commercial product

Mesosilver®. The characterization of the three AgNPs was performed in Milli-Q water using a set of complementary techniques such as DLS, TEM, AFM and UV-vis spectroscopy, ISE-electrode for % ionic silver and Atomic Absorption Spectroscopy (AAS) to measure total silver concentration. In addition the NM-300 AgNPs were characterized in relevant media as bacterial broth media and in Milli-Q water with different concentrations of NaCl, the most abundant salt in the marine environment. It was expected that in media with high concentration of NaCl, the persistence of AgNPs as single nanoparticles would be low with a tendency to agglomerate/aggregate through the time and dissolve progressively.

1.2.2. Study of the antibacterial mechanisms of AgNPs

The toxicity of AgNPs is bacterial species-specific, for this reason the susceptibility of wild marine bacterial strains to AgNPs (Gram negative and Gram positive bacteria identified with molecular techniques based on a partial sequence of the 16S rRNA gene) were investigated. This work was carried out by monitoring bacterial growth under different concentrations of AgNPs and by having ionic silver $AgNO_3$) as a positive control. The inhibitory/bactericidal concentrations for each species of interest obtained from this preliminary work would support the experimental design of the microcosm experiment as for example the dose of AgNPs. Furthermore the data obtained with the work carried out with pure cultures will increase the toxicity data available relating to the inhibitory concentrations of different AgNPs types against wild bacterial strains isolated from the marine environment. This information is currently scarce and essential for the environmental risk assessment of AgNPs as to date the existing studies have been carried mostly with a few model species. In addition, toxicity tests with pure cultures not only provide valuable information relating to inhibitory concentrations, but also the biological responses of bacterial cells under the presence of AgNPs such as EPS production which is an important mechanism of defence against metals in general. On the basis of previous studies, it was hypothesized that the toxicity of AgNPs would be bacterial species-specific.

1.2.3. Microcosm study

The main objective of this research project was to investigate the effects of AgNPs on the functioning of estuarine bacterial communities with a series of microcosm experiments to model realistic environmental conditions. The microcosms were established with sediments and water samples collected from the Firth of Forth estuary (Scotland, UK) and the pollution of sediments with AgNPs was achieved by a single dose of AgNPs in the overlaying water. This is the first study to investigate the

effects of AgNPs on the bacterial functioning in marine estuarine sediments in order to assess whether the ecosystem services provided by these organisms could be disrupted. One of the main research questions was to investigate if AgNPs could affect negatively bacterial communities that inhabit estuarine and coastal areas under environmentally-relevant conditions. As under high concentrations of chloride silver is potentially more mobile than in a fresh water (Luoma et al., 1995) and exhibit higher antibacterial activity (Gupta et al., 1998; Levard et al., 2013), to pose one of the possibly worst case scenarios, the conditions in the microcosms were typically marine (salinity 31‰).The bacterial community structure and function in sediments were assessed using phospholipid fatty acid analysis (PLFAs) and community level physiological profile (CLPP) with the Biolog EcoPlate™, respectively. These two techniques have been used in previous ecotoxicological studies as they comprise the functioning of different bacterial groups within the community and can identify physiological and structural patterns at the community level. The effect of AgNPs on the physiological status of the whole microbial communities that inhabit the water column was analyzed with respirometry. In well aerated estuarine waters the microbial community is expected to be aerobic. Thus if AgNPs affects negatively the metabolic activity of bacteria and also the viability of the bacterial cells, a decrease in the O_2 uptake rate was expected after exposure to AgNPs. Two different culture independent methods were used to quantify bacterial abundance and bacterial production in the water column; these are 1) direct counts with Epifluorescent microscopy and 2) flow cytometry. The bacterial cell viability of heterotrophic groups that inhabit the water and sediments was assessed with bacterial plate counts. A final aim in the present study was to investigate the effects of AgNPs on the abundance of selected functional groups with the culture-independent method with quantitative polymerase chain reaction (qPCR), as the ammonia oxidizing bacteria (AOB) that play a crucial role in the nitrogen cycle. It was also important to examine the effects of the NM-300 on the AOB, as the dispersant of the AgNPs contained ammonium, as described in section 2.1.2.

Chapter 2 Materials and Methods

2. Materials and methods

2.1. Preparation of silver nanoparticle suspensions

The type of silver nanoparticles (AgNPs) used in the exposures ideally should be homogenously dispersed in the stock and exposure media, in order to achieve repeatability of the experiments and minimize variability within the same treatments. Two different types of AgNPs were used in the present research project, AgNPs purchased from Sigma Aldrich and 300-NM AgNPs from LGC Standards. In addition, the cleaning product "Mesosilver Hot tube ^{TM} " for domestic use advertised as an AgNPs containing product, was characterized and its toxicity assessed in order to compare the toxicity of a reference AgNPs type against a consumer product containing AgNPs.

2.1.1. Sigma Aldrich Silver nano; Ø< 100 nm

This type of nanoparticle was purchased from Sigma Aldrich in nanopowder form (product code**:** 576832-5G), an uncoated AgNP type, was used to develop toxicity tests with pure cultures, and has been used previously in similar studies (Bradford *et al.*, 2009, Mühling *et al.*, 2009, Maity *et al.*, 2011) and well characterized in natural waters (Teo and Pumera, 2014).

Procedure

Five 5 or 10 mg of the AgNPs nanopowder were dispersed in 100 ml of sterile Milli-Q depending on the desired final concentration (50 or 100 mg L^{-1}) and sonicated for 30 minutes in an ultrasonic bath with ice. Shaking approximately every 5 minutes enhanced dispersion.

2.1.1.1. Optimization of the homogeneity of the AgNPs dispersion

The influence of AgNPs concentration and the addition of bovine serum albumin (BSA) as a dispersant, on the homogeneity and stability of the suspension were investigated. This was important because, as discussed previously, may improve the repeatability of the experiments and minimize variability within the same treatments. To do this, AgNPs stock suspensions at different concentrations (50 and 100 mg L^{-1}) were prepared. BSA (final concentration 0.1% BSA) was added to one of the dispersions at 50 mg L^{-1} to investigate its efficiency in enhancing the stability of the AgNPs dispersion (Ravindran *et al.*, 2010). Several aliquots were sampled from the suspensions

which were shaken and not stirred between sampling events. Afterwards the concentration of total silver in the aliquots before and after acidification (HNO_3 10%) was measured with Atomic Absorption Spectroscopy.

It was observed that at higher concentrations of AgNPs, and without the addition of BSA, the amount of silver recovered from the stock suspension decreased per aliquot according to the order of extraction (Figure 2.1). There was a statistically significant negative correlation (p-value < 0.001 Pearson correlation coefficient r = - 0.794) between the total silver and the order of extraction in the suspension prepared at 100 mg L^{-1} of AgNPs. The differences in terms of total silver between aliquots indicated that a suspension of 100 mg L^{-1} was less homogenous, or less stable, than AgNPs stock suspensions prepared at a final AgNPs concentration of 50 mg L^{-1}. At 50 mg L^{-1} the order of extraction did not influence the total silver recovered from the stock suspension but the addition of BSA increased the amount significantly (independent t-test p-value < 0.001).

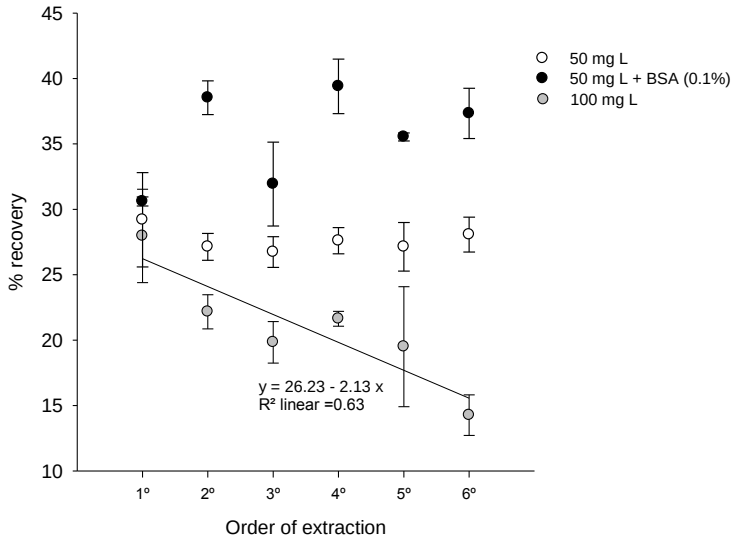

Figure 2. 1Recovery of total Ag (Sigma Aldrich) over the nominal concentration expressed as the mean % ± SD, n=3

2.1.2. NM-300 Silver Ø< 20 nm purchased from LGC Standard

The silver nanoparticles used in the microcosm exposures were the NM-300 Silver Ø < 20 nm purchased from LGC Standards, a reference nanomaterial accredited by the Organisation for Economic Co-operation and Development (OECD) Working Party on Manufactured Nanomaterials (WPMN) international testing programme (Gaiser *et al.*, 2013). NM-300 Silver was provided in an aqueous dispersion with 10% nominal total silver concentration. The stabilizing agents were 4% w/w polyoxyethylene glycerol trioleate and Tween 20 and 7% NH_4NO_3 (Kermanizadeh *et al.*, 2012).

These AgNPs have been well characterized by the JRC at the Institute for Health and Consumer Protection. They reported that the average size of these AgNPs is 17.24 ± 3.17 nm based on Transmission Electron Microscopy (TEM) analysis. AgNPs suspensions were prepared as described in Appendix I following the manufacturer's protocol (Klein *et al.*, 2011) and as previously reported in the literature for other AgNP dosing experiments (Kermanizadeh *et al.*, 2012, Bradford *et al.*, 2009).

The working suspensions used in toxicity tests with pure cultures (section 2.4) were prepared at a final concentration of 200 mg L^{-1} and the effects of broth medium on particle size were investigated with TEM and AFM microscopy.

Working suspensions for dosing the microcosm (section 2.5) were prepared at a concentration of 360 mg L^{-1} in sterile Milli-Q water. Before dosing the water column, the AgNPs dispersion was vigorously shaken for 4 min and ultrasonicated twice for 15 min in an ultrasonic bath containing ice.

The effect of NaCl on the physiochemical characteristics of this type of nanoparticle was investigated as described in the section 2.3.

2.1.3. Hot tub AgNPs Mesosilver^{MT} purchased from Purest Colloids

The Mesosilver product comes in a liquid form and no further preparation was required apart from diluting the product in Milli-Q water prior to characterizing the suspension.

2.2. Characterization of silver nanoparticles

In the present section a set of techniques used to characterize the physicochemical characteristics of AgNPs are described.

2.2.1. Ultraviolet–visible (UV–vis) spectroscopy

UV-vis spectroscopy was used to monitor nanoparticle persistence, aggregation and dissolution. AgNPs exhibit a characteristic absorbance peak around 400 nm, but can range from 390 nm to greater wavelengths as particle size increases. The absorbance along the UV-vis spectrum (300-700nm) depends not only on the particle size, but also particle shape, particle aggregation and AgNPs concentration. For this reason (UV–vis) spectroscopy is an inexpensive method suitable for characterizing and monitoring AgNPs in aqueous media (Chinnapongse *et al.*, 2011, MacCuspie *et al.*, 2011, Zook *et al.*, 2011). Further details relating to the materials and equipment can be found in the Appendix II.

2.2.2. Dynamic light scattering (DLS) and zeta potential

Dynamic Light Scattering (DLS) is one of the techniques used to analyze particle size and surface charge in liquid dispersion (Malvern Instruments, 2014a). DLS measures the scattered light produced when a laser beam (λ = 633nm instrument used in this study) impacts on a small particle or molecule. The photons interact with the electric field of the particles and the energy radiated is called scattered light. The Rayleigh theory that states that the intensity of the scattered light is proportional to the diameter (d) of the particle (Figure 2. 2) can be applied if particles are small, 1/10 of the laser wavelength (< 63.3 nm in this study). The DLS measurements are also based on the velocity of the particles under Brownian motion, smaller particles move faster than bigger particles. This velocity is defined by the translational diffusion coefficient (D) and the hydrodynamic parameter (d_H) can be derived from D based on the Stokes – Einstein equation [Eq 1]:

$$d_H = \frac{k\,T}{3\tau\mu D}$$

Where:

k: Boltzmann's constant
T: absolute temperature
μ= viscosity

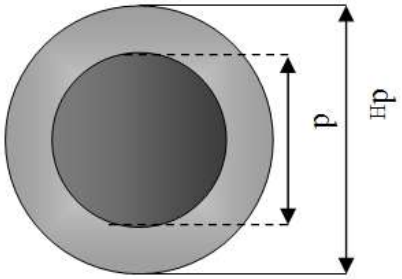

Figure 2. 2 Graphical representation of a particle with a core diameter "d" and its associated "d_H".

The DLS informs about the average particle size named as the Z-Average parameter that is estimated based on the d_H of a sphere of the same average diffusion coefficient. As the size reported by DLS refers to the hydrodynamic diameter of the particle, it is expected that size measurements obtained with this technique will be higher than size measurements carried out with microscopy techniques that measure the core diameter of the particle. The Z-Average can be very sensitive to small changes in the sample dispersion such as the particle agglomeration. If the d_H increases > (λ/10) the Rayleigh theory cannot be applied. When particles are greater than 63.3 nm the Mie theory is applied to estimate the diameter of the particles, and in presence of big agglomerates > 633 nm (λ) then more complex functions need to be applied to relate the light intensity to the d_H. In addition agglomerated or aggregated particles with a large d_H are analyzed as a single particle. The analysis of these big "particles" may interfere with the analysis of smaller particles that can be overlooked.

DLS might not be the most suitable technique to measure the size of AgNPs as metallic nanoparticles tend to settle down. The sedimentation process leads to unstable sample suspensions, and any other motion of particles different to the Brownian (e.g. sedimentation) will produce unreliable measurements (Malvern Instruments). In addition the composition of liquid medium or solvent used to disperse the nanoparticles can interfere with the surface charge of the nanoparticles as previously explained in section 1.1.5. To support the assessment of the results obtained with the DLS measurements and evaluate the adequacy of the data obtained, a quality report is generated with every DLS measurement. This report includes the parameters Polidispersity Index (PdI) and the Y-intercept (see "result quality" Figure 2. 3) estimated from the correlation curve also known as the correlation function.

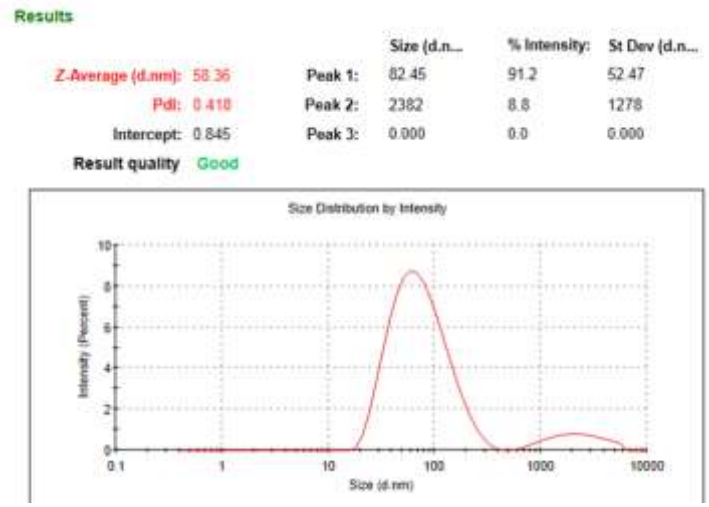

Figure 2. 3 Representation of the Z-Average results report

The Polidispersity Index (PdI) is a dimensionless number related to the size distribution of the samples (Malvern Instruments, 2014a). If PdI > 0.7 then the sample exhibits a very broad distribution and DLS is not the technique recommended for the analysis of particle size. An ideal signal produce a Y-intercept value of 1 (value of the correlation curve when x = 0), but values greater than 0.6 are also regarded as good, and the best ones are > 0.9 (Figure 2. 4). The cumulants for error should be < 0.005 (Malvern, personal communication).

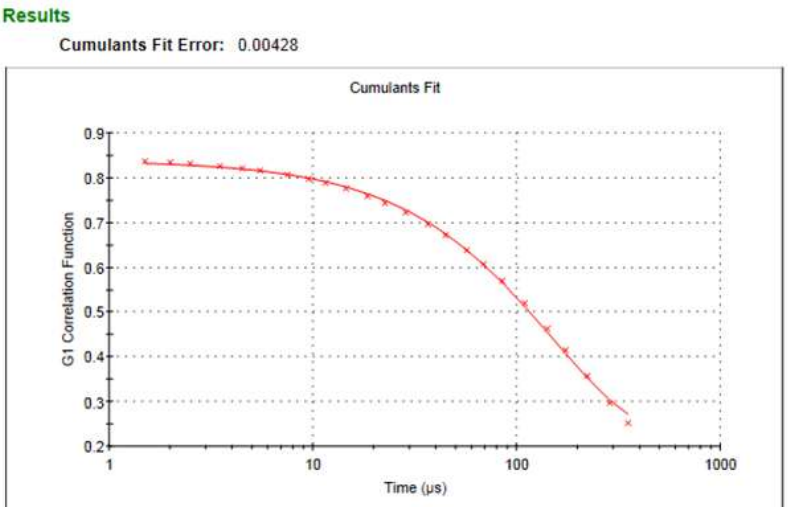

Figure 2. 4 Cumulants fit plot

Zeta potential analysis was used to investigate particle surface charge. The zeta potential is the potential in the slipping plane of the particle and depends on the ionization process taken place in the surface of the particle and the adsorption of other ionic species to this surface, which also depends on the surrounding solvent. As a result of this the charge in this plane may not be the same as the particle surface charge (Figure 2.5). The principle to measure the zeta potential is based on measuring the electrophoretic mobility of the particles (see Eq2) when an electric field is applied through the dispersion. The particles with surface charge in the slipping plane will move to the electrode of opposite charge at a velocity proportional to the magnitude of the zeta potential.

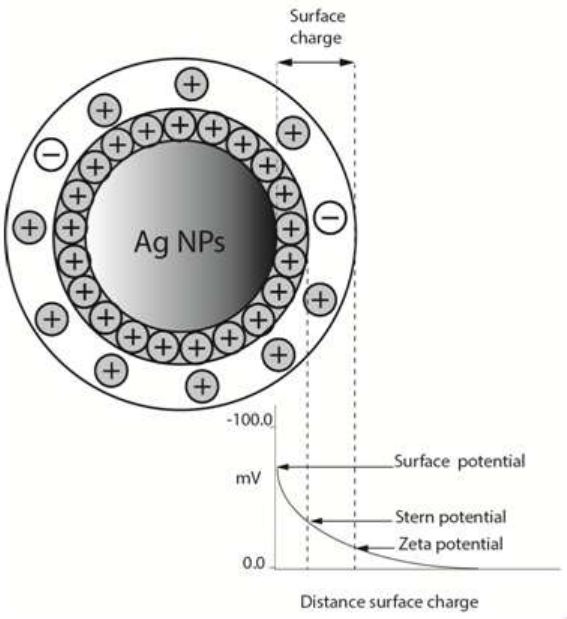

The zeta potential can be obtained from the Henry equation [Eq 2]:

$$Ue = \frac{2\varepsilon\, Z\, F\,(ka)}{3\,\eta}$$

Where
Ue: Electrophoretic mobility
ε : Dielectric constant
Z: zeta potential
η: viscosity
$F\,(ka)$:Henry's function

Figure 2. 5 Particle surface charge of AgNPs negatively charged. Diagram modified from Malvern Instruments. http://www.malvern.com/labeng/technology/zeta_potential/zeta_potential_lde.htm

The zeta potential will influence the interaction of the nanoparticles in a suspension, the repulsion and attraction forces between them as a result the stability of the suspensions. The zeta potential can take positive or negative values, and values in the order of < -30mV or $> +30$ mV are regarded as high values leading to very stable nanoparticle suspensions (Malvern, 2004).

Both parameters, particle size and surface charge, were measured in folded capillary cells with a Malvern instrument, ZS series. Similarly to UV-vis spectroscopy analysis, the size and zeta potential were measured immediately after filling the capillary cell with AgNPs suspended in aqueous media at pH 7.5.

Sample preparation

The samples were immediately analyzed after preparation in capillary cells (Malvern ref. DTS1060). The capillary cells were rinsed first with ethanol and then with Milli-Q water. First a small volume of sample should be injected in the cell to soak the walls of the cell. Then the cell is emptied and filled with approximately 0.75 ml of sample and stoppers inserted.

Measurement settings

Prior to the analysis of a sample with DLS it is required to specify the following parameters: the dispersant refractive index (RI) and viscosity, the RI of the material (AgNPs in this study) and its absorption, the temperature of analysis (20ºC in this study) , type of cuvette and equilibration time of the sample (60-120 seconds). The advised number of measurements per sample is 5 (Facility for Environmental Nanoscience Analysis and Characterisation (FENAC), personal communication). To measure the Z-Average the duration is set up as "automatic". The analysis model advised by Malvern Instruments was "General Purpose" as it is regarded as an appropriate model for the majority of the dispersions. When measuring the zeta potential, if the conductivity of the sample is high (> 5 mS cm^{-2}) the number of measurements should be also 5 but the number of runs per measurement should not exceed 20 to avoid overheating and consequently damaging the electrodes of the cuvette. The analysis model recommended by Malvern is "Auto mode", as it allows the software to determine the most suitable analysis to perform after measuring the conductivity of the sample. Similarly to the Z-Average report, in the "results quality" field the quality of the analysis performed is informed (Figure 2.6).

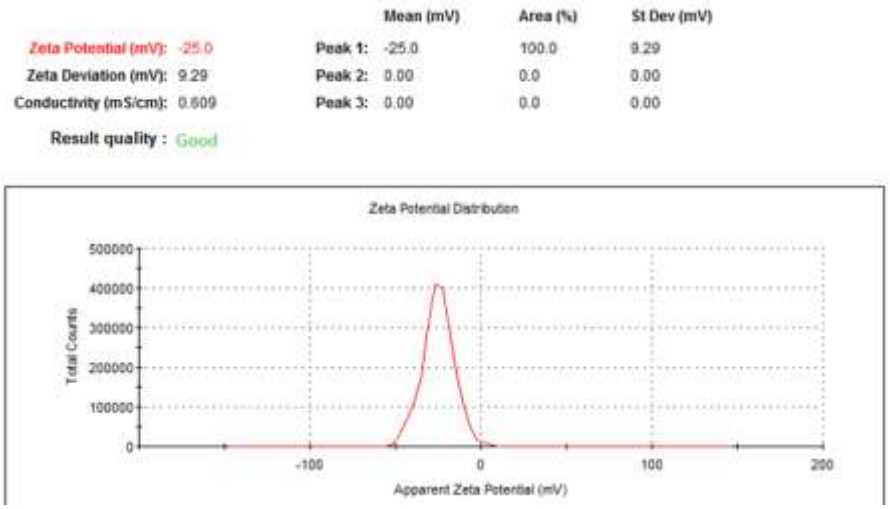

Figure 2.6 Representation of the Zeta Potential report

2.2.3. Analysis of ionic silver in AgNPs suspensions prepared in Milli-Q water

2.2.3.1. Ion Selective Electrode

The ionic silver content of fresh AgNPs stock suspensions was measured in milli-Q water with an Ion selective electrode (ISE, Nico 2000 Ltd) following the manufacturer guidelines (http://www.nico2000.net/analytical/silver.htm). For further details see Appendix III.

2.2.3.2. Ultracentrifugation

The ultracentrifugation technique can be used to separate particles according to different sizes by varying the time and rotation speed. The procedure relating to this technique (sample preparation and how to use an ultracentrifuge) was demonstrated at FENAC. At FENAC this technique is normally used to concentrate NPs after synthesis. The demonstration was carried out with the NM-300 and Mesosilver ^{TM} AgNPs.

AgNPs silver suspensions were prepared at a concentration of 100 ppm (in ultracentrifugation tubes, Beckman/ Ultra clear TM tubes, 9/16 x 3 ¾ inches Ref. 344060, vol. in 12. 8 ml) in milli-Q water. The tubes were closed with paraffin and placed gently in the tube case of the rotor (Figure 2. 7) followed by ultracentrifugation at 30,000 rpm (162994 *g*) at 10 °C, for 1 hr with a Beckman L7 Ultracentrifuge.

Figure 2. 7 Ultracentrifugation tubes used at

After the ultracentrifugation process the supernatant of the NM-300 suspension was yellowish (Figure 2. 8) and the UV-vis spectroscopy analysis showed a peak at the 400 nm (Figure 2. 9) that confirmed the presence of AgNPs.

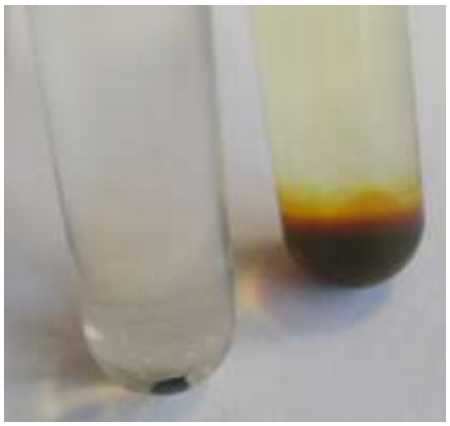

Figure 2. 9 AgNPs in the tube after ultracentrifugation. Mesosilver (left) and NM-300(right).

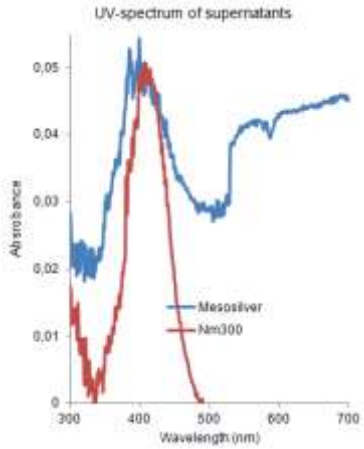

Figure 2. 8 Absorbance of the AgNPs in the UV-vis spectrum.

The equation (CPS Instruments Europe) used to estimate the minimum particle size centrifuged down is depicted below [Eq 3]:

$$t=[18\eta \ln(x_2/x_1)]/[d^2(\rho-\rho_0)\omega_2]$$

t = time in seconds
η = viscosity of suspension, poise
x_2 = distance from centre of rotor to bottom of tube, (cm)
x_1 = distance from centre of rotor to top of fluid (cm)
d = diameter of particles (cm)
ρ = density of particles (gcm^{-3})
ρ_0 = density of suspending medium (gcm^{-3})
ω = angular rotation speed (radians per second)

Based on this formula, particles greater than 7.85 nm were spun down. To bring down particles < 1 nm higher speed or/and longer centrifugation period of time should be applied. In addition the DLS analysis revealed the presence of big particles, and one of the hypotheses is that AgNPs could have been aggregated if the surfactants were spun down with big NPs (Dr. Christine Elgy, FENAC, personal communication).

2.2.4. Transmission electron microscopy (TEM) for particle size

TEM images of metallic nanoparticles exhibit a good contrast facilitating the analysis of the particle size in 2D. TEM was also used in the present study to measure the projected diameter of the approximately spherical AgNPs. Sample preparation and examination was carried out at FENAC.

The samples were prepared by placing a 10 µl aliquot of AgNPs suspension on to copper grids (mesh 400 holey carbon film, Agar scientific), allowed to air dry for one hour, washed twice in Millipore water for 30 seconds and air dried for 2-24 hr. Samples were examined by members of the staff at FENAC with the instrument Jeol 1200 TEM. TEM images were processed with ImageJ. This is open source image analysis software that enables the measurement of various particle parameters, including diameter.

2.2.5. Atomic force microscopy (AFM) for particle size

Atomic force microscopy is a type of scanning probe microscopy, and consists essentially of a sharp metallic tip mounted on a cantilever that scans a surface. The interaction forces created between the tip and the surface cause the cantilever deflection. The changes in the cantilever deflection are detected by a laser beam (aligned with the tip). The laser beam reflects off in the backside of the cantilever and is collected afterwards by the Position Sensitive Photo Detector (PSPD) (PSIA, 2002). The laser signal is then processed to translate the changes in the cantilever deflection into differences in the z axe (height). As a result, when using AFM to analyze particle size, the actual dimension measured is the height of the particles, which corresponds to the diameter of the AgNPs, providing these are spherical. This technique has been successfully applied to monitor the growth of metallic nanoparticles such as gold NPs with the ability to detect small clusters down to 1 nm size (Georgiev *et al.*, 2013). AFM can be used in different modes, depending on the type of cantilever used, which can make this technique less invasive than the electron beam used in TEM analysis.

Contact mode AFM (CM-AFM)

The tip is in contact with the sample thus high resolution images are obtained. This mode is recommended to examine hard surfaces, as soft samples (e.g. biological samples) could be damaged (Paniagua *et al.*, 2014). When working in CM-AFM the tip can also be damaged more easily than when working in other AFM modes (Dr. Christine Elgy, FENAC, personal communication).

Amplitude-modulated AFM (AM-AFM) or tapping mode

The cantilever oscillates across the surface with an amplitude between 10-20 nm preventing the tip from getting stuck in the fluid layer when tapping the sample at a given frequency, and as a result there is a better preservation of the sample and the tip (Zhong *et al.*, 1993). It is a useful technique to detect variations in the composition of a surface as it can detect differences in adhesion and viscoelasticity (García and Pérez, 2002).

Frequency modulation atomic force microscopy (FM-AFM) also known as Non-contact mode AFM

The cantilever oscillates with amplitude smaller than 10 nm (Digital Instruments, 2000). The tip and samples damage is minimized. It allows atomic resolution and accurate tip-sample interaction, very relevant for materials characterization. In the present study the AgNPs analysis was carried out with non-contact cantilevers in non-contact mode at ambient conditions.

Procedure

i. Sample preparation

AgNPs samples were prepared on fresh cleaved mica sheet (Agar scientific). 40 µl aliquots of NPs suspension were added to the mica (Figure 2. 11) left to air dry for one hour, washed twice in Milli-Q water for 30 seconds and air dried for 2-24 hr. Finally the mica was placed on a magnetic steel mounting (Figure 2. 10) to ensure a flat surface under the microscope. AFM samples were examined with a XE-100 Microscope and images obtained were analyzed with the XEI imaging software.

Figure 2. 11 AgNPs suspension on 0.25 cm^2 of mica. .

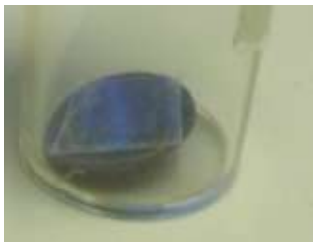

Figure 2. 10 Mica sheets are stick to a steel mounting dish and examined under the XE-100 SPM Microscope.

ii. Image analysis

Images were captured and analyzed with XEI Imaging software (PSIA Corporation). The size of the AgNPs was analyzed as depicted in the Figure 2.12 and a 3D view in Figure 2. 13.

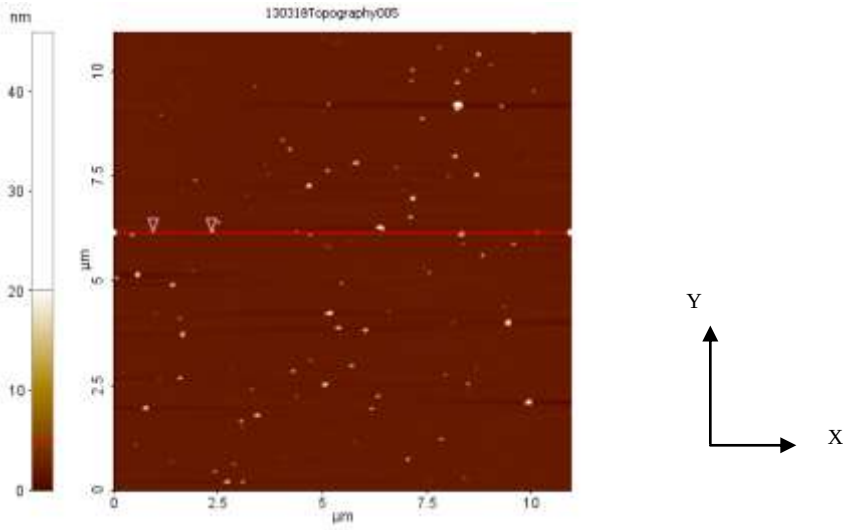

Figure 2.12 AFM topography data obtained with XEI software depicting the presence of nanoparticles on x-y axes.

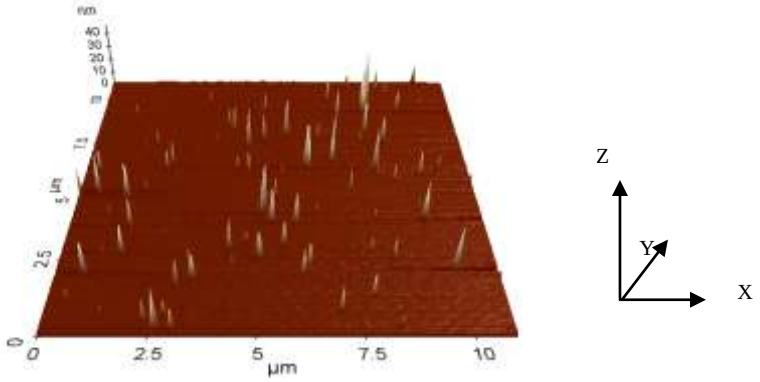

Figure 2. 13 3D surface plot of a scanned area with AgNPs. Z axe the size of the nanoparticle (nm).

The size of the particles is calculated by positioning the pair or cursors, one on the flat line and the second at the highest value of the particle Figure 2. 14. The difference in height corresponds to the height/size of the particle.

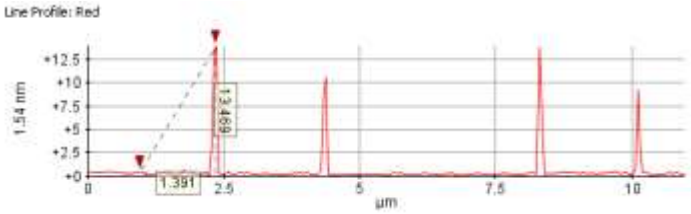

Figure 2. 14 The profile of the line shows the presence of a few particles on a line.

2.2.6. Raman microspectroscopy

Raman microspectroscopy is a technique accepted for nanomaterial characterization (Lin *et al.*, 2014, Al-Shaeri *et al.*, 2013) and in the present study was applied to investigate the fate of AgNPs in sediments during microcosm exposures. Raman microspectroscopy analyzes the interaction of a laser with the molecular vibrations of the element that is being examined. The energy of the laser photons shifts or Raman shift is reported as the relative intensity at a given wavenumber cm^{-1}. The different peaks obtained in the Raman spectra are obtained based on the relative intensity of the Raman shifts. The instrument used was an "inVia Raman" spectrometer with an integrated Renishaw microscope. Different laser wavelengths and output power can be applied. In the present study samples were examined under 785-nm laser operating at 25mW output power for 1 second. Shorter wavelengths could heat the sample and change its properties.

Procedure

For the sample preparation a thin layer of the sample was placed on a quartz slide and cover by another quartz slide. The instrument was calibrated with a piece of silicon. The sample was placed under the microscope and the particle or region of interest was examined. Using a × 50 objective the transmitted light optical images of the sample were captured with a camera (Leica) and the Raman spectra of the same region (Figure 2. 15). The bands obtained were related to a discrete point.

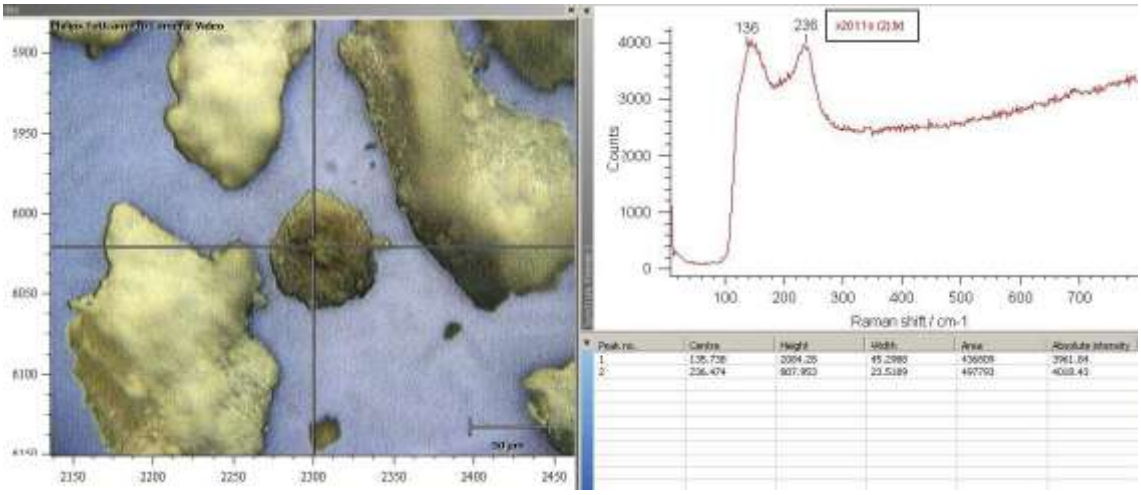

Figure 2. 15 Sample of pure AgCl salt examined under Raman spectroscopy (left) and Ram spectra obtained (right).

Different silver compounds ($AgNO_3$ (Figure 2.16 and Figure 2. 17) and AgCl Figure 2.18 and Figure 2. 19) were analyzed and the peaks obtained in the Raman

spectra were identified by the associated molecular bonds according to the information available in the literature (Downs *et al.*, Wang *et al.*, 1999, Martina *et al.*, 2012).

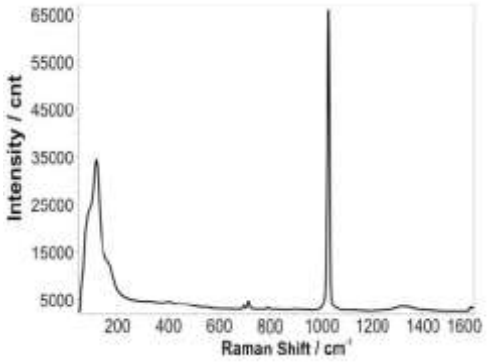

Figure 2.16 Raman spectrum of standard $AgNO_3$ (37 mW, 50x low working distance (lwd), 1 s) by Martina et *al.*, (2012)

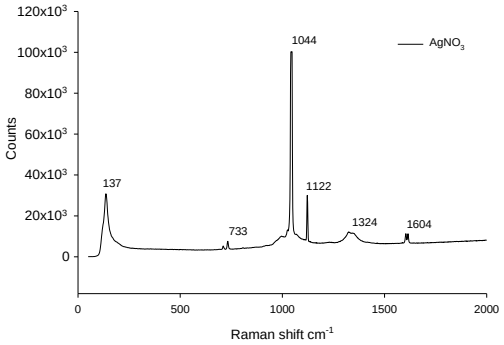

Figure 2. 17 Raman spectrum of standard $AgNO_3$ (25 mW, 50x, 1 s) measured at Heriot-Watt.

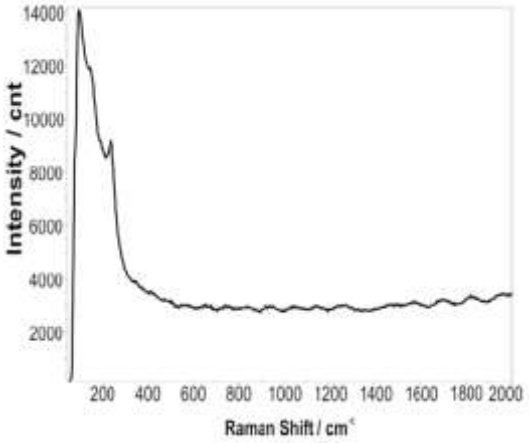

Figure 2. 19 Raman spectrum of standard AgCl (37 mW, 50x lwd, 1 s) by Martina et *al.*, (2012)

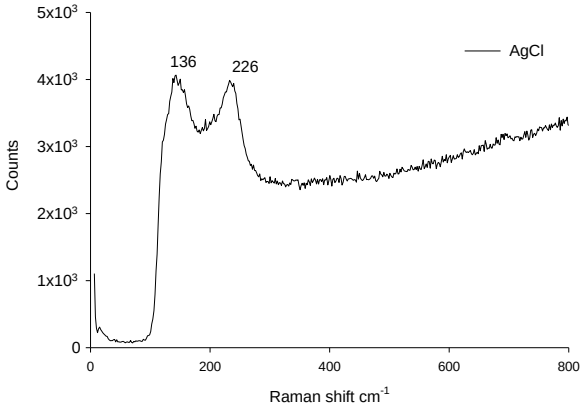

Figure 2. 18 Raman spectrum of standard AgCl (25 mW, 50x , 1 s) measured at Heriot-Watt.

2.2.7. Analysis of total silver with Atomic Absorption Spectroscopy (AAS)

The concentration of total silver in the AgNPs stock suspensions, bacterial culture, water and sediments was measured with Atomic Absorption Spectroscopy (AAS) using a Perkin Elmer AAnalyst TM 200 spectrometer. The lower detection limit of the AAS was 30 ppb. Bacterial culture media was acidified with HNO_3, 5% final concentration. Water and sediment samples collected from the microcosms were digested according to the USEPA methods 3005A and 3050B respectively (Appendix VII), with the following modifications:

Method 3005A (water)

Water samples were not filtered as AgNPs and other silver aggregates could be trapped in the filter and as a result the concentration of silver can be underestimated.

Method 3050B (sediments)

The concentration of concentrated HCl was 2.5 ml instead than 10ml (5% final concentration in 50 ml final volume of sample) due to HCl increases the Cl^- concentration that can complex the Ag^+ and precipitate as AgCl affecting the homogeneity of the digested sample. In addition HCl at concentrations between 15-20% v/v of HCl is not recommended as can damage the AAS instrument. The effect of HCl on the digestion of the samples was investigated by comparing the recovery of silver with and without the addition of HCl in triplicates of the soil reference material. The adequacy of the digestion method was confirmed with a soil reference material (Sigma Aldrich Metals in Soil, number SQC- 001). The efficiency of this method to digest sediments was accepted as the average recovery of silver in the soil reference material was 97% (the mean value of the soil reference material was 39.3 ±0.942 mg Ag/ kg soil) and was always within the acceptance limits (16.6 – 62 mg Ag/ kg soil). Adding HCl during the digestion increased the recovery of silver to 99.8 ± 2.3%, compared to 94.1±1.9% without HCl, however this was not statistically significant different (One Way ANOVA p-value = 0.071).

2.3. Effects of chloride on the physicochemical properties of the NM-300 AgNPs

The influence of chloride ions on the physicochemical properties of AgNPs was determined by dispersing AgNPs in different concentrations of NaCl. Particle agglomeration and surface charge were measured by ultraviolet–visible (UV–vis) spectroscopy (Shimadzu 1650 UV-VIS Spectrophotometer), dynamic light scattering (DLS) and zeta-potential (Zetasizer Nano-ZS, Malvern Instruments). Briefly, AgNPs

(final concentration: 1.5 mg L^{-1}) were exposed in the dark to different concentrations of NaCl in triplicates (0, 10, 20 and 30 g L^{-1}), 0.1 M HEPES, pH 7.5, at a temperature of 20ºC, and gently continuously shaken at 125 rpm on a xyz shaker. The absorbance in the UV-spectrum, particle size and zeta-potential were monitored at three different time points, 0, 24 and 48 hr. Details of the reagents are provided in the Appendix V.

2.3.1. Silver speciation

The silver speciation in media containing 10 and 20 g L^{-1} NaCl (pH 7.5, temperature 20ºC) and in seawater (31 ‰, pH 7.9, temperature 10 ºC) was calculated with Visual MINTEQ (version 3.1), a free software available on line (http://vminteq.lwr.kth.se/). The input parameters applied are depicted in Table 2. **1**.

Table 2. 1 Input data applied to analyze silver speciation

Sample	Na^+ (mMol)	Cl^- (mMol)	Ag^+ (mMol)	Temperature (ºC)	pH	Eh (mV)
NaCl (10 g/L)	171.12	171.12	0.013915	20	7.5	
NaCl (20 g/L)	342.23	342.23	0.013915	20	7.5	
Seawater (31 ‰)	415.45	483.46	0.009276	10	7.9	230

2.4. Toxicity tests with pure bacterial cultures

The aim was to develop toxicity tests with different bacterial species in order to study the susceptibility of different wild bacterial strains to the NM-300 AgNPs to sustain the design of the microcosm experiments (e.g. initial AgNPs dose) and also to support the analysis of the results obtained. The NM-300 AgNPs is a reference nanomaterial used by the OECD, therefore to work with the NM-300 was more relevant for comparison purposes with other studies. A second objective of the work with pure cultures was to investigate the susceptibility of different bacterial species to different AgNPs types, with the aim of analyzing the nanoparticle toxicity according to their physicochemical properties. This information could also support a better insight into the antibacterial mechanisms of AgNPs. To do this several bacterial strains were isolated from water and sediments samples collected from the Firth of Forth estuary. All the work that involved handling bacteria was carried out under a laminar flow to ensure sterile conditions and avoid contamination that could produce misleading results.

2.4.1. Isolation and identification of estuarine bacteria

2.4.1.1. Bacteria isolation

The species present in superficial sediments are the ones that could be the most exposed to AgNPs as the particles suspended in the water column tend to accumulate in the top layer of the sediments (Bradford *et al.*, 2009) and here the redox potential is normally higher and could increase the bioavailable forms of this metal (Christopher and Raina, 2003). For this reason surface water and intertidal sediment samples (depth < 1 cm) were collected in sterile plastic tubes and immediately inoculated in liquid and solid broth once in the laboratory. Two different types of media were used: (1) low nutrient medium consisting of ZM/10 agar (Green *et al.*, 2004) (75% natural sea water, 25% distilled water, 0.05% Bacteriological Peptone(Oxoid), 0.01% yeast extract(Oxoid), 1.4% Bacteriological Agar (Oxoid)) and (2) marine agar (MA) (75% natural sea water, 25% distilled water, 0.5% Tryptone, 0.25% yeast extract, 1.4% Bacteriological Agar). The sediment grains were plated directly on to the surface of the agar with the aim of enhancing the growth of bacteria firmly attached to the sediment grains. Plates were incubated at room temperature (20ºC) and growth was monitored during the following days in order to identify fast and slow growers. The bacterial colonies of interest were isolated, grown in liquid marine broth medium for 2-5 days depending on the strain, and preserved in 25% glycerol at -70°C for further work.

2.4.1.2. Phenotypic bacterial identification

The phenotypic characterization of the bacterial isolates started with a direct examination of the colony morphology, colour and texture. The Gram staining technique was carried out to classify bacteria as Gram positive or Gram negative. The β-agarase, catalase and oxidase enzyme production and cell motility were analyzed as described bellow:

β-agarase enzyme production

Pure colonies were streaked on plates containing low nutrient agar medium (ZM/10) and incubated at room temperature. Positive result for β- agarase enzyme production was obtained if the agar was degraded.

Catalase test

A bacterial colony was scraped from an agar plate with a plastic sterile loop, and resuspended in a drop of H_2O_2 (3%) on a slide. The formation of bubbles or effervescence as a confirmation of the catalase production was examined immediately (Gerhardt P, 1994).

Oxidase test

An ashless filter paper (Whatman no. 40, quantitative grade) was place on a petri dish and wet it with a few drops of 1% solution of tetramethyl-p-phenyledediamine. A colony was picked up with a plastic- sterile loop and rubbed on to the wet filter paper. A positive catalase test is obtained if the filter paper turns blue-purple.

Motility test

Marine agar (MA) was prepared as described in section 2.4.1.1 but at a lower concentration of agar (0.4%). A small amount of bacterial biomass was taken from a colony with a tooth-pick and placed very gently on to the surface of the agar. Plates were incubated at room temperature and examined during the next days in order to detect spreading zones around the initial inoculating point.

2.4.1.3. Molecular identification based on a partial sequence of the 16S RNA gene

The bacterial isolates of interest were identified at species level based on a partial sequence of the 16S RNA gene. The phenotypic information obtained supported the selection of the primers to use in the molecular work. Details of the specific apparatus and reagents used are provided in Appendix VI.

i. Extraction of DNA from bacterial strains

PCR was carried out. A pin-tip sized amount of bacterial growth from colonies of pure cultures was transferred to 20 ml sterile milli-Q water using a sterile 200 µl pipette tip prior to PCR.

ii. Universal bacterial 16S rRNA primers

Two different sets of primers (27F/685R, 341F/A976R) were used due to differences in the specificity of the primers for each genus:

U341F (Forward) 5' – CCTACGGGAGGCAGCAG-3' (Muyzer *et al.*, 1998)

A976R (Reverse) 5'-CCGGCGTTGAMTCCAATT-3' (Wang and Qian, 2009) cites the work of (Baker *et al.*, 2003)

27F (Forward) 5'-AGAGTTTGATCCTGGCTCAG-3' (DeSantis *et al.*, 2007)

E685R (Reverse) 5'-TCTACGCATTTCACCGCTAC-3' (Wang and Qian, 2009)

iii. PCR reaction mixture

The following reagents were added at a final volume of 25 µl to 1 illustra^{TM} PuRe Taq Ready-to-go TM PCR bed (GE Healthcare) in a 0.2 ml thin walled PCR tube in the following order: 22 µl sterile HPLC-grade water (Fisher), 1 µl 25 pM forward primer, 1 µl 25 pM reverse primer, 1 DNA template from 20 µl suspension of cells.

iv. PCR settings

PCR was carried out using a thermal cycler (Techne) and the Touchdown program was chosen and the following settings were established: 5 min 94 °C, 25 x (1 min 94 °C (DNA denaturation), 1 min 57°C (primer annealing), 3 min 72 °C (primer extension)), 7 min 72 °C

Touchdown method increases the probability of amplifying the correct DNA fragments. At higher annealing temperature the specificity between primers and targeted sequence of DNA increases. At lower temperatures the primers may be less specific, more readily stick to other fragments other than the sequence of interest, producing a

poor quality PCR product. Other factors that may affect the final results are, for example 1) concentration of cations as Mg^{2+} and Mn^{2+} and 2) polymerase mutations.

v. Agarose gel preparation

Procedure: Place the mixture (TBE + agarose) in the microwave for a 1 minute approximately and stop it when bubbling. Cool down the sample until "hand temperature". Then add 2 µl Ethidium Bromide (EthBr) (EthBr binds the DNA and it is the agent that makes DNA fluorescent). Mix well. Poor the agarose in the gel box and wait for 30 min.

vi. Set up of the PCR samples

The following reagents were added to an Eppendorf tube and centrifuged briefly in "quick run" mode 5µl PCR sample, 2 µl of water, 1 µl of loading buffer. A marker was prepared as a reference for the PCR sample as follows: 2 µl of commercial marker, 5 µl of water, 1 µl of loading buffer. The gel was run for 30 minutes.

vii. Depuration of PCR product

The following reagents were added to an Eppendorf tube: 30 µl deionised distilled water, 20 µl PCR sample, 200 µl PureLink buffer. Then the tube was placed in a microcentrifuge for 1 min at 10,000 *g* (in this way the DNA was allowed to move into the spin column). Then 650 µl of ethanol were added (wash buffer), centrifuged for 1 min at 10,000 *g* and again 13,000 *g* for 3 min. The supernatant was discarded and 50 µl of Elution buffer added, after which the samples were incubated for 1 min at room temperature. The samples were the centrifuged for 2 min at maximum speed (13,000 *g*) and the DNA sample collected in the Eppendorf tube.

viii. Preparing the sample for sequencing

To a 500 µl Eppendorf tube 4 µl of molecular grade water and 1.5 µl of the PCR sample were added. Samples ready for sequencing were stored at -20°C until delivery to the GenePool (University of Edinburgh) for sequencing.

ix. DNA sequence analysis

DNA sequences were edited with the BioEdit Sequence Alignment Editor (v7.0.9) followed by the sequence analysis with Basic Local Alignment Search Tool (BLAST). This tool searches for similar sequences in databases available at the "National Center for Biotechnology (NCBI) for 16S ribosomal RNA sequences (Bacteria and Archaea)" and returns the name and details of the most similar bacterial species found.

2.4.2. Determination of the relationship of bacterial cell number to absorbance - building the bacterial growth curve

The objective of this experiment was to establish a relationship between the number of colony forming units (CFU) and absorbance or optical density (OD), for each bacterial strain of interest. It is accepted that each CFU corresponded to one viable cell in the culture. In this way, when carrying out toxicity tests it is sufficient to measure the OD of the culturing media in order to estimate the number of viable bacterial cells per unit volume. As dead cells contribute to OD, the exponential phase or log phase (when cell doubling occurs at a constant rate) is the most adequate phase to compare the growth curves under different AgNPs concentrations or different AgNPs types. The OD of the cell culture was measured at 600 nm as at this wavelength the turbidity is related to the number of cells and there were no interferences with bacterial pigments or AgNPs plasmon resonance. The absorbance of the cell culture was measured in the UV-vis spectrum (300-700nm) to confirm that no interferences occurred at 600 nm owing to pigments or AgNPs.

For the exposures to AgNPs it was decided to use liquid low nutrient medium (ZM/10) in order to minimize the concentration of compounds such as thiol groups (-SH) that exhibit high affinity by ionic silver, reducing their toxicity and increasing the concentration of AgNPs needed to inhibit bacterial growth.

Bacterial cultures were prepared in triplicates and incubated at 25ºC at 125 rpm in 50 ml flasks. The OD_{600} was measured with a Shimadzu 1650 UV-VIS spectrometer by collecting 1 ml aliquots collected from each experimental flask at different time intervals. Immediately after measuring the OD the corresponding CFU were measured by plating 40 µl of a series of 10-fold dilutions of the bacterial cultures on Tryptone agar plates using an alcohol-sterilised glass spreader. The CFU were counted after 2-5 days of incubation period depending on the species. The OD_{600} and CFU were monitored at different time intervals for 12 – 50 hr depending on the species, until OD_{600} stabilized.

2.4.3. Monitoring bacterial growth by means of dry weight and total nitrogen

The growth of some species such as *Streptomyces sp.* could not be monitored by measuring the OD as this species formed clumps as it grew thereby interfering with the homogeneity of the turbidity of the cell culture. Ultrasonication in a water bath was carried out to break down the clumps but it did not work efficiently and probe sonication was not available. For this reason other methods to quantify the growth of

this species were explored such us quantification of (1) total biomass by measuring the dry weight of the cell culture and (2) protein production by measuring total nitrogen using the Kjeldahl method.

2.4.3.1. Total biomass

1 ml aliquots of cell culture were collected in 1.5 ml microcentrifuge tube after 48 hr of exposure, centrifuged and the supernatant discarded. The pellet of bacterial biomass was air-dried at room temperature. The biomass or dry weight per ml was estimated as the difference between the tube with the dry biomass (*w2*) and the empty tube (*w1*):

$$\boldsymbol{dry\ weight\ (mg/ml) = (w2 - w1)} \qquad \text{[Eq 4]}$$

2.4.3.2. Kjeldahl method

The amount of nitrogen in cells is regarded as a suitable parameter to estimate bacterial growth. The Kjeldhal method has been widely applied to measure the total nitrogen in biological material and it has also been used previously to quantify N as an indicator of bacterial growth (Youmans, 1946). It is based on the oxidation of the organic matter to $(NH4)_2SO_4$ through the digestion of the sample with H_2SO_4.

The NH_4 ions are release in presence of NaOH during the distillation process and the NH_4 is complexed by Boric acid and quantified by titration with HCl.

The following procedure was followed:

i. Sample preparation

10 ml of cell culture were pipetted into a clean dry Kjeldhal tube. The next steps were carried out in the fume hood due to the risks associated to the different chemicals used. The following reagents were added in each tube: 2 silicon antifoam tablets (containing 0.97 g Sodium Sulphate and 0.03 g Silicon Antifoam) , one tablet of selenium catalyst tablet (containing 5 mg of Selenium) and 12 ml of concentrated H_2SO_4 with a dedicated dispenser for this task.

ii. Digestion

Samples were placed in the digestion block on the extraction thimble lid and the water extraction was switched on. Samples were heated gradually up to 440ºC and kept at this temperature for 15 min. Then the heating was set down to 20ºC and the samples were left to cool down. The colour of the sample turned blue/green during this process.

iii. Distillation

The distillation was performed in a distillation unit (Foss Kjeltec TM 8100) that injects distilled water first to reduce the violence of the reaction when NaOH is added to

release the NH_4. The NH_4 steam was distilled and transferred to a flask containing 25 ml of Boric acid solution (4%) with indicator (Boric acid solution + indicator, BDH 4.5 product code 19231 6H, VWR-Prolabo).

iv. Titration

The sample was titrated after distillation against 0.1 N Hydrochloric Acid (AVS Titrinorm, VWR Prolabo) and back titration with a Metrohm Herisau Multi-Burette E485 20 ml. The end point is grey/discolouration of the blue indicator.

Total Nitrogen calculation

$$\boldsymbol{mg\ N\ mg/10\ ml} = \frac{\boldsymbol{Titre\ (mls) \times M \times 14.007 \times 10}}{\boldsymbol{Volume\ of\ sample\ in\ mls}} \quad \text{[Eq5]}$$

2.4.4. Exposure of bacterial pure cultures to AgNPs

The exposure of pure bacterial cultures to AgNPs was carried out in ZM/10 liquid medium under the same incubation conditions used to determine the bacterial growth curve, 25ºC at 125 rpm (section 2.4.2). Depending on the particle type, the exposures were carried out in different containers, small volume tubes (3 ml), 50 ml flasks and 250 ml bottles/flasks as explained in the following subsections. The experimental containers were inoculated with different volumes of the AgNPs suspensions in triplicates, in order to get different concentrations of AgNPs. Immediately afterwards, the experimental flasks containing broth medium and AgNPs were inoculated with the bacterial culture (a single bacterial species) in stationary phase at a concentration 1:100 (cell culture/broth). ZM/10 liquid broth with different concentrations of AgNPs (without bacteria), were used as blanks to correct the OD_{600}.

The end point of the exposures was established when the bacterial growth in the control treatments (without AgNPs) reached the stationary phase, when the OD stabilized. The end point for the *Streptomyces sp.* was established at 48 hr as it was observed "by eye" that cell density did not increase thereafter.

To investigate the immediate bactericidal effects of AgNPs, aliquots of the cell cultures were plated at the beginning of the exposure, t = 0 hr. At the end of the exposures bacterial cultures were acidified with HNO_3 (final concentration 5%) and kept at 4ºC in the dark for total silver analysis with AAS.

Developing exposures in liquid medium was the preferred option to carry out the exposures as in this way bacteria-nanoparticle interaction is allowed in contrast to other methods such as using discs impregnated with AgNPs (Ojha *et al.*, 2013). The antibacterial mechanism of AgNPs in discs can be only associated to the release of ionic silver.

2.4.4.1. Sigma Aldrich AgNPs exposures with pure cultures

The AgNPs suspensions were prepared as described in section 2.1. Exposures were carried out in a final volume of 100 ml in 250 ml bottles as depicted in the Figure 2. 20. A wave motion was created in order to enhance particle dispersion as this type of AgNPs settled down quickly.

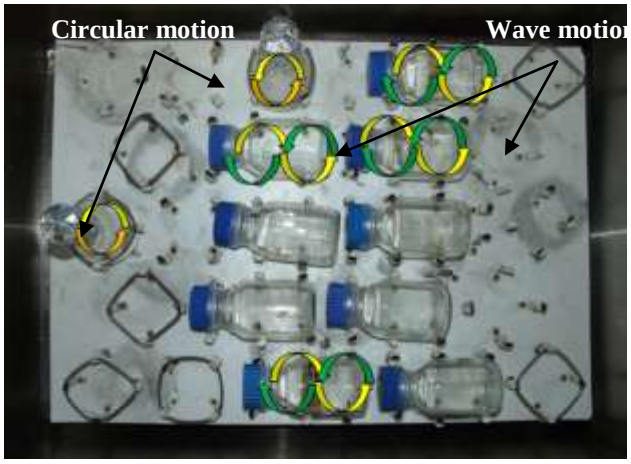

Figure 2. 20 View from above of the orbital incubator.

2.4.4.2. 300-NM and Hot Tub Mesosilver AgNPs exposures with pure cultures

The screening for the inhibitory concentrations of these two different types of AgNPs and also $AgNO_3$ was carried out initially in low volume borosilicate test tubes containing 3 ml of cell culture (Figure 2. 21).

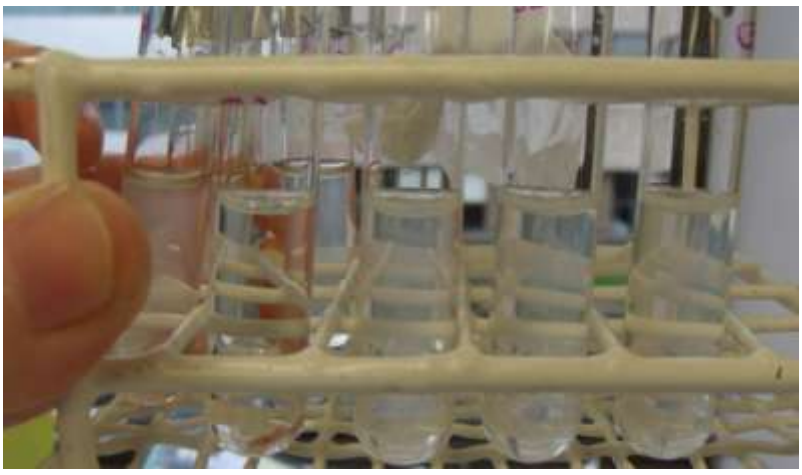

Figure 2. 21 Test tubes used to investigate the AgNPs inhibitory concentrations

2.4.4.3. Exposures in 50 ml flasks

The exposure of pure bacterial cultures to AgNPs was carried out in 50 ml Pyrex flasks, in a final volume of 40 ml of sterile ZM/10 Figure 2. 22.

Figure 2. 22 Example of cell cultures in 50 ml flasks used during the exposures to AgNPs

2.5. Microcosm exposures

In the present study estuarine conditions were modelled by establishing a series of microcosms with sediments and water samples collected from the Firth of Forth estuary in order to investigate the effects of AgNP on the functioning of bacterial community inhabiting the sediments and the water column.

The type of AgNPs used was the 300-NM as it is a very well characterized AgNPs and the stock suspensions were stable; AgNPs do not settle down as quick as the Sigma Aldrich type, and dispersed more homogenously in the water column, as a result with the 300-NM nanoparticle type less variability within the AgNPs treatment was expected. In addition the NM-300 AgNPs is a reference nanomaterial used by the OECD, therefore to work with the NM-300 was more relevant for comparison purposes with other studies.

2.5.1. Microcosms set up

2.5.1.1. Sampling of water and sediments

The microcosms were established with intertidal sandy sediments and water samples collected at extreme low tides from Cramond, Scotland, United Kingdom (Figure 2. 23), Firth of Forth estuary (coordinates 55 º 58’ 59.19’’N, 3 º 17’ 50.11’’W), To minimize sediment exposure time to air during low tide, the bacterial communities inhabiting sediments in the present study were collected at the extreme lower eulittoral during springtides and therefore were mostly subtidal.

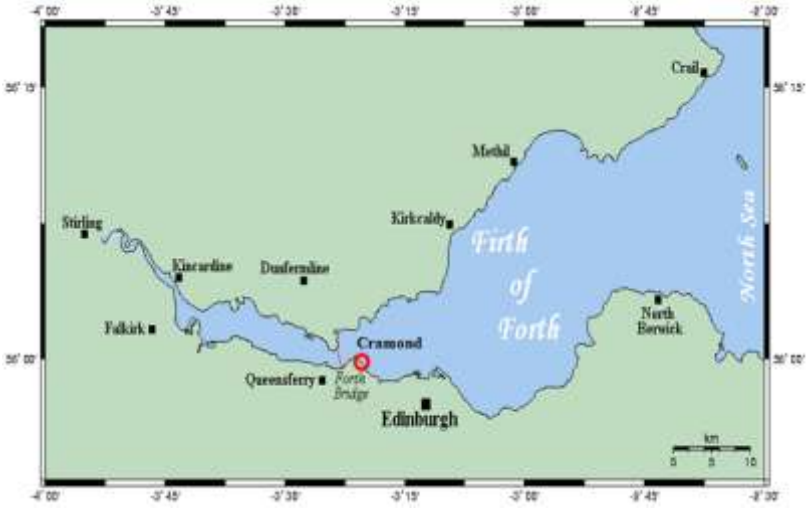

Figure 2. 23 Location of the Cramond sandflats in the Firth of Forth estuary

In the present study we focused on the communities inhabiting the water column and the first mm (< 3 mm) as it is in sediments where silver was expected to accumulate initially (Bradford *et al.*, 2009). Highlight that, sandy sediments, in a strong tidal setting, will not retain fine sediments and by extension nanoparticles. Ensuring that

undisturbed sediments were collected was a priority in order to minimize the variability of the bacterial community as bacterial diversity varies with depth (Tšertova *et al.*, 2013).

The picture depicted in the Figure 2. 24 illustrates the difficulties encountered to place the sediment samples in the tanks. The rectangular sections of sediments could not be placed into the tanks without disturbing the sample.

Figure 2. 24 Disrupted sediment sample

The most suitable option to sample undisturbed sediments was to use as a core sampler built with one of the buckets used as the containers (or tanks) in the microcosm. The bottom of the bucket was cut-off and the walls of the sampler reinforced with a section of a plastic pipe (see orange part of the assemblage) Figure 2. 25 . With this sampler oxic sediments were collected with minimal perturbation (depth < 10 cm) and placed in 5 L polypropylene (PP) cylindrical containers (∅ 19.5 cm).

Figure 2. 25 The core sampler was built with an identical model of bucket used as tanks during the microcosm exposures.

All the containers for sampling and preparing the microcosms were cleaned with Decon Neutracon and 10% v/v HNO_3 and sterilized at 121°C for 15 min.

2.5.1.2. Dosing the microcosms

A single pulse exposure at an initial nominal concentration of AgNPs in water (1 mg L^{-1}) similar to concentrations used in previous studies (Bradford *et al.*, 2009,

Colman *et al.*, 2012, Colman *et al.*, 2014) To achieve this concentration 3 L of well mixed estuarine water were dosed with 8.33 ml of the initial AgNPs working suspension (360 mg L^{-1}), and then gently poured on to the surface of the sediments in each microcosm, and sediments were subsequently contaminated through precipitation of the AgNPs contained in the overlaying water. The accumulation of silver in the sediments was supported by a previous study (Bradford *et al.*, 2009). As the aqueous matrix of the AgNPs contained stabilizing agents it was necessary to investigate the effects of this dispersant separately. The dispersant or carrier control was prepared similarly to the AgNPs treatment with the appropriate concentrations of sterile dispersant (JRCNM03001a) but in the absence of AgNPs. Three different treatments were established, the AgNPs treatment containing dispersant (T1), the dispersant alone (T2), and the control treatment (TC) consisting of tanks dosed with an equivalent volume of sterile Milli-Q water.

2.5.1.3. Aeration

In estuaries superficial sediments are in direct contact with the dissolved O_2 in the water column, and the superficial sediment layers is where the concentration of O_2 is the highest across vertical horizons. Continuous aeration in the surface of the sediments and along the water column with minimal sediment disturbance was achieved using a bubble-wall system (Figure 2. 26) to mimic aeration provided by the tide. The use or air-stones is not recommended as they tend to disturb sediments more easily.

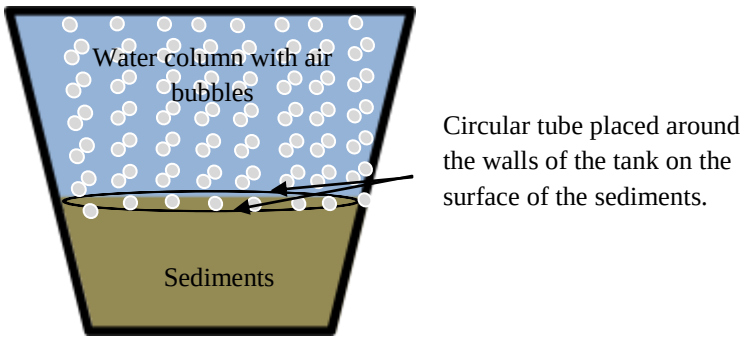

Figure 2. 26 Drawing representing the water column and sediment compartments in microcosm tanks, and the air bubbles formed from the surface of the sediments along the water column.

2.5.1.4. Sampling water and sediments from the microcosms for biological and chemical analysis

Water and sediment samples were collected with a cut sterile 5 ml pipette tip (diameter 5 mm). The sampling areas in the sediments were delimited with an empty

sterile corer in order to avoid repeatedly sampling the same spot. These corers were placed on the sediments with sterile forceps Figure 2. 27.

Figure 2. 27 View of the surface of the sediments with cylindrical plastic piece marking the area where sediments were collected in previous time points. It is also observed the circular black tube that creates a gentle aeration across the water column and superficial sediments.

The visibility across the water column in the tanks was good due to the low concentration of suspended solids (not measured) achieved by the gentle aeration system established and the low concentration of organic material in the sandy sediments. The good visibility through the water column in the tanks facilitated the collection of superficial sediments. Preliminary experiments with silty sediments and very rich in organic matter, also collected from the mudflats at Cramond, complicated the collection of the samples due to lack of visibility caused by suspended solids in the water as depicted in Figure 2. 28.

Figure 2. 28 View of the microcosms established with sediments collected from mudflats.

2.5.1.5. Temperature

The annual average temperature of the water registered in a nearby area, Crombie, in the Firth of Forth estuary is 9.4 ± 4 ºC (data provided by the Scottish

Environmental Protection Agency, SEPA, years 2010-2011). The ambient temperature was maintained at 12 °C in March 2012, 16 ºC in August 2012 and 10 ºC in January 2013. In January 2013 the temperature measured *"in - situ"* at the time of sampling collection was 5.8ºC. This temperature was not feasible in the existing facilities at Heriot-Watt at that time and also for consistency with the microcosms run in 2012 the ambient temperature was set up at 10ºC.

2.5.2. Environmental parameters monitoring and analysis

2.5.2.1. Dissolved oxygen, temperature and salinity

The dissolved oxygen (DO), temperature and salinity were measured *in-situ* with a YSI 85 probe. The salinity was monitored during the exposures in the water samples collected from the tanks at different time points. Preliminary experiments showed that the DO and the salinity remained stable for 120 hr. To avoid cross contamination between the experimental tanks (the YSI 85 probe cannot be sterilized) the probe was submerged in the tank only at the end of the experiment. The instrument maintenance and calibration was conducted following manufacturer's guidelines.

2.5.2.2. pH

The pH was measured in the water column by collecting water samples from the microcosms at different time points. The pH meter used Thermo Orion model 420. The pH was measured in continuously stirred samples.

2.5.2.3. Redox potential

The redox potential in the superficial sediments of the microcosms was measured in the first 3 mm. The redox potential electrode used was Sentek (type n° 01/CER/ball/1M/BCN) 3 M KCl saturated with AgCl. The functioning of the instrument was tested with ZoBell's solution prepared as follows: The following chemicals (they should be dried overnight before use) were required 1.4080 g $K_4Fe(CN)_6 \cdot 3H_2O$ (Potassium ferrocyanide), 1.0975 g $K_3Fe(CN)_6$ (Potassium ferricyanide), 7.4557 g KCl (Potassium chloride). These chemicals were dissolved in deionized water and stored in a dark bottle at 4°C (Nordstrom and Wilde, 2005). The reading of the following solution should be 238 mV at 25°C.

When measuring the redox potential on the surface of the sediments the electrode readings were taken when the measurement stabilized ± 5mV.

2.5.2.4. Total organic carbon in sediments (TOC)

The total organic carbon in sediments was measured with loss on ignition (LOI) method following the following procedure: sediments were dried overnight at 105 ºC.

Then 2.0 g of sediments were weighed in a porcelain crucible and placed into a furnace overnight at 440ºC (Schumacher, 2002). The percentage of total organic carbon was calculated as follows where Wi corresponds to the initial weight and Wf to the final weight:

$$\text{TOC (\%)} = \frac{(Wi - Wf)}{Wi} \; x \; 100 \qquad \text{[Eq 6]}$$

2.5.2.5. Grain size

Sediments samples collected from the first 10 cm were dried at 50 ºC overnight and sieved using mesh size ranging between 2 mm and 63 µm.

2.5.2.6. Porosity

The porosity of the sediments (the sediment pores were 100% water saturated) was measured by gravimetric analysis. Water saturated sediment samples were collected in plastic cores (volume 45 cm^3) and weighed. Then samples were dried overnight at 105º C and the dry weights registered. The porosity was calculated with the formula depicted below (Mudroch *et al.*, 1996):

$$\textbf{\textit{Porosity}} \; (\%) = \frac{(Mws - Mds)}{Vws \times \rho w} \times 100 \qquad \text{[Eq 7]}$$

Where:

Mws is the mass of the wet sediments (g)

Mds is the mass of the dry sediments (g)

Vws is the volume of the wet sediments (cm^3)

ρw is the density of the water (g/cm^3). As the conditions are typically marine (salinity 31 ‰), the value adopted for the ρw in the present study is 1.025 g/ml (Safarov *et al.*, 2012)

2.5.3. Sample collection and preservation for chemical and biological analysis

Water and sediment samples, collected at different time points (0, 24, 72 and 120 hr), were collected as described in section 2.5.1.4 and preserved at -70°C for biological analysis and at -20°C for chemical analysis. Water samples were collected in 50 ml sterile and metal-free plastic tubes. Sediment samples were collected from the superficial sediments (< 3 mm depth) with sterile plastic cores (5 mm diameter). Three samples were taken from each tank and pooled together. Samples collected to measure bacterial viability and community physiological profile were preserved at 4ºC and processed within 12 hr.

2.5.4. Chemical analysis

2.5.4.1. Silver analysis

Water and sediment samples collected at different time points were digested according to the USEPA methods as described in section 2.2.7. .

2.5.4.2. Inorganic Nitrogen

The concentration of inorganic Nitrogen species in the overlaying water was analyzed during the course of the experiment. Samples were defrosted overnight in the fridge (4ºC) and the temperature of the samples was allowed to increase up to room temperature before the analysis, as recommended by the manufacturer. The concentration of ammonium (NH_4^+) was analyzed with Ammonia Nitrogen by the Salicylate Method (DL 0.004 mg L^{-1}, Hach Method 8155. Nitrite (NO_2^-) with the NitriVer® 3 diazotization method (DL 0.002 mg L^{-1}) and Nitrate (NO_3^-) was analyzed with the NitraVer® 5 cadmium reduction method, Hach method 8171 (DL 0.04 mg L^{-1}). These three methods are recommended for the analysis of N in seawater. The spectrophotometer used was a Hach Lange DR 2010 and the volume of water analyzed was 10 ml. The accuracy of the methods should have been analyzed with reference materials run alongside.

HACH methods are commercial kits widely used to monitor water quality. In the present study the precision of the Hach Method 8155 to detect differences between samples was tested by measuring the concentration of NH_4 in a series of standards Figure 2. 29 prepared as follows: 152.83 mg of NH_4Cl (BDH product number 27149, purity 99%) were dissolved in milli-Q water up to a final volume of 40 ml to get a final concentration of 1 mg/ml of N. The high correlation coefficient (R^2=0.9994) confirmed the precision of the method and its practicality to detect differences between samples if any.

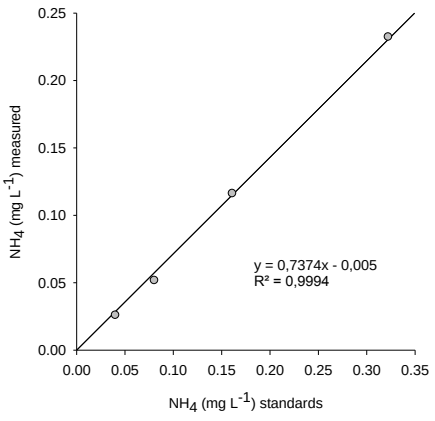

Figure 2. 29 NH_4 measured versus nominal concentration of NH_4 prepared with NH_4Cl.

The dispersant contains 7% (w/w) of NH_4NO_3 (Kermanizadeh *et al.*, 2012) versus 10% (w/w) of total silver ($AgNPs^+$ residual ionic silver), thus the extra amendment of NH4 and NO_3 in the treatments dispersant and with AgNPs is estimated as follows:

i) Mass ration AgNPs: NH_4NO_3 = 10:7= 1.43

ii) If the final concentration of AgNPs is 1 mg L^{-1} then the final concentration of NH_4NO_3 is expected to be proportional to the ratio: 1 mg L^{-1} ÷ 1.43 = 0.7 mg L^{-1}.

The addition of 0.7 mg L^{-1} of NH_4NO_3 is equivalent to 0.16 mg L^{-1} of NH_4 and 0.56 mg L^{-1} of NO_3.

2.5.4.3. Chemical Oxygen Demand

The chemical oxygen demand (COD) in the water was analyzed with the mercury-free small scale (2 ml) flask digestion procedure using chromium(III) potassium sulphate and silver nitrate solutions (1986 method D; closed-tube); limit of detection is typically 9 mg L^{-1} (Environment Agency 2007). A detailed procedure for this experiment is provided in the Appendix VIII. This parameter is used as an indirect measure of organic matter content and is based on the oxidation of the organic matter by a strong oxidant, in this case dichromate CrO_7^{2-}. The excess or residual dichromate is titrated with Iron (II) ammonium sulphate solution and the COD of each sample is estimated as follows:

$$\text{COD} = \mathbf{4000} \times \mathbf{DF} \times \mathbf{M}\,(\mathbf{Vb} - \mathbf{Vs})\ (\text{mg L}^{-1}) \qquad \text{[Eq 8]}$$

where: Vb is the volume (ml) of iron (II) ammonium sulphate solution used in the titration of blank solutions; Vs is the volume (ml) of iron (II) ammonium sulphate solution used in the titration of the sample (D4.4.1); DF is the dilution factor, in the present study it was always as there was not need to dilute the samples; M is the molarity of standardised iron (II) ammonium sulphate solution

This method was preferred against the commercial kits available because the detection limit of the commercially available kits suitable for the analysis of COD in seawater was not low enough. Double amounts of chromium (III) potassium sulphate $KCr(SO_4)_2$ and silver nitrate ($AgNO_3$) solutions were added (see Appendix VIII) due to the concentration of chloride in the water samples collected from the microcosm was greater than 2000 mg L^{-1}. The chloride interferences with the CrO_7^{2-} are detailed below:

Chloride interferences reaction

Oxidation reaction: $Cr_2O_7^{2-} + 8H^+ \rightarrow 2Cr^{3+} + 4H_2O + 3O$ [Eq9]

Iron (II)/dichromate titration: $6Fe^{2+} + Cr_2O_7^{2-} + 14H^+ \rightarrow 6Fe^{3+} + 2Cr^{3+} + 7H_2O$ [Eq10]

Chloride ions complexed by $KCr(SO_4)_2$ and $AgNO_3$:

$$Cr^{3+} + 6Cl^- \rightarrow [CrCl_6]^{3-}$$
$$Ag^+ + Cl^- \rightarrow AgCl \quad [Eq11]$$

The concentration of chloride in the water samples was estimated on the basis of salinity. As chloride is a major component of the seawater and proportional to the salinity, if the salinity is 31 ‰ then the concentration of chloride was 17.14 g L^{-1} (Millero *et al.*, 2008). To test the accuracy of the COD method and the ability to assess the difference between samples, the COD was analyzed in samples containing 30 g L^{-1} of NaCl (containing to 18,200 mg L^{-1} of chloride) with different concentrations of glucose (0, 6.25, 12.5, 25, 50 to 100 mg L^{-1}). To oxidize 1 mol of glucose (180 g), 6 mol of O_2 (192 g) are required. Based on this ratio it is estimated that to oxidized 1 mg of glucose, 1.07 mg of oxygen is required.

Glucose oxidation: $C_6H_{12}O_6 + 6O_2 \rightarrow 6CO_2 + 6H_2O$ [Eq12]

Thus 1.0 mg L^{-1} glucose is equivalent to 1.07 mg L^{-1} of COD. The correlation between COD and glucose at high chloride concentrations with the method used in the present project is depicted in Figure 2. 30.

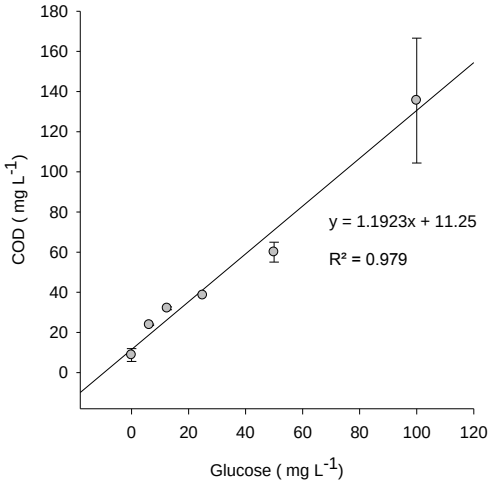

Figure 2. 30 COD versus glucose concentration expressed as mean ± SD, n= 2 except for 25 mg L^{-1} glucose n=1, one sample was lost during the processing.

The use of $HgSO_4$ (mercury (II) sulphate) was avoided as mercury is highly toxic and it is recommended to minimize the exposure to this compound.

2.5.5. Biological analysis of water samples

2.5.5.1. Respirometry Assay

Respirometry assays have been widely used in ecotoxicology to study the effects of pollutants on the metabolism of microbial communities in soils (Taccari *et al.*, 2011), WWTPs (Ricco *et al.*, 2004) and very recently to evaluate the antimicrobial effects of AgNPs on natural stream water (Colman *et al.*, 2012). This assay was applied to study the physiological status (by means of O_2 uptake) of pure bacterial cultures and natural microbial communities inhabiting the water column collected from the microcosms. The instrument used in the present study was the Strathtox® respirometer (Figure 2. 31)that has been used previously with soil microbial communities (Aspray *et al.*, 2007). This equipment measures the concentration of dissolved O_2 in the water samples in a continuous mode and incorporates a built-in magnetic stirrer and a water bath with a temperature controller to ensure that O_2 measurements are carried out under continuous stirring and electrodes are maintained at a constant temperature ± 0.1 ºC.

Figure 2. 31 Strathtox® respirometer used to measure the O_2 uptake rate.

Cleaning procedure

To avoid cross contamination between samples the vessels and stirring bars were thoroughly cleaned between different sample measurements with metal-free detergent (Decon Neutracon) and 70% ethanol and rinsed thoroughly with sterile distilled water. The electrodes were cleaned thoroughly with water and ethanol (ethanol was used carefully to prevent O_2 membrane probe damage)

Verifications

The performance of the respirometer in seawater and Milli-Q was analyzed, with and without dispersant and AgNPs, in order to ensure that none of these components

affected the normal functioning of the O_2 probes. The NM-300 AgNPs did not interfere with the readings of the electrodes, nor the associated dispersant.

2.5.5.1.1. Pure cultures

The exposures were carried out with ZM/10 liquid medium and the preparation of the cell cultures and AgNPs were prepared as explained in section 2.4.4.2 in a final volume of 20 ml.

2.5.5.1.2. Microcosm exposures

Water samples

The respirometry assay measured the O_2 uptake of the whole microbial community inhabiting the water column, providing an insight of the overall physiological status of the community including non culturable bacterial groups. Water samples were collected at different time points during the course of the microcosm exposures and O_2 uptake rate was monitored at least for 30 min. The working temperature varied according to the time of the year. In summer the temperature was set at 20-22°C (August 2012) and at 15°C during the winter time (January 2013). There is an inverse relation between temperature and dissolved O_2, for this reason the water samples were acclimated in the water bath for 30 min prior to measure the O_2 uptake in order to ensure that changes in the concentration of dissolved O_2 were exclusively due to microbial respiration and not due to changes in the temperature of the water samples. Up to six samples were run each time as this is the number of vessels in the respirometer.

Sediment samples

Sediment slurries were prepared to investigate the O_2 uptake of microbial communities inhabiting this environmental compartment. Sediments were mixed with sterile seawater similarly to the procedure followed to extract the microbial community from sediments (section 2.5.6.1). However due to the presence of fine grains of sediments the tight sealing between the vessel and the electrode failed and the experiment was cancelled. No further attempts were carried out with sediment samples due to time constraints.

Data analysis

The O_2 uptake rate was estimated by dividing the difference of the dissolved O_2 at the beginning and at the end of the assay by the time period. A 30 min time period was established to analyze the O_2 uptake rate in the water samples collected from the

microcosm as the main aim was to take a shot of the physiological status of the microbial community. During this 30 minute period the concentration of dissolved O_2 in the water sample and time exhibited a linear relationship as observed in the user interface of the respirometer (Figure 2. 32). The user can decide the start and end time point of the assay and analyze the concentration of dissolved O_2 in each vessel.

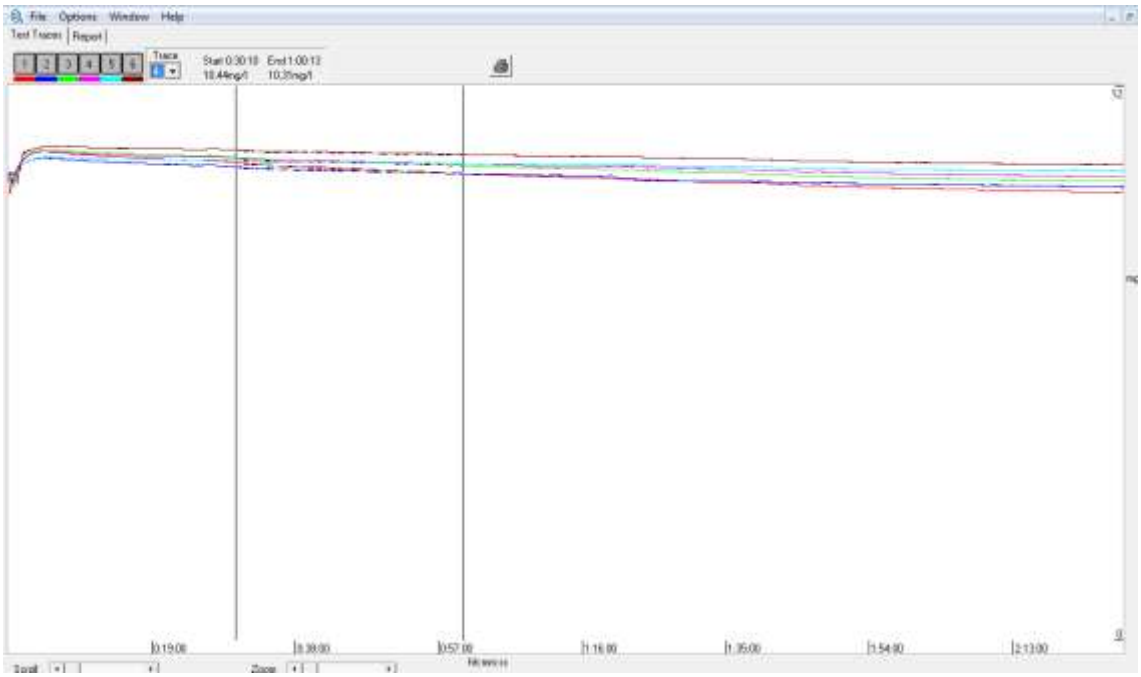

Figure 2. 32 The Strathtox® respirometer user interface is shown. The two vertical selector bars can be dragged to select the section of the trace, start and the end time.

2.5.5.2. Microbial abundance in the water column

2.5.5.2.1. Bacterial plate counts

The procedure followed to plate water aliquots was similar to the one described in section 2.5.6.1 (Bacterial plate counts in sediments) with the difference that no bacterial extraction from sediments was required. Dilutions plated ranged between 10^{-1} and 10^{-3}.

2.5.5.2.2. Direct counts with Epifluorescence microscopy

DAPI (4', 6-diamidino-2-phenylindole) is a fluorescent stain that binds and stains the DNA of bacterial cells a white-blue colour. This method has been widely used to count marine bacteria (Pernthaler *et al.*, 2001). Details of the specific reagents are available in the Appendix XI and the procedure is described below.

i. Fixation

Fixation of the cells was carried out as described in Porter and Feig (1980). Fixation is necessary with DAPI staining at salinities higher than 12% (Zweifel and Hagstrom, 1995), and also provides physical rigidity to the bacterial cell membranes

and allows the preservation of the samples at < - 20ºC until further analysis. In addition fixation helps the stain to penetrate the membranes (Howard-Jones *et al.*, 2001). The procedure used was as follows: harvest 1ml of bacterial culture and place in a 1.5 ml tube. The dilution of the sample may be needed, depending on the bacterial concentration. Add 81µl (38 % w/w formaldehyde) to a final concentration of approximately 3 % of formaldehyde in the sample. Incubate cells at room temperature for 1 h in the dark (or covered with tin foil). Place a moistened support filter (GF/C or GF/F) and a 25 mm a polycarbonate membrane filter of 0.2 µm into a filtration tower.

ii. Filtration

Filter the fixed sample by applying a gentle vacuum. Support filters may be utilized for several samples. After complete sample filtration, wash the filter with 15 ml of sterile Milli-Q water; remove the water by vacuum. Put the membrane filter in a plastic petri dish, cover and allow to air-drying. Label the samples immediately after with a pencil.

iii. Dehydration

Each filter was dehydrated by placing it in ethanol (EtOH) (50 %) for 5 min, then placing it in 80 % EtOH for a further 5 min and then in 100 % EtOH for a further 5 min. Filters were allowed to air-drying and stored at -20˚C until further analysis. Dehydration is an important step as prevents the formation of ice crystals that could break cells and also enhances pore formation that will lead to a better staining of the cell.

iv. Slide preparation

Filters were mounted on a glass slide (cell side up), and 15µl of Fluoroshield™ with DAPI were added (Sigma-Aldrich). Then the filter was covered with a cover-slip.

v. Epifluorescence microscopy and cell counts

The filters were examined using a Zeiss Axiscope fitted with a 100x objective microscope illuminated by UV light. The DNA of the cells was fluorescent and the individual bacteria were easy to identify (Figure 2. 33). DAPI stained cells were photographed using an Axio digital camera and ZEN 2011 imaging software. Between 15 and 20 consecutive microscope field were photographed along a 1/4 of the filter.

Bacterial counts was performed by the with CellC software (Selinummi *et al.*, 2005). This software processes the images (see Figure 2. 34) and counts the cells. The accuracy of the CellC software was satisfactory; the cells of a few pictures were counted manually and the results obtained were compared with the counts obtained with the number estimated by CellC.

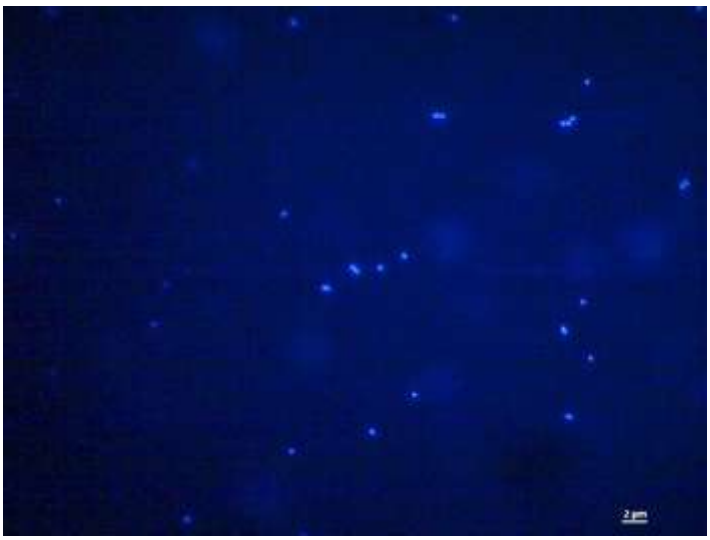

Figure 2. 33 Image depicting cells inhabiting the water column stained with DAPI and observed with Epifluorescent microscopy.

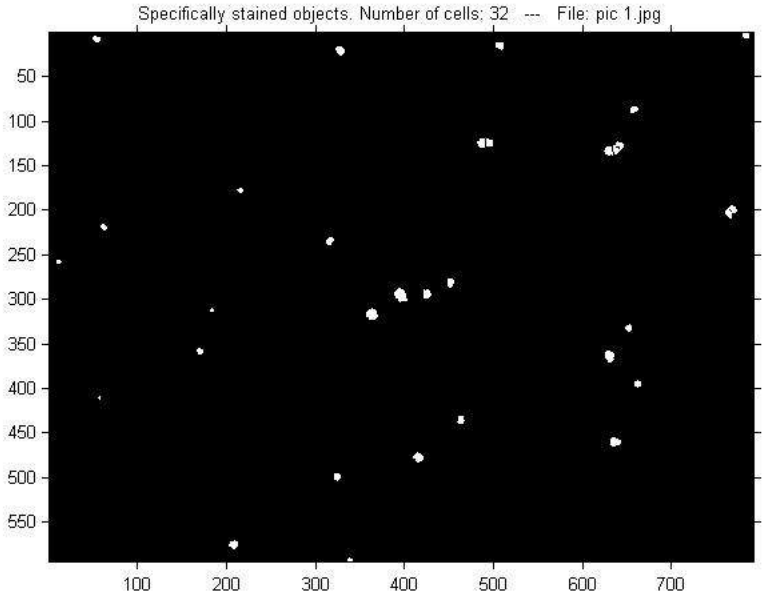

Figure 2. 34 Image processed with CellC software showing the cells counted.

2.5.5.2.3. Flow cytometry

Flow cytometry is a technique widely used to analyze cell abundance. It also can provide useful information about the cell status by means of measuring its granularity (also known as internal complexity of the cell) and fluorescence intensity. The foundations of this technique are based on measuring the forward-scattered light (FSC) or diffracted light resulting from a laser light impacting on the cell surface. The FSC is proportional to the cell size, cell shape and surface and also to other granular components inside the cell. The cell granularity is proportional to the side-scattered light (SSC) and is normally collected by a lens located in an angle that makes a 90° angle with the laser beam. The correlation between FSC and SSC is used to classify different types of cells.

The flow cytometer used in the present study, the CyFlow (Partec) incorporates a laser that emits light at emission 488 nm. This light is absorbed by the electrons in the fluorescent dye used to stain the cells. The electron will go back to its normal energy level and the excess of energy will be released by the emission of a photon. The SYTO®9 (SYTO® 9 Green Fluorescent Nucleic Acid Stain, Life Technologies) was the dye used in the present study, which binds nucleic acids, RNA and DNA. The emission wavelength is also characteristic of the fluorescent dye (SYTO®9 emissions wavelengths are 501 and 498 for RNA and DNA respectively). Fluorescence enhances the signal produced by each cell and enables the analysis of different cell types or cells in different physiological status; higher metabolic activity is associated to higher RNA content. In the present study the use of a fluorescent dye can help to discriminate between different bacterial populations according to different nucleic acid content, higher fluorescence is associated to higher RNA/DNA content, that can be used as a way to measure cell status: higher or lower metabolic activity or viability.

The parameters used to analyse the bacterial populations were FSC (relative size), SSC (relative granularity), and the fluorescence emission of SYTO®9 at 520 nm band pass filter. The FSC and SCC were established by running pure cultures of bacteria exhibiting different morphology and water samples collected from the Firth of Forth estuary.

Procedure

Samples were fixed with formaldehyde (3 % final concentration) and kept at -70°C until further analysis (section 2.5.2.5). Before the analysis with FC, samples were thawed at room temperature. 1 ml sample aliquots were stained with SYTO®9 at a final concentration of 1.5 µM (0.3 µl SYTO®9/ ml water sample) as recommended by the manufacturer. Then vortex to mix and incubated for 30 min prior to analysis with FC.

2.5.5.3. Ammonia oxidizing bacteria (AOB) abundance

Water samples were collected at the beginning of the microcosm exposures (0 hr) and at the end (120 hr) to analyze the effects of AgNPs on the abundance of AOB groups with quantitative polymerase chain reaction (qPCR). The methodology applied for the bacterial DNA extraction, primers, commercial master mix (that include the fluorescent acid nucleic stain) and qPCR cycle settings, described next and the information relating to the equipment and materials needed are detailed in Appendix XII.

i. Water sample filtration

For the analysis of AOB abundance, 250 ml water samples were filtered through 0.22µm filters (Millipore) at the beginning and at the end of the exposures (time points 0 hr and 120 hr) with a manifold. The manifold cups were thoroughly cleaned with Decon 90, HNO_3 (10% v/v), rinsed thoroughly with milli-Q water and sterilized in the autoclave at 121°C for 15 min. The filters were stored at -70°C until DNA extraction takes places with a commercial kit.

ii. DNA extraction from filters

Commercial DNA extraction kits reduce the variability during the DNA extraction process, a crucial step for quantitative polymerase chain reaction (qPCR). In the present study two different commercial kits have been used in preliminary experiments, Power Water ® (catalog No 14900-50-NF) and the Rapid Water ® (catalog No 14810-50-NF) DNA extraction from MoBio, both combine mechanical and enzymatic lysis following manufacturer's protocol.

iii. Positive control for the amoA gene

The positive control template used for the *amoA* gene responsible for the production of ammonia monooxygenase was obtained from the strain *Nm51* belonging to the *Nitrosomonas sp*. marine cluster. For details of the *Nm51* strain cultivation given in the Appendix XIII. Cells were harvested by centrifugation of the cell culture, the supernatant was discarded and the cell pellet transferred to a microcentrifuge tube. Bacterial cells were boiled at 95 ºC for 10 min, then immediately chilled on ice and centrifuged for 5 min at 13.000 ×*g* and 4 ºC (Hornek *et al.*, 2006). The supernatant was collected and ready to use for PCR.

iv. DNA purification

The DNA concentration and purity from the environmental samples was analyzed with NanoDrop ®.

v. Primers

End point PCR preliminary experiments were carried out with different qPCR master mix to optimize the qPCR settings. The efficiency at amplifying the *amoA* gene of the pairs of primers detailed below was investigated. The concentration of primers in the final reaction tube was varied between 100 and 500 nM in order to optimize the mixture and minimize the production of primer dimmers, a by-product of the PCR than can create undesirable secondary peaks in the qPCR melting curve.

amoA-1F	GGGGTTTCTACTGGTGGT	(Rotthauwe *et al.*, 1997)
amoA-2R	CCCCTCKGSAAAGCCTTCTTC	(Rotthauwe *et al.*, 1997)

amoA-1F	GGGGTTTCTACTGGTGGT	(Rotthauwe *et al.*, 1997)
amoAr NEW	CCCCTCBGSAAAVCCTTCTTC	(Hornek *et al.*, 2006)
amoA-1F	GGGGTTTCTACTGGTGGT	(Rotthauwe *et al.*, 1997)
amoAr NEW	CCCCTCBGSAAAVCCTTCTTC	(Hornek *et al.*, 2006)
amoA-1F	GGGGTTTCTACTGGTGGT	(Rotthauwe *et al.*, 1997)
amoAr NEW 2.0	CCCCTCIGSAAAICCTTCTTC	(Hornek *et al.*, 2006)
A189	GGHGACTGGGAYTTCTGG	(Holmes *et al.*, 1995)
amoA-2R'	CCTCKGSAAAGCCTTCTTC	(Okano *et al.*, 2004)

The polymerases used were provided in qPCR master mix commercial products that are detailed below:

- SsoFast master mix (Bio-Rad)
- QuantiFast SYBR Green PCR (Qieng)
- Quanti Tec SYBR green Master Mix (Qieng)
- GoTaq® qPCR Master mix (Promega)
- GoTaq® Probe qPCR Master Mix Promega)

vi. Preparation of the PCR reaction mixtures

PCR and qPCR reactions were carried out in 20 µl final volume as described in Appendix XII.

vii. Thermal profile used for amplification of the amoA gene sequence

End point PCR settings

The PCR settings were the following: activation temperature 95 ºC for 1 min, 35(cycles) × (DNA denaturation temperature 95 ºC for 45 s, primers annealing temperature 55 ºC for 45s, DNA extension temperature 72 º C for 45s), 72 º C for 7 min (Rotthauwe *et al.*, 1997). To detect the most adequate annealing temperature the PCR was run with a gradient of temperatures ranging between 54 and 60 ºC.

qPCR settings

The qPCR settings were based on the PCR settings and were established as follows: 35(cycles) × (DNA denaturation temperature 95 ºC for 45 s, primers annealing temperature 58 ºC for 45s, DNA extension temperature 72 º C for 45s and 80 ºC for 20 s). A 4th step at 80ºC was included to reduce the florescence of non specific products (Long *et al.*, 2014).

viii. Analysis of the PCR and qPCR products on agarose gel

A final volume of 5 µl of the PCR and qPCR products together with 1 µl of the commercial marker were run in agarose gel prepared as explained in section 2.4.1.3

with the difference that the agarose gel in this experiment was prepared at a higher concentration (1.5% agarose) for better resolution of the PCR products.

qPCR standard curves

The DNA sequence of the *amoA* template obtained from the bacterial strain *Nm51* was purified and a series of dilutions between 10^3 and 10^7copies/µl were used to plot the standard curve.

2.5.6. Biological analysis of sediment samples

2.5.6.1. Bacterial plate counts

Bacterial extraction from sediments was carried out by the addition of 10 ml of sterile water (75% sea water and 25% deionized water) to the wet sediments (~ 2 g) and vortexing and vigorous shaking (5 min). Dilutions plated ranged between 10^{-3} and 10^{-4}.

A volume of 40 µl of a series of ten-fold dilutions of the suspensions were plated onto two different media: (1) ZM/10 agar (75% natural sea water, 25% deionized water, 0.05% Bacteriological Peptone, 0.01% yeast extract, 1.4% Bacteriological Agar (Oxoid, Thermo Scientific)) and (2) Marine Agar (MA, Difco, Detroit, MI, USA) slightly modified from Lebaron (Lebaron *et al.*, 2001): the nutrient concentration was reduced to 1:2 and complemented with natural sea water (0.25% peptone, 0.05%, yeast extract 17.5% natural sea water, 82.5% Milli-Q water, 1.4 % Bacteriological Agar).Plates were incubated at 15°C under a 12 hr light photoperiod, and the formation of colonies was monitored and the number of colonies counted after 8 days of incubation. The plate counts bacterial differences obtained between (1) ZM/10 and (2) Marine agar are shown in the Appendix IX.

2.5.6.2. Community-Level Physiological Profiles (CLPP)

The Biolog EcoPlate™ (Biolog Inc., Hayward, CA) include 31 different environmentally relevant carbon sources that are distributed in triplicate in a 96 well plate. Each well contains a single carbon substrate together with a tetrazolium violet redox dye. NADH is produced during the tricarboxylic acid (TCA) cycle that forms part of the metabolic pathway of the carbon substrates included in the Ecoplate Figure 2. 35. The inner membrane dehydrogenases, such as NADH dehydrogenase, reduce the tetrazolium dye via the electron transport chain (ETC). Tachon *et al.* (2009) observed that the reduction site depended on the growth conditions, in the inner part of the membrane in liquid and not active bacteria, and outside the cell in the outer part of the membrane in bacteria growing on agar plates.

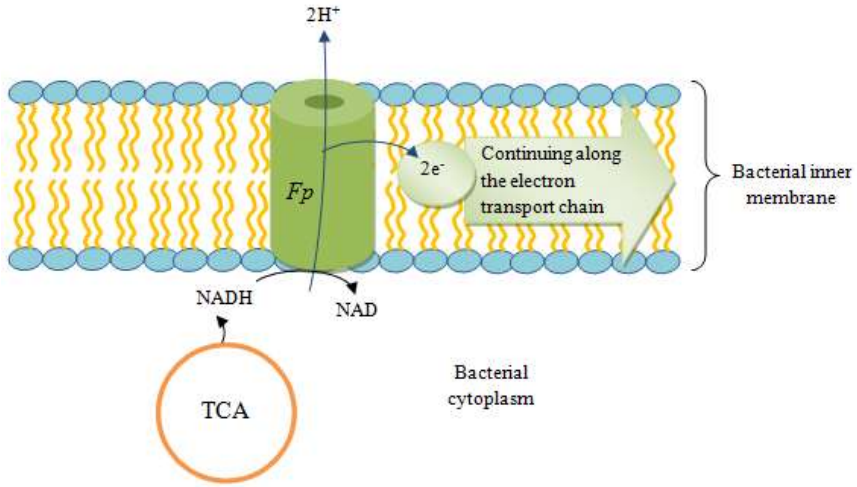

Figure 2. 35 Diagram representing NADH generated during the TCA cycle is the most important proton donor in the electron transport chain (ETC) located in the bacterial inner membrane. In *E.coli* a flavoprotein (Fp) is one of the hydrogen carriers. Modified from (Neidhardt *et al.*, 1990).

Under aerobic conditions the highest amounts of ATP and $NADH_2$ are produced. The tetrazolium violet redox dye is reduced by the NADH producing formazan and turning the well purple indicating a positive utilization of the carbon substrate (Figure 2. 36).

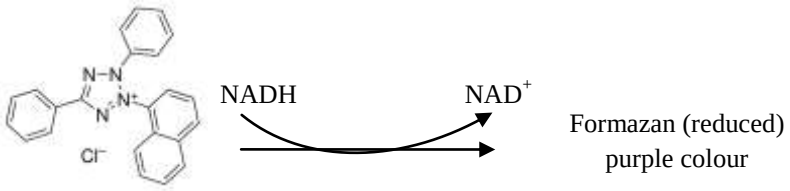

Figure 2. 36 Tetrazolium violet ($C_{23}H_{17}ClN_4$) chemical structure (Extracted from Sigma) is reduced by NADH.

Plates were inoculated with 140 µl (Anderson *et al.*, 2002) of bacterial suspension extracted from sediments at a 1:100 dilution, as described above and incubated at 15 ºC without agitation (Garland and Mills, 1991). In the present study 140

µl were inoculated in each well rather than 150 µl to prevent the overflowing of the cell culture from any of the wells that could cause well cross-contamination.

The utilisation of each carbon substrate (Figure 2. 37) was monitored with repeated plate readings measured approximately every 24 hr by reading the optical density at 590 nm (OD_{590}) and by direct observation of the colour development in each single well (Figure 2. 38) until uptake of the carbon substrates stabilized. The optical density was measured with a SpectraMax® M5 Molecular Devices spectrophotometer.

A1 Water	A2 β-Methyl-D-Glucoside	A3 D-Galactonic Acid γ-Lactone	A4 L-Arginine	A1 Water	A2 β-Methyl-D-Glucoside	A3 D-Galactonic Acid γ-Lactone	A4 L-Arginine	A1 Water	A2 β-Methyl-D-Glucoside	A3 D-Galactonic Acid γ-Lactone	A4 L-Arginine
B1 Pyruvic Acid Methyl Ester	B2 D-Xylose	B3 D-Galacturonic Acid	B4 L-Asparagine	B1 Pyruvic Acid Methyl Ester	B2 D-Xylose	B3 D-Galacturonic Acid	B4 L-Asparagine	B1 Pyruvic Acid Methyl Ester	B2 D-Xylose	B3 D-Galacturonic Acid	B4 L-Asparagine
C1 Tween 40	C2 i-Erythritol	C3 2-Hydroxy Benzoic Acid	C4 L-Phenylalanine	C1 Tween 40	C2 i-Erythritol	C3 2-Hydroxy Benzoic Acid	C4 L-Phenylalanine	C1 Tween 40	C2 i-Erythritol	C3 2-Hydroxy Benzoic Acid	C4 L-Phenylalanine
D1 Tween 80	D2 D-Mannitol	D3 4-Hydroxy Benzoic Acid	D4 L-Serine	D1 Tween 80	D2 D-Mannitol	D3 4-Hydroxy Benzoic Acid	D4 L-Serine	D1 Tween 80	D2 D-Mannitol	D3 4-Hydroxy Benzoic Acid	D4 L-Serine
E1 α-Cyclodextrin	E2 N-Acetyl-D-Glucosamine	E3 γ-Hydroxybutyric Acid	E4 L-Threonine	E1 α-Cyclodextrin	E2 N-Acetyl-D-Glucosamine	E3 γ-Hydroxybutyric Acid	E4 L-Threonine	E1 α-Cyclodextrin	E2 N-Acetyl-D-Glucosamine	E3 γ-Hydroxybutyric Acid	E4 L-Threonine
F1 Glycogen	F2 D-Glucosaminic Acid	F3 Itaconic Acid	F4 Glycyl-L-Glutamic Acid	F1 Glycogen	F2 D-Glucosaminic Acid	F3 Itaconic Acid	F4 Glycyl-L-Glutamic Acid	F1 Glycogen	F2 D-Glucosaminic Acid	F3 Itaconic Acid	F4 Glycyl-L-Glutamic Acid
G1 D-Cellobiose	G2 Glucose-1-Phosphate	G3 α-Ketobutyric Acid	G4 Phenylethyl-amine	G1 D-Cellobiose	G2 Glucose-1-Phosphate	G3 α-Ketobutyric Acid	G4 Phenylethyl-amine	G1 D-Cellobiose	G2 Glucose-1-Phosphate	G3 α-Ketobutyric Acid	G4 Phenylethyl-amine
H1 α-D-Lactose	H2 D,L-α-Glycerol Phosphate	H3 D-Malic Acid	H4 Putrescine	H1 α-D-Lactose	H2 D,L-α-Glycerol Phosphate	H3 D-Malic Acid	H4 Putrescine	H1 α-D-Lactose	H2 D,L-α-Glycerol Phosphate	H3 D-Malic Acid	H4 Putrescine

Figure 2. 37 Carbon sources included in the Biolog EcoPlate™.

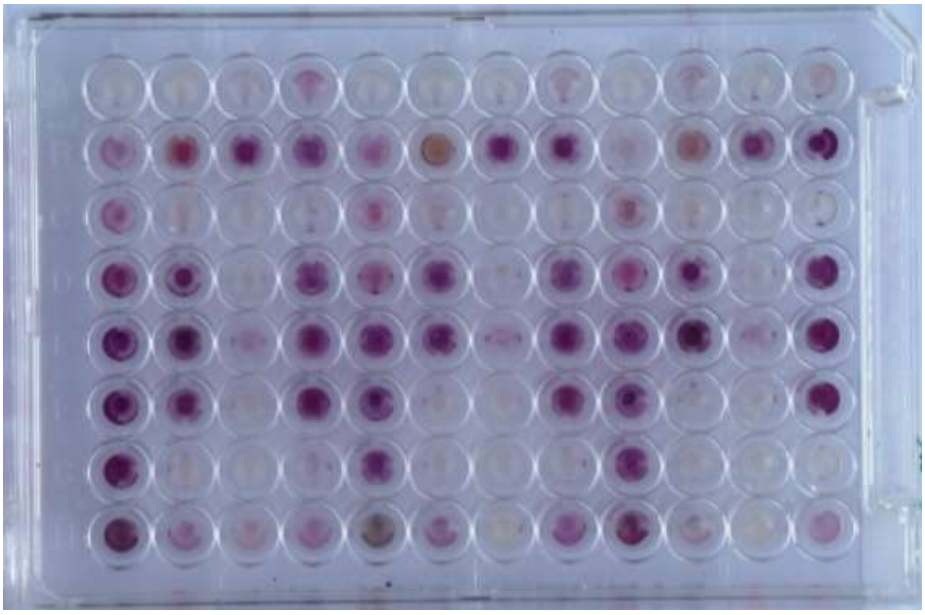

Figure 2. 38Biolog EcoPlate™ showing wells turned purple revealing that there is a positive utilization of the given carbon source.

2.5.6.3. Phospholipid fatty acid analysis (PLFAs) to study community structure and bacterial abundance

Sediment samples were analysed by lipid extraction with a single phase chloroform mixture, fractionation on a SPE Si column and the lipids subjected to a mild methanolysis (Bligh and Dyer, 1959, White *et al.*, 1979, Frostegård *et al.*, 1991, Frostegård and Bååth, 1996). The PLFAs extraction and the analysis with gas chromatography flame ionisation detection (GC-FID, 6890N, GC System, Agilent Technologies) were carried out at the James Hutton Institute (Aberdeen, UK). GC-FID is a technique used to separate compounds that can be volatized without degradation that uses an inert gas, (Helium in the present study) as a carrier of the sample and the stationary phase was liquid, Polyethylene glycols (PEG), widely used as it remains liquid under GC conditions. The different compounds of the sample will elute in the stationary phase, and the retention time in the stationary phase varies depending on the compound. When a compound elutes in the column, it enters the detector heated to approximately 300ºC. This reaction produced an electrical signal registered as a peak in a chromatogram as depicted in Figure 2. 39. When analyzing the composition of a sample it is necessary to run pure compounds as internal standards to use their retention time and the size of the peak as a reference. PLFAs can be identified and quantified with this technique through the analysis of their respective fatty acid methyl esters (FAMEs). Thus before the GC-FID step it is necessary to transform the PLFAs into FAMEs with methanolysis. The peak area of the FAME derivatised from their respective PLFA is used to estimate the concentration of PLFAs in the sample. The description of the procedure and materials required are available in the Appendix X.

Analysis of the chromatograms

The analysis with GC-FID of the present FAMEs was performed by members of the staff at the James Hutton institute. They used GC ChemStation (Rev A.09.03 [1417] (Agilent Technologies) to collect and analyze the output obtained from the GC-FID. The data obtained from this first analysis was analyzed with Visual Basic macros software developed at the James Hutton institute to support the selection of the peaks related to the FAMEs of interest. This in-house software also takes into account the relative retention time of the internal standard, C19:0 methyl ester. Then the area of the relevant peaks was corrected by subtracting the background (Thornton *et al.*, 2011).

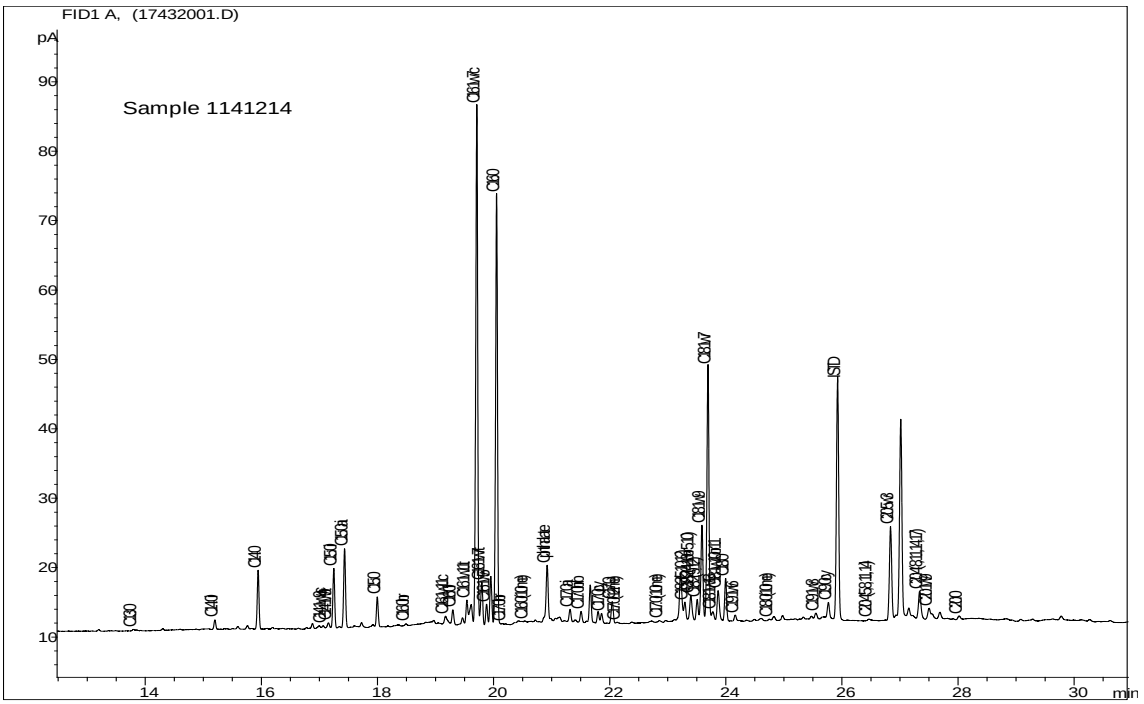

Figure 2. 39 Example of a chromatogram obtained with flame ionization detector -mass spectrometry (GC-FID). Each peak represents a single PLFA.

PLFA nomenclature

PLFAs are named by reference to the C atoms, the first number indicates the number of C atoms in the aliphatic chain and the second the number of double bonds, e.g. 16:0 indicates 16 C atoms and zero double bonds and 18:2 indicates 18C atoms and 2 double bonds. Branched chain fatty acids are indicated by "I"(iso), "a" (anteiso), "br" (unconfirmed position) and "cy" (a cyclopropyl group). "Iso" indicates a branch on the second carbon and "anteiso" indicates a branch on the third carbon from the methyl end. A number followed by "Me" indicates the position of a methyl group attached to that carbon from the carboxyl end of the molecule.

PLFAs denomination was based on standard nomenclature (Zogg *et al.*, 1997, Frostegard *et al.*, 1993) and grouped according to different bacterial groups as follows: Gram positive bacteria (Zogg *et al.*, 1997) (i15:0, ai15:0, i16:0, 10 Me l6:0, 17:0i, 17:0ai, 10 Me l7:0, 10 Me l8:0) Gram negative bacteria (Zogg *et al.*, 1997) (16:1ω7c, 16:1ω7t, 16:1ω5, 17:0cy, 18:1ω7, 19:0cy), unclassified bacterial PLFA (Frostegård and Bååth, 1996, Zogg *et al.*, 1997) (15:0, 17:0), Actinobacter (Frostegård and Bååth, 1996) (10 Me l6:0, 10 Me l7:0, 10 Me l8:0). The PLFA 16:1ω5 also known by the systematic name as *cis*-11-hexadecenoic acid [16:1(11)], was included as a specific biomarker for bacteria. This PLFA is often associated with arbuscular mycorrhizal fungi (Olsson *et al.*, 1995) and Gram negative bacteria (Butler *et al.*, 2003) specifically in nitrate-oxidizing bacteria (Lipski *et al.*, 2001). As arbuscular mycorrhizal fungi are not

expected to be dominant in the estuarine sediments of the present study, the 16:1ω5 has been associated with the presence of Gram negative bacteria.

PLFA Data analysis

The abundance of the PLFAs was reported in terms of abundance of their respective FAME in terms of μg g^{-1} dry sediment with a precision of 0.01 μg g^{-1}. These values were recalculated as moles g^{-1} to obtained PLFAs abundance as moles g^{-1}.

2.6. Data analysis

The statistical analysis was performed with SigmaStat 2.03 (Systat Software) and IBM® SPSS® Statistics 21, and graphs were produced with SigmaPlot®. Normality of the data for ANOVA analysis was analyzed by SigmaStat and the homogeneity of variances with SPSS.

2.6.1. Characterization of AgNPs

The effects of different concentrations of NaCl and time on the surface charge (zeta potential) and hydrodynamic diameter (z-average) were analyzed with a two way ANOVA with a level of significance of 0.05, followed by Bonferroni post hoc test. The normality of the data relating to particle size distribution was analyzed with the Kolmogorov-Smirnov and Shapiro –Wilk tests. When the data did not follow a normal distribution, the differences between samples were analyzed with the Mann-Whitney test for independent samples and the Wilcoxon signed-rank test for related samples.

2.6.2. Susceptibility of bacteria to AgNPs

Differences between treatments in terms of bacterial growth measured as colony forming units (CFU) and bacterial biomass as nitrogen concentration were analyzed with One Way ANOVA followed by Bonferroni post hoc test with a level of significance of 0.05. CFU data were log10-transformed prior to ANOVA analysis.

2.6.3. Microcosm experiments

2.6.3.1. Chemical analysis

The total concentration of silver in water and sediments was compared at different time points with One Way Repeated Measures ANOVA (RM-ANOVA). The concentration of inorganic forms or nitrogen and COD was compared across the treatments with a One Way ANOVA.

2.6.3.2. Biological analysis in water samples

The data relating to bacterial abundance obtained with the bacterial plate counts, flow cytometry and epifluorescence microscopy counts were log10-transformed prior to ANOVA analysis followed by Bonferroni Post Hoc test. The differences between treatments relating to the O_2 uptake rate were analyzed with an independent t-test.

2.6.3.3. CLPP Data analysis

Absorbance values were blanked against the absorbance of each respective well (A_0) at the beginning of the assay and the average well colour development (AWCD) at each time point for each sample was estimated as follows:

$$\boldsymbol{AWCDi = \Sigma(Ai - A0) \,/\, n} \qquad \text{[Eq 13]}$$

Where *Ai* is the absorbance in each well at time t_i , and *n* the number or carbon sources (Garland and Mills, 1991). The average AWCD for each treatment was plotted at each time point and the uptake rate was estimated by averaging the slope of the curves when the relationship between time and AWCD was linear.

Relationships among samples and shifts in the pattern of single carbon substrate utilization were assessed by principal component analysis (PCA) using the absorbance values recorded in each well at a single time point (Garland, 1996). PCA analysis was carried out at two different time points (6 and 14 days incubation) to explore whether the selection of a time point significantly influenced the results.

Prior to the PCA analysis, as recommended by former studies (Garland and Mills, 1991, Garland, 1996), *Ai* values of each sample were transformed into A_i', by dividing the absorbance of each well by the AWCD of their respective sample in order to avoid the relative bacterial abundance in the samples influencing the PCA analysis. The carbon substrates that were included in the PCA analysis fulfil the following criteria: colour development with a net OD > 0.25 (Garland, 1996) and statistical requirements: Kaiser-Meyer-Olkin Measure of Sampling Adequacy (KMO) >0.5, Bartlett's test of sphericity <0.05, non-redundant residuals < 50% in reproduced correlation matrix with absolute values greater than 0.05 (Field, 2009). These statistical criteria were applied in the present study to all the PCA analyses performed, including PLFAs. The analysis of the variance and PCA analysis were performed with IBM® SPSS® Statistics 21.

2.6.3.4. PLFAs

The abundance of single PLFAs and bacterial groups was compared across the treatments with a One Way ANOVA. The shift patterns of the community structure were explored with PCA component analysis on the basis of the relative abundance of each PLFA. The PLFAs included in the analysis were those regarded as relevant bacterial biomarkers and comprised ≥ 1% total phospholipid fatty acids biomass (mol) as recommended by Zogg *et al.*, (1997)

Chapter 3 Results

3. Results

3.1. Characterization of silver nanoparticles

3.1.1. Sigma Aldrich AgNPs nanopowder < 100nm

The Sigma Aldrich AgNPs dispersed in milli-Q water (purchased from Sigma Aldrich 576832-5G) settled down and quickly reduced the stability and the homogeneity of the suspension. Figure 3. 2 shows this type of AgNPs tended to aggregate. DLS analysis in milli-Q showed that the average particle size (Z-Average) was 191.8 nm ± 55.8. The TEM analysis showed that these nanoparticles form agglomerates/aggregates (Figure 3.1A) and this may explain the detection of big particles (> 100 nm) with the DLS. The Zeta Potential analysis indicated that this AgNPs type is negatively charged (- 23.1 ± 8.4 mV; n = 8). The absorbance analysis in the visible UV-vis spectrum of the AgNPs (dispersed in Milli-Q water) showed a peak absorbance value at 409 nm (Figure 3.1 B).

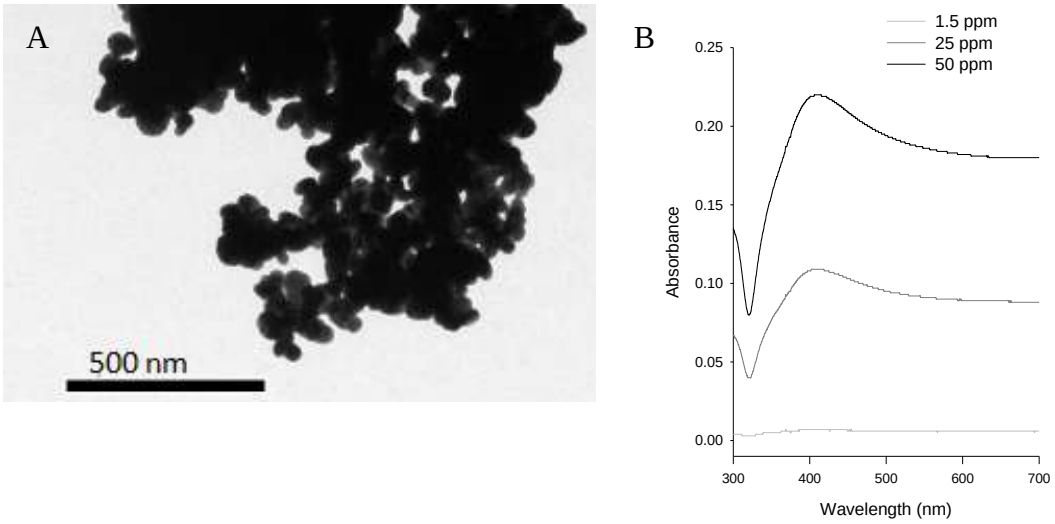

Figure 3. 1 TEM image of Sigma Aldrich AgNPs (courtesy of Mr Iain Hannah) (A) and UV-vis spectrum of different concentrations of the Sigma Aldrich AgNPs (right).

3.1.2. NM-300 AgNPs

The UV-vis spectrum analysis of the NM-300 (LGC Standards Figure 3. 2 left) in Milli-Q water exhibited a maximum absorbance peak at 412 nm. The TEM images showed that this type of AgNPs was spherically shaped (Figure 3. 2; right). DLS

analysis in milli-Q measured a Z-Average diameter of 58.25 ± 2.74 and negatively charged, Zeta Potential was -22.3 ± 3.3 (n = 3) in Milli-Q water.

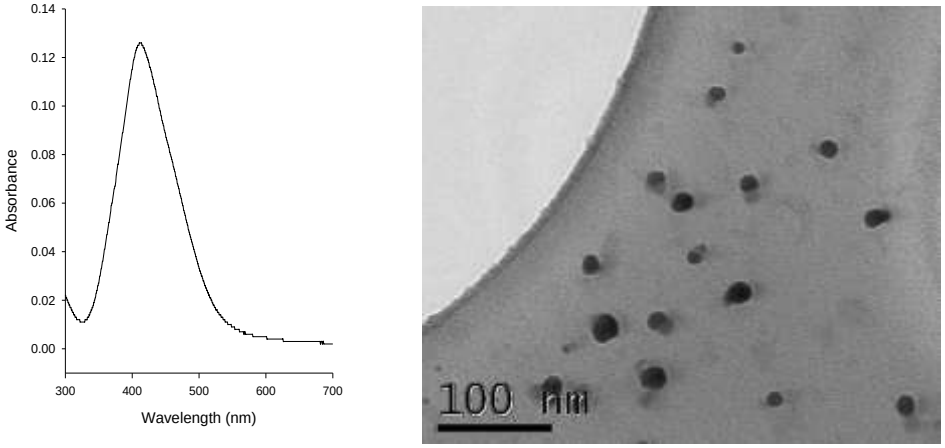

Figure 3. 2 UV-vis spectrum (left) of the 300-NM AgNPs and TEM image (right).

The particle size of the NN-300 AgNPs was analyzed in Milli-Q water with TEM Figure 3. 3. The particle size between samples was compared with the non-parametric test Mann-Whitney test as the particle size distribution did not follow a normal distribution.

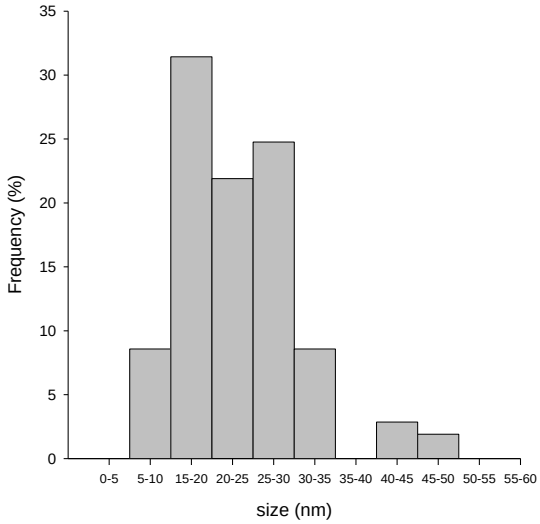

Figure 3. 3 Frequency distribution of NM-300 AgNPs according to particle size analyzed with TEM Mean ± SD =18.2 ± 7.3nm, Median =16.6; Q_{25} =13.4; Q_{75}=21.7; n= 105.

3.1.2.1. Effects of salinity on NM-300 AgNPs physicochemical properties

The effects of NaCl on AgNPs stability were analysed with DLS and UV–vis spectroscopy depicted in Figure 3. **4** and Figure 3. **5** (a-c) respectively. A two way ANOVA found that the factors of time and NaCl concentration, and the interaction of

both factors affected significantly the average particle size of the AgNPs ($p < 0.001$) (Figure 3. 4 A). The Bonferroni post-hoc test determined statistically significant differences ($p<0.05$) between the three different concentrations of NaCl, and between the 0 hr and the other two time points (24 and 48 hr). On the other hand, the concentration of NaCl affected significantly the zeta potential of AgNPs ($p < 0.001$) whereas the factor time did not. The Bonferroni post-hoc test found statistically significant differences ($p<0.001$) between the zeta potential of the AgNPs dispersed in 0 g L^{-1} of NaCl and the AgNPs dispersed in 10 and 20 g L^{-1} NaCl (Figure 3. 4 B).

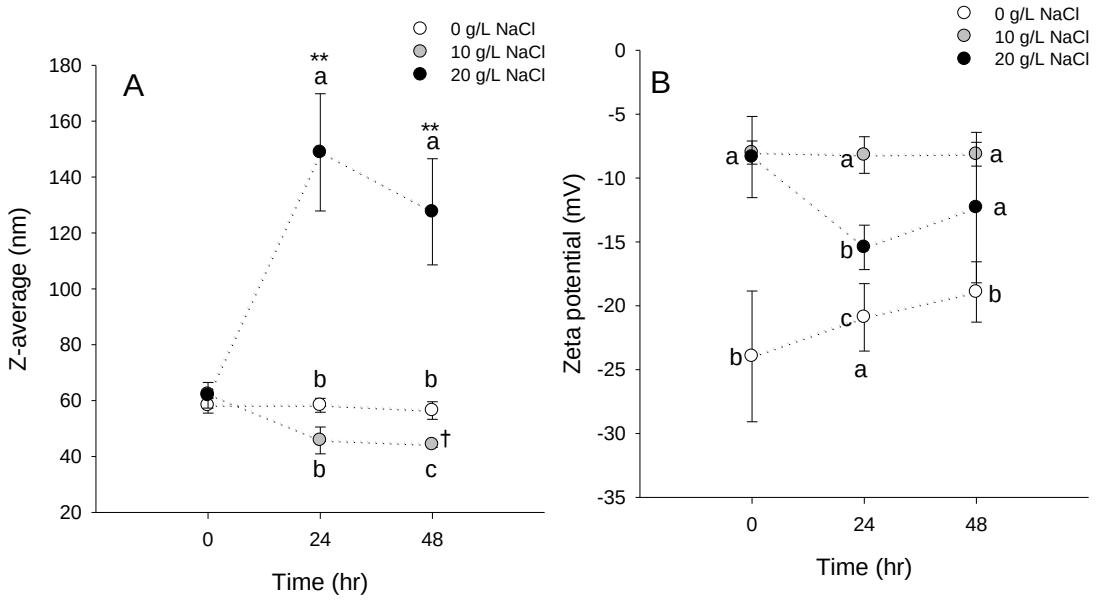

Figure 3. 4 Average particle size or z-average (left, A) and zeta potential (right, B) of the NM-300 AgNPs suspensions expressed as the mean ± SD (n=3). ** symbolizes statistically significant differences ($p< 0.010$, RM-ANOVA) within the treatment NaCl 20 g L^{-1} between the time points 0 hr -24 hr and 0 hr - 48 hr. † symbolizes statistically significant differences (RM ANOVA, $p< 0.05$) within the treatment NaCl 10 g L^{-1} between the time points 0 hr -48 hr and 24 hr - 48 hr. Data points with different letters show statistically significant differences between NaCl concentrations ($p< 0.05$, One way ANOVA).

The UV–vis analysis showed that at higher NaCl concentrations, the intensity of the peak absorbance of the AgNPs suspensions became lower during the course of the exposure.

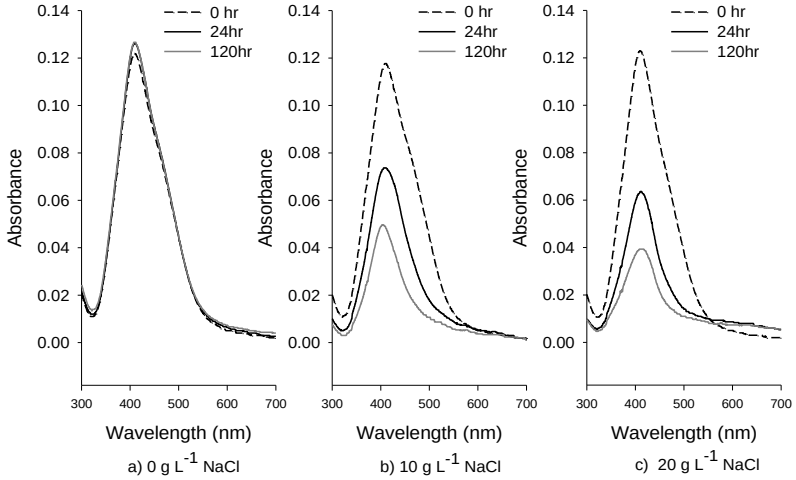

Figure 3. 5 Absorbance (mean value, n=3) of AgNPs in the UV-spectrum exposed to different salinities: a) 0 g L^{-1} NaCl; b) 10 g L^{-1} NaCl and c) 20 g L^{-1} NaCl.

Preliminary analysis with UV-vis spectroscopy and NaCl concentration ranging between 0 and 30 g L^{-1} showed no apparent differences in the persistence of the NM-300 AgNPs at 20 and 30 g L^{-1} (Figure 3. 6).

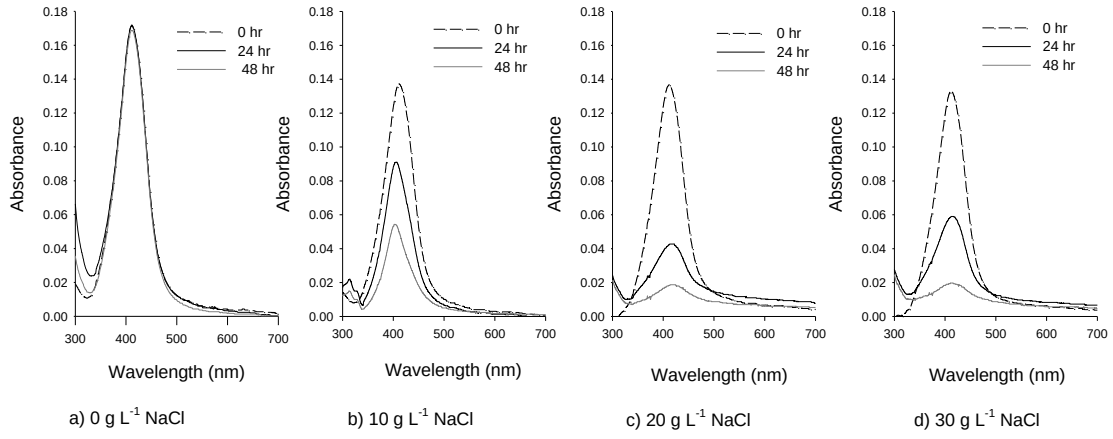

Figure 3. 6 Absorbance (mean value, n=3) of AgNPs in the UV-spectrum exposed to different concentrations of NaCl: a) 0 g L^{-1} NaCl; b) 10 g L^{-1} NaCl c) 20 g L^{-1} NaCl and d) 30 g L^{-1} NaCl.

3.1.2.2. Silver speciation calculated with Visual MINTEQ (3.1)

The speciation of silver dissolved from AgNPs in media containing NaCl (10 and 20 g L^{-1}) and seawater (31 ‰) was calculated with Visual MINTEQ (3.1). The results obtained show that Na, Cl and Ag species would dissolve completely, see the output of Visual Minted in Figure 3. 7.

Distribution of components between dissolved, sorbed and precipitated phases **10 g L^{-1} NaCl**
(Concentrations in molal)

Component	Total dissolved	% dissolved	Total sorbed	% sorbed	Total precipitated	% precipitated
Ag+1	1.3915E-05	100.000	0	0.000	0	0.000
Cl-1	1.7112E-01	100.000	0	0.000	0	0.000
H+1	-2.7456E-07	100.000	0	0.000	0	0.000
Na+1	1.7112E-01	100.000	0	0.000	0	0.000

Distribution of components between dissolved, sorbed and precipitated phases **20 g L^{-1} NaCl**
(Concentrations in molal)

Component	Total dissolved	% dissolved	Total sorbed	% sorbed	Total precipitated	% precipitated
Ag+1	1.3915E-05	100.000	0	0.000	0	0.000
Cl-1	3.4223E-01	100.000	0	0.000	0	0.000
H+1	-3.0554E-07	100.000	0	0.000	0	0.000
Na+1	3.4223E-01	100.000	0	0.000	0	0.000

Distribution of components between dissolved, sorbed and precipitated phases **Seawater (31‰)**
(Concentrations in molal)

Component	Total dissolved	% dissolved	Total sorbed	% sorbed	Total precipitated	% precipitated
Ag+1	9.2760E-06	100.000	0	0.000	0	0.000
Cl-1	4.8346E-01	100.000	0	0.000	0	0.000
H+1	-3.1358E-07	100.000	0	0.000	0	0.000
Na+1	4.1545E-01	100.000	0	0.000	0	0.000

Figure 3. 7 Distribution of components calculated with Visual MINTEQ.

The species distribution calculated with Visual MINTEQ (Figure 3. **8**) shows that at a concentration of 10 g L^{-1} NaCl, the 0.024% of the total concentration of silver will remain as Ag^{+}. In contrast, at 20 g L^{-1} NaCl and in seawater, all the silver would be complexed with chloride.

10 g L^{-1} NaCl		
Component	% of total concentration	Species name
Cl-1	95.429	Cl-1
	4.553	NaCl (aq)
	0.012	AgCl2-
Ag+1	0.024	Ag+1
	21.707	AgCl3-2
	4.837	AgCl (aq)
	73.431	AgCl2-
Na+1	95.447	Na+1
	4.553	NaCl (aq)

20 g L^{-1} NaCl		
Component	% of total concentration	Species name
Cl-1	92.261	Cl-1
	7.730	NaCl (aq)
Ag+1	37.036	AgCl3-2
	2.005	AgCl (aq)
	60.953	AgCl2-
Na+1	92.270	Na+1
	7.730	NaCl (aq)

Seawater (31‰)		
Component	% of total concentration	Species name
Cl-1	90.248	Cl-1
	9.748	NaCl (aq)
Ag+1	52.948	AgCl3-2
	1.014	AgCl (aq)
	46.036	AgCl2-
Na+1	88.657	Na+1
	11.343	NaCl (aq)

Figure 3. 8 Visual MINTEQ output: species distribution.

3.1.2.3. Characterization of the NM-300 AgNPs in broth medium ZM/10

The particle size of the NM-300 in the broth medium (ZM/10) where toxicity tests were carried out was analyzed with TEM and AFM. The concentration of Na^+ and Cl^- in ZM/10 broth medium based on the salinity measurement is 13.3 g L^{-1} Cl^- and 7.4 Na^+ (75% sea water) , equivalent to 20 g L^{-1} of NaCl (previous section 3.1.2.1).

3.1.2.3.1. Size characterization in broth medium with AFM

The size of the NM-300 AgNPs dispersed in ZM/10 broth medium was analyzed with AFM at the beginning of the exposures and after 24 hr (Figure 3. 9 a-b).

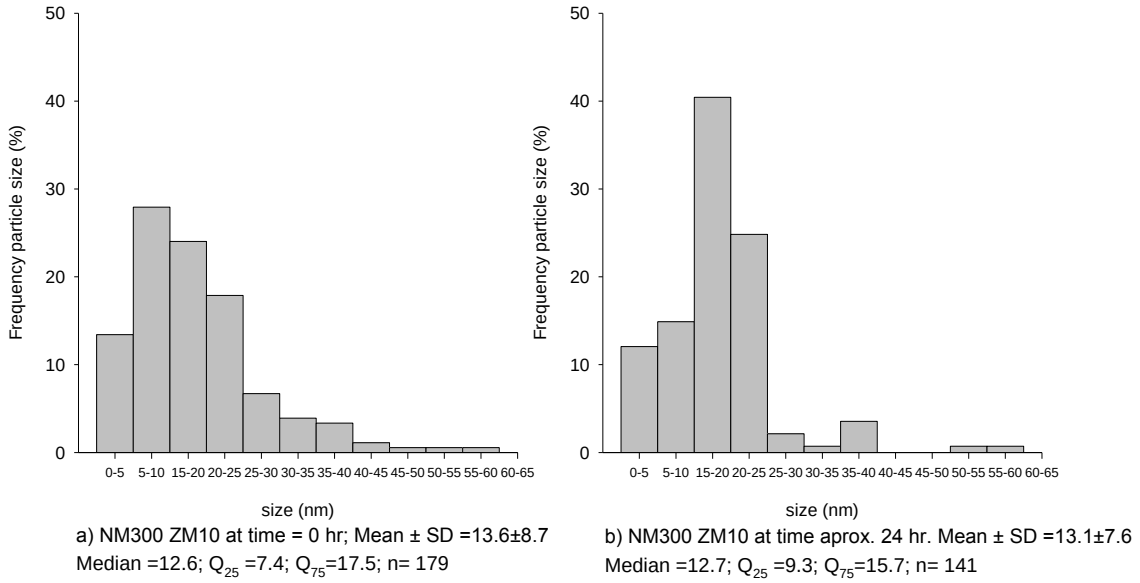

Figure 3. 9 Frequency size distribution of the NM-300 AgNPs in bacterial broth medium (ZM/10) analyzed with AFM after (a) 0 hr and (b) 24 hr.

Particle size data did not follow a normal distribution (data analyzed with Kolmogorov-Smirnov and Shapiro –Wilk tests), and for this reason the particle size at the two different time points (0 and 24 hr) was compared with the non parametric Wilcoxon signed-rank test for related samples (the AgNPs analyzed at 0 hr and 24 hr were not the same, but they were extracted from the same suspension), and no statistically significant differences were found in terms of the mean particle size (p-value = 0.914). If the samples at time 0 hr and 24 hr are regarded as independent samples, the Mann-Whitney test can be used to compare particle size at 0 hr and 24 hr. No statistically significant differences between the mean size at 0 and 24 hr were found (Mann-Whitney test, p-value = 0.98), similar to the analysis performed with Wilcoxon signed-rank test. However, the particle size frequency distribution revealed a shift towards greater particle sizes: at 0 hr the dominant particle size range (28%) was between 5-10 nm whereas 24 hr later 40% of the NPs ranged between 15 – 25 nm. The AFM images showed that particle density was higher at 0 hr than after 24 hr (Figure 3.10 a-b respectively). The presence of big aggregates that could be AgNPs, silver-complexes or salts was observed (Figure 3.10 b-B3).

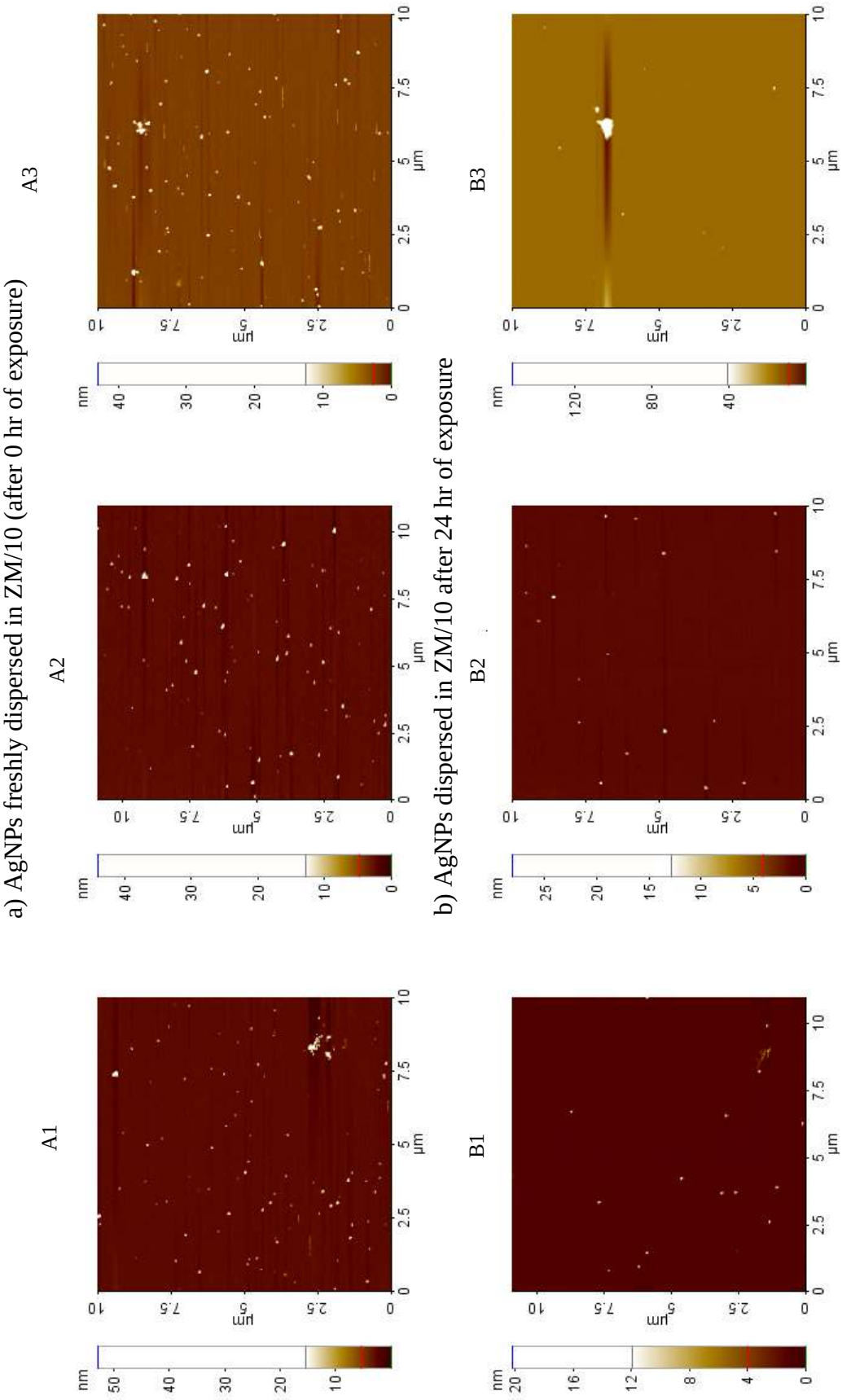

Figure 3. 10 AFM images of the NM-300 AgNPs dispersed in ZM/10 broth medium (a) freshly prepared (0 hr) and (b) after 24 hr exposure

3.1.2.3.2. Characterization in broth medium ZM/10 with TEM

TEM images of AgNPs dispersed in ZM/10 at 0 hr (Figure 3. 12) and after 24 hr (Figure 3. 13) were analyzed with ImageJ®. The particle size data was analyzed similarly to the data obtained with AFM. The frequency intervals to depict the frequency distribution of the particles according to their size were established at 5 nm. The number of particles in each interval was depicted as the relative percentage over the total number of particles (Figure 3. 14). The particle size distribution was not normally distributed (Kolmogorov-Smirnov and Shapiro–Wilk tests, p-value = 0.000) but contrary to AFM results, the mean particle size was statistically significantly higher after 24 hr in ZM10 broth medium (Mann Whitney test p-value = 0.016).

No differences in particle size were found between the AgNPs dispersed in Milli-Q water and the AgNPs just dispersed in the ZM/10 broth medium at time 0 hr (Mann Whitney test, p-value = 0.983). As observed with the AFM particle size analysis, there was a shift towards higher particle sizes between both time points. The relative frequency between 15-20 nm decreased from 24 to 17.3% and the number of particles ranging between 25-30 nm increased from 17 to 24 %.

The AgNPs 300-NM dispersed in ZM/10 medium after 0 hr and 24 hr of exposure and imaged with TEM are depicted in Figure 3. 12 and Figure 3. 13

Figure 3. 11 AFM images of the NM-300 AgNPs dispersed in ZM/10 broth medium (a) freshly prepared (0 hr) and (b) after

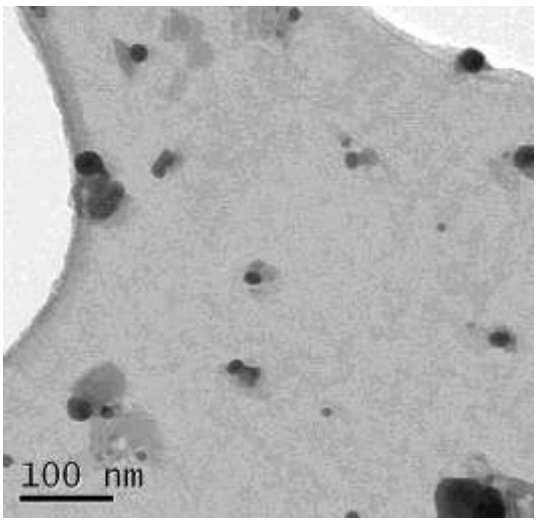

Figure 3. 12 TEM image of the NM-300 AgNP type freshly dispersed (t = 0 hr) in ZM/10

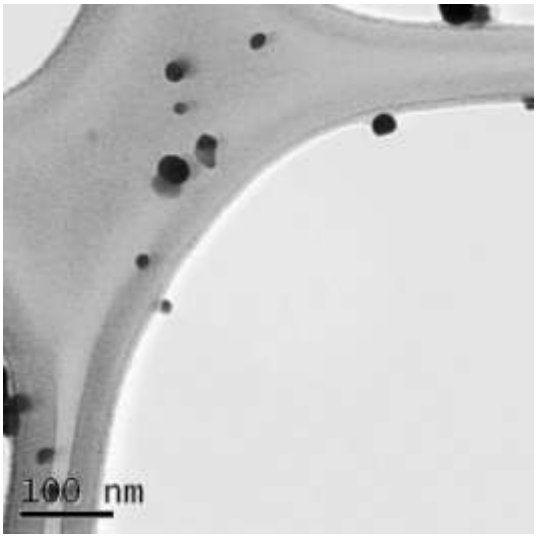

Figure 3. 13 TEM image of the NM-300 AgNP type after 24 hr of exposure in ZM/10

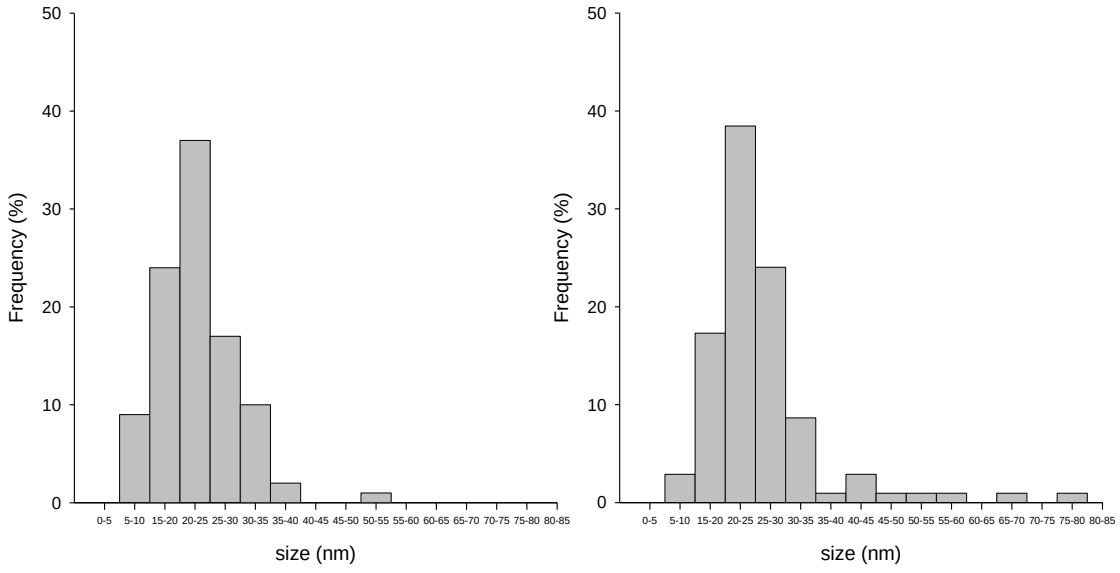

Figure 3. 14 Frequency of the particle size distribution of the NM-300 AgNPs dispersed in bacterial broth medium (ZM/10) analyzed with TEM after (a) 0 hr and (b) 24 hr.

Differences in terms of the particle size analyzed with AFM and TEM in broth medium ZM/10 were compared at each time point 0 and 24 hr with the non-parametric Mann Whitney test (when samples were regarded as independent) and Wilcoxon Signed Rank test (when samples were regarded as paired). With both tests it was estimated that the difference in the median values of the particle size measured with TEM was significantly larger (p-value < 0.001 and 0.016 respectively) than the particle size analyzed with AFM. A summary of the particle size characterization of the NM-300 AgNPs in different media and time points is provided in Table 3.1. The TEM and DLS values measured in Milli-Q are similar to the values reported by the JCR. However the

DLS analysis showed that after 24 hr, AgNPs agglomerated in medium containing 20 g L^{-1} NaCl.

Table 3. 1 Summary of the particle size (nm) of the NM-300 AgNP type measured with DLS, AFM and TEM in different media, milli-Q and ZM/10 or NaCl at two different time points.

	JCR (Klein *et al.*, 2011)		**Milli-Q**			**NaCl[a]** **(20 g L^{-1})**	**ZM/10 (containing ~ 20 g L^{-1} NaCl)**	
Time (hr)	DLS	TEM Nanopure water	DLS	AFM	TEM	DLS	AFM	TEM
0	50-70	17.24±3.17	58.25±2.74	N/A	18.2 ± 7.3 Q_{25}: 13.4 Median: 16.6 Q_{75}:21.7	61.9 ± 4.59	13.6 ± 8.7 Q_{25}: 7.4 Median: 12.6 Q_{75}:17.5	17.8 ± 6.5 Q_{25}: 13.7 Median: 16.6 Q_{75}:22.4
24			58.33 ±2.47	n/a	n/a	148.84 ± 21	13.1 ± 7.6 Q_{25}: 9.3 Median: 12.7 Q_{75}:15.7	20.8 ± 9.6 Q_{25}: 15.8 Median: 19.2 Q_{75}:22.0

[a] Equivalent concentration of chloride in the ZM/10 medium

N/A: not available

3.1.3. Mesosilver AgNPs

The Mesosilver Hot Tube ® product was analyzed with UV-vis spectroscopy, DLS and microscopy (TEM and AFM) in order to identify the presence of nanoparticles and their size. The concentration of total silver with AAS and ionic silver with the ISE confirmed that the product contained silver. The peak at 390 nm (Figure 3.15a) is characteristic of the AgNPs surface plasmon resonance and the TEM microscopy images (Figure 3.15b) indicated the presence of nanoparticles in the Mesosilver product. The quality of the TEM images of Mesosilver AgNPs dispersed in Milli-Q water was poor, for this reason the TEM image of nanoparticles freshly dispersed in ZM/10 is depicted in (Figure 3.15 b).

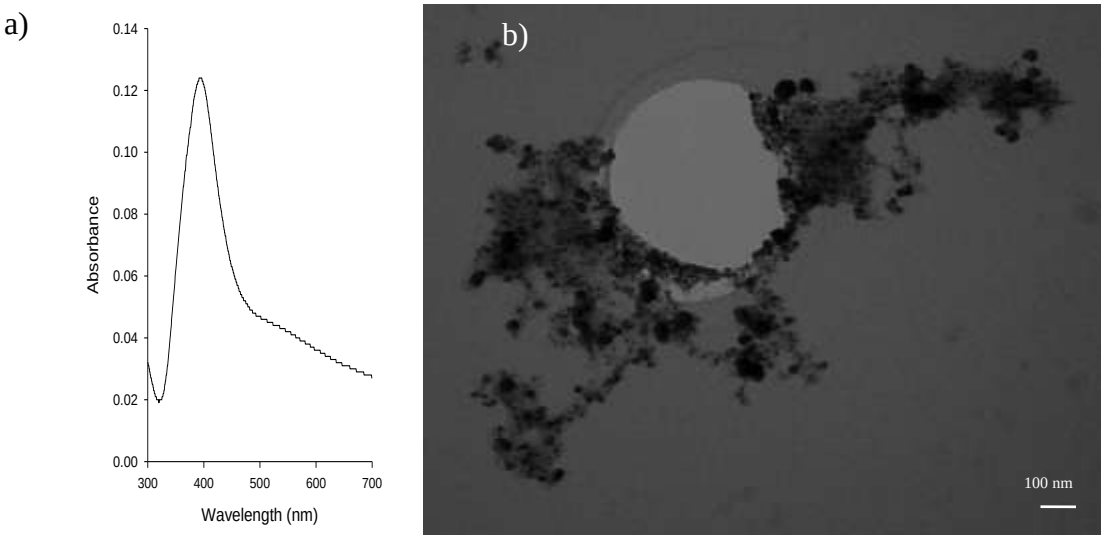

Figure 3.15 Mesosilver AgNPs freshly dispersed absorbance in the UV-vis spectrum in Milli-Q water (left) and b) image obtained with TEM (t = 0 hr) in ZM/10 TEM (right).

The DLS analysis of Mesosilver AgNPs in Milli-Q water showed that the suspension was very polydispersed (Figure 3.15), which was confirmed by the quality report analysis; the particle distribution exhibited very different size ranges as was also observed with the particle size TEM analysis. The analysis of the particle with TEM was not feasible due to the low magnification of the images (x 40000), however the AFM analysis was feasible and the particle size distribution is depicted in Figure 3.17.

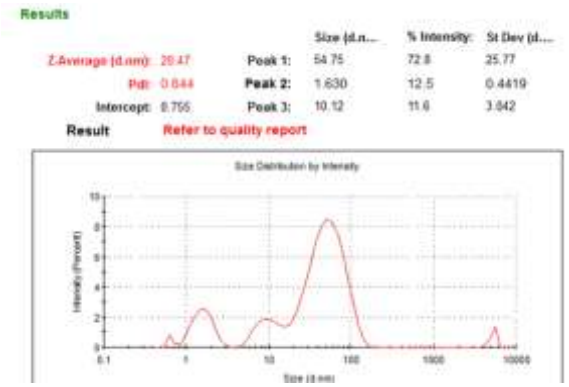

Figure 3.16 Size distribution analyzed by intensity using DLS.

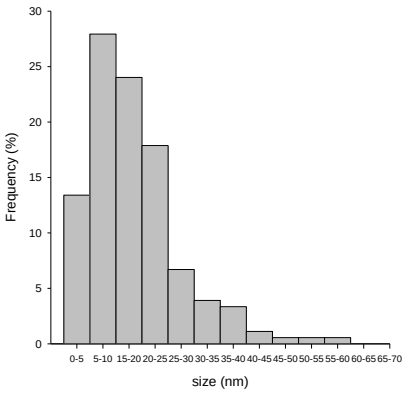

Figure 3.17 Particle size distribution of Mesosilver AgNPs analyzed with AFM in milli-Q water. Mean ± SD 10.5 nm ± 8.9, Median = 9.9 nm; Q_{25} =5.3; Q_{75}=13.6; n= 156.

The Zeta-Potential analysis in Milli-Q water indicated that the Mesosilver AgNPs were negatively charged, the mean value ± SD was -26 ± 10.86 mV (n=4). The quality report of the results was not always good, for this reason the most reliable value for the Zeta-Potential for this type of AgNPs was around -35.8 ± 2.545 mV (n=2). A good measurement of the Zeta-Potential analysis for this nanoparticle type is depicted in the Figure 3. 18.

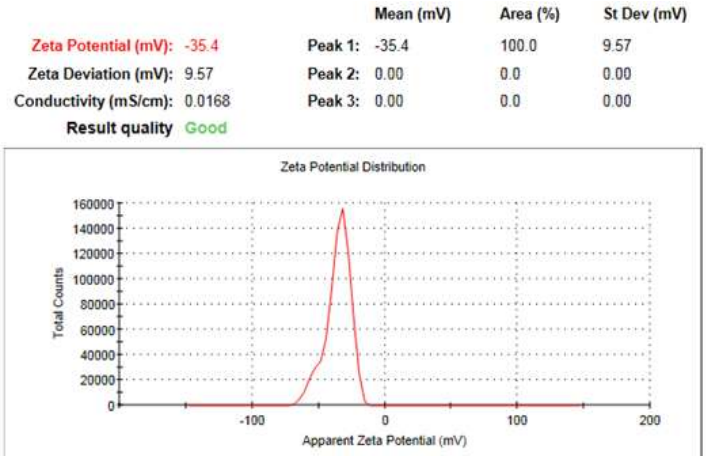

Figure 3. 18 DLS report related to the Zeta-Potential analysis of the Mesosilver Hot tube suspension.

The atomic absorption spectroscopy (AAS) analysis of the Mesosilver product determined that the concentration of total silver in the product was 101.76 ± 0.928 mg L^{-1}. The percentage of ionic silver measured with the ISE corresponded to 14.6%. The sensitivity of the ISE to distinguish between different concentrations of ionic silver according to different concentrations of the Mesosilver product was assessed. The matrix of the standards used to calibrate the ISE Electrode was 100% milli-Q water. For this reason the measurements of Mesosilver suspensions diluted in milli-Q product may be more reliable due to greater similarities in the composition of the matrix. This is

confirmed by the better correlation observed between the difference of potential measured (mV) with the ISE (ionic silver) and the concentration of the Mesosilver when the product has been diluted in milli-Q water (Figure 3. 19).

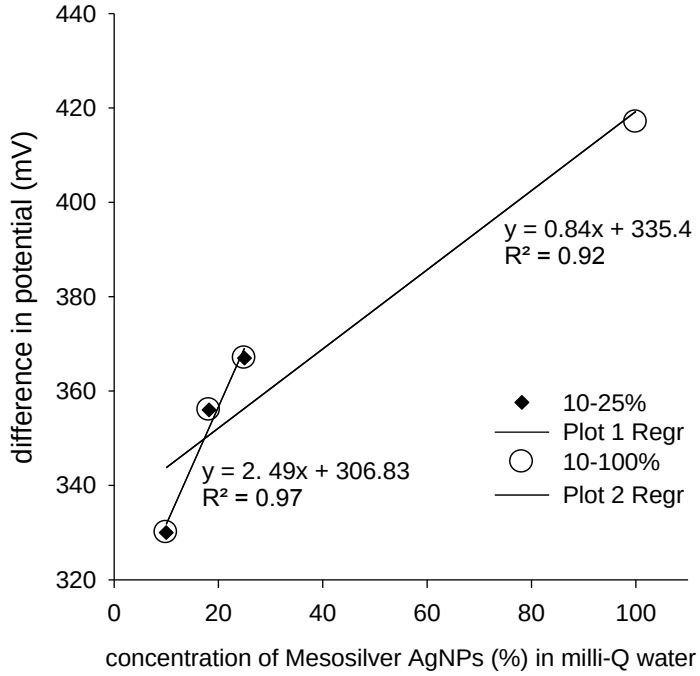

Figure 3. 19 Relation between different dilutions (different concentrations of Mesosilver AgNPs expressed as %) of the Mesosilver and difference in potential (n=1).

The manufacturer of the Mesosilver product described the product as colloidal silver dispersed in water, however they did not provide any certificate of analysis, thus there is uncertainty about the exact composition of the product. The label on the Mesosilver Hot tube bottle indicated that the concentration of silver in the product was 200 ppm (uncertified, ionic silver concentration was not specified) whereas the AAS analysis revealed it was 50% lower (101.76 ± 0.928 ppm).

3.1.4. Summary

A summary of the physicochemical characteristics (in Milli-Q water) of the three different AgNP types are summarized in Table 3. 2.

Table 3. 2 Summary of the physicochemical characteristics of the AgNPs under study

AgNP type	Z-Average (nm)	Zeta potential (mV)	Size (TEM) (nm)	Size (AFM) (nm)	% ionic silver	UV-vis peak absorbance (nm)
NM-300	58.25±2.74	-22.3 ± 3.3	18.2 ± 7.3	13.6 ± 8.7	4.93	~ 412
Mesosilver Hot tub	17.13±2.31	-26 ± 10.86	N/A	10.5 ± 8.9	11.63	~ 394
Sigma Aldrich	191.8 ± 55.8	- 23.1 ± 8.4	N/A	N/A	8.23	~ 410

N/A: Not available

3.2. Toxicity tests with pure cultures

The bacterial strains depicted in Table 3. 3 were used in the AgNPs exposures.

Table 3. 3 Characteristics of the bacterial species exposed to different AgNP types

Species name(16S RNA gene partial sequence)	Phenotypic characteristics	Cell	Colony
Arthrobacter agilis	Catalase(-) Oxidase (+++) Agarase (-) Motility(-) Gram positive		
Streptomyces koyangensis	Catalase(-) Oxidase (++) Agarase (-) Motility(-) Gram positive	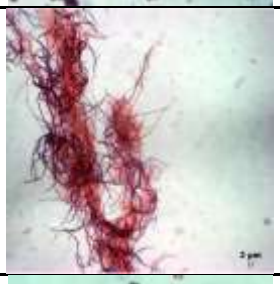	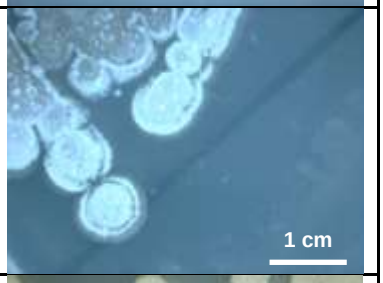
Bacillus weihenstephanensis	Catalase(++) Oxidase (-) Agarase (-) Motility(-) Gram positive		
Pseudoalteromonas aliena	Catalase(+) Oxidase (+) Agarase (+) Motility(+) Gram negative	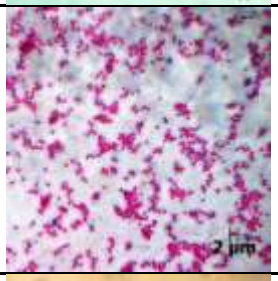	
Pseudoalteromonas arctica	Catalase(+) Oxidase (+) Agarase (+) Motility(+) Gram negative	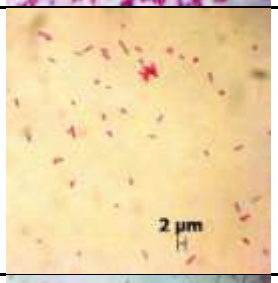	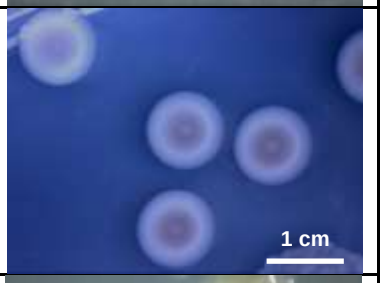
Cellulophaga fucicola	Catalase(+) Oxidase (-) Agarase (++) Motility(+) Gram negative		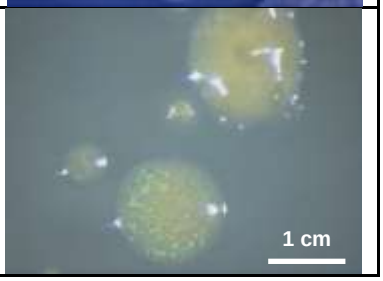

-: negative result for the test; +: weak positive response; ++:moderate positive response; +++: strong positive response

The strains included in Table 3.3 exhibit very different phenotypic differences not only in terms of the bacterial envelope structure (Gram positive/Gram negative), but they were also very different in terms of size, shape, life style (i.e. single cells or forming aggregates).

3.2.1. Growth curves

Four different strains (*P.aliena, C.fucicola, A.agilis* and *B. weihenstephanensis*) were chosen to develop toxicity tests with the NM-300 and Mesosilver AgNPs as these were the most adequate candidates based on the characteristics of their bacterial envelope (Gram positive/ Gram negative), size and cell morphology (surface area). These were relevant characteristics to investigate the antibacterial properties of AgNPs. The relationship between the optical density (OD 600nm) and the colony forming units CFU) on plates was calculated and depicted in Figure 3. 20.

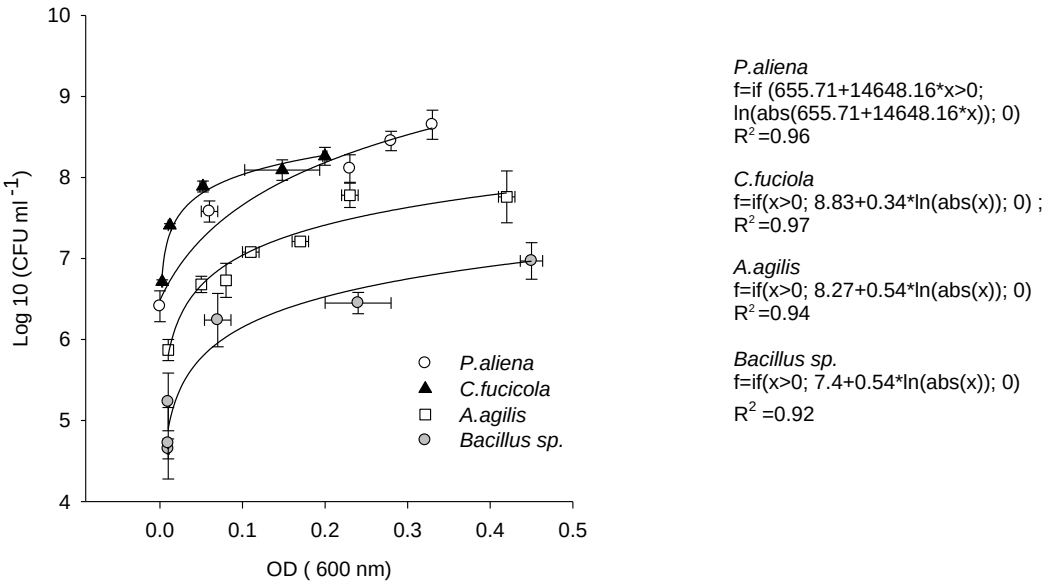

Figure 3. 20 Regression curves and associated equations estimated for the relation between the OD (600 nm) and CFU ml $^{-1}$ for the different bacterial species exposed to 300-NM AgNPs.

3.2.2. Toxicity of NM-300 and Mesosilver AgNPs in 50 ml flasks

The growth of four bacterial species, monitored with OD_{600}, under different concentrations of the 300-NM will be covered in the present section. The effect of the NM-300 AgNP type on the bacterial viability was also investigated with bacterial plate counts. Overall it was observed that at higher concentrations of AgNPs the lag phase was extended.

3.2.2.1. Cellulophaga fucicola

The bacterial growth measured with OD_{600} showed low variability within the different treatments (Figure 3. 21a). The nominal IC_{50} OD_{600} for NM-300 was 375 ppb (measured concentration 307 ppb, Figure 3. 21b). There was no apparent recovery of growth at 1500 ppb (nominal) , although cell cultures were found to still be viable (CFU formed on agar plates free of AgNPs, data not registered) after 24 hr of exposure.

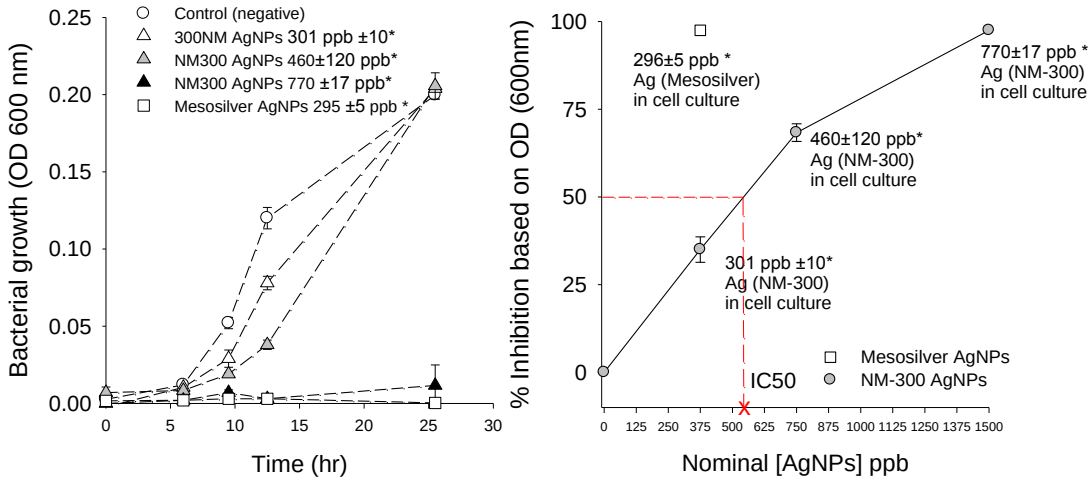

a) *C.fucicola* OD vs time

b) Bacterial growth inhibition based on OD

Figure 3. 21 Growth of *C. fucicola* under different concentrations of NM-300 AgNPs measured with OD_{600} (a) expressed as the Mean (OD 600 nm) ± SD, and (b) growth curve inhibition (%) based on the OD measurements (registered at t=13 hr) expressed as Mean (% inhibition) ± SD.* indicates the total concentration of silver measured with AAS in the cell cultures after the exposures.

The bacterial plate counts showed that the bacterial viability was statistically significantly lower at 1500 ppb compared to the beginning of the exposures (One Way ANOVA, p=0.044). Over the following hours differences in bacterial viability were observed between the control treatment and the treatment containing AgNPs at 750 ppb (Figure 3. 22). The bacterial viability recovered in the presence of AgNPs (750 ppb) after 12.75 hr of exposure.

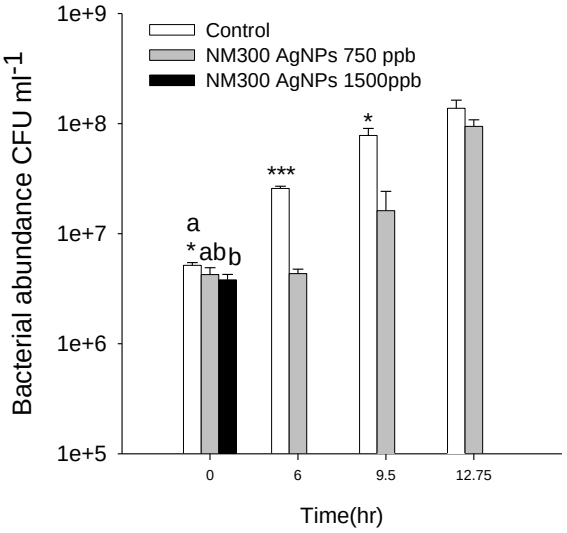

Figure 3. 22 Cell viability expressed as the Mean ± SD of the CFU formed in agar plates under different concentrations of NM-300 AgNPs. Columns with different letters are significantly different, (One Way ANOVA, $p<0.05$). *, **, *** symbolizes statistically significant differences ($p < 0.05$), ($p < 0.01$), ($p < 0.001$), respectively.

Black aggregates formed and settled out in presence of AgNPs (Figure 3. 23). These aggregates were only observed in *C. fucicola* cultures, but not in any other bacterial species at similar AgNPs concentrations.

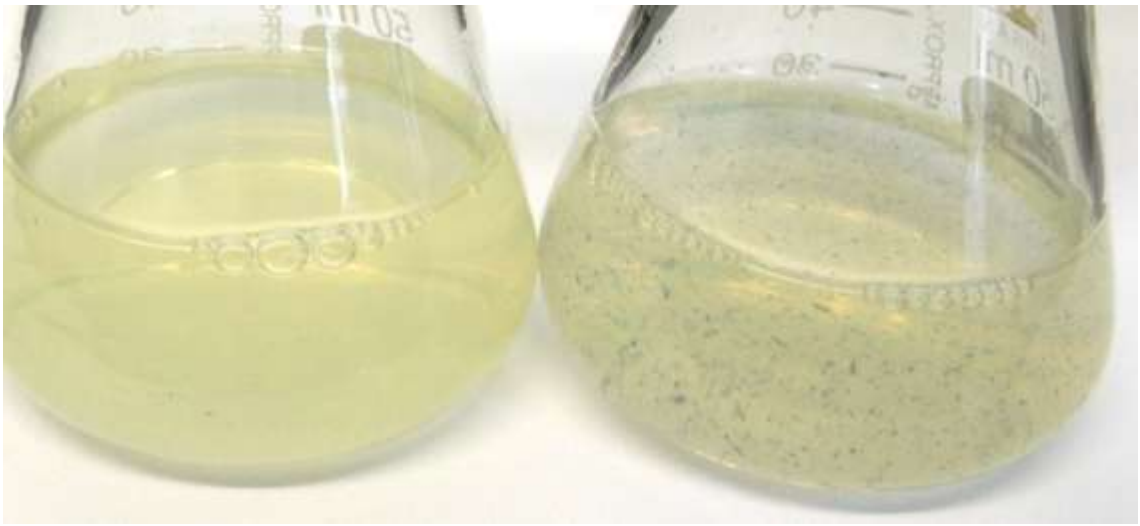

Figure 3. 23 Cell cultures of *C.fucicola*, control (left) and at 750 ppb (right). In presence of AgNPs black aggregates are formed.

3.2.2.2. Arthrobacter agilis

Similarly to *C.fucicola*, the growth of *A.agilis* was delayed with increasing concentrations of the NM-300. At higher AgNPs concentration the lag phase was prolonged (Figure 3. 24a). The NM-300 (IC_{50}) estimated was 125 ppb (66 ppb measured with AAS Figure 3. 24b).

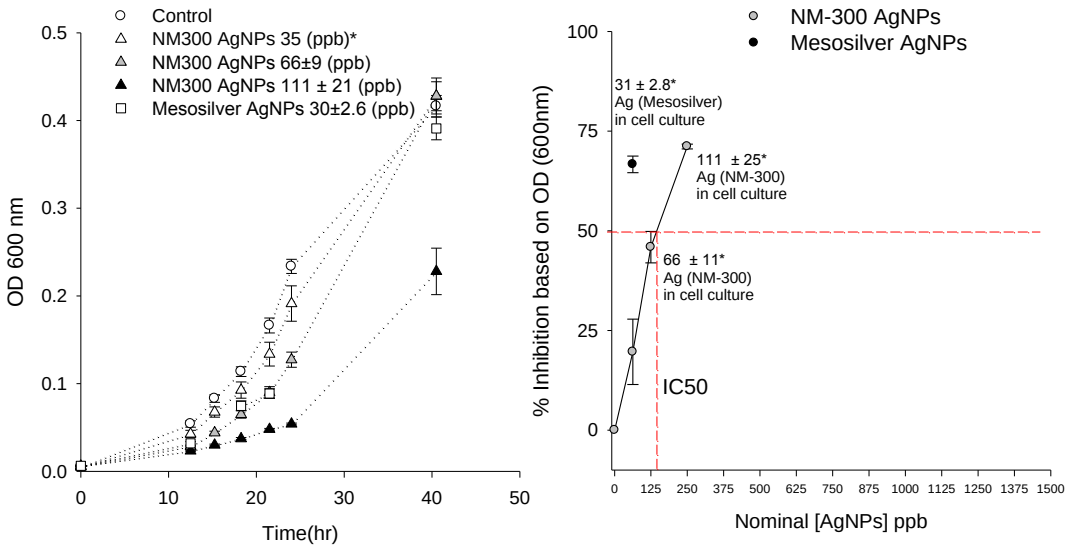

Figure 3. 24 Growth of *A.agilis* under different concentrations of NM-300 AgNPs measured with OD_{600} (a) expressed as the Mean (OD 600 nm) ± SD, and (b) Inhibition curve (OD %) based on the OD measurements (registered at t=21hr) expressed as Mean (% inhibition) ± SD. * indicates the total concentration of silver measured with AAS in the cell cultures after the exposures.

The lag phase observed with the OD_{600} measurements registered at the different concentrations of AgNPs is in agreement with the results related to cell viability obtained with the plate counts (Figure 3. 25).

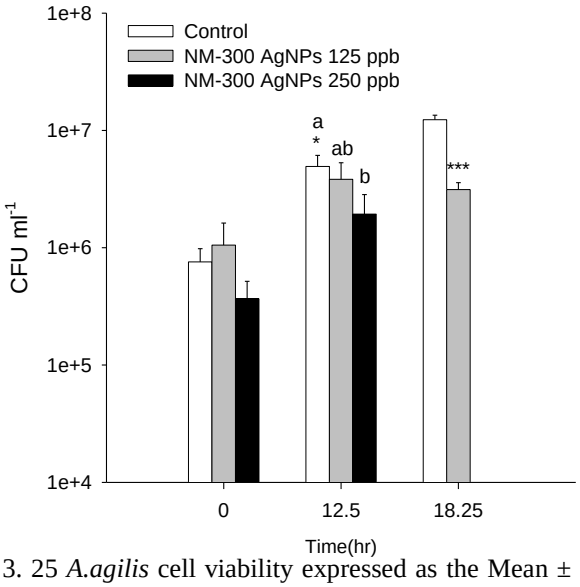

Figure 3. 25 *A.agilis* cell viability expressed as the Mean ± SD of the CFU formed in agar plates under different concentrations of NM-300 AgNPs, n=3. Columns with different letters are significantly different, (One Way ANOVA, $p<0.05$). *, *** symbolizes statistically significant differences ($p < 0.05$), ($p < 0.01$) $p < 0.001$), respectively.

The respirometry results showed inhibition at concentrations of NM-300 AgNPs ≥ 0.25 mg L^{-1} (Table 3. 4). Inhibition of O_2 uptake is calculated having as a reference the value measured in the control treatment (n=1). Thus negative values in the column

named as "Inhibition (%)" means that bacterial activity was greater than in the control treatment, thus no inhibition occurred but a hormetic response was observed at low concentrations < 0.25 mg L^{-1}.

Table 3. 4 Respiration of *A.agilis* at different concentrations of NM-300

Tube	Treatment	Concentration AgNPs (mg L^{-1})	Respiration rate (mg/l/h)	Inhibition (%)
1	Control	0.0	0.28	
2	Dispersant[a]	0.5	0.46	-64.3
3	AgNPs	0.05	0.43	-52.9
4	AgNPs	0.1	0.38	-36.7
5	AgNPs	0.25	0.26	7.6
6	AgNPs	0.5	0.17	39.8

[a] Equivalent concentration of dispersant in 0.5 mg L^{-1} of AgNPs

3.2.2.3. Pseudoalteromonas aliena

It was not possible to determine the IC_{50} for the NM-300 and, based on the results obtained, was estimated to be greater than 1000 ppb (Figure 3. 26b).

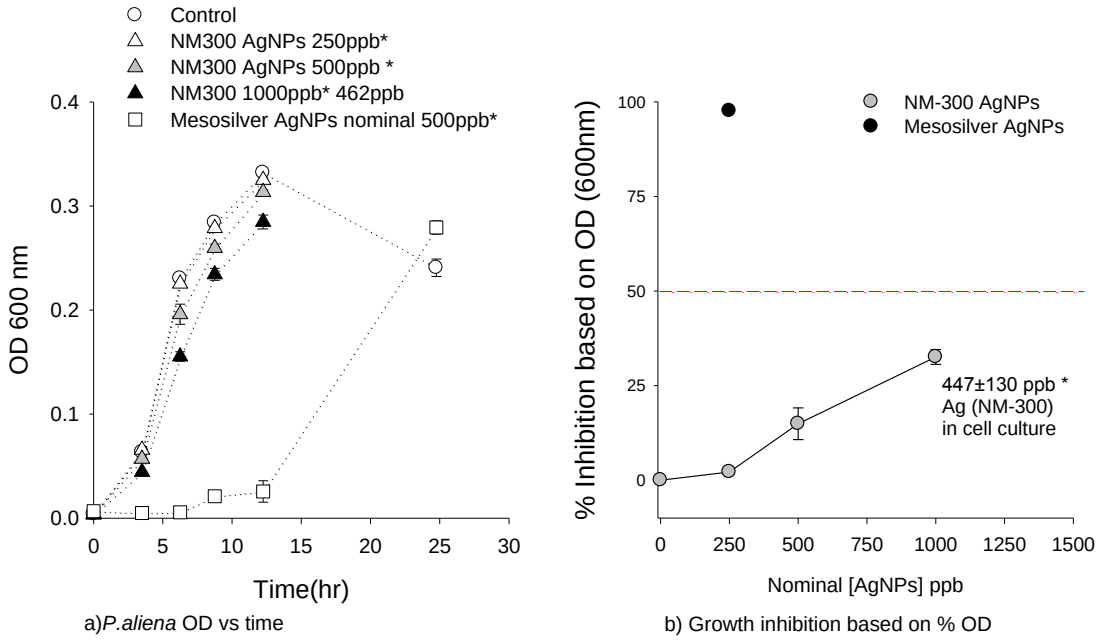

Figure 3. 26 Growth of *P.aliena* under different concentrations of NM-300 AgNPs measured with OD_{600} (a) expressed as the Mean (OD 600 nm) ± SD, and (b) growth inhibition curve (%) based on the OD measurements (t = 6 hr) expressed as Mean (% inhibition) ± SD, n=3. .* indicates the total concentration of silver measured with AAS in the cell cultures after the exposures.

No significant differences in cell viability were observed when the highest difference in the OD_{600} between the control and the treatment at 1000 ppb (nominal) occurred (after 6 hr of exposure) Figure 3. 27.

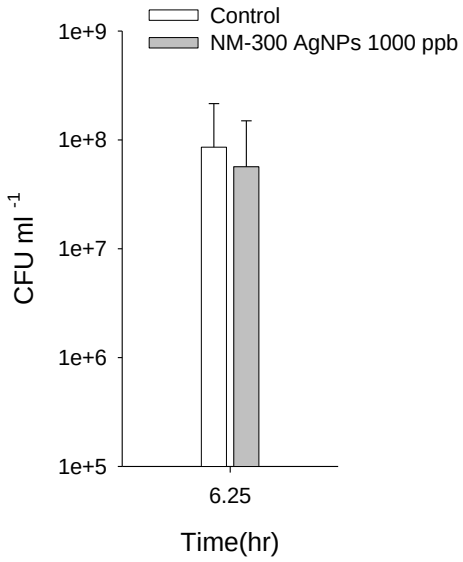

Figure 3. 27 *P.aliena* cell viability expressed as the Mean ± SD of the CFU formed in agar plates, n=3.

The black complexes in the cell culture of *P.aliena* were not formed (Figure 3. 28) as observed previously in the experiment with the *C.fucicola* (Figure 3. 23).

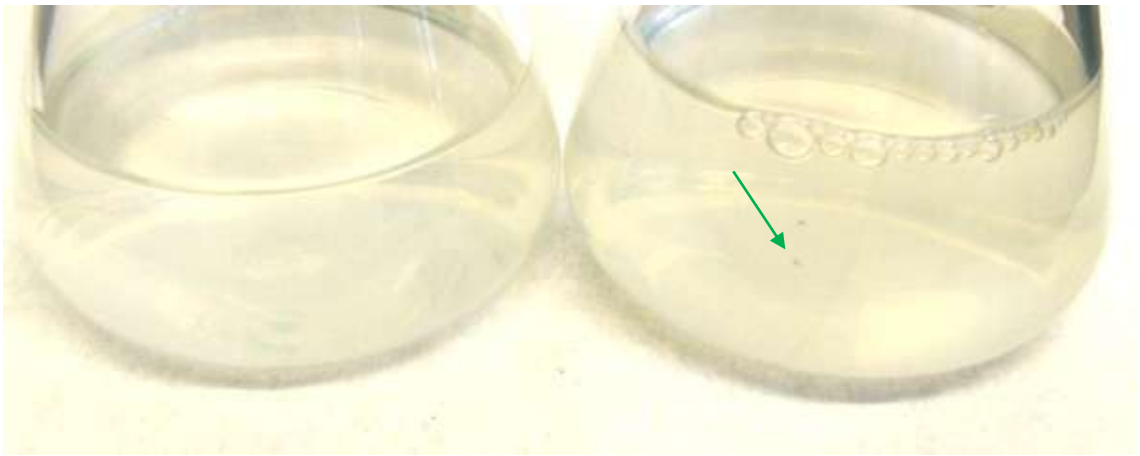

Figure 3. 28 Control (left) and at 1000 ppb (right). Agglomerated AgNPs are observed (green arrow).

The results with respirometry showed inhibition at concentrations of NM-300 AgNPs ≥ 0.1 mg L^{-1} (Table 3. 5).

Table 3. 5 Respiration of *P.aliena* at different concentrations of NM-300

Tube	Treatment	Concentration AgNPs (mg L^{-1})	Respiration rate (mg/l/h)	Inhibition (%)
1	Control	0.0	1.53	
2	Dispersant[a]	1.0	1.92	-25.2
3	AgNPs	0.1	1.31	14.1
4	AgNPs	0.25	1.12	26.9
5	AgNPs	0.5	1.10	28.2
6	AgNPs	1.0	1.07	30.4

[a] Equivalent concentration of dispersant in 1 mg L^{-1} of AgNPs

3.2.2.4. Bacillus sp.

Bacillus sp. was exposed to 300-NM and Mesosilver AgNPs, and based on the results obtained it was concluded that the IC_{50} for NM-300 was between 250 and 125 ppb (nominal, between 99 and 143 ppb measured) see Figure 3. 29. The Mesosilver AgNP at 125 ppb (nominal, approximately 35 ppb real estimated concentration) inhibited the concentration of the *Bacillus sp*., but bacterial growth was restored after 20 hr of exposure.

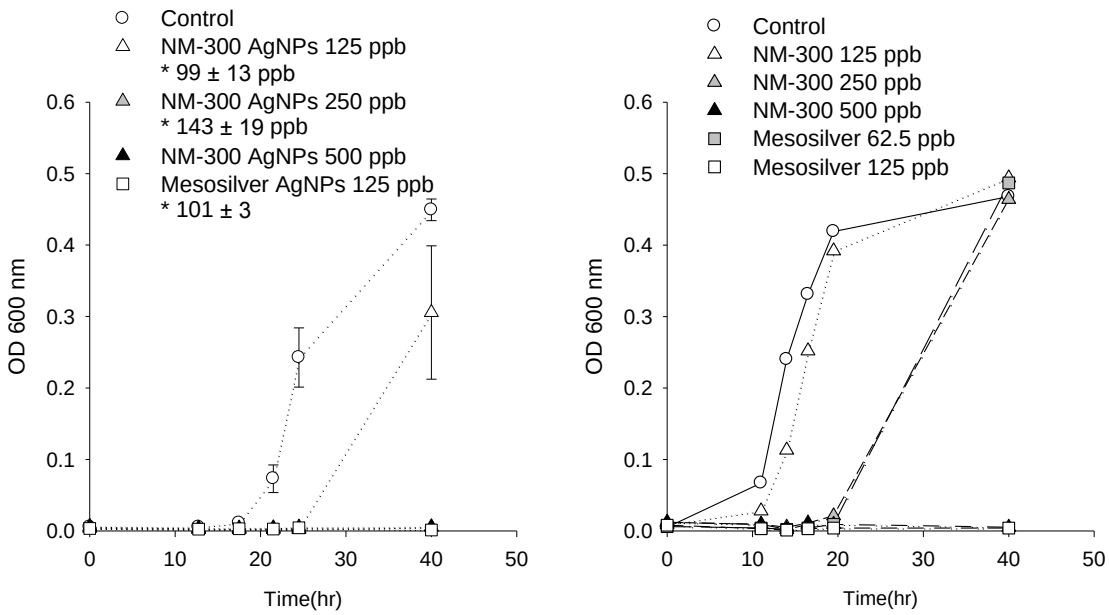

Figure 3. 29 Growth of *Bacillus sp.* under different concentrations of NM-300 and Mesosilver AgNPs measured with OD_{600} expressed as the Mean (OD 600 nm) ± SD, n=3. .* indicates the total concentration of silver measured with AAS in the cell cultures after the exposures.

A summary of the inhibitory concentrations (IC_{50}) of the NM-300 and Mesosilver AgNPs, and $AgNO_3$ are depicted in the Table 3. 6 depicted below:

Table 3. 6 NM-300 and Mesosilver AgNPs inhibitory concentrations (ppb)

Bacterial species	**NM-300**	**Mesosilver**	**$AgNO_3$**
Bacillus	IC_{50} < 143	IC50 <101	IC50<50
C.cellulophaga	IC50=301	IC50 < 296	IC50<100
A.agilis	IC50=66	IC50=31	IC50 ~10
P.aliena	IC50>447	IC50<250	IC50<50

3.2.3. Toxicity test in small volume versus 50 ml flasks

Bacterial growth under different concentrations of the NM-300 was monitored in small volumes (3 ml) for rapid screening of inhibitory concentrations of the NM-300 and Mesosilver AgNPs. Once the IC_{50} values were estimated, similar experiments were carried out in a greater volume of liquid broth medium, 40 ml of the ZM/10 in 50 ml flasks. The bacterial growth in the control treatment was always higher in the 50 ml flasks for all the species tested.

3.2.3.1. A.agilis

The growth of *A.agilis* was 10 times lower in the small test tubes (Figure 3. 30 a) than in the 50 ml flasks (Figure 3. 30 b). Even though the growth measured in the 3 ml volume was low, growth was noticeable by eye, as the cells of this bacterium are pigmented dark pink. The results obtained with small volumes estimated that the NM-300 IC_{50} ranged between 100 ppb and 250 ppb (nominal) agreeing with the results obtained in the 50 ml flasks that indicated an IC_{50} at 125 ppb (nominal).

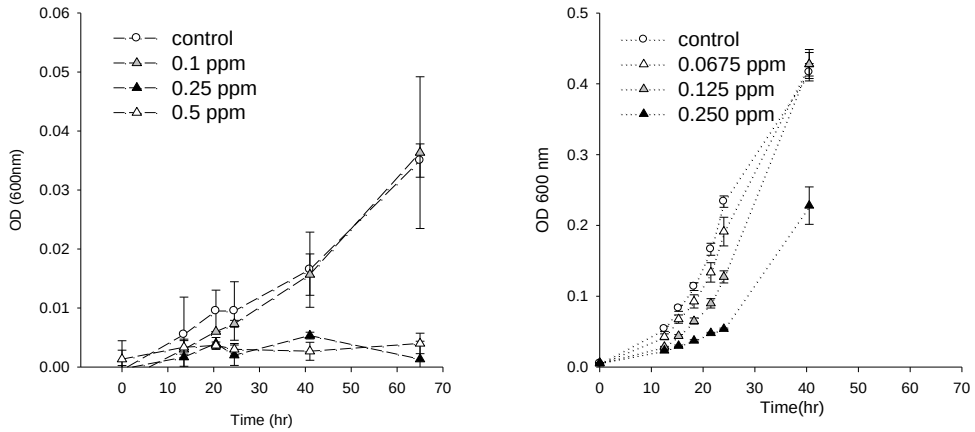

a) *A.agilis* growth monitored with OD in 4 ml volume

b) *A.agilis* growth monitored with OD in 50 ml flask

Figure 3. 30 Growth of *A.agilis* monitored by measuring the OD_{600} under different concentrations of NM-300 in different volumes (a) 3 ml and (b) 40 ml in 50 ml flasks (40 ml final volume). Growth expressed as the Mean (OD_{600}) ± SD, n=3.

3.2.3.2. Bacillus sp.

Similarly to *A.agilis*, the growth of *Bacillus sp.* was lower in the 3 ml than in 50 ml flasks (Figure 3. 31). The IC_{50} observed in small tubes was around 250 ppb, similar to the IC_{50} estimated in 50 ml flasks that ranged between 125 ppb and 250 ppb.

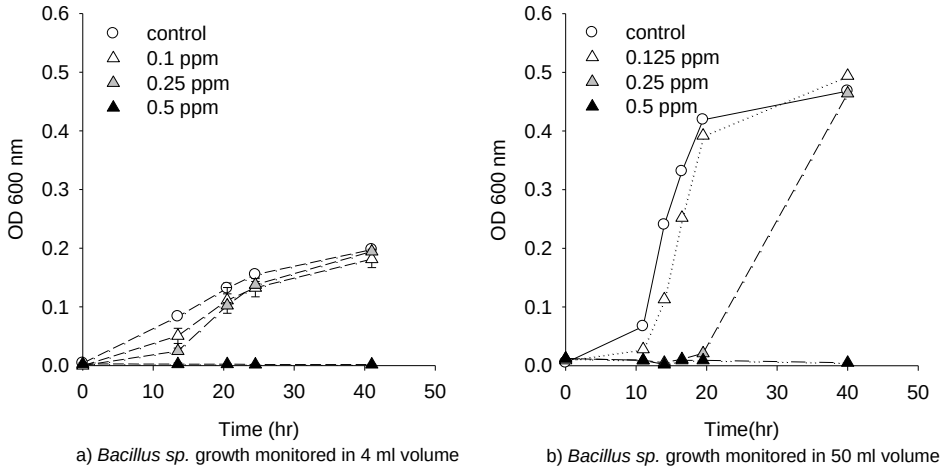

a) *Bacillus sp.* growth monitored in 4 ml volume b) *Bacillus sp.* growth monitored in 50 ml volume

Figure 3. 31 Growth of *Bacillus sp.* monitored by measuring the OD_{600} under different concentrations of NM-300 in different volumes (a) 3 ml and (b) 40 ml in 50 ml flasks. Growth expressed as the Mean (OD_{600}) ± SD, n=3.

3.2.3.3. P.aliena

The IC_{50} observed in 3 ml (Figure 3. 32 a) was lower than in 50 ml flasks (Figure 3. 32 b). It was observed that at 1000 ppb (nominal) the lag phase was longer in a 3 ml volume than in a 50 ml flask, the bacterial growth in the control was also lower, as observed with other species previously.

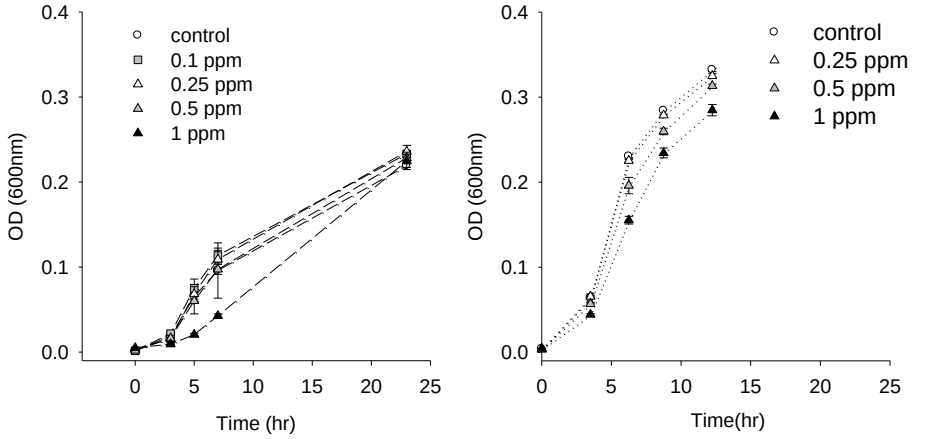

a) *P.aliena* growth monitored with O.D in 4 ml volume b) *P.aliena* growth monitored with O.D in 50 ml flasks

Figure 3. 32 Growth of *P.aliena* monitored by measuring the OD_{600} under different concentrations of NM-300 in different volumes (a) 3 ml and (b) 40 ml in 50 ml flasks. Growth expressed as the Mean (OD_{600}) ± SD, n=3.

3.2.4. Exposure of two different species of the *Pseudoalteromonas* genus to NM-300

The inhibitory concentration of the 300-NM AgNPs on the growth of members of the *Pseudoalteromonas* genus, a very ubiquitous group in the marine and estuarine environment, was investigated in small volumes (3 ml). The results obtained indicated that the IC_{50} was around 500 ppb for both species, although *P.aliena* (Figure 3. 33 a) exhibited higher resistance to NM-300 than the *P.arctica* (Figure 3. 33 b) as the lag phase at 1000 ppb was shorter than for the *P.aliena* species.

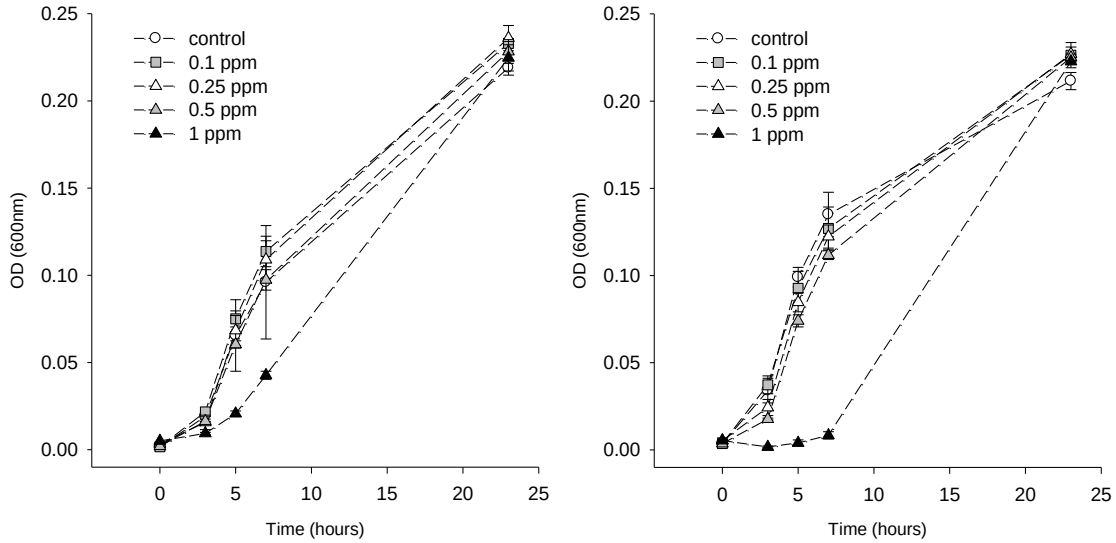

Figure 3. 33 Growth of *P.aliena* (a) and *P.arctica* (b) monitored by measuring the OD_{600} under different concentrations of NM-300 in different volumes (a) 3 ml and (b) 40 ml in 50 ml flasks. Growth expressed as the Mean (OD_{600}) ± SD, n=3.

3.2.5. Comparing toxicity NM300 versus Sigma Aldrich AgNPs

3.2.5.1. Pseudoalteromonas arctica

Preliminary experiments with *P.arctica* indicated that the NM-300 AgNP type (Figure 3. 34b) was more toxic than the AgNPs purchased from Sigma Aldrich (Figure 3. 34a).

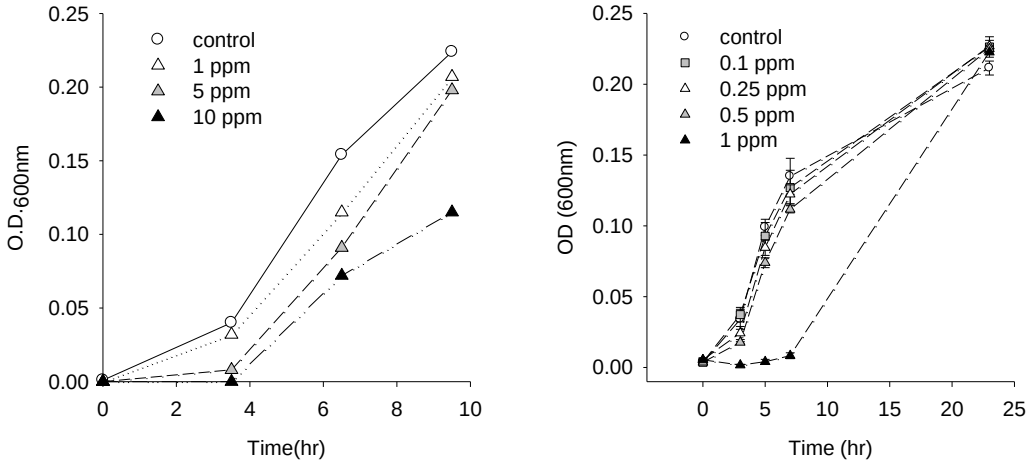

a) *P.artica* (exposure to Sigma Aldrich AgNPs) b) *P.artica* (exposure to NM-300)

Figure 3. 34 Growth of *P.arctica* exposed to different concentrations of Sigma Aldrich in 100 ml volume (a) and NM-300 in 3 ml volume (b) AgNPs. Growth expressed as the Mean (OD_{600}) ± SD, n=3.

3.2.5.2. Pseudoalteromonas aliena

To compare the toxicity of the Sigma and NM-300 AgNPs under the same experimental conditions, *P.aliena* was exposed to different concentrations of these two different AgNP types. The Sigma Aldrich AgNPs were dispersed in the NM-300 dispersant and exposures took place in test tubes in a final volume of 3 ml (Figure 3. 35).

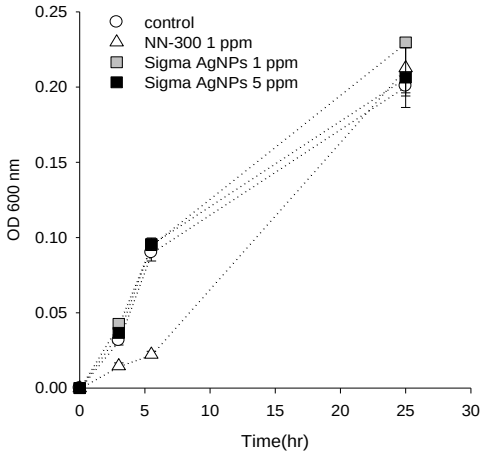

Figure 3. 35 Growth of *P.aliena* exposed to different concentrations of Sigma Aldrich (a) and NM-300 in 3 ml volume (b) AgNPs. Growth expressed as the OD_{600} Mean ±SD, n=3.

3.2.5.3. Streptomyces koyangensis

Similarly to *P.arctica*, the *S. koyangensis* species exhibited greater resistance to the Sigma Aldrich AgNPs (Figure 3. 36a) than to the NM-300 AgNP type (Figure 3. 36b). Both experiments might not be directly comparable as the bacterial growth of the cultures exposed to the Sigma Aldrich AgNPs was quantified by measuring the dry weight whereas the total Nitrogen was the parameter used to investigate the inhibitory concentrations of the NM-300. However as the composition of nitrogen is relatively constant in the total bacterial biomass it was assumed that differences in bacterial biomass are directly proportional to the nitrogen content. No statistically significant differences were found between the various concentrations of AgNPs (ANOVA, Sigma Aldrich p-value = 0.121 and NM-300 p-value = 0.067). The total Nitrogen concentration was statistically significantly higher (p-value = 0.040; t-test) in the control than at 500 ppb (NM-300 AgNP type).

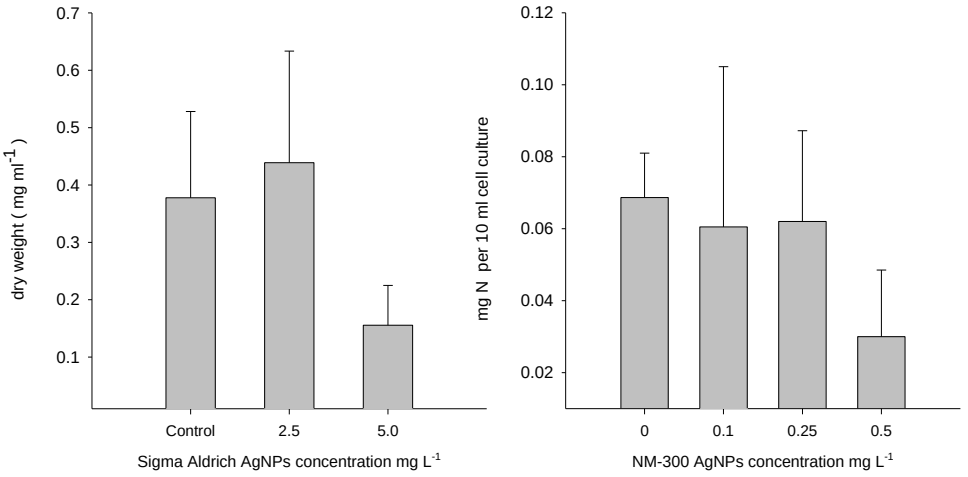

a) Bacterial growth expressed as mean of the dry weight (±S.D.), n=3.

b) Bacterial growth expressed as mean weight of total Nitrogen in mg per 10 ml of cell culture (±S.D.), n=3. In the treatment 100 µg L-1 one of the replicates exhibited a negative value for total N, then this value was zero it.

Figure 3. 36 *S. koyangensis* growth under different concentrations of Sigma AgNPs (a) and 300-NM (b)

It was noticed that in presence of AgNPs (Sigma Aldrich) the *S.koyangensis* did not grow homogenously but forming clumps (Figure 3. 37)

Figure 3. 37The *S. koyangensis* formed clumps in presence of 5 ppm of the Sigma Aldrich

The results with respirometry are in agreement with the results obtained my measuring total nitrogen in the cell cultures after 48 hr exposure. The NM-300 AgNPs inhibited respiration at concentrations ≥ 0.5 mg L^{-1} as observed in Table 3. 7. Inhibition of O_2 uptake is calculated having as a reference the value measured in the control treatment (n=1). Thus negative values in the column named as "Inhibition (%)" means that bacterial activity was greater than in the control treatment, no inhibition occurred.

Table 3. 7 Respiration of *S. koyangensis* at different concentrations of NM-300 AgNPs

Tube	Treatment	Concentration AgNPs (mg L^{-1})	Respiration rate (mg/l/h)	Inhibition (%)
1	Control	0.0	0.30	
2	Dispersant[a]	1.0	0.57	-92,9
3	AgNPs	0.1	0.66	-123,2
4	AgNPs	0.25	0.47	-58,6
5	AgNPs	0.5	0.15	50,2
6	AgNPs	1.0	0.17	44,5

[a] Equivalent concentration of dispersant in 1 mg L^{-1} of AgNPs

3.2.5.4. *A.agilis and Bacillus sp*

A.agilis and *Bacillus* sp. exposed to the Sigma Aldrich AgNPs did not grow at concentrations ranging from 2.5 to 10 ppm (OD_{600} represented in Figure 3. 38 a-b, and cell viability is depicted in Figure 3. 39 a-b. These results indicated that members of the *Pseudoalteromonas* spp. are more resistant to AgNPs than *A.agilis* and *Bacillus* sp species, independent of the AgNPs type.

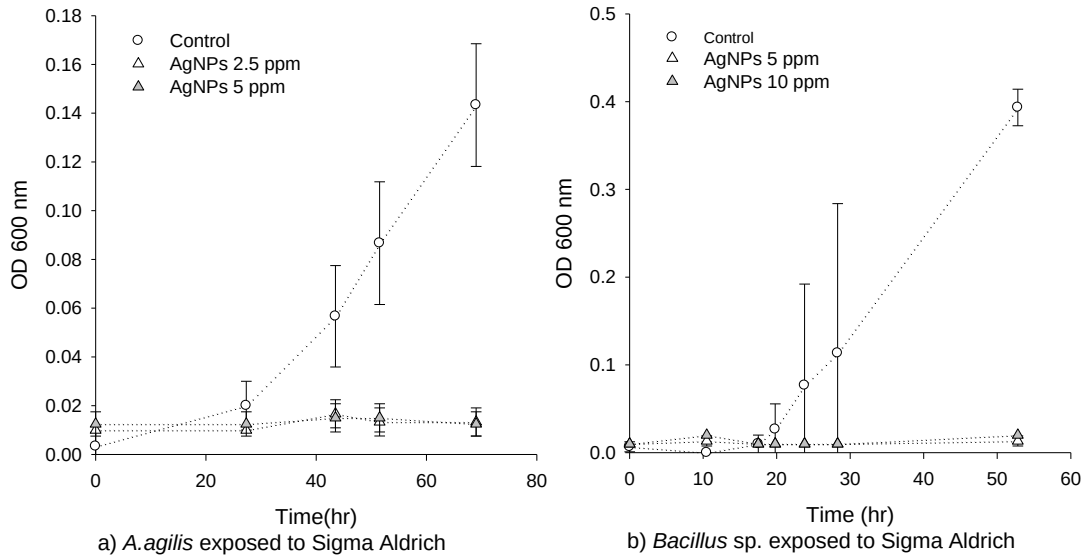

Figure 3. 38 Growth of (a) *A.agilis* and (b) *Bacillus* sp. exposed to different concentrations of Sigma Aldrich AgNPs. Growth expressed as the OD_{600} Mean ±SD, n=3.

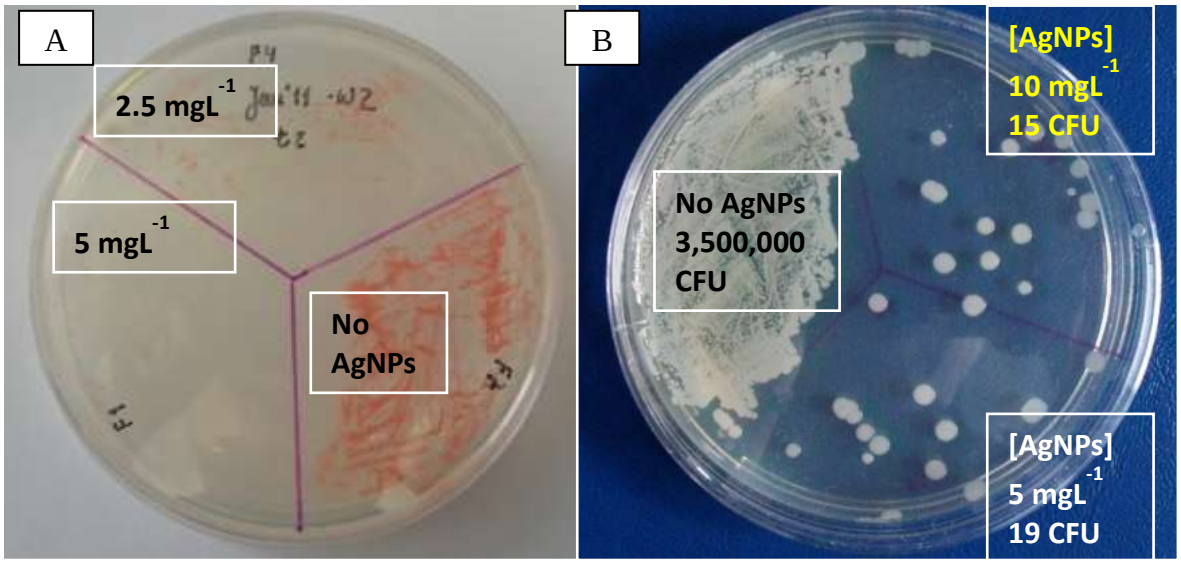

Figure 3. 39 Image showing CFU after (a) *A.agilis* after 43.5 hr exposure and (b) *Bacillus sp.* after 23 hr exposure to Sigma Aldrich AgNPs.

3.3. Microcosm exposures

In the present section the results of the chemical and biological analysis performed with water and sediment samples obtained from different microcosm experiments are presented.

3.3.1. Sediment physical analysis

The granulometric analysis of sediments showed that the sand class fractions were dominant. The total sand fraction comprised up to the 97.54% of the total weight (expressed as percentage o dry sediment weight) of sediments (Table 3. 8). The size class of sediments (sand) was in agreement with the porosity of the sediments, the mean ± SD was 44.10 ± 1.67% (n=3).

Table 3. 8 Granulometric analysis of sediments

Mesh Ø (µm)	% Weight	Size class
710< Ø >500	0.20	Coarse sand
500< Ø >250	47.44	Medium sand
250 < Ø>125	43.00	Fine sand
125<Ø>63	6.90	Very fine sand

3.3.2. Chemical analysis

The concentration of total silver was measured in water and sediment samples collected during the course of the microcosm exposures. The chemical oxygen demand and inorganic forms of nitrogen were measured in the water column.

3.3.2.1. Concentration of silver in water and sediment samples

The concentration of total silver was monitored during the course of the microcosm experiments in the water column and sediments and the results obtained in August 2012 and January 2013 showed a very similar trend (Figure 3. 40). The concentration of total silver in the water column decreased significantly (p-value <0.001 RM-ANOVA concentration total silver at the beginning of the exposure, t = 0 hr and the other sampling time points 24, 72 and 120 hr) during the first 24 hr and concomitantly increased in sediments. The concentration of silver in the control treatment was below the detection limits in water and sediments.

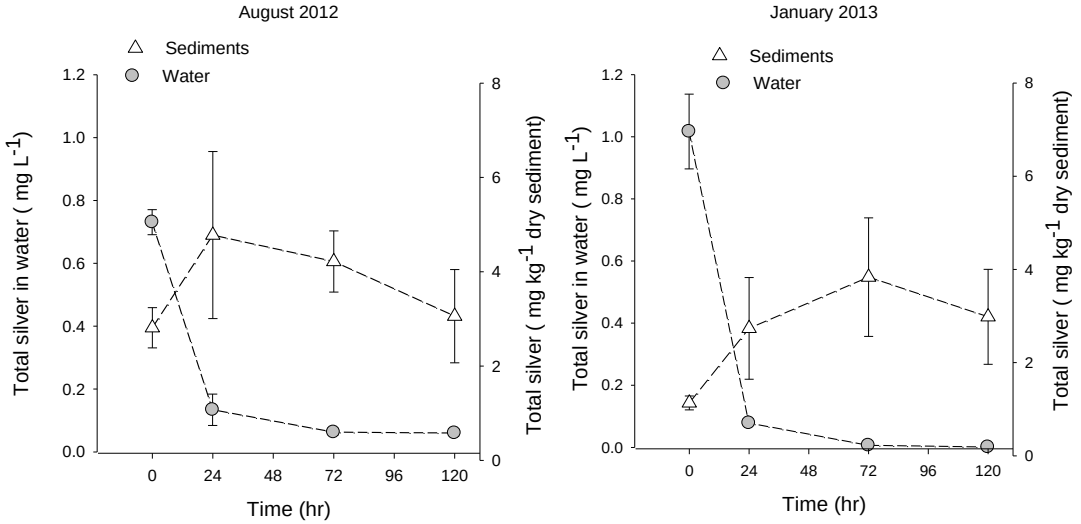

Figure 3. 40 Mean (± SD) concentrations of total silver in water and sediment samples collected from the microcosms during the course of the experiment, n=4.

3.3.2.2. Investigating the fate of AgNPs in sediments with Raman microspectroscopy

The transformation of the NM-300 AgNPs into other silver-complexes in sediments (collected from the microcosms experiment) was investigated by examining the sediment samples exposed to AgNPs (NM-300) with Raman microspectroscopy (Figure 3. 41 a-b). The peaks at 136 (a), 143 b) and 131 (c) are associated to Ag-lattice vibrational mode. The peaks at 290,327 and 409 (b) could be due to Ag-Cl stretching modes and (c) 1099 and 1122 to Ag-O to stretching/bending modes.

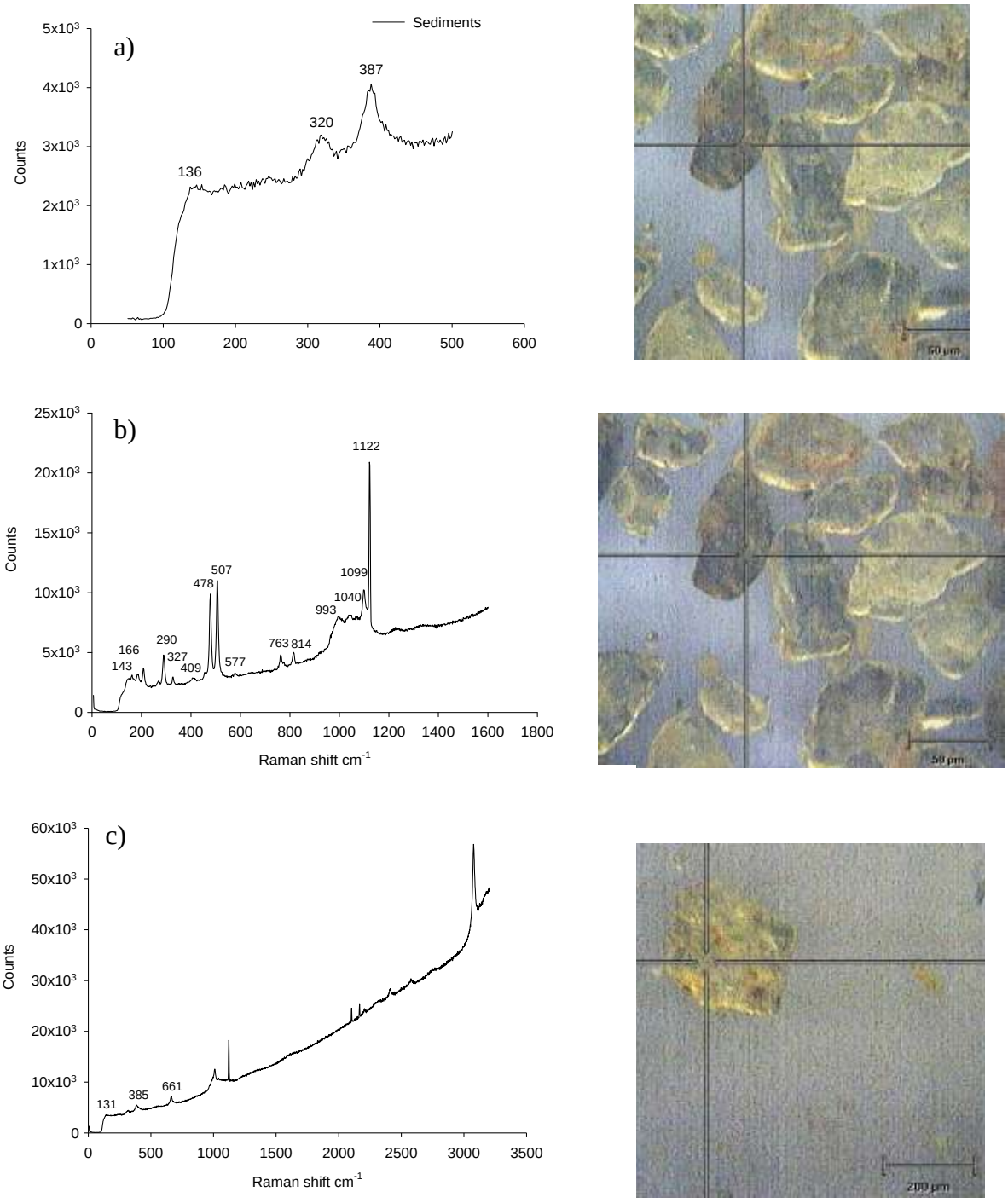

Figure 3. 41 Sediment samples exposed to NM-300 AgNPs, examined under Raman spectroscopy (right) and Raman spectra obtained (left) in different spectral ranges: (a) 600, (b) 1800 and (c) 3500 Raman .

Figure 3.42 (a-c) shows the previous 3 spectra aligned to enable comparison between samples.

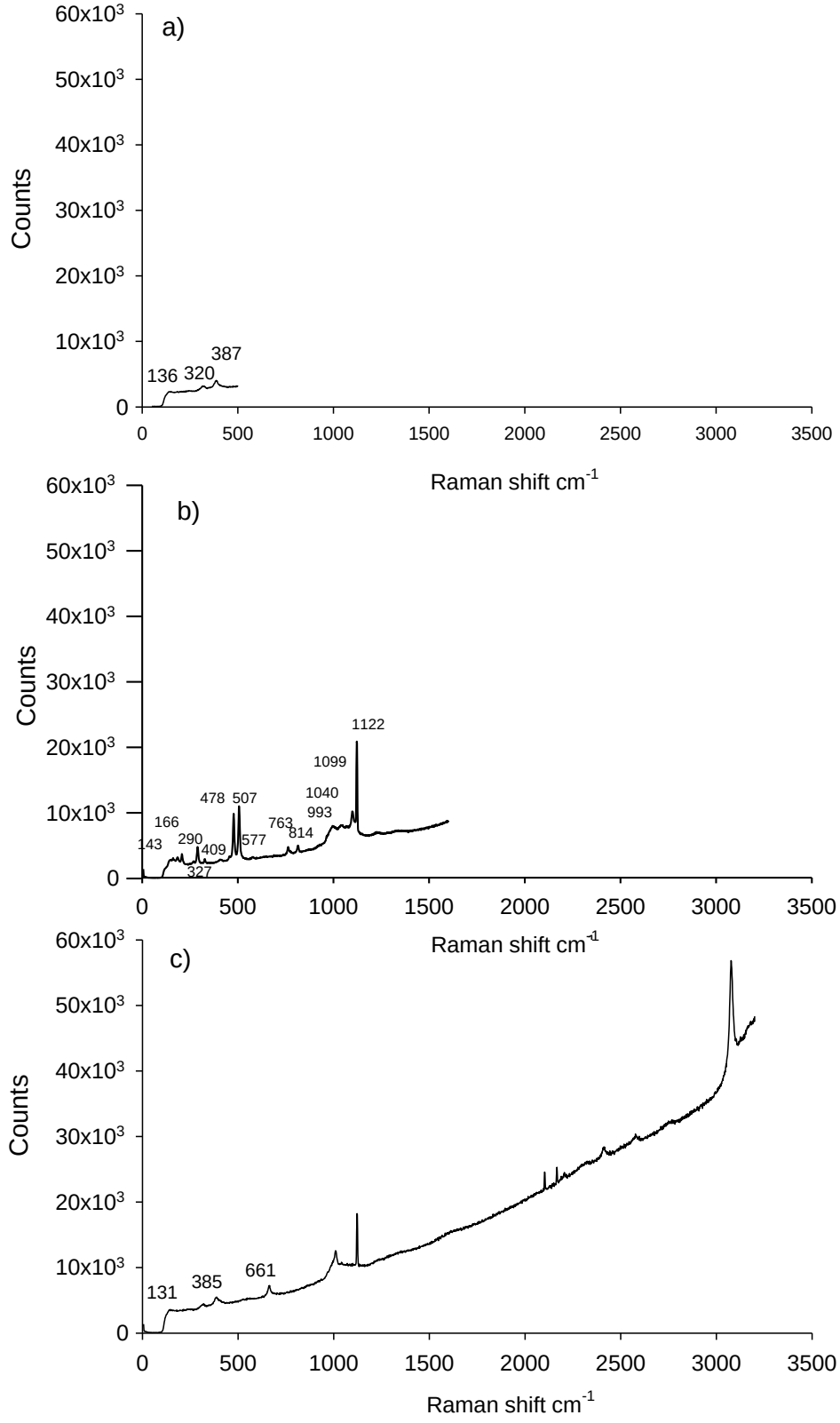

Figure 3. 42 Raman spectra of sediment samples exposed to NM-300 AgNPs in different spectral ranges: (a) 600, (b) 1800 and (c) 3500 Raman .

The Figure 3.43 Represents the Raman spectra for (a) the reference $AgNO_3$ and below (b) the spectra obtained for sediment samples exposed to the NM-300 AgNPs. Highlight the presence in sediments (b) of the peaks 1099 and 1122 corresponding possibly to Ag-O.

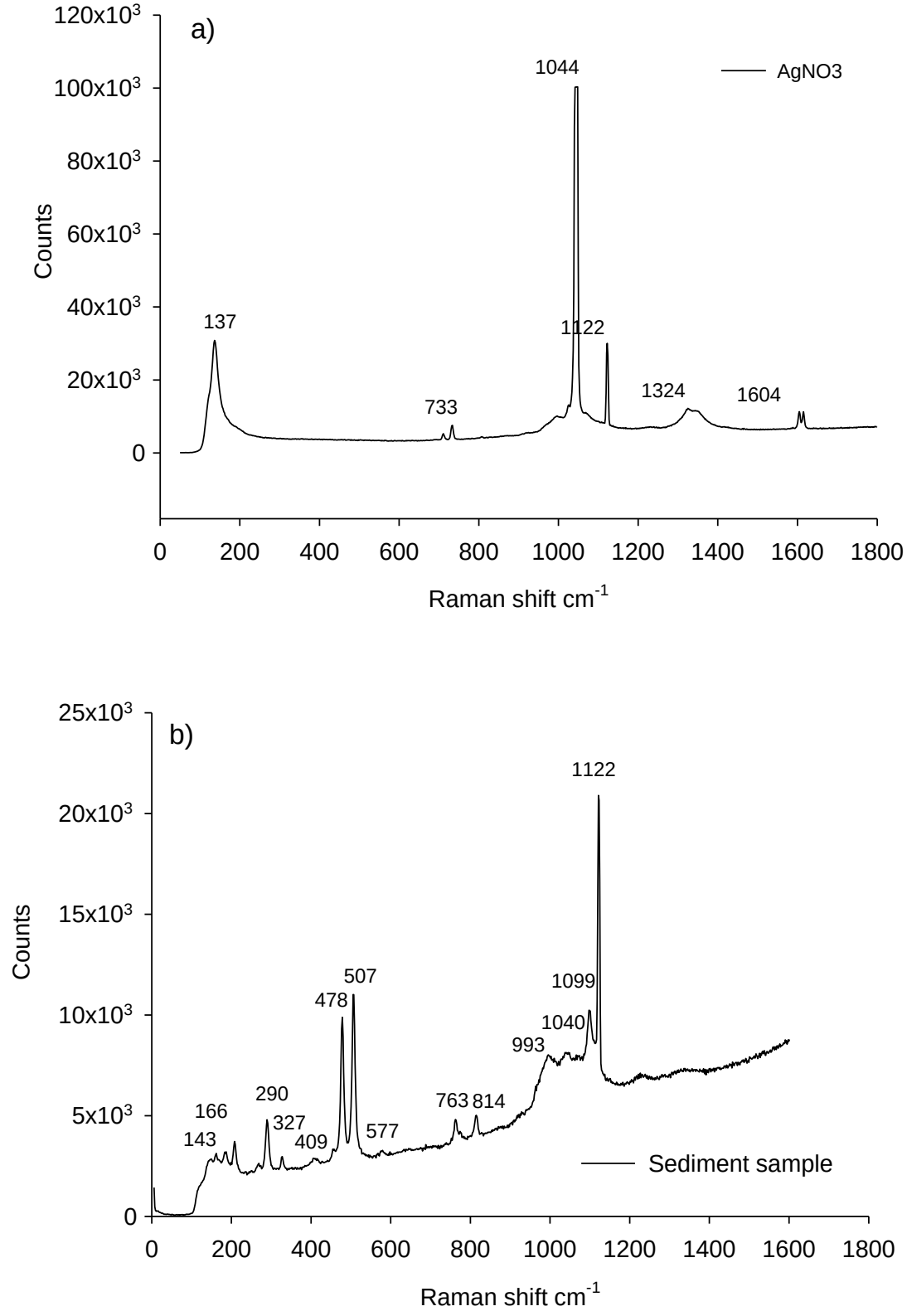

Figure 3. 43 Raman spectra of (a) pure $AgNO_3$and (b) sediment sample after exposure to NM-300 AgNPs

The Figure 3.44 Represents the Raman spectra for (a) the reference AgCl and below (b) the spectra obtained for sediment samples exposed to the NM-300 AgNPs. Highlight the presence in sediments (b) of the peak 136 corresponding possibly to Ag-Cl.

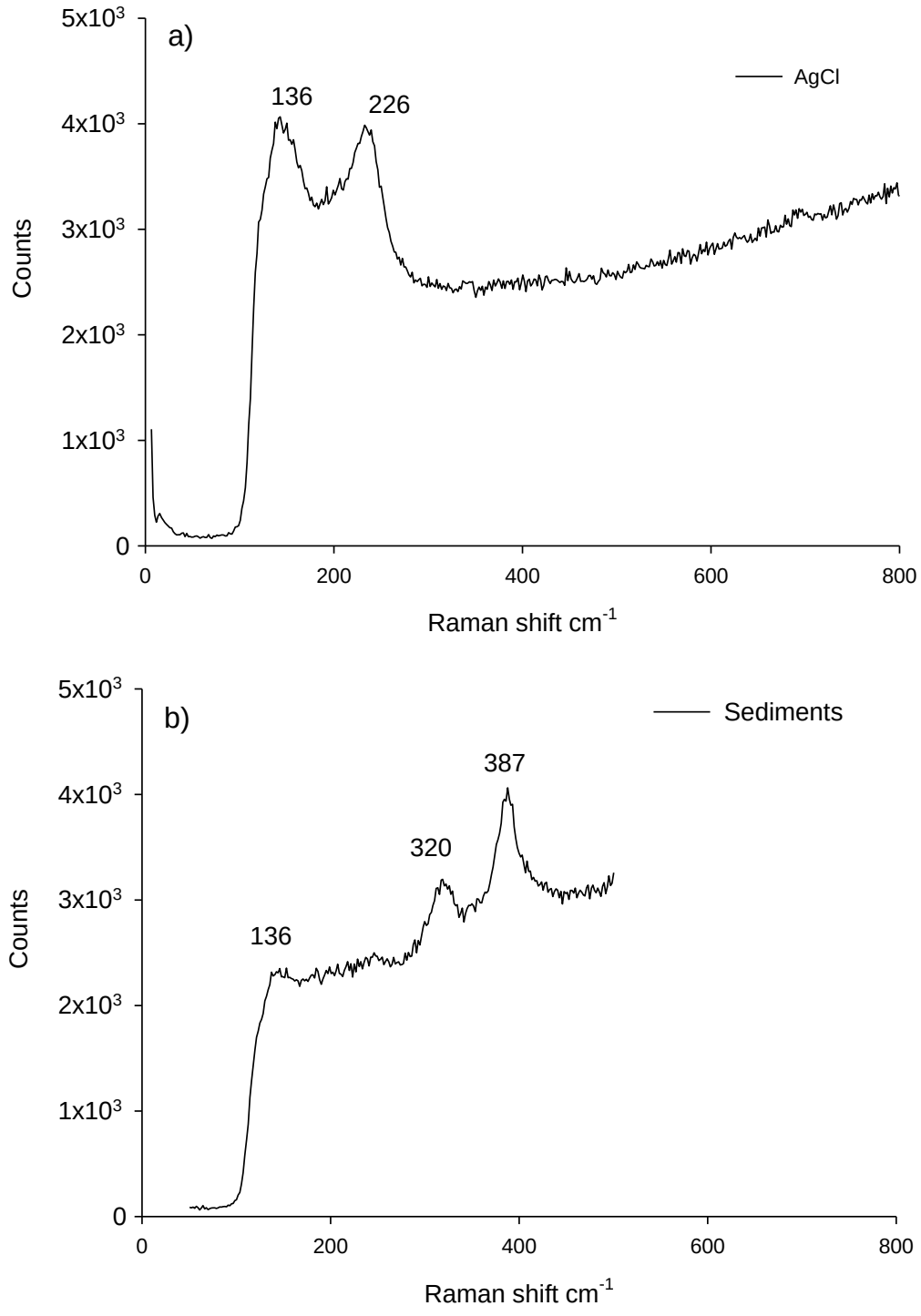

Figure 3. 44 Raman spectra for (a) the reference AgCl and below (b) the spectra obtained for sediment samples exposed to the NM-300 AgNPs.

3.3.2.3. COD analysis

COD results did not show statistically significant differences between treatments (t-test in August 2012 (2 treatments) and One Way ANOVA in January 2012 (3 treatments), $p<0.05$) at different time points (0, 24, 72 and 120 hr) in any of the microcosms run during the summer 2012 and winter 2013 (Figure 3. 45).

In both microcosm experiments, August 2012 and January 2013, it was observed that overall COD increases in the water column during the first 24 hr, decreased at 72 hr and increased after 120 hr of exposure.

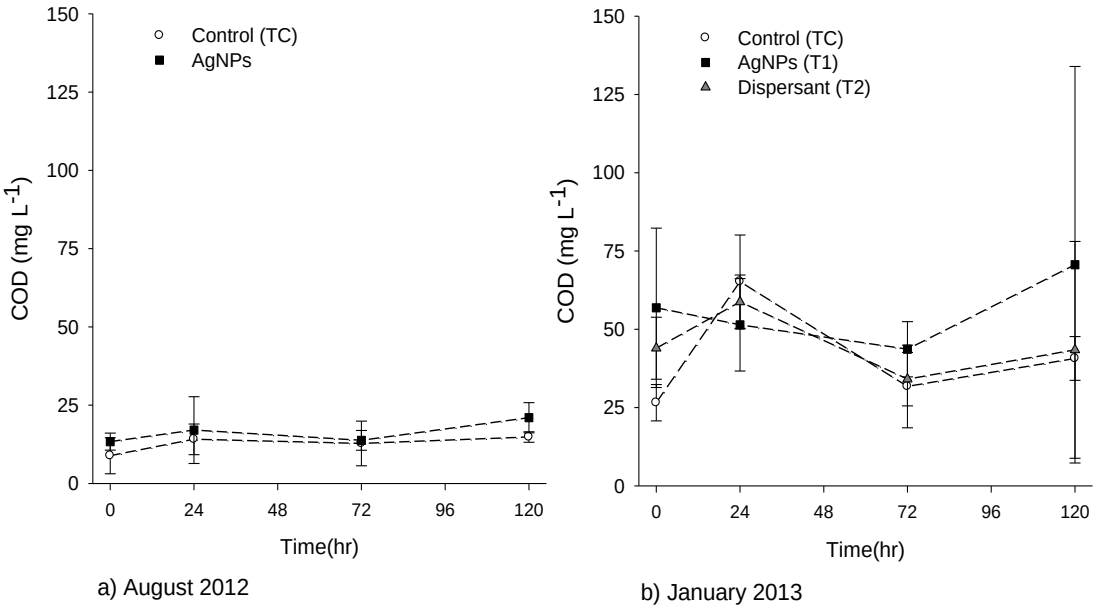

Figure 3. 45 COD measured in the water column during the course of the experiment in August 2012 (a) and January 2013 (b), expressed as mean ± SD, n=4.

3.3.2.4. Inorganic nitrogen analysis

3.3.2.4.1. Ammonium (NH_4)

The concentration of NH_4 in the water column was measured at different time points during the course of the microcosm experiments and the trends observed in August 2012 and January 2013 were very different (Figure 3. 46a-b). During both microcosm experiments the initial concentration of NH_4 was always higher in dispersant-containing treatments (T1 and T2). In August 2012 the concentration of NH_4 increased during the first 24 hr and it did not change after 120 hr. In contrast, in January 2013, the concentration of NH_4 decreased during the first 24 hrs. This drop was more dramatic in the dispersant (T2) treatment than in the presence of AgNPs.

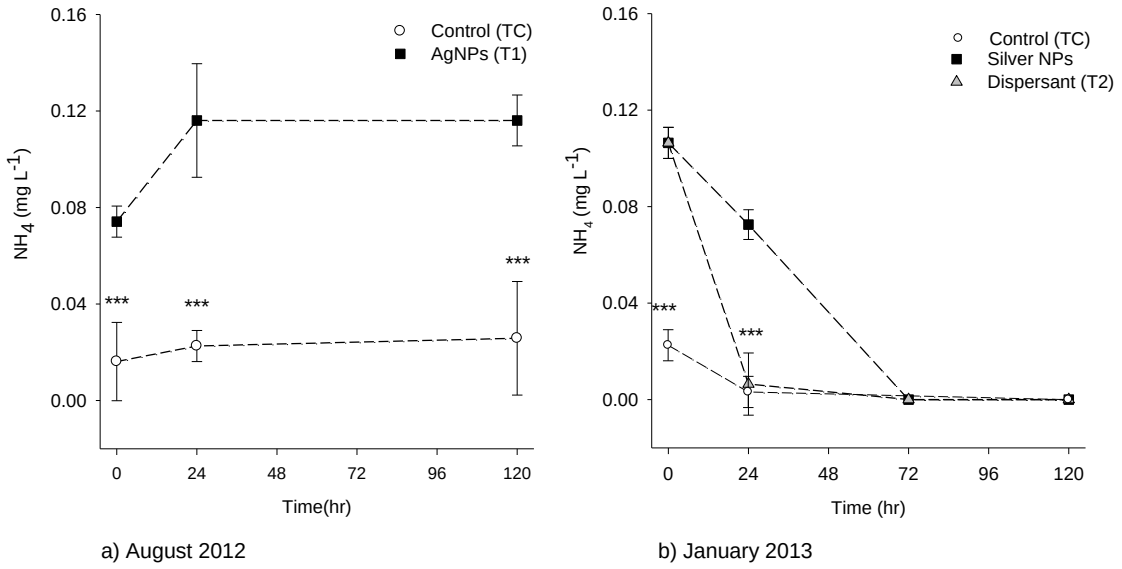

Figure 3. 46 NH_4 measured in the water column during the course of the experiment in August 2012 (a) and January 2013 (b), expressed as mean ± SD, n=4 except. *** symbolizes statistically significant $p < 0.001$).

3.3.2.4.2. NO_2 analysis

The concentration of NO_2 in August 2012 and January 2013 oscillated around the same ranges (Figure 3. 47 a-b), between 0.005 and 0.015 mg L^{-1}.

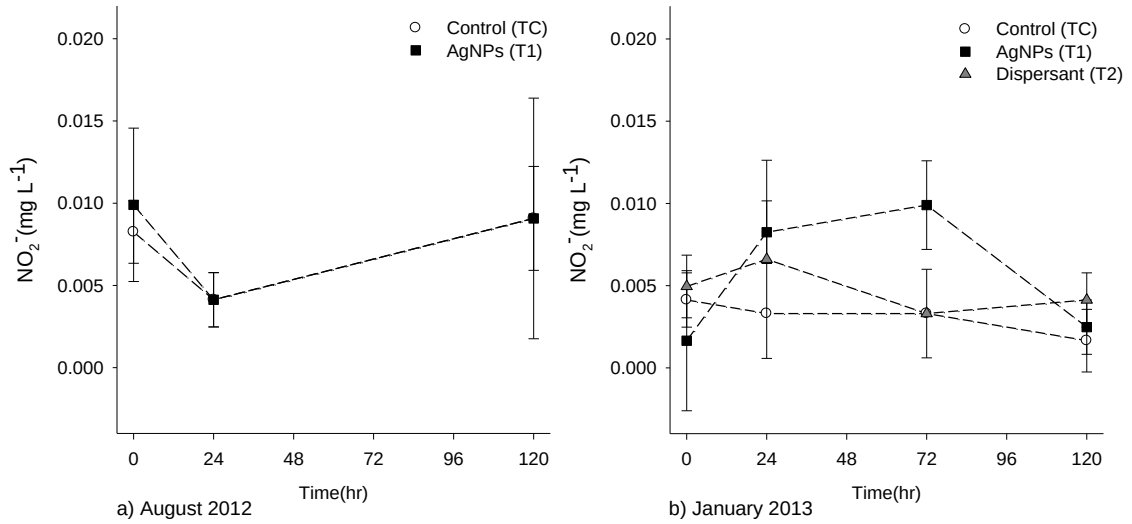

Figure 3. 47 NO_2 measured in the water column during the course of the experiment in August 2012 (a) and January 2013 (b), expressed as mean ± SD, n=4.

3.3.2.4.3. NO_3 analysis

The concentration of NO_3 in the water column showed a very different trend between the two microcosms. In August 2012 the NO_3 concentration oscillated between 0.2 and 0.8 mg L^{-1} (Figure 3. 48a). In January 2013 the NO_3 concentration increased as NH_4 decreased (Figure 3. 48b).

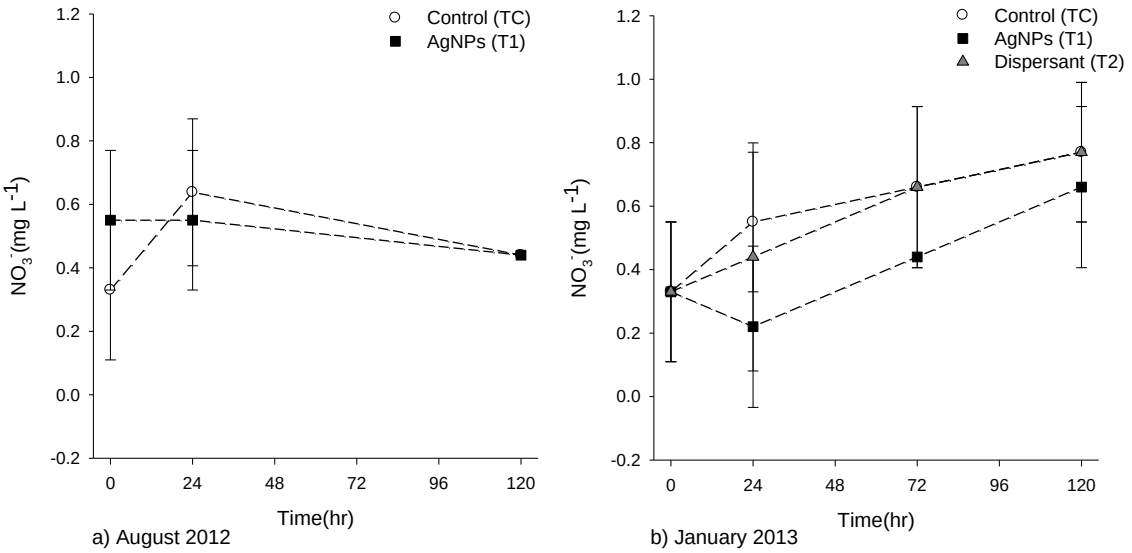

Figure 3. 48 NO_3 measured in the water column during the course of the experiment in August 2012 (a) and January 2013 (b), expressed as the mean ± SD, n=4.

3.3.3. Biological analysis in the water column

3.3.3.1. Bacterial plate counts

The viability and abundance of heterotrophic bacteria inhabiting the water column was monitored with plate counts. In the three microcosm experiments developed in March and August of 2012, and January 2013, it was observed, that in the presence of AgNPs, the bacterial abundance was reduced during the first 72 hr of exposure. The bacterial abundance recovered completely after 120hr of exposure, except in August 2012, when no increase in the bacterial abundance following exposure to AgNPs was observed (Figure 3. 49). The CFU counts were log10-transformed and the statistical analysis indicated that the reduction in the bacterial abundance was significant at the beginning of the exposures (0 hr) in March 2012 and August 2012 (independent t-test, p-value = 0.004 and 0.022 respectively). In January 2013 after 24 hr of exposure there was a reduction in the bacterial abundance in the presence of AgNPs (One Way ANOVA, p-value <0.001, MA agar). No CFU developed in the plates after 24 hr of exposure in August 2012, possibly due to a human error when performing the dilution series. In January 2013 the abundance in the ZM/10 plates was too high owing to a miscalculation and, as a result of this, the CFUs were too high and uncountable. No differences in bacterial plate counts were observed between the ZM/10 and the Difco MA except at 72 hr in the AgNPs (T1) treatment (t-test, p= 0.030).

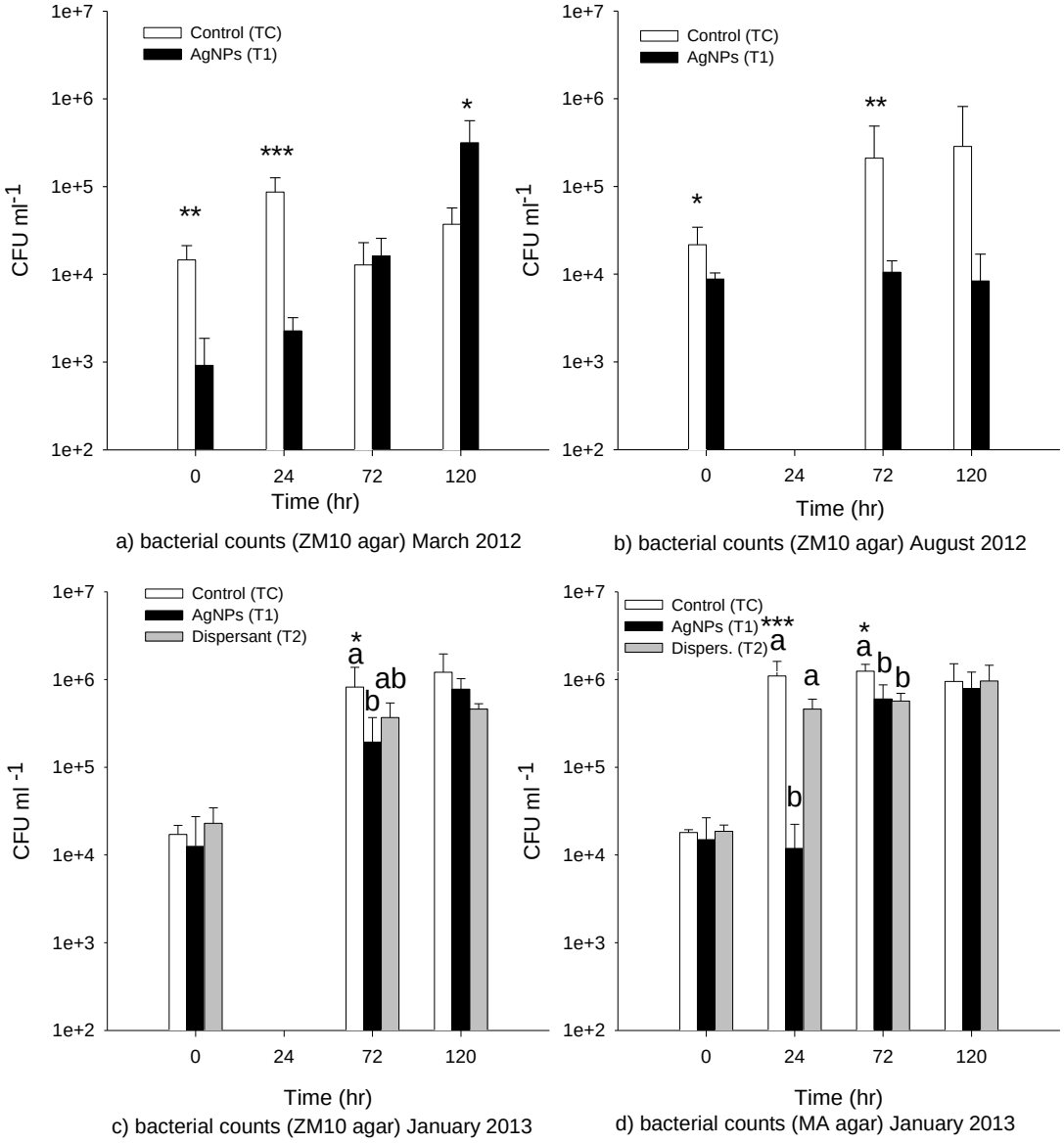

Figure 3. 49 Bacterial abundance in the water column expressed as the mean ± SD of the log 10 (CFU). Columns with the same letters are not significantly different from each other. t-test, March 2012 and August 2012, and ANOVA, January 2013, p< 0.05), *, **, *** symbolizes statistically significant differences (p < 0.05), (p < 0.01) p < 0.001), respectively).

3.3.3.2. Microbial abundance in the water column (January 2013)

The microbial abundance in the water column was measured with two different culture-independent techniques, direct counts with Epifluorescence microscopy (DAPI) and flow cytometry (FC) (Figure 3. 50 a-b). At the beginning of the exposures (0 hr) the counts obtained with both methods are in agreement, however the counts obtained with DAPI were greater thereafter. The differences between the treatments regarding DAPI counts and (FC) are presented below.

Time point 0 hr: At the beginning of the exposures the cell counts analyzed with FC indicated that the cell concentration in the control (TC) was statistically significantly

lower (ANOVA p< 0.05) than in the treatment with AgNPs (T1)(Figure 3. 50b). These unexpected results are discussed in Chapter 4, section 4.5.2.2 .

Time point 24 hr: the results obtained with FC and DAPI counts indicated that in the control and dispersant treatments (TC and T2), the cell abundance was statistically significantly higher than in the treatment with AgNPs (T1). In the AgNPs treatment (T1) the FC counts showed a more dramatic decrease in the microbial abundance (changed from 5.9 $x10^5$ to 2.1 x 10^5 counts ml^{-1}) than the reduction observed with the bacterial plate counts (previous section). In the AgNPs (T1) treatment the DAPI counts did not change between the 0 and 24 hr, however in the treatments without silver, (TC and T2), the microbial abundance increased significantly during the first 24 hr (paired t-test p-value < 0.01).

Time point 72 hr and 120 hr: The cell abundance in the AgNPs (T1) increased after 72 hr. The FC analysis did not find differences in the microbial abundance between treatments after 120 hr of exposure whereas the DAPI counts estimated that microbial abundance was significantly higher in the control (TC) treatment than in presence of AgNPs (T1). However, the DAPI and FC counts showed a similar trend, with bacterial abundance increasing during the first 24 hr and then stabilizing.

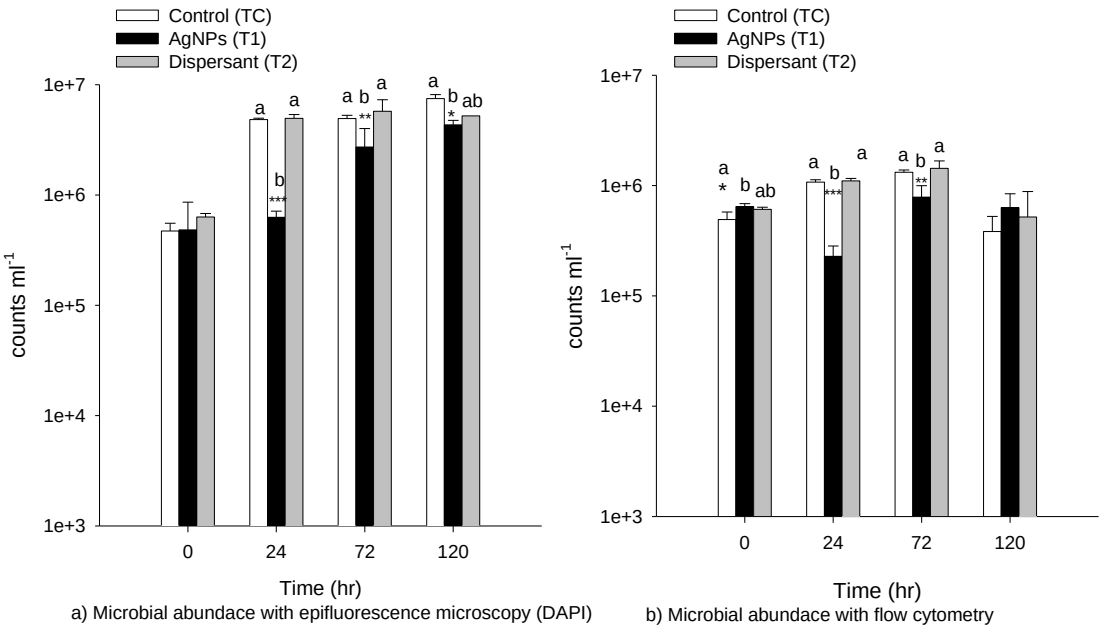

Figure 3. 50 Microbial abundance in water expressed as the mean ± SD of the log 10 (counts ml^{-1}). Columns with the same letters are not significantly different. ANOVA , $p < 0.05$, n=4), *, **, *** symbolizes statistically significant differences ($p < 0.05$), ($p < 0.01$) $p < 0.001$), respectively.

Both techniques, DAPI and FC found statistically significant differences between treatments at 24 and 72 hr. A linear regression analysis confirmed that FC and

DAPI counts are positively correlated ($p < 0.000$, Pearson's correlation coefficient (R) =0.972, Figure 3. 51).

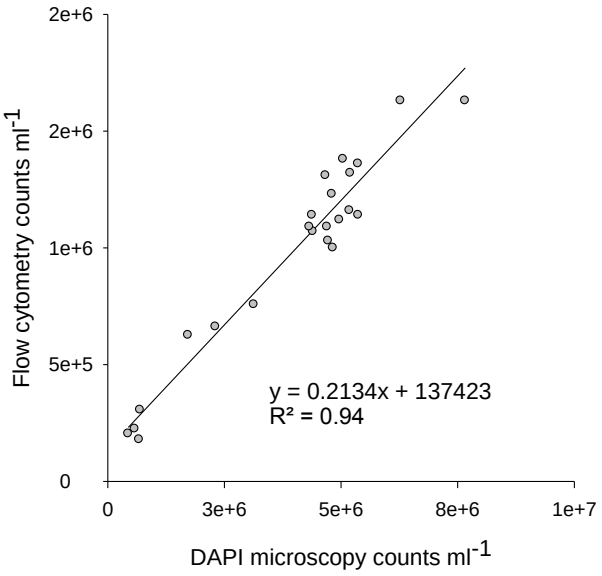

Figure 3. 51Relation between the DAPI and flow cytometry counts measured at 24 and 72 hr, n= 23.

3.3.3.3. O_2 uptake rate

During the course of the microcosm the O_2 uptake of the whole microbial community inhabiting the water column was measured. This parameter provided an insight into the overall physiological status of the communities inhabiting the water column, including non culturable bacterial groups. Water samples were collected at different time points during the course of the experiment and O_2 uptake rates were monitored for 30 min prior to stabilization of the samples in the Strathtox® respirometer. In both microcosm experiments, August 2012 and January 2013, it was observed an increase in the O_2 consumption during the first 48 hr of exposure and a decrease afterwards, however the O_2 uptake in the absence of AgNPs (control treatment TC) was higher in January 2013 than in August 2012 (Figure 3. 52) and consistent with nitrate (NO_3) production (Figure 3. 48). At the beginning of the exposures no differences in the O_2 uptake rate per hour were detected between the AgNPs (T1) and the control (TC) (March 2012) or the dispersant (T2) treatment in January 2013. In the following hours the O_2 uptake rate decreased in the water column in the AgNPs (T1) treatment. In contrast, in the treatments without silver (control (TC) and dispersant (T2)), the O_2 uptake increased steadily during the first 48 hrs in August 2012 and 72 hrs in January 2013, and then progressively decreasing afterwards.

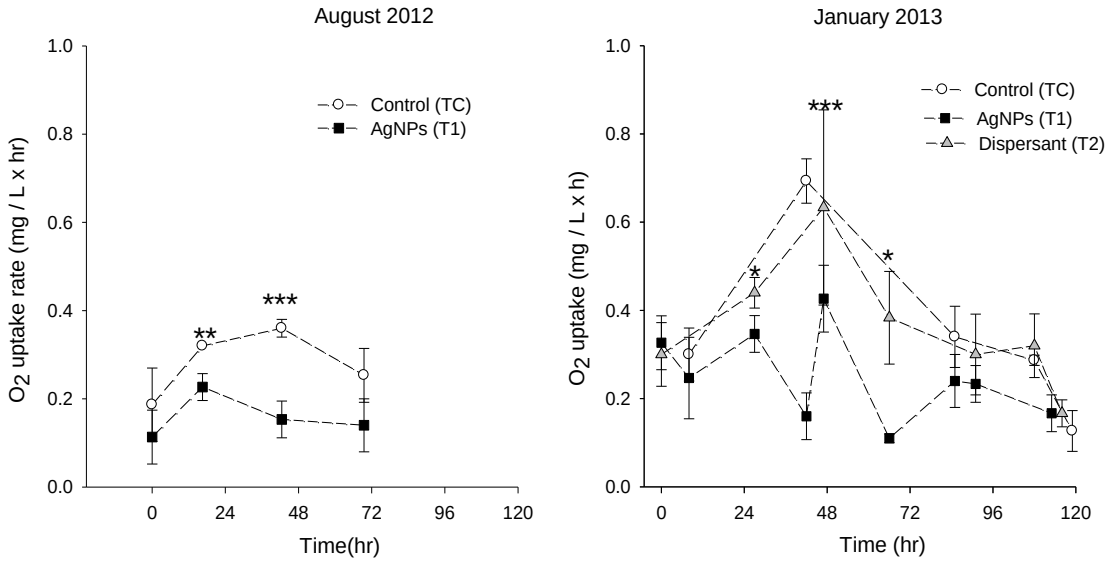

Figure 3. 52 O_2 uptake rate of the microbial communities during the course of the experiment expressed as the Mean value of the oxygen uptake ± S.D., n= 3. The differences between treatments where analyzed with the Student's t-test for independent samples. *, **, *** symbolizes statistically significant differences at a p-value < 0.05, 0.01, 0.001 respectively.

3.3.3.4. Relationship between different biological parameters

In Table 3. 9 the statistical parameters related to the correlation between the different sets of biological data (bacterial plate counts, prokaryotic abundance with DAPI counts and flow cytometry (FC) and the O_2 uptake rate) are depicted. Data obtained at all time points were pooled together for the analysis otherwise the population size (N) was small ($12 \geq N \geq 6$).

Table 3. 9 Correlation between the biological parameters measured in the water

Technique	Statistical parameters	O_2 uptake (mg L^{-1}×hr)	Plate counts (CFU ml^{-1})	DAPI (counts ml^{-1})
Flow cytometry (FC) (counts ml^{-1})	Pearson Correlation	0.392*	0.377*	0.525***
	p-value (2-tailed)	0.035	0.011	0.000
	N	29	45	41
O_2 uptake (mg L^{-1})	Pearson Correlation		-0.558**	
	p-value (2-tailed)		0.002	
	N		29	
Plate counts (CFU ml^{-1})	Pearson Correlation			0.639***
	p-value (2-tailed)			0,000
	N			43

*, **, *** symbolizes statistically significant differences at a p-value < 0.05, 0.01, 0.001 respectively

The bacterial abundance and the physiological status of the community changed during the course of the experiment. Therefore the correlations between the different sets of data were separated according to the time point of sampling, and the corresponding correlation analysis is depicted in

Table 3. 10. Only after 24 hrs of exposure there was a statistically significant correlation between the four biological parameters.

Table 3. 10 Correlation between the biological parameters measured in the water at different time points (0 hr, 24 hr and 72 hr). Empty cells indicate no statistically significant correlation.

Time (hr)	Technique	Statistical parameters	Plate counts (CFU ml^{-1})	DAPI counts ml^{-1}	Flow cytometry counts ml^{-1}	O_2 uptake mg L^{-1}×hr
0	Plate counts (CFU ml^{-1})	Pearson Correlation		-0.632*	-0.16	-0.63
		p-value (2-tailed)		0.037	0.62	0.07
		N		11	11	9
24	DAPI counts ml^{-1}	Pearson Correlation	0.810**		0.994***	0.846*
		p-value (2-tailed)	0.003		0.000	0.034
		N	11		11	6
	Flow Cytometry counts ml^{-1}	Pearson Correlation	0.671*	0.994***		0.868*
		p-value (2-tailed)	0.017	0.000		0.025
		N	12	11		6
	O_2 uptake (mg L^{-1})	Pearson Correlation	0.821*	0.846*	0.868*	
		p-value (2-tailed)	0.045	0.034	0.025	
		N	6	6	6	
72	DAPI counts ml^{-1}	Pearson Correlation	0		0.966**	0.813*
		Sig. (2-tailed)	0.825		0.00	0.049
		N	12		12	6

*, **, *** symbolizes statistically significant differences at a p p-value < 0.05, 0.01, 0.001 respectively

3.3.3.5. Effects of AgNPs on the abundance of ammonia oxidizing bacteria (AOB)

3.3.3.5.1. End point PCR results

The end point PCR showed the presence of AOB in the water samples collected from the microcosm established in August 2012. Before performing the qPCR it was necessary to obtain a clean amplification product (PCR product) for the sequence of interest of the *amoA* gene. To do this, the end PCR product obtained with different combinations of primers, DNA extraction kits and qPCR master mix (including a DNA polymerase and SYBR GREEN as a fluorescent stain) was examined. The end point PCR performed with the different pairs of primers yielded a 491-bp fragment of the *amoA* gene. In (Figure 3. 53) some of the results obtained relating to the PCR amplifications products produced with Quanti Tec SYBR green Master Mix (Qieng) and GoTaq® qPCR Master mix (Promega) are shown. No PCR product was obtained in the environmental samples mixed with Quanti Tec. In contrast the GoTaq® master mix produced a few bands.

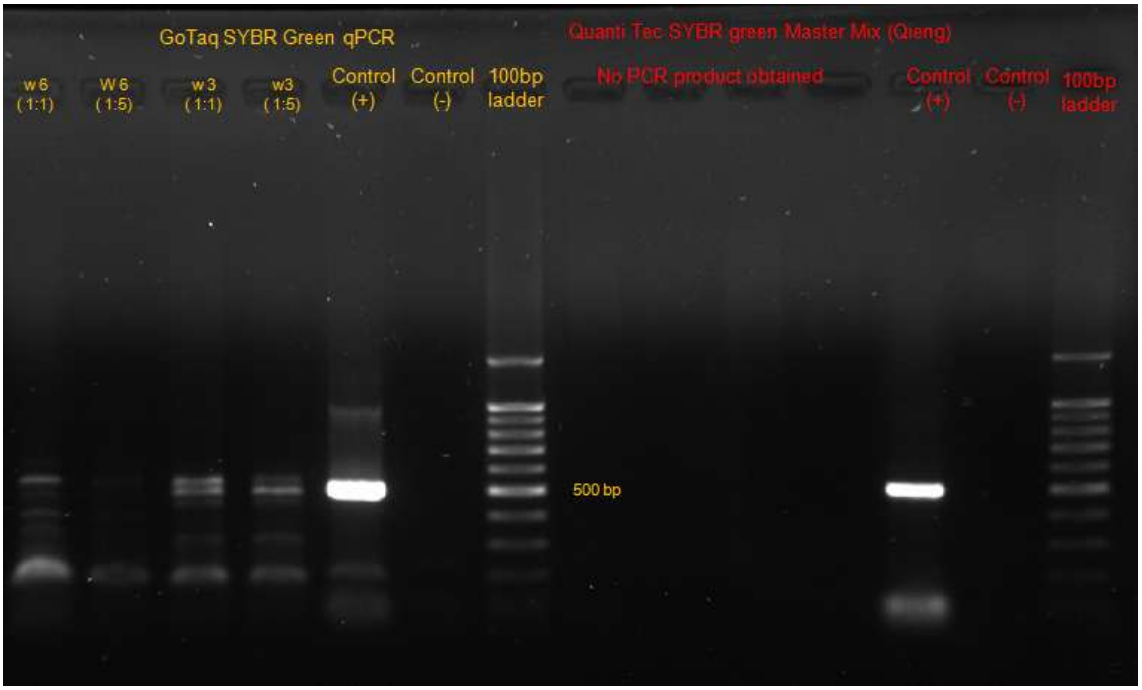

Figure 3. 53 PCR amplification of a specific sequence of the *amoA gene*. Two different samples (w3 and w6) at different dilutions 1:1 and 1:5 were amplified.

The addition of DMSO (1%) enhanced the specificity of the DNA polymerase (the polymerase is included in the GoTaq® master mix) for the sequence of interest and reduce the formation of secondary products. The cleanest product was obtained with the GoTaq® qPCR Master (Promega) with the addition of DMSO (1%) and the pairs of primers amoA-1F / amoA-2R. The DNA extraction kit that produced the purest product

(1 band) for the *amoA* gene fragment was the Rapid Water ® (catalog No 14810-50-NF) DNA from MoBio compared to the few bands obtained with the second extraction kit tested, Power Water ® (catalog No 14900-50-NF) as depicted in Figure 3. 54.

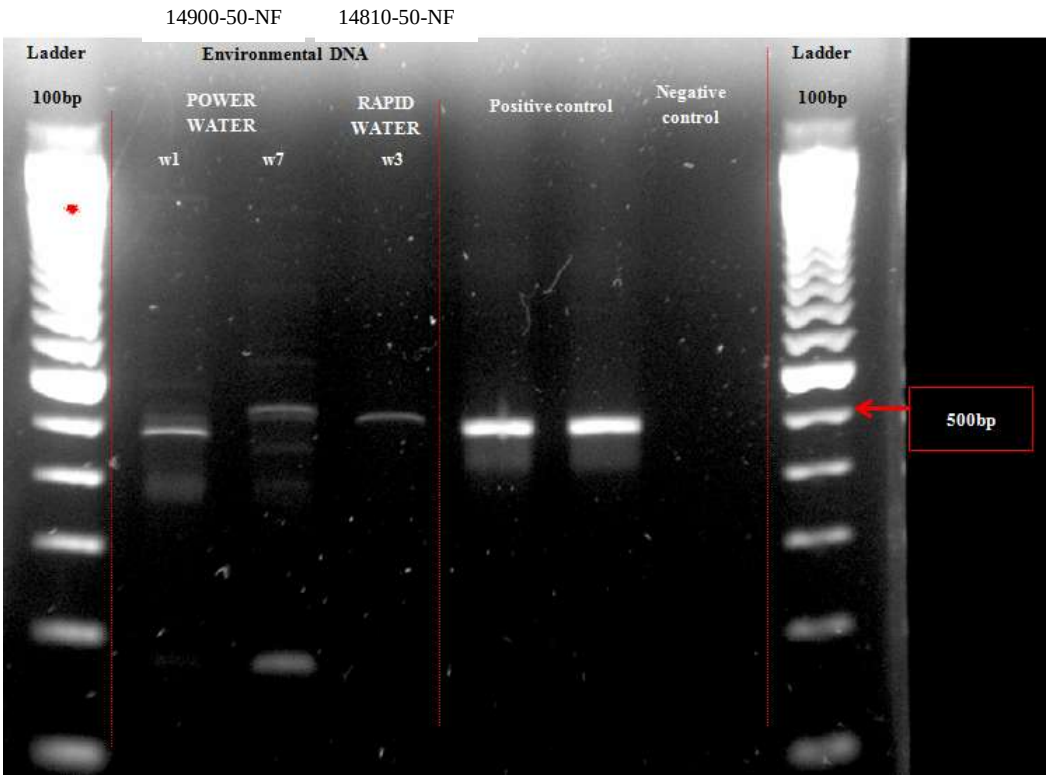

Figure 3. 54 PCR amplification of a specific sequence of the *amoA* gene. No bands observed in the negative control two positive controls were included and three environmental samples. The sample identified as w3 corresponds to the DNA extracted from filtered water with the Rapid Water® kit, whereas the DNA from samples w1 and w7 was extracted with Power Water ®. The master mix was GoTaq® qPCR Master (Promega).

3.3.3.5.2. qPCR results

The qPCR amplification performed to quantify the abundance of AOB groups did not work properly. First the amplification of the standard curves did not work, the correlation coefficient was 0.95 (Figure 3. 55) with only 4 points as one of the standards failed. Moreover a correlation coefficient of 0.95 is regarded as low by the manufacturer of the reagents (Life Technologies^{TM}) for this type of work, when we aimed for > 0.990.

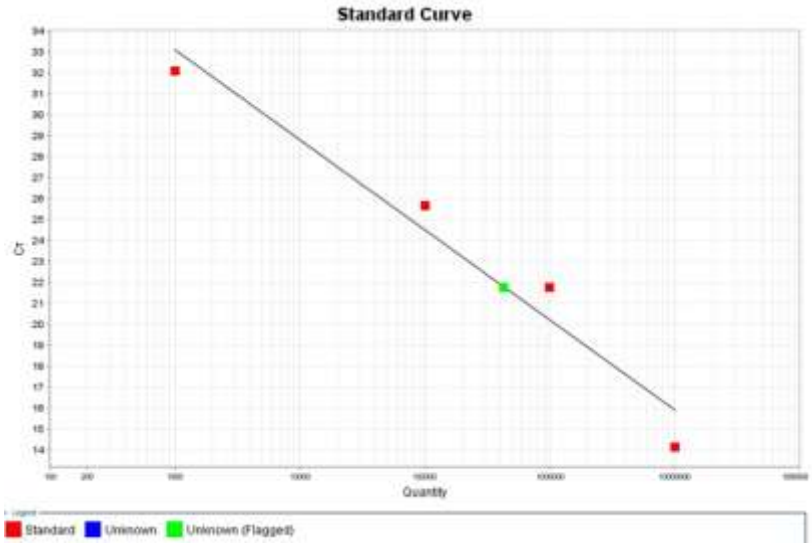

Figure 3. 55 Standard curve obtained with Go Taq Master mix represented by the red squared-dots. The threshold cycle (Ct) is shown in the Y-axis and the starting concentration of DNA template ranging between 10^3 and 10^7 copies/µl in the X-axis. The green squared-dot represents an environmental sample.

The melt curve obtained showed that the qPCR amplification did not produce a good quality standard curve as the maximum peaks of fluorescence did not occur at the same melting temperature (Tm), the adequate temperature for the sequences to hybridize (Figure 3. 56). Tm was 81.99 ºC for the standards at the concentrations, 10^5, 10^6 and 10^7copies/µl and was lower (Tm =78.3ºC) for the standard prepared at a concentration of 10^3copies/µl. The negative controls (prepared without DNA template) showed a maximum peak of fluorescence at 79 ºC and also secondary peaks were formed in the standards. These undesired peaks formed in the negative controls and standards may be due to the formation of primer dimmers and contamination.

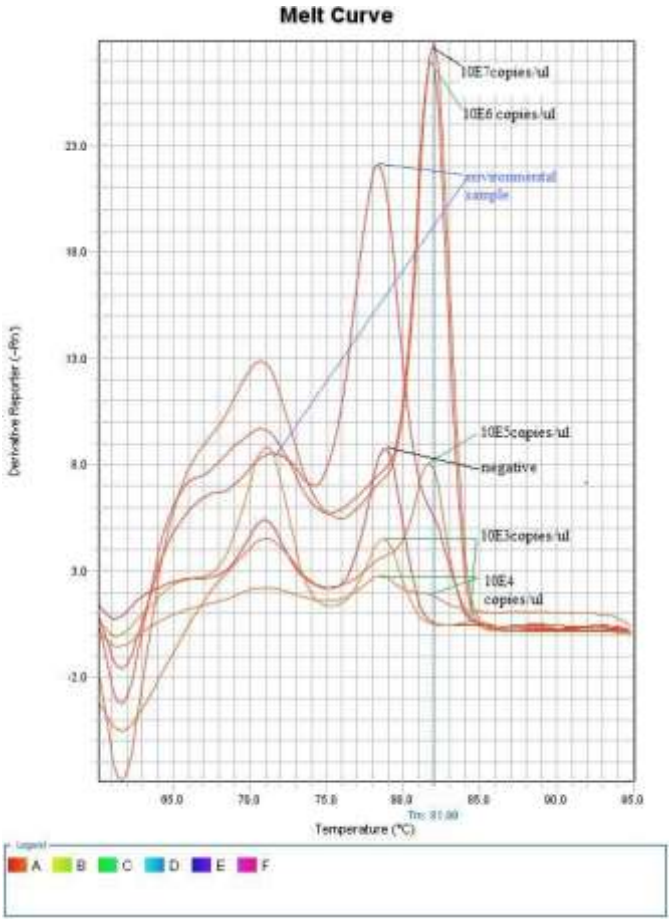

Figure 3. 56 Melt curve obtained during the qPCR is plotted represented by the changes in fluoresce vs time (derivative reporter, -Rn) shown in the Y-axis and the temperature in the X-axis.

3.3.4. Bacterial counts obtained from sediment samples

The growth of heterotrophic bacteria was monitored with plate counts. It was observed that in the presence of AgNPs (T1) the bacterial viability was reduced during the first 24 hrs of exposure and increased after 72 hrs, which was similar to the effects of AgNPs on the bacterial communities inhabiting the water column. AgNPs reduced bacterial viability during the first 24 hrs in March 2012 and August 2012 significantly (t-test, $p < 0.05$) (Figure 3. 57 a-b). The bacterial plate counts obtained in January 2013 showed similar trends to the results obtained in March and August 2012 (Figure 3. 57 c-d). The plate counts in the AgNPs (T1) were always statistically higher than in the control treatment (TC) after 120 hrs of exposure similar to a hormetic response. No statistically significant differences were found between the control (TC) and dispersant treatment (T2).

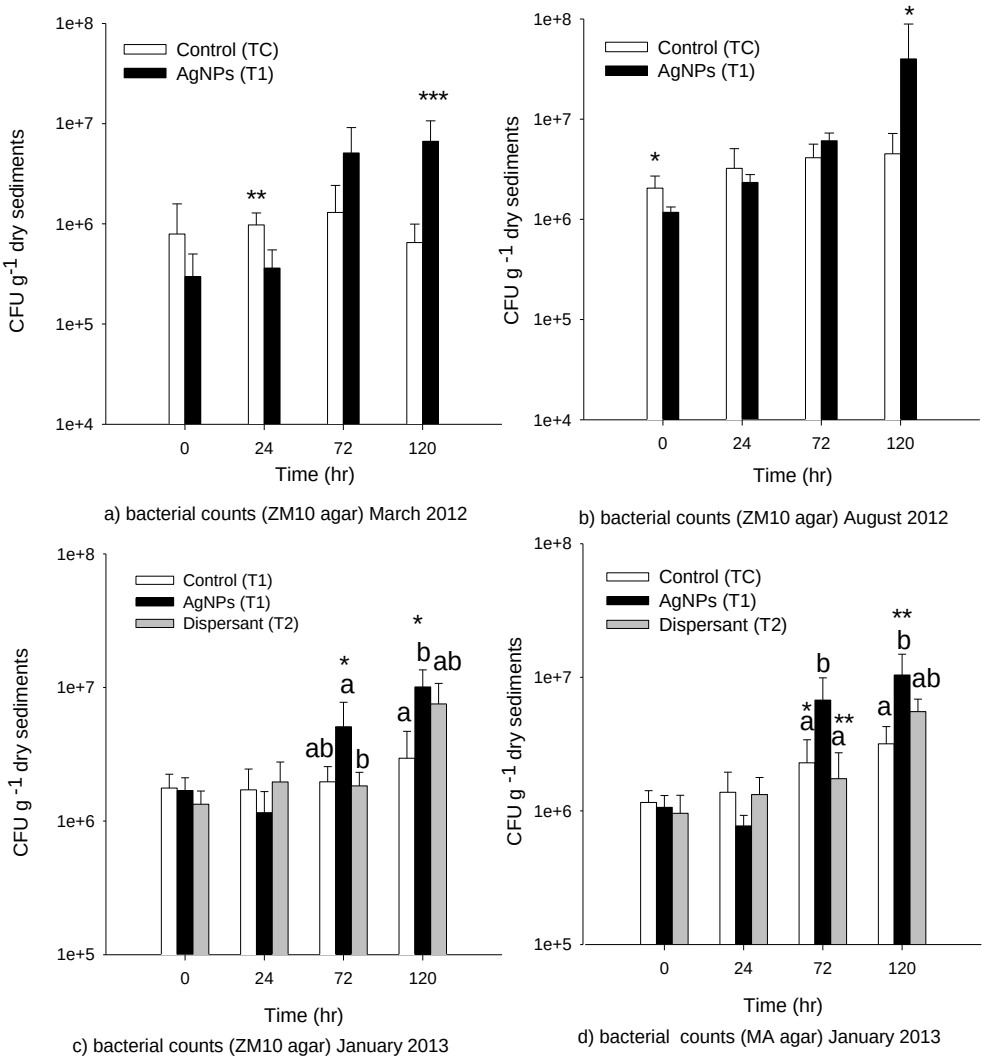

Figure 3. 57 Bacterial abundance expressed as the mean ± SD of the log 10 (CFU). Columns different letters are significantly different. t-test, March'12 and August '12, and ANOVA , January'13, $p < 0.05$), *, **, *** symbolizes statistically significant differences ($p < 0.05$), ($p < 0.01$) $p < 0.001$), respectively.

The bacterial plate counts in January 2013 were statistically significantly higher in the ZM/10 medium that in the Difco MA at time 0 hrs in the AgNPs (T1) (ZM/10 *vs* Difco MA t-test , p-value= 0.40) and Control (TC) treatments (ZM/10 *vs* Difco MA , t-test p-value=0.047) (see related graph in the Appendix IX Figure A3).

3.3.5. Study of the community function with Biolog Ecoplates

The overall utilization of the different carbon sources included in the Biolog EcoPlate™ was investigated at two different time points, 24 and 120 hours after the beginning of the AgNP exposures, and in two different microcosms established in different seasons, in summer (August 2012) and in winter (January 2013). These two time points were chosen on the basis of the results obtained with plate counts in March 2012. The preliminary data showed that after 24 hours of exposure to AgNPs (T1) the viability of heterotrophic groups was negatively affected, but recovered fully to resemble the control (TC) treatment after 120 hours of exposure. The results related to the carbon substrates utilization rates and the community level physiological profiles are described in the following subsections.

3.3.5.1. Average well colour development and carbon utilization rate

The average well colour development (AWCD) related to the average carbon substrates utilization included in the Biolog Ecoplate was always higher in the absence of AgNPs. The AWCD varied depending on the time of exposure (after 24 hr or 120 hr) in both seasons, in August 2012 decreased after 120 hr whereas in January 2013 increased.

3.3.5.1.1. AWCD August 2012

The linear relationship between OD_{590} and time was found between the incubation times of 14-114 hrs for samples collected after 24 hr of exposure (Figure 3. 58 a) and between 25-143 hr for samples collected after 120hr of exposure (Figure 3. 58 b). The uptake rate was always higher in the control (TC) treatment and statistically significantly different after 24 hr of exposure (ANOVA, $p<0.001$).

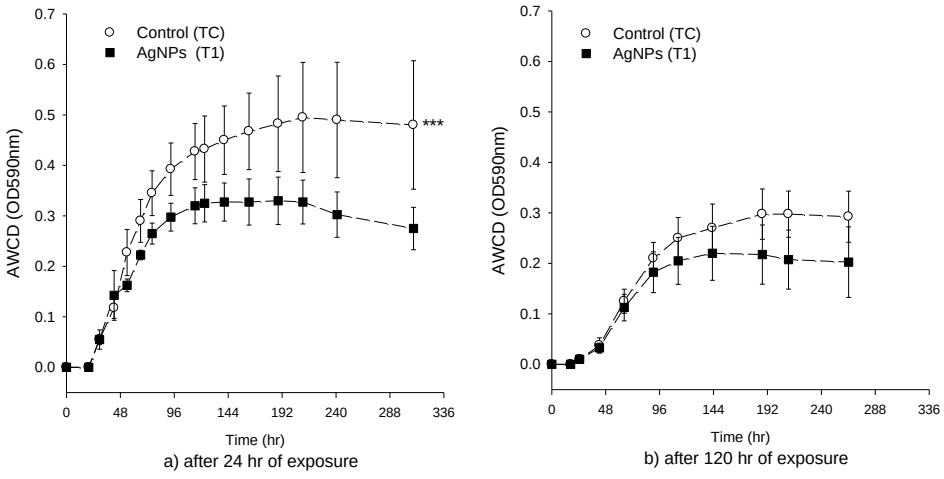

Figure 3. 58 Average utilization rate of the carbon substrates included in the Biolog EcoPlate™ after (a) 24 hr and (b) 120 hr of exposure, expressed as the mean value of OD (590 nm) ± SD, n=4. Symbol *** indicate significant difference ($p < 0.001$) between treatments.

The uptake rate of the individual carbon substrates was analyzed and summarized in the Table 3. 11. A positive uptake for a carbon source (per treatment and time of exposure) was determined if at least 3 out 4 wells (75%) for a given carbon substrate exhibited a positive utilization (if the colour of the well turned purple). The uptake rate for each carbon source was estimated when there was a linear relationship between the OD_{590}. After 24 hr of exposure the utilization of the following carbon substrates was inhibited in presence of AgNPs (T1): 4-hydroxy benzoic acid, D – xylose, N-acetyl-D-glucosamine, D-galacturonic acid, L-phenylalanine and putrescine. The utilization of most of these substrates recovered after 120 hr of exposure except the aminoacid L-phenylalanine. After 120 hr of exposure the utilization of pyruvic acid methyl ester was affected by the exposure to AgNPs (T1). Glucose-1-phosphate was utilized in the bacterial communities exposed to AgNPs (T1) after 120 hr however in the control (TC) no positive uptake was observed.

Table 3. 11 Summary of carbon utilization (+[1]/-[2]) August 2012

Carbon group	Carbon source	After 24 hr		After 120 hr	
		Control TC	AgNPs T1	Control TC	AgNPs T1
Phenolic compounds	2-Hydroxy Benzoic acid	–	–	–	–
	4-Hydroxy Benzoic acid	+	–	+	+
Carbohydrates	D - Mannitol	+	+	+	+
	D - Xylose	+	–	+	+
	D-Cellobiose	+	+	+	+
	D-Galactonic Acid γ- Lactone	–	–	–	–
	,L-α-Glycerol Phosphate	–	–	–	–
	N-Acetyl-D-Glucosamine	+***	+	+	+
	i- Erythritol	–	–	–	–
	α - D - Lactose	+	+	+	+
	β - Methyl -D-Glucoside	–	–	+	+
	Glucose-1-Phosphate	+	+	–	+
Carboxylic acids	γ-hydroxybutyric acid	–	–	–	–
	α - Ketobutyric Acid	–	–	–	–
	D-Galacturonic Acid	+	–	+	+
	D-Glucosaminic Acid	–	–	–	–
	Itaconic Acid	–	–	–	–
	D- Malic Acid	–	–	–	–
	Pyruvic acid Methyl Ester	+	+	+*	–
Amino acids	L-Arginine	+	+	+	+
	L-Asparagine	+	+	+	+
	L-Phenylalanine	+	–	+	–
	L-Serine	+	+	+	+
	L-Threonine	+	+	+	+
	Glycyl-L-Glutamic Acid	+	+	+	+
Amines	Phenyethyl-amine	–	–	–	–
	Putrescine	+	–	+	+
Polymers	Tween 40	+	+	+	+
	Tween 80	+	+	+	+
	α - Cyclodextrin	+	+	+	+
	Glycogen	+	+	+	+

[1](+) symbolizes positive growth observed in at least the 75% of the wells, [2](-) means the opposite. Carbon substrates with the same letters are not statistically significantly different. * symbolizes statistically significant differences (independent t-test $p < 0.05$).

3.3.5.1.2. AWCD January 2013

The overall carbon utilization rate was calculated between 16-135 hr for samples collected after 24 hr of exposure (Figure 3. 59a) and between 52-166 hr for samples collected after 120hr of exposure (Figure 3. 59b), when there was a linear relation between AWCD and time. Similarly to the results obtained in August 2012, the uptake rate was always higher in the absence of AgNPs (T1), and statistically significantly different between the dispersant (T2) and the AgNPs (T1) after 120 hr of exposure (ANOVA, $p<0.05$). In contrast to August 2012, the average uptake in all treatments (TC, T1 and T2) was higher after 120 hr of exposure than after 24 hr. This increase was higher in the dispersant only treatments and AgNPs (T1 and T2, 50% increase) than in the control treatment (TC, 10% increase).

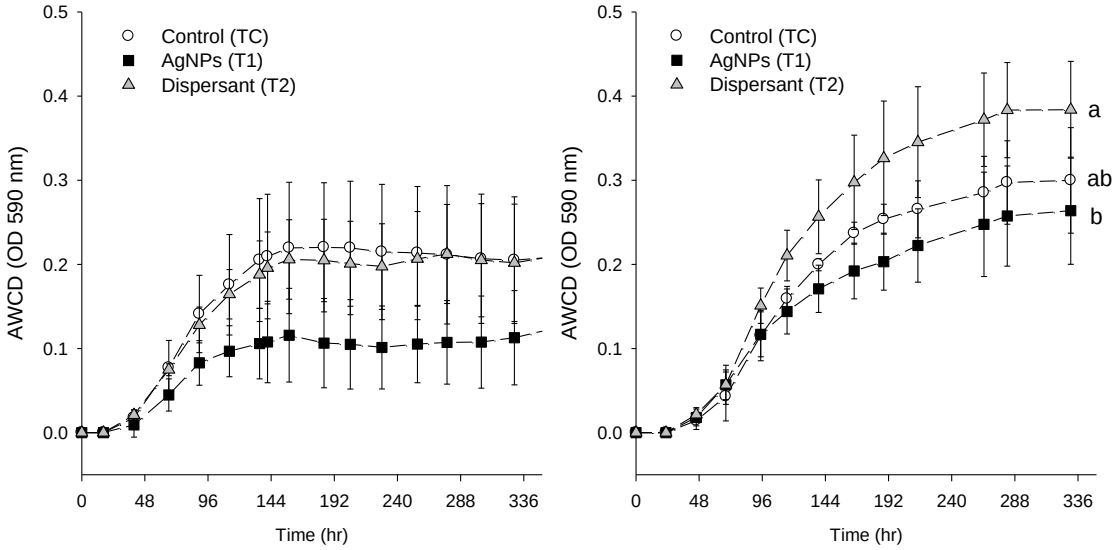

Figure 3. 59 Average utilization rate of the carbon substrates included in the Biolog EcoPlate™ after 24 hr (a) and 120 hr. (b) of exposure, expressed as the mean value of OD (590nm) ± SD, n=4. Lines with different letters indicate significant difference ($p<0.05$) between treatments.

The analysis related to each individual carbon source was performed in the same way to August 2012, and a summary is depicted in the Table 3. 12. The utilization of the following carbon sources was negatively affected by the exposure to AgNPs after 24 hr exposure: D-mannitol, L-arginine, L-asparagine and L-phenylalanine. After 120 hr of exposure a positive uptake of these carbon sources was observed. In the dispersant treatment (T2) no utilization of putrescine was observed after 24 hr but a positive uptake took place after 120 hr. After 120 hr of exposure the utilization of the following carbon sources was statistically significantly higher in the dispersant treatment (T2) than in the AgNPs (T1): D-cellobiose, N-acetyl-D- glucosamine and pyruvic acid methyl ester.

Highlight that the use of the amine phenyethyl-amine was positive only in the dispersant (T2) treatment after 120 hr of exposure.

Table 3. 12 Summary of carbon utilization (+[1]/-[2]) at different time points of exposure

Carbon group	Carbon source	after 24 hr exposure			after 120 hr exposure		
		Control (TC)	AgNPs (T1)	Dispersant (T2)	Control (TC)	AgNPs (T1)	Dispersant (T2)
Phenolic compounds	2-Hydroxy Benzoic acid	–	–	–	–	–	–
	4-Hydroxy Benzoic acid	–	–	–	–	–	–
Carbohydrates	D - Mannitol	+	–	+	+	+	+
	D - Xylose	–	–	–	+	+	+
	D-Cellobiose	+	+	+	+(ab)	+(b*)	+(a)
	D-Galactonic Acid γ- Lactone	–	–	–	–	–	–
	D,L-α-Glycerol Phosphate	–	–	–	–	–	–
	N-Acetyl-D-Glucosamine	+	+	+	+(ab)	+(b*)	+(a)
	i- Erythritol	–	–	–	–	–	–
	α - D - Lactose	+	+	+	+	+	+
	β - Methyl -D-Glucoside	+	+	+	+	+	+
	Glucose-1-Phosphate	–	–	–	–	–	–
Carboxylic acids	γ-hydroxybutyric acid	–	–	–	–	–	–
	α - Ketobutyric Acid	–	–	–	–	–	–
	D-Galacturonic Acid	–	–	–	+	+	+
	D-Glucosaminic Acid	–	–	–	–	–	–
	Itaconic Acid	–	–	–	–	–	–
	D- Malic Acid	–	–	–	–	–	–
	Pyruvic acid Methyl Ester	+	+	+	+(ab)	+(b*)	+(a)
Amino acids	L-Arginine	+	–	+	+	+	+
	L-Asparagine	+(a)	+(b*)	+(ab)	+	+	+
	L-Phenylalanine	+	–	+	+	+	+
	L-Serine	+	+	+	+	+	+
	L-Threonine	+	+	+	+	+	+
	Glycyl-L-Glutamic Acid	+	+	+	+	+	+
Amines	Phenyethyl-amine	–	–	–	–	–	+
	Putrescine	+	+	–	+	+	+
Polymers	Tween 40	+	+	+	+	+	+
	Tween 80	+	+	+	+	+	+
	α - Cyclodextrin	+	+	+	+	+	+
	Glycogen	+	+	+	+	+	+

[1](+) symbolizes positive growth observed in at least the 75% of the wells, [2](-) means the opposite. Carbon substrates with the same letters are not statistically significantly different. * symbolizes statistically significant differences (ANOVA, $p < 0.05$).

3.3.5.2. Effects of NM-300 at the community level physiological profile (CLPP) or community function

The CLPP was analyzed with principal component analysis (PCA) using two different sets of data, the data obtained with the Biolog EcoPlate™ in January 2013 and a second analysis using the same data together with the Biolog EcoPlate™ results obtained in August 2012.

3.3.5.2.1. CLPP in January 2013 analyzed with PCA

PCA analysis of the absorbance data sets, measured 6 days (PCA_6, Figure 3. 60) or 14 days (PCA_{14}, Figure 3. 62) after incubation showed similar distribution of the samples in the plots depicted by three principal components PC1, PC2 and PC3, that explained approximately up to the 70% of the total variability between samples. The outlying samples are identified in the graphs. After the first 24 hr of exposure the samples associated to the control (TC) and dispersant (T2) treatments grouped together indicating that communities in both treatments exhibit a similar CLPP. In contrast the samples in the AgNPs (T1) treatment were segregated revealing a different CLPP after 24 hr. After 120 hours of exposure all treatments grouped together in the PC1 *vs.* PC2 and PC1 *vs.* PC3 axes indicating that the bacterial communities from the three treatments exhibited a similar CLPP. The carbon substrates included in the analysis and their loadings represented by the principal components PC1 *vs.* PC2 and PC1 *vs.* PC3, are depicted in Figure 3. **61** (PCA_6) and Figure 3. **63** (PCA_{14}).

CLPP after 6 days incubation time (PCA_6)

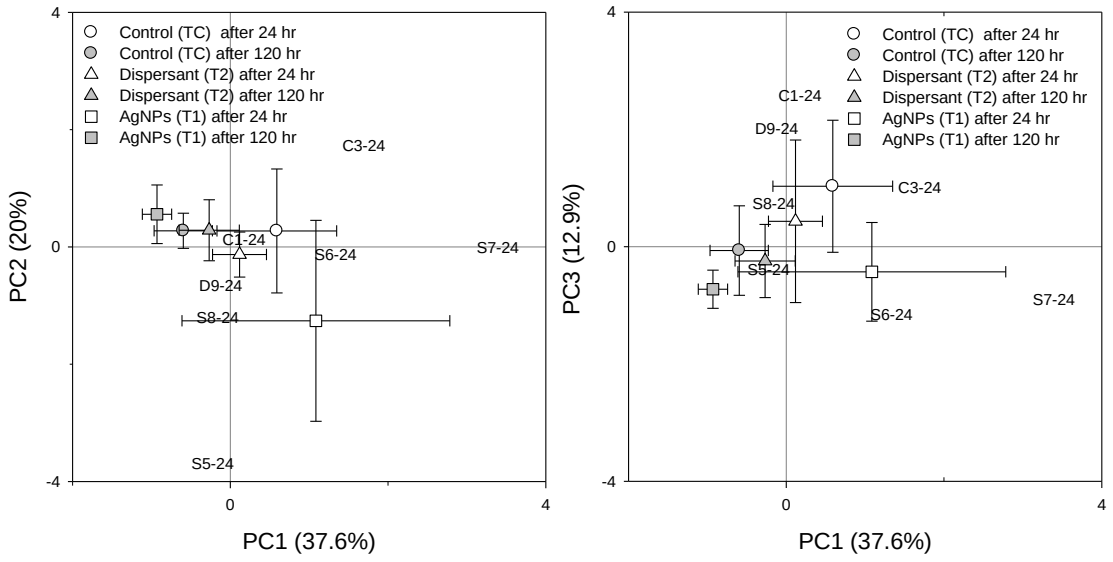

Figure 3. 60 Principle Component Analysis of the CLPP of the three different treatments based on the utilization of different carbon substrates included in Biolog EcoPlates™ with absorbance measurements after 6 days of incubation. The values of the principal component scores are expressed as the mean ±SD; n=4. C1-24, C3-24 (Control); S5-24, S6-24, S7-24, S8-24 (AgNPs) and D9-24 (Dispersant) treatments, respectively, following 24 hr exposure.

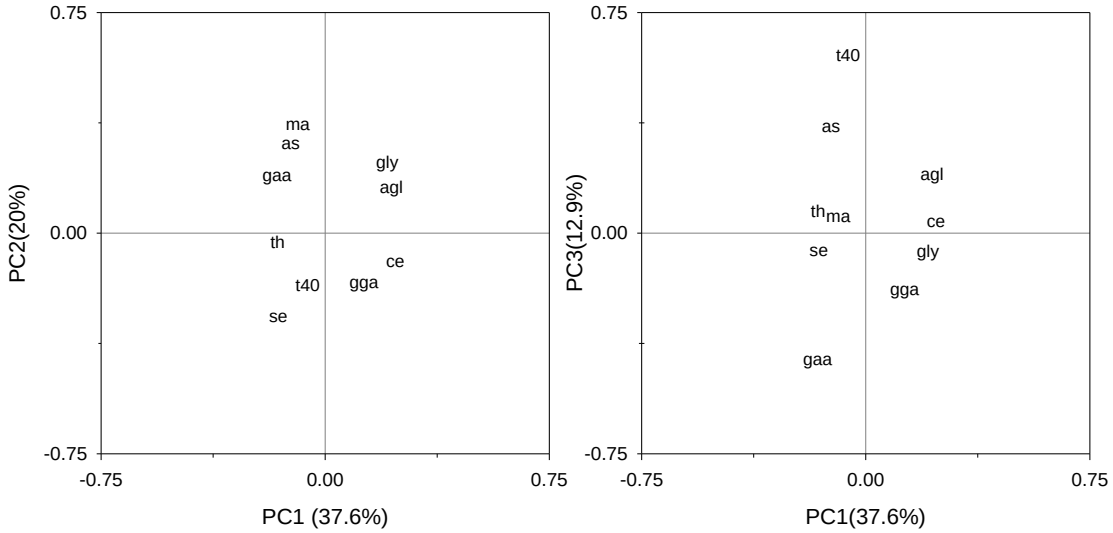

Figure 3. 61 Loading of the carbon substrates included in the PCA analysis in the PC1 *vs*. PC2 and PC1 *vs*. PC3 axes. Carbon substrates with O.D.590nm >0.25 after 6 days incubation period and fulfilling the statistical criteria for PCA were included in the analysis (gly: glycogen; t40:Tween 80; ce: D-cellobiose; gaa: D-galacturonic acid; agl: N-acetyl-D-glucosamine; gga: glycil-L-glutamic acid; ma: D-Mannitol; se: L-serine; th: L-threonine; as: L-asparagine).

CLPP after 14 days incubation time (PCA_{14})

In the PCA_{14} the number of carbon substrates included (factors) was higher than in the PCA_6, because after 14 days incubation, more carbon substrates exhibited a Mean OD_{590} > 0.25.

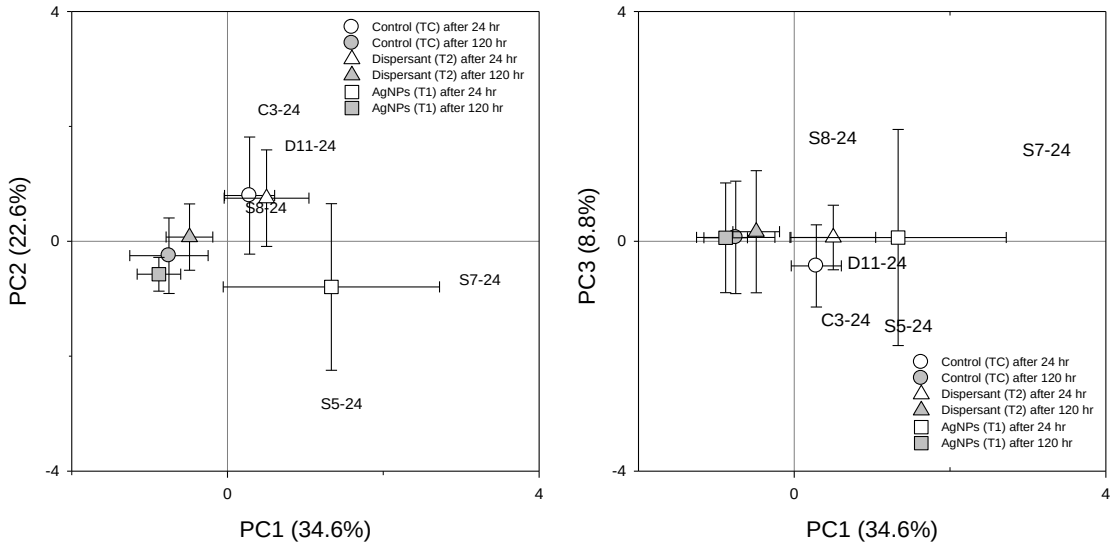

Figure 3. 62 Principle Component Analysis of the CLPP of the three different treatments based on the utilization of different carbon substrates included in Biolog EcoPlates™ with absorbance measurements after 14 days of incubation. The values of the principal component scores are expressed as the mean ±SD; n=4. C3-24 (Control); S5-24, S7-24, S8-24 (AgNPs) and D11-24 (Dispersant) treatments, respectively, following 24 hr exposure.

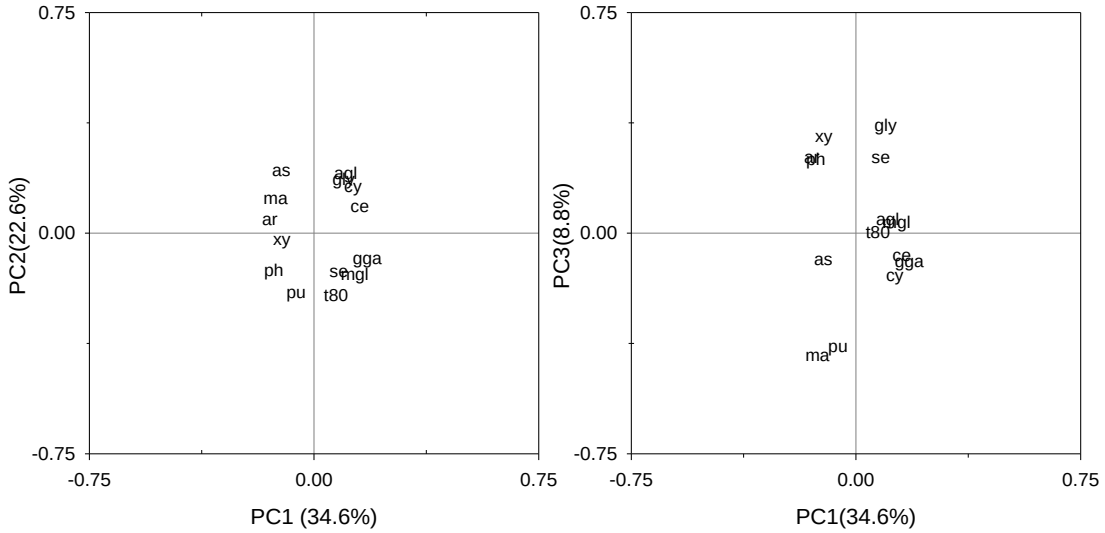

Figure 3. 63 Loading of the carbon substrates included in the PCA analysis in the PC1 vs. PC2 and PC1 *vs.* PC3 axes. Carbon substrates with O.D.590nm >0.25 after 14 days incubation period and fulfilling the statistical criteria for PCA were included in the analysis (cy: α-cyclodextrin; gly: glycogen; t80:tween 80; ce: D-cellobiose; agl: N-acetyl-D-glucosamine; gga: glycil-L-glutamic acid; ph: L-phenylalanine; mgl: β-methyl-D-glucoside; ma: D-Mannitol; se:L-serine ;as: L-asparagine, ar: L-arginine; pu:putrescine; xy: D-xylose).

3.3.5.2.2. CLPP in August 2012 and January 2013 analyzed with PCA

The CLPP of the bacterial communities inhabiting the sediments in August 2012 and January 2013 were analyzed together with PCA. The patterns depicted by the sample distribution in the PC1 *vs.* PC2 and PC1 *vs.* PC3 explained up to 53.7 % of the total variability between samples (Figure 3. 64 a-b). The CLPP of the bacterial communities differed depending on the season, summer or winter, August 2012 and January 2013, respectively. The samples associated with August 2012 distributed in the positive side of the x-axis (PC1), whereas the samples from January 2013 are organized on the negative side of the x-axis. In the PC1 *vs.* PC2 plot it can be seen that the samples of the different treatments (TC and T1 in August 2012; TC, T1 and T2 in January 2013) grouped closely after 120 hr indicating a similar CLPP (encircled in red).

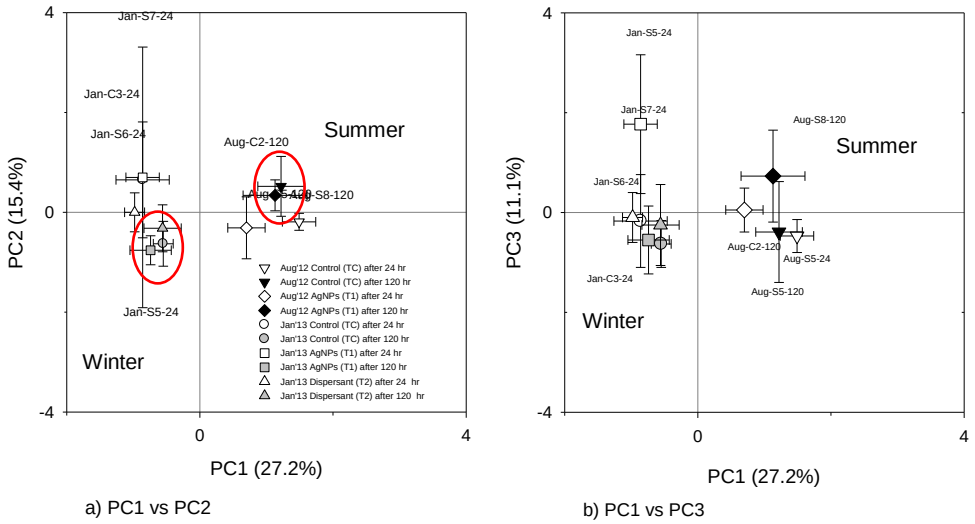

Figure 3. 64 Principle Component Analysis of the CLPP based on the utilization of different carbon substrates included in Biolog EcoPlates™ in microcosms experiments carried out in August 2012 and January 2013.The values of the principal component scores are expressed as the mean ±SD; n=4. Aug or Jan stands for August 2012 or January 2013 respectively, C,S and D for Control, AgNPs and Dispersant and 24 or 120 according to the time of exposure, after 24 hr of after 120 hr.

The carbon substrates included in the analysis and their loadings represented by the principal components PC1 *vs.* PC2 and PC1 *vs.* PC3 are depicted in Figure 3. 65.

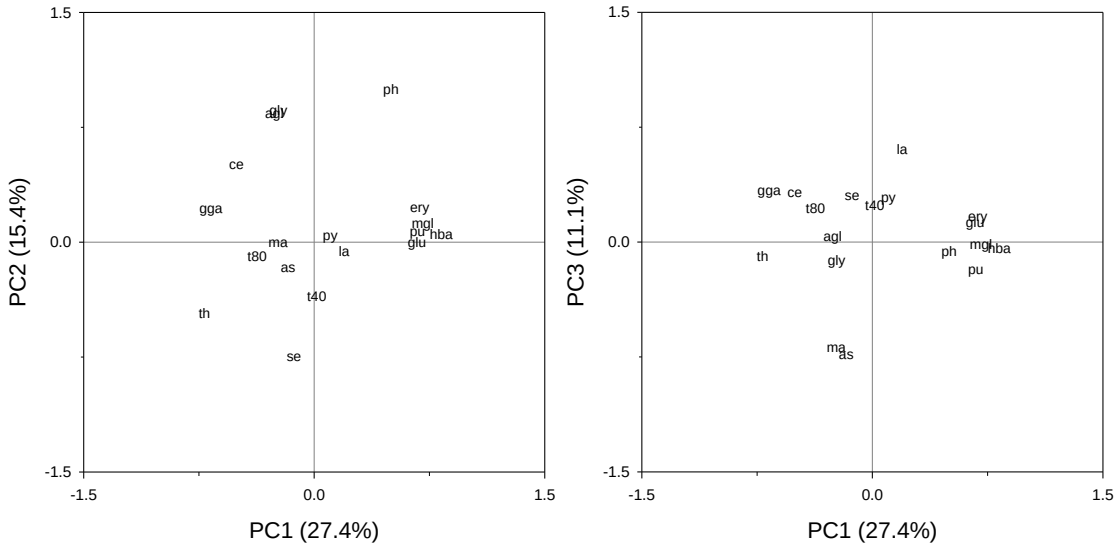

Figure 3. 65 Loading of the carbon substrates included in the PCA analysis in the PC1 *vs*. PC2 and PC1 *vs.* PC3 axes. Carbon substrates with OD_{590}nm >0.25 after 14 days incubation period and fulfilling the statistical criteria for PCA were included in the analysis (gly: glycogen; t40:tween 40; t80:tween 80; ce: D-cellobiose; agl: N-acetyl-D-glucosamine; gga: glycil-L-glutamic acid; ph: L-phenylalanine; mgl: β-methyl-D-glucoside; ma: D-mannitol; se:L-serine ;as: L-asparagine; pu:putrescine; xy: D-xylose;ery:i- i-erythritol; α-D-lactose; hba: γ-hydroxybutyric acid; py: pyruvic acid methyl ester; th: L-threonine).

3.3.6. PLFAs analysis: effects on the community structure

The PLFAs analysis of microbial community inhabiting sediments was carried out with the samples collected during the microcosm established in January 2013.

3.3.6.1. Abundance of bacterial groups

The abundance of Gram negative bacteria across treatments after 120 hr of exposure showed statistically significant differences (p=0.041) between treatments (Figure 3. 66b).

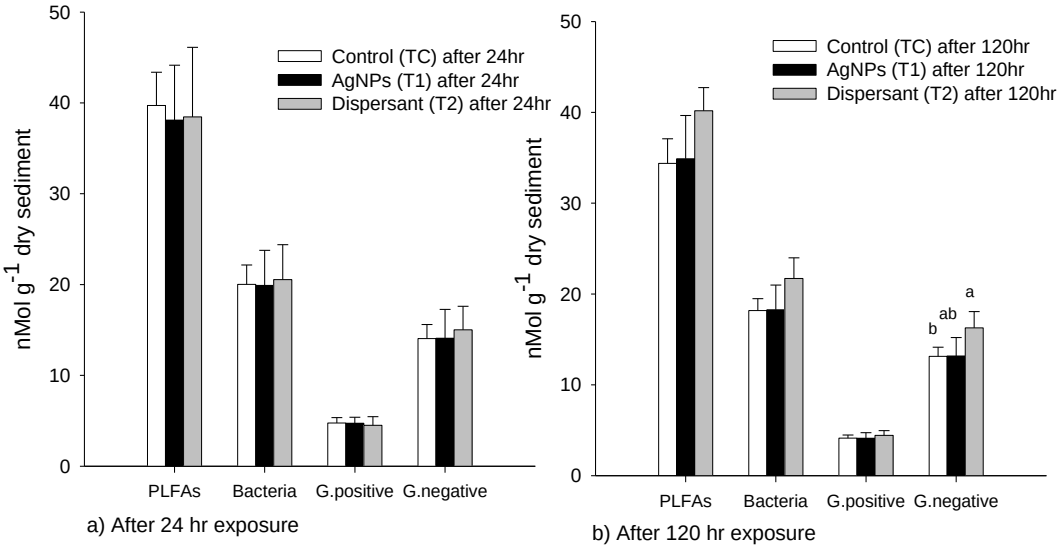

Figure 3. 66 Total PLFAs, total bacteria, Gram positive and Gram negative groups after 24 hr (a) and 120 hr (b) of exposure expressed as mean ± SD, n= 4. Columns with different letters indicate significant difference ($p < 0.05$) between treatments ($p < 0.05$). The Bacteria bar chart includes the sum of the Gram positive and Gram negative bacteria abundance in addition to the unclassified bacterial PLFAs(the ones may be present in both bacterial groups). Gram positive bacteria(Zogg *et al.*, 1997) (i15:0, ai15:0, i16:0, 10 Me l6:0, 17:0i, 17:0ai, 10 Me l7:0, 10 Me l8:0), Gram negative bacteria (Zogg *et al.*, 1997) (16:1ω7c, 16:1ω7t, 16:1ω5, 17:0cy, 18:1ω7, 19:0cy), unclassified bacterial PLFA (Frostegård and Bååth, 1996, Zogg *et al.*, 1997)(15:0, 17:0).

Pairwise comparisons indicated that the abundance of Gram negative groups was statistically significantly higher in the dispersant (T2) than in the control (TC) treatment (t-test p-value=0.022). The use of a paired sample t-test to compare the abundance of Gram negative groups between both time points (24 hr and 120 hr) found statistically significant differences in the control (TC) treatment (p-value=0.029). The abundance of fatty acids 16:1ω7c and 16:1ω7t was reduced by approximately 10% and 25%, respectively. The reduction in the abundance of the 16:1ω7t was statistically significant in the control (TC) treatment between both time points (Paired samples t-test, p-value=0.019). The biomass of bacterial PLFAs increased in the dispersant (T2) treatment coinciding with a higher utilization of carbon substrates following 120 hr of exposure. A summary of the statistically significant paired t-tests performed for each individual PLFAs is provided in the Appendix XIV Table A1.

3.3.6.2. Abundance of individual PLFAs

The abundance of the individual PLFAs is depicted in Figure 3. 67, the associated data is available in the Appendix XIV Table A2.

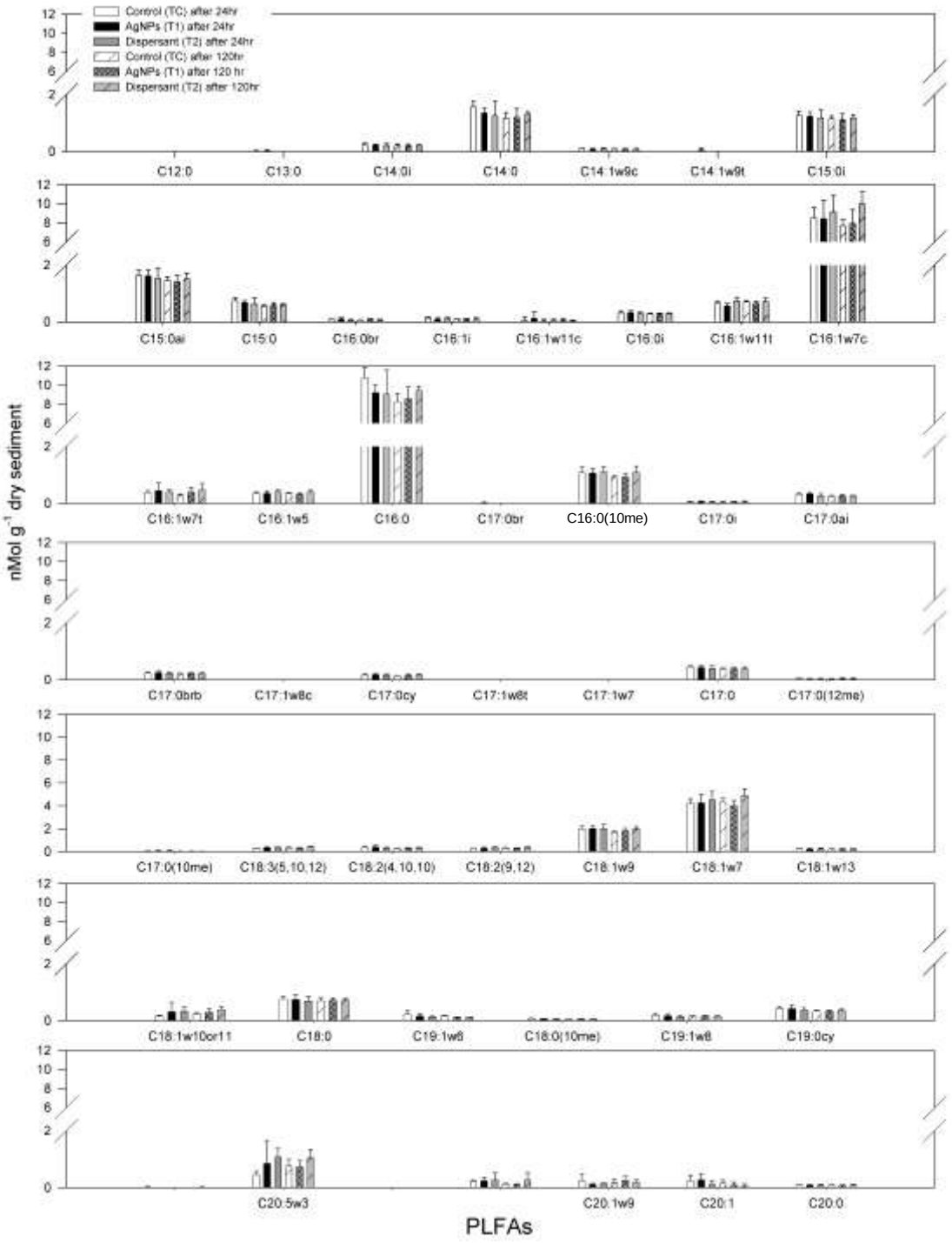

Figure 3. 67 Bar chart showing the abundance of individual PLFAs after 24 and 120 hr of exposure. Data expressed as the mean ± SD, n=4.

The analysis of each PLFA (ANOVA, $\alpha = 0.05$) showed that after 24 hr exposure the abundance of the PLFAs C18:2(9,12) was significantly higher in the dispersant (T2) treatment than in the control (TC) (p-value=0.033). After 120 hr of exposure the abundance of the C16:1ω7c was also higher in the dispersant (T2) than in the control

(TC) (Independent t-test p-value=0.02) and the abundance of the C18:3 (5,10,12) was also significantly higher in the dispersant (T2) than in the AgNPs (T1) treatment (p-value=0.018). The abundance of the C19:1w6 was significantly higher in the control (TC) than in the AgNPs (T1) after 120 hr of exposure (p-value=0.013). A summary of the ANOVA statistical analysis and the Bonferroni post-hoc analysis are depicted in the Table A3 and Table A4 respectively (Appendix XIV).

3.3.6.3. Community structure

The profiling of the microbial community structure based on the PLFAs after 24 and 120 hours of exposure to AgNPs was analyzed with PCA (Figure 3.67). The PLFAs included in the analysis and their respective loadings in the PCA are depicted in the Figure 3. 69. Most of the variability was distributed between two principal components, PC1 and PC2 that explained up to the 72.9% of the total variability between samples, 48.8% and 24.1%, respectively. The samples from the control (TC) and AgNPs (T1) treatment shifted in a similar direction between the 24 and 120 hr time points, revealing a similar community structure based on the relative abundance of PLFAs. No shift between either time points of exposure was observed in the dispersant treatment (T2).

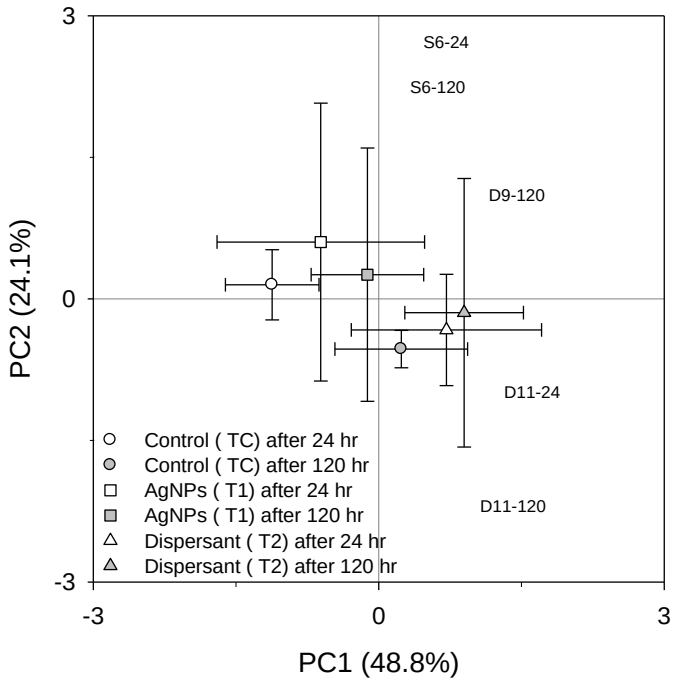

Figure 3. 68 PCA analysis of the bacterial community structure on the basis of the relative abundance of bacterial PLFAs. The values of the principal component (PC) scores are expressed as the mean ± SD, n= 4. The values of the principal component scores are expressed as the mean ±SD; n=4. S6-24, S6-120 (AgNPs T1) and D9-120, D11-24, D11-120 (Dispersant T2) treatments, respectively, following 24 or 120 hr of exposure.

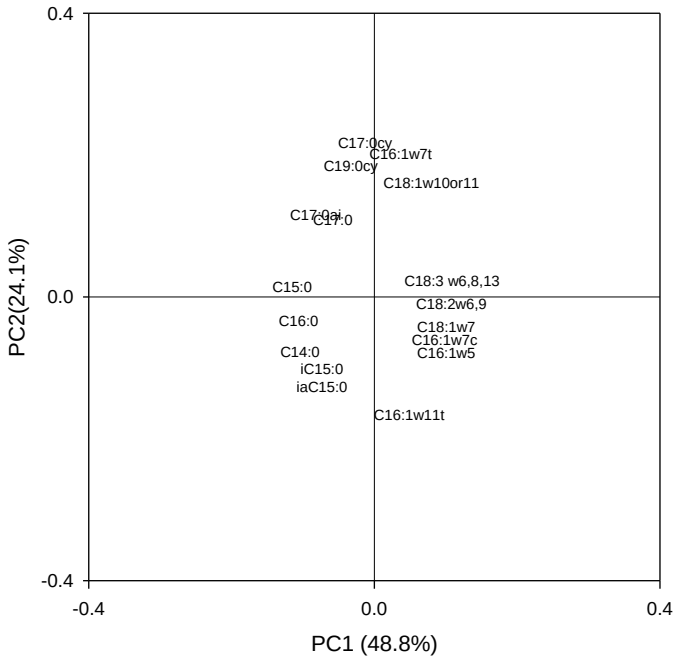

Figure 3. 69 Loading values for the PLFAs included in the PCA analysis. The PLFAs 14:0;16:0; 16:1ω11t; 18:1ω10 or 11 and 18:3ω6,8,13 are not associated to specific bacterial groups but they account for the 30% of the total PLFAs biomass. Gram positive bacteria34 (ic15:0, iac15:0, 17:0ai), Gram negative bacteria34 (16:1ω7c, 16:1ω7t, 16:1ω5, 17:0cy, 18:1ω7, 19:0cy), unclassified bacterial PLFA 33, 34(15:0,17:0)

.

Chapter 4 Discussion

In the present chapter the results relating to the characterization of the physicochemical properties of the different types of AgNPs and their antibacterial properties are discussed first. In the second part of this section the fate of the AgNPs in the water column and sediments is described. Afterwards the findings relating to the ecotoxicity of the AgNPs on the benthic bacterial communities, that inhabit these ecological compartments, are addressed.

4.1. Characterization of Sigma Aldrich, NM-300 and Mesosilver (Hot tube) AgNPs in milli-Q water

The characterization of the physicochemical properties of the AgNPs was needed to explain the antibacterial properties of AgNPs. During the AgNPs characterization process it was observed that to work with the NM-300 AgNPs was going to produce more reproducible results due to the fact that the NM-300 AgNPs stock suspensions were more homogenous as the nanoparticles did not settle out of the suspension, as observed with the Sigma Aldrich. Bondarenko *et al.*, (2013) also observed that uncoated AgNPs (Sigma Aldrich) showed a quick sedimentation and had problems to characterize the AgNPs suspensions with UV-vis spectroscopy. In addition, the NM-300 AgNPs is a reference nanomaterial used by the OECD, therefore to work with the NM-300 was more relevant for comparison purposes with other studies. For this reason the NM-300 AgNPs was the nanoparticle chosen in the present study to compare the susceptibility of different bacterial species to AgNPs and to develop the microcosm exposures. Thus most of the characterization work (bacterial broth media and different chloride concentrations) focused on the NM-300 AgNPs.

4.1.1. Stability of the stock suspensions

4.1.1.1. Sigma Aldrich vs. NM-300 AgNPs

The homogeneity of the AgNPs working suspensions was a key factor in obtaining reproducible results in the toxicity tests with pure bacterial cultures. In the present project it was observed that Sigma Aldrich AgNPs stock suspensions at a concentration of 100 mg L^{-1} were less stable than at 50 mg L^{-1}. This is because at higher concentrations of the AgNPs suspension the particle interaction is enhanced (Lim *et al.*, 2013) leading to higher NP agglomeration/aggregation. At a concentration of 100 mg L^{-1} the AgNPs settled down quickly and, as a result of this, the homogeneity of the suspension decreased, increasing the variability of the concentration between the different aliquots obtained from the suspension. This issue can be a source of variability

in the results obtained within treatments and can also reduce the reproducibility of the toxicity tests. The addition of BSA (final concentration 0.1%) in the AgNPs suspensions at 50 mg L^{-1} enhanced the stability/homogeneity of the AgNPs dispersion. However, BSA may affect the physicochemical properties of the AgNPs (Ravindran *et al.*, 2010), and as a result also the toxicity of the nanoparticles that may produce misleading results. BSA possibly reduces the toxicity of AgNPs by coating the nanoparticles and preventing particle dissolution and the release of silver ions, which is regarded as the main antibacterial mechanisms of AgNPs (Xiu *et al.*, 2012, Levard *et al.*, 2013). The Sigma Aldrich AgNPs settled down quickly in the broth medium and showed a tendency to form big aggregates/clumps during orbital shaking. Therefore, to ensure that AgNPs dispersed well in the experimental flasks, vigorous shaking was required. Orbital shaking was avoided as it enhanced particle aggregation, and conventional flasks were replaced with DURAN ®bottles placed in a horizontal position in order to create a wave motion that increased the AgNPs dispersion in the liquid media. The NM-300 AgNPs was a more adequate AgNP type to develop the toxicity tests with pure cultures than the Sigma Aldrich AgNPs, as the NM-300 dispersed more homogenously (the NM-300 AgNPs did not settle out of the suspension) in the different media (broth media and sea water) without the need of very vigorous shaking.

4.1.1.2. Mesosilver AgNPs

Although the manufacturer of the Mesosilver Hot tube cleaner claimed that this product contained nanosilver, it was still necessary to confirm the presence of AgNPs as some products have been advertised falsely as AgNPs-containing products (Chao *et al.*, 2011). The UV-vis spectroscopy analysis showed the characteristic peak absorbance of AgNPs near the 400 nm (measured at 390 nm) and TEM and AAS confirmed the presence of nanoparticles and silver, respectively. More information could have been obtained with TEM analysis together with Energy-dispersive X-ray spectroscopy (EDS, EDX, or XEDS) to corroborate that the NPs observed with TEM corresponded to AgNPs. However this analysis was not performed as it was not a priority within the scope of the present project.

4.1.2. Comparison of the techniques used to analyze particle size

As expected on the basis of former studies with metallic nanoparticles, the particle size (Z-average) reported by the DLS in Milli-Q water was greater than the size values reported with microscopy techniques (AFM and TEM). This is because the Z-average refers to the value of the hydrodynamic diameter (d_H) whereas AFM and TEM measured the actual size of the nanoparticle, with TEM regarded as the most suitable

technique due to the high contrast of the images (Georgiev *et al.*, 2013). In addition, as DLS is biased towards large particles or aggregates, which scatter more, the analysis of smaller nanoparticles can be overlooked due to their the relative intensity decreases. The results obtained with the different techniques showed the following results, where the particle size or diameter is represented by the symbol Ø: $Ø_{DLS} > Ø_{TEM} > Ø_{AFM}$. These results are in agreement with previous studies that compared the particle size of metallic nanoparticles (Fe_3O_4 NPs). The DLS analysis always reported the largest values followed by TEM NPs (Lim *et al.*, 2013), while the AFM analysis provided the smallest particle size value (Pelletier *et al.*, 2010). TEM/SEM and AFM are the most adequate techniques to measure particle size and shape of metallic nanoparticles including AgNPs, especially when NPs suspensions are polydispersed (Tomaszewska *et al.*, 2013).

4.1.3. Effects of chloride and broth medium on the physicochemical properties of the NM-300 AgNPs

4.1.3.1. Effects of chloride

Salinity is one of the environmental parameters responsible for the high variability of estuarine conditions. It is defined as the amount of dissolved salts in water, and in the seawater is mostly due to dissolved sodium (Na^+) and chloride (Cl^-) ions. Chloride exhibits high affinity for Ag^+, leading to the formation of the low solubility silver chloride (AgCl) salt. For this reason the concentration of chloride can significantly influence the persistence and toxicity of AgNPs, thus the effects of this anion on the AgNPs dissolution and agglomeration were investigated.

4.1.3.1.1. Surface charge and NPs agglomeration/aggregation

The electric double layer surrounding AgNPs depends on the ionic strength of the aqueous suspension. The NM-300 AgNPs are not coated, thus at higher ionic strength there is a reduction in the electric double layer of nanoparticles, and as a result the absolute value of the zeta potential also decreases. The high ionic strength leads to a reduction in the particle surface charge of the AgNPs. This results in enhanced nanoparticle surface interaction and reduced suspension stability (Leo *et al.*, 2013) and settling out of AgNPs (Badawy *et al.*, 2010). AgNPs agglomeration was confirmed with DLS analysis that detected an increase of the average particle diameter in the AgNPs suspended in 20 g L^{-1} NaCl. The UV-vis analysis of the particles in this suspension also reflected particle agglomeration showing a shift towards longer wavelengths (Chinnapongse *et al.*, 2011).

4.1.3.1.2. Dissolution

The intensity of the peak absorbance observed with UV-vis spectroscopy at 10, 20 and 30 g L^{-1} NaCl decreased in agreement with the results obtained by Šiller *et al.*, (2013). Similarly to Zook et *al.*, (2011) and Kent and Vikesland (2011), the results obtained in the present study showed that AgNPs may have dissolved due to nanoparticle oxidation by the dissolved O_2 in the suspension, thereby releasing Ag^+ ions subsequently scavenged by the Cl^- ions (Liu and Hurt, 2010). Zook et *al.*, (2011) showed that UV-vis spectrum analysis was a suitable technique for measuring the dissolution of AgNPs in environmental media with high chloride concentration such as seawater, and demonstrated empirically that dissolution leads to lower absorbance since the plasmon resonance is specific to NPs . Zook *et al.*, (2011) also calculated that AgNPs would dissolve completely at a Cl^- concentration of 339 mMol (12 g L^{-1}), equivalent to the Cl^- concentration in 20 g L^{-1} of NaCl, in agreement with the results obtained with Visual Minteq in the present study that calculated a 100% dissolution for all the components, Ag and NaCl. UV-vis analysis is an inexpensive technique that allowed the semi-quantitative analysis of particle dissolution at different NaCl concentrations and the persistence of the AgNPs in the water column. Ultracentrifugation has been used in earlier studies to analyze AgNPs (Bondarenko *et al.*, 2013, Joshi *et al.*, 2012), however, in the present study this technique was discarded initially, because the AgCl precipitation and accumulation in the solid phase during the ultracentrifugation step could have led to an underestimation of the dissolution of AgNP. However this hypothesis was erroneous according to recent studies that showed that at the Cl/Ag molar ratio 1: 26,750 (close to the experimental conditions of the present study Cl/Ag molar ratio 1: 24,595 in the suspension with 20 g L^{-1} of NaCl) no solid AgCl would form (Levard *et al.*, 2013), in agreement with the output provided by Visual Minteq in the present work that calculated the following silver speciation: 2% AgCl (aqueous form), 61% $AgCl_2^-$ and 37% $AgCl_3^{2-}$. The analysis of NM-300 AgNPs dissolution in ZM/10 media and at different NaCl concentrations was included in a NERC proposal to gain access to the Facility for Environmental Nanoscience Analysis and Characterisation (FENAC) in the University of Birmingham. The characterization of the dissolution of the NM-300 AgNPs in relevant media is an important parameter to assess their toxicity. However this topic of research was not regarded as relevant by the NERC committee as previous studies indicated that AgNPs would dissolve completely in seawater (Levard *et al.*, 2012, Levard *et al.*, 2013, Zook *et al.*, 2011, Liu *et al.*, 2010) under aerobic conditions, as the presence of dissolved O_2 is required for the oxidation of

the AgNPs and the release of silver ions (Liu and Hurt, 2010, Xiu *et al.*, 2012). Nevertheless there was the opportunity to explore the ultrafiltration technique at FENAC, thus AgNPs suspensions in Milli-Q at 100 ppm (NM-300 and Mesosilver) were centrifuged for 1 hr at 30,000 rpm. The presence of AgNPs in the supernatant (based on its yellowish colour) was suspected and the UV-vis spectroscopy analysis showed a peak in the ~ 400 nm and confirmed the presence of the NM-300 AgNPs. The optimum settings of the ultracentrifugation process, such as time, could be investigated in further work in order to quantify the NM-300 dissolution in different media (ZM/10 and estuarine water) at more relevant concentrations (~1 ppm maximum concentration used in the microcosms and in the toxicity test with pure cultures). Ultracentrifugation has been used also to study AgNPs dissolution for the removal of the larger AgNPs (> 26 nm) together with other techniques as ultrafiltration (Ma *et al.*, 2011) as very small nanoparticles can be retained in the supernatant (Maurer *et al.*, 2013). Ultrafiltration and dialysis methods have been used to determine the AgNPs dissolution under different concentrations of chloride that showed that at higher chloride concentrations the dissolution rate increased (Angel *et al.*, 2013) and was prolonged through the time (Burchardt *et al.*, 2012). Preferably a set of complementary techniques should be used to investigate AgNPs dissolution. One of the limitations is that the lower limit of detection of the instruments used to quantify the concentration of silver in the different separated fractions can be high, being 30 ppb for AAS in the present study. Furthermore the most sensitive technique, the ICP-MS, cannot be used with samples containing high concentrations of NaCl as marine water samples. It has been observed that at concentrations of NaCl > 0.1 g L^{-1} the results obtained with internal standards do not produce satisfactory results and the system is blocked after running three samples (Dr. Christine Elgy, FENAC, personal communication).

4.1.3.2. Characterization of the NM-300 AgNPs in ZM/10 medium

The particle size of the NM-300 AgNPs dispersed in the broth medium ZM/10 was analyzed at two different time points with AFM and TEM. Both techniques showed a shift towards higher particle sizes between both time points, although the median particle size measured with AFM between 0 and 24 hr was not statistically significantly different. In contrast the particle size analyzed with TEM was statistically significantly higher after 24 hr. The salinity of the ZM/10 was 24‰ and pH 8.1. At this salinity the concentration Na^+ and Cl^- were estimated to be 7.4 g L^{-1} and 13.3 g L^- respectively (Millero *et al.*, 2008), similar to the highest concentration of NaCl, 20g L^{-1} (7.87 g L^{-1} Na^+, 12.13 g L^{-1} Cl^-) used to investigate the effects of chloride on the NM-300 AgNPs

fate. The NM-300 AgNP was not characterized in ZM/10 broth medium with the DLS analysis as the media composition (bacteriological peptone and yeast extract) cannot be defined in the settings prior to analysis. However due to the high chloride concentration in the ZM/10 it is likely that a reduction of the surface charge and particle aggregation occurred, as observed in medium with 20 g L^{-1} of NaCl. Future work to investigate the stability of the AgNPs dispersed in ZM/10 (with UV-vis spectroscopy) and AgNPs dissolution could be useful to understand better their main antibacterial mechanisms, especially dissolution. Previous studies measured the ionic silver released from AgNPs and compared the toxic effects of these AgNPs with the toxicity of equivalent concentrations of silver ions (normally added as $AgNO_3$ form). When the toxic effects of AgNPs were higher than the effects of $AgNO_3$ at equal concentrations of dissolved silver there was a reason to believe that this higher toxicity was attributable to a "particle-effect" as AgNPs may enhance the formation of ROS (Fabrega *et al.*, 2009a), AgNPs might penetrate inside the bacterial cell (Joshi *et al.*, 2012) and direct contact between the AgNPs and bacterial membranes increases the uptake of ionic silver (ionic silver associated to AgNPs) inside the bacterial cell (Bondarenko *et al.*, 2013).

4.2. Toxicity tests with pure bacterial cultures

The toxicity tests with pure bacterial cultures produced useful information relating to the different bacterial sensitivity to the NM-300 AgNPs. The knowledge gained through the work carried out with pure cultures, supported the analysis of the results obtained with the microcosm experiments, as they provided an insight into the susceptibility of natural estuarine bacteria to the NM-300 AgNPs. In the present work it was observed that the antibacterial properties of AgNPs are bacterial species-specific as described in earlier studies and associated to differences in the bacterial envelope between Gram positive and Gram positive species (Morones *et al.*, 2005, Suresh *et al.*, 2010) and discussed further in section 4.4.1. The minimum inhibitory concentrations (MICs) of the NM-300 AgNPs observed in the present study were lower (MIC values between 0.125 and 1 mg L^{-1}) compared to the results obtained by Suresh *et al.*, (2010) that ranged between 0.5 and 6.5 mg L^{-1} with a similar approach (monitoring bacterial growth under different concentrations of AgNPs). This is possibly due to different bacterial species and different AgNPs types were used. The existing differences in terms of AgNPs types and bacterial species used by different research groups make the direct comparison of the results across studies difficult, but similarities in terms of the bacterial resilience to AgNPs have been observed. Recently the antibacterial properties of the same AgNP type (NM-300K AgNPs, different batch) were investigated on

different *Salmonella* serotypes by Losasso *et al.*, (2014). Higher AgNPs concentrations were used (10- 200 mg L^{-1}) to study their bactericidal effects. For this reason their results are not directly comparable with the NM-300 MICs obtained with estuarine bacteria. Nevertheless, the results are in agreement in terms of the initial antibacterial effects observed by a reduction in the CFU counts followed by a recovery of the bacterial numbers within 72 hr. The type of broth medium used (aminoacid containing –SH groups as cysteine may complex silver ions reducing the AgNPs toxicity) and the cultivation conditions as well as the shape or size of the container may also affect the MICs obtained as described below.

4.3. Effect of the incubation conditions on growth: shake flasks *vs*. tubes

In order to speed up the process of screening for AgNPs MICs the exposures were carried out in small glass test tubes (75 mm×12mm, 3 ml of broth). However, it was observed that for all the bacterial species tested, growth was higher and faster (lag phase was shorter) in the 50 ml flasks (broth medium volume 40 ml) than in smaller tubes (3 ml). This is because in 50 ml flasks the ratio between the volume and the air space is higher than in small tubes, thus the gas exchange (not only O_2) between the air and the liquid phase can be improved, and also the nutrient availability and the exchange of waste products, favouring the growth of aerobic bacteria (Breznak and Costilow, 1994). The species *P.aliena* and *P.arctica* exhibited different growth patterns comparing to *A.agilis* and *Bacillus sp*. The *Pseudoalteromonas spp*. are fast growing bacteria compared to the other species, and also motile. Pseudoalteromonas spp. grew more homogenously in the liquid medium than the other species under low agitation. In contrast *A.agilis* and *Bacillus sp*. showed a tendency to settle down at the bottom of the flask, thus a continuous gently shaken at 100-125 rpm was required for optimum growth of these Gram positive species, whose growth was remarkably higher in 50 ml flasks. It was also observed that the variability within treatments was lower in the 50 ml flasks than in small test tubes. For these reasons it was more adequate to run the toxicity tests in 50 ml flasks to investigate the inhibitory concentrations of NM-300 AgNPs than in smaller volumes. The toxicity tests were conducted in low nutrient medium (ZM/10, 0.05% Bacteriological peptone, 0.01% yeast extract, 75% sea water, 25% distilled water). The use of low nutrient media aimed to minimize the complexation of AgNPs with the organics contained in the medium that could reduce the toxicity of the AgNPs and increase the MICs values. The NM-300 AgNPs concentration (total silver) values obtained with the AAS were always lower than the expected nominal concentration (recovery 58.37 ± 18.23%). However the concentration of total silver measured in the

AgNPs stock suspensions was in agreement with the nominal concentration. Prior to the AAS analysis, the cell cultures exposed to AgNPs were transferred from the 50 ml conical flasks to Falcon® tubes and acidified thereafter. Thus some AgNPs and their derived dissolved forms could have adhered to the conical flask walls (which may also increase the apparent MIC) and this may explain the differences between the nominal concentration and the values measured with AAS. On the other hand the respirometry assay was very useful to determine the inhibitory concentrations of the NM-300 AgNPs on those bacterial species whose growth cannot be measured with OD, as the filamentous forming bacterium *S.koyangensis*. Overall the respirometry assay was a quick technique to determine the range of the inhibitory concentrations of the NM-300 AgNPs as they were in agreement with the results obtained with the other techniques used: monitoring OD and measuring total nitrogen. However the OD technique was more sensitive to detect inhibition at lower concentrations of AgNPs and also greater differences between 1:2 concentrations of AgNPs were detected. This may be due to OD measured bacterial growth between 0 and 40 hr whereas the respirometry assay measured O_2 uptake during the first 1-2 hr of exposure therefore the inhibitory concentrations obtained with both techniques can be in the same range however may not coincide completely. This is possibly because the immediate bacterial response to AgNPs exposure could have increased some resistance mechanisms causing an increase in respiration as observed previously with other antibiotics such as amoxicillin (Händel *et al.*, 2013). The stimulation of bacterial activity under a low dose of a toxic agent, in this particular case AgNPs, is a phenomena known as hormesis, and it has been observed in previous studies that investigated the antibacterial properties of AgNPs (Xiu *et al.*, 2012). In contrast, bacterial cell division is inhibited in presence of ionic silver as they cause DNA condensation (Feng *et al.*, 2000), and this antimicrobial mechanism is also associated to AgNPs.

4.4. Bacterial susceptibility to different AgNP types

The minimum inhibitory concentrations (MICs) observed for the NM-300 AgNPs was always higher than the MICs estimated for the Mesosilver AgNPs. The higher toxicity of the Mesosilver AgNPs suspension could be due to the higher concentration of ionic silver (by 2.2 times higher) and their smaller particle size. The particle size of the Mesosilver AgNPs was also smaller, favouring interaction with the bacterial membranes and previous studies observed that small AgNPs are more toxic (Morones *et al.*, 2005, Lu *et al.*, 2013). Smaller nanoparticles exhibit higher surface area that generally increases dissolution (Dobias and Bernier-Latmani, 2013, Mitrano *et al.*,

2014, Xiu *et al.*, 2012) and surface interaction with biological membranes (Choi and Hu, 2008, Morones *et al.*, 2005). Nanoparticle-membrane interaction can negatively affect cell membranes as a consequence of mechanical interaction (Taglietti *et al.*, 2012) and it also enhances particle dissolution and the intracellular uptake of Ag ions (Bondarenko *et al.*, 2013). On the other hand, *Pseudoalteromonas arctica* was more susceptible to the NM-300 AgNPs than to the Sigma Aldrich AgNPs even though the silver ionic content was higher in the working suspensions of the Sigma Aldrich AgNPs. Preliminary studies with *A.agilis* and *Bacillus sp*. appeared to indicate the same, that the NM-300 AgNP type was more toxic than the Sigma Aldrich AgNPs, however not enough data is available to confirm this. The NM-300 AgNPs were more toxic than the Sigma Aldrich possibly due to their smaller particle size as observed with the DLS analysis. Further characterization of the Sigma Aldrich AgNPs in the bacterial broth media as dissolution and aggregation state would be required. Bondarenko *el at.* (2013) obtained similar results with the AgNPs purchased from Sigma Aldrich AgNPs: low antibacterial toxicity, the formation of large aggregates and high sedimentation. One possible explanation for the lower toxicity of the Sigma Aldrich AgNPs compared to the NM-300 is that the Sigma Aldrich NPs aggregated more (AgNPs clumps were observed by eye) thus the dissolution rate and interaction with biological membranes decreased. These changes in the physicochemical properties of the AgNPs possibly reduced the AgNPs bacterial toxicity.

4.4.1. Resistance of pure bacterial cultures to AgNPs

The results obtained with pure bacterial cultures isolated from the estuary indicated that the Gram negative species (*Pseudoalteromonas* spp. and *C.fucicola sp.)* were more resistant then the Gram positive (*A.agilis* and *Bacillus sp*.) to the NM-300 AgNPs. In the present study *Pseudoalteromonas* spp. exhibited the highest resistance to the NM-300 AgNPs. Members of the *Pseudoalteromonas* genus are known for producing EPS that confers them resistance to metals (Gutierrez *et al.*, 2008). EPS can sequester metals and thus could have trapped the silver ions and prevent their entry into the bacterial cell (Kang *et al.*, 2013). EPS can also enhance cell aggregation, reducing the cell surface area exposed to nanoparticles (Joshi *et al.*, 2012). Abundant black clumps were observed in the cell culture of the *C.fucicola* after exposure to AgNPs (NM-300 and Mesosilver). These floating black clumps were not observed in the cultures of other species after exposure to AgNPs. *C.fucicola* in solid low nutrient media as ZM/10 exhibits a swarming behaviour and degrades agar, similar to other species belonging to the family of the *Flavobacteriaceae,* which are known for

producing extracellular enzymes that degrade polysaccharides (Du *et al.*, 2011). It is possible that extracellular enzymes, such as some glycoside hydrolases containing thiol groups (Ito *et al.*, 2014) present in the amino acid cysteine (a metal binding amino acid), were produced by the *C.fucicola*, and complexed with the AgNPs leading to the formation of the black clumps. In future more work is needed to confirm if *C.fucicola* and the *Pseudoalteromonas* spp. used in the present research project produce EPS. If this is affirmative, the interaction between EPS and AgNPs would be an interesting case of study.

The differences between the Gram negative and Gram positive bacteria groups regarding the resistance to AgNPs have been investigated extensively (Suresh *et al.*, 2010, Kim *et al.*, 2007, Amato *et al.*, 2011, Ojha *et al.*, 2013, Bondarenko *et al.*, 2013), including ionic silver (Jung *et al.*, 2008, Feng *et al.*, 2000). However, based on these studies it is not possible to conclude which group is more susceptible to ionic silver and AgNPs, as different species and different types of AgNPs were used as discussed previously in section 1.1.4. Moreover the physicochemical properties of AgNPs depend on the environmental conditions (as the composition of the nutrient media, pH and temperature). Regarding the bacterial susceptibility to silver, it would be interesting to examine whether the most resistant bacteria to AgNPs (*Pseudoalteromonas* spp.) are also the most resistant to ionic silver.

One of the objectives of the present research project was to investigate the interaction between the bacterial membranes and AgNPs with AFM at the minimum inhibitory concentrations (MIC). This study was supported by a NERC Grant to carry out a pilot study at the FENAC. To do this bacterial samples (prepared on mica sheet pre-treated with Poly-L-Lysine as described in Bolshakova *et al.*, (2001)) were examined with AFM in non contact mode to avoid the tip of the cantilever damaging the sample. After five days of work no results were obtained due to the instrument limitations. The instrument available at FENAC, model XE-100 SPM Microscope was not suitable for bacterial examination in liquid broth medium (personal communication Dr Mohammed Baalousha, FENAC). In a liquid environment the oscillatory conditions of the cantilever are different than those in air conditions. Thus the resonance frequencies produced by the cantilever will also change (Korayem *et al.*, 2011) and this type of issues could not be overcome at FENAC.

4.5. Microcosm exposures

Toxicity tests with pure bacterial cultures are relevant to screen for the antibacterial activity of different nanoparticle types and additionally to determine the most susceptible bacterial groups. However, bacterial communities are typically formed by mixed populations of bacterial species and the interactions may be competitive, but can also be syntrophic or beneficial (such as mutualism and commensalism) (Morris *et al*., 2013). A key advantage of this microcosm approach was that it took the whole bacterial community into account as they were established with fresh undisturbed sediment samples and water from the estuary. The main aim of the present piece of work was to assess the bacterial community functional response to a single pulse of AgNPs in water.

4.5.1. Fate of the NM-300 AgNPs in the microcosm

In the present study the initial Cl/Ag molar ratio in the water column was 52,360:1, as a result the formation of soluble forms of silver chloro-complexes such AgCl, $AgCl_2^-$ and$AgCl_3^{2-}$ was possibly favoured as calculated with Visual MINTEQ and supported by previous work (Levard *et al.*, 2013). These ionic forms of silver are bioavailable and able to cross bacterial cell membranes and (based on studies carried out with the Gram negative bacterium *Escherichia coli* (Gupta *et al.*, 1998)) at high concentrations can decrease the bacterial resistance to ionic silver. This is in agreement with the study developed by Crémazy *et al.*, (2014) whose findings showed that metal toxicity may not be associated solely to free ionic forms and the Biotic Ligand Model (BLM) theory should take this into account. The concentration of sulphides in the water column was not measured in the present study as they are expected to be low in estuaries between 1.7 and 100 µg L^{-1} (Liu *et al.*, 2011), and Ag-S interactions were expected to be negligible under the microcosm conditions that are mainly marine and aerobic (Levard *et al.*, 2012). The measurements obtained in the microcosms showed that the water column was well aerated (dissolved oxygen 7.8 mg L^{-1}) and superficial sediments were essentially oxic (redox potential measured in the first 5 mm was + 230 mV). Well oxidized sediments containing iron and manganese oxides exhibit high affinity for ionic silver (Luoma *et al.*, 1995). It is known that other components in the water matrix such as certain types of organic matter (Fabrega *et al.*, 2009a) and clays (Zhou *et al.*, 2012) can influence the physicochemical properties of AgNPs by absorbing the nanoparticles. Previous studies have revealed that natural organic matter (NOM), such as humic and fulvic acids are able to reduce the dissolution of AgNPs through surrounding the AgNPs and protecting them from oxidative species (Liu *et al.*,

2010). Some organics such as Suwannee River humic acids (SRHA) can enhance the disaggregation of the AgNPs (this is the reason why SRHA is commonly used to enhance the dispersion of nanomaterials when developing ecotoxicity tests (Al-Shaeri *et al.*, 2013)) and reduce the toxicity of AgNPs through particle surface modification (Fabrega *et al.*, 2009a). Na^+ and Cl^- are always in the same proportion in the sea water (Millero *et al.*, 2008) and as the value of total salinity in the water of the microcosm was 31‰, the concentrations of Na^+ and Cl^- were estimated to be 9.55 g L^{-1} and 17.14 g L^{-1} respectively. The NM-300 AgNPs in the water column of the microcosm appeared to dissolve and agglomerate in a similar way to the AgNPs exposed to the highest concentration of NaCl (20 g L^{-1}), following deposition onto the sediments (confirmed with AAS). Preliminary experiments showed no differences between the persistence of the AgNPs at 20 and 30 g L^{-1} (equivalent to seawater salinity of NaCl of 21.92 ‰ and 32.87 ‰ respectively (Cox *et al.*, 1967)). Therefore in the experiments addressing the effects of chloride on the persistence of AgNPs, the highest concentration of NaCl tested was 20 g L^{-1}.

4.5.1.1.1. Raman microspectroscopy

Raman microspectroscopy was the technique used to examine the type of silver species accumulated in the surface of the sediment samples collected from the microcosm. This technique has been used successfully to analyze polluted sediments with heavy metals (Villanueva *et al.*, 2008) and microplastics (Van Cauwenberghe *et al.*, 2013). The preliminary results obtained in the present study confirmed the presence of AgCl and silver oxides (Ag-O stretching/bending modes) in sediments. It would be interesting to investigate more deeply the applicability of this technique in order to analyze the transformation of AgNPs in marine sediments. The construction of a database including Raman shifts relating to the diverse mineralogy present in sediments to use it as a background control may be required. The Raman microspectroscopy analysis allows the identification of substances and particle types (Santos *et al.*, 2010). It is also a non-destructive technique that preserved the physicochemical properties of the samples and as result of this the AgNPs of silver-complexes are conserved. This technique on its own does not allow the analysis of nanoparticles but it could be used in conjunction with other complementary techniques such as symmetric-flow field flow fractionation (Gigault and Hackley, 2013).

Based on the preliminary results obtained with the Raman microspectroscopy and the effects of chloride in the AgNPs together with the AAS analysis, the silver

species in the sediments of the microcosms possibly included silver chloride and AgNPs agglomerated or/and complexed with organic matter that in the first millimetres of the superficial sediments of the microcosm can be susceptible to oxidation followed by the formation of more bioavailable forms of silver such as detailed previously (Levard *et al.*, 2013). The sulfidation of silver is not expected to occur as in aerobic environments sulphate is the predominant form of sulphur, and it does not react with silver (Liu *et al.*, 2011).

4.5.2. Effects of NM-300 on the bacterial abundance, community structure and function

The bacterial abundance analyzed with bacterial plate counts showed a similar trend in the water column and sediments, independently on the season (winter versus summer) as observed with the microcosm experiments established in March of 2012 (end of the winter), August 2012 (summer) and January 2013 (winter). Overall in presence of AgNPs (T1) the bacterial production is reduced and bacterial abundance is lower than in the control (TC) and dispersant (T2) treatments. The bacterial production in the AgNPs (T1) treatment recovered at the end of the exposures (120 hr) in the water column (except in August 2012) and earlier in sediments (72 hr). In subsections 4.5.2.1 and 4.3.2.2 the discussion is focused mainly in the results obtained in January 2013 as up to four complementary techniques were applied to investigate the effects on AgNPs on the bacterial community that inhabit the water column. More resources were invested to investigate the effects of the AgNPs on the metabolic profile and structure of bacterial communities inhabiting sediments due to the scarce studies performed to date relating of the effects of AgNPs on bacteria inhabiting this ecological compartment (see section 4.5.3 and related subsections).

4.5.2.1. Effects of AgNPs on planktonic bacteria (water column)

The analysis of the water samples with different techniques to investigate the effects of AgNPs on planktonic bacteria in January 2013 (bacterial plate counts, Flow Cytometry (FC) and direct counts with Epifluorescence microscopy) showed that bacterial production and bacterial activity was negatively affected in presence of the NM-300 AgNPs during the first 72 hr of exposure and recovered at the end of the exposures (120 hr). The increase in the bacterial abundance was observed in all treatments. A similar trend in the abundance of heterotrophic groups has been reported previously in studies with marine microcosms, and associated with confinement in the tanks and the environmental conditions *ex-situ* (Ferguson *et al.*, 1984, Lebaron *et al.*, 2001). The plate counts indicated that bacterial viability was reduced in presence of

AgNPs in agreement with the results obtained with the respirometry assay that showed a decreased in the O_2 uptake rate during the first 72 hr. On the basis of the information provided by the bacterial plate counts and the respirometry assay it can be confirmed that the physiology of the microbial community inhabiting the water column was negatively affected by the exposure to AgNPs. A reduction in the metabolic activity of the bacterial community possibly reduced the uptake of NH_4, as this is the most relevant source of inorganic N for assimilation and also essential for bacterial growth (Neidhardt *et al.*, 1990). This could explain why the concentration of NH_4 decreased more dramatically in the dispersant (T2) than in the AgNPs (T1) treatment. The dispersant contained ammonium nitrate (NH_4NO_3) (Kermanizadeh *et al.*, 2012) and explained the higher concentration of ammonium in the AgNPs (T1) and dispersant (T2) treatments at the beginning of the experiment. The recovery in the bacterial abundance after the exposure to AgNPs measured with flow cytometry has been reported in earlier studies in fresh water at concentrations of AgNPs ranging between 0.05 and 0.5 mg L^{-1} (Das *et al.*, 2012) and seawater environments at 0.05 mg L^{-1}(Doiron *et al.*, 2012). This recovery can be associated with the proliferation of more resistant bacterial species to AgNPs (Das *et al.*, 2012). Two other hypotheses may also explain the bacterial recovery in the AgNPs (T1) treatment:

1) Removal of the antibacterial agent

The results obtained with *C.fucicola* and the recovery of the bacterial abundance in the microcosms shows the ability of some species to recover from acute exposure after the antibacterial agent has been removed. The concentration of total silver decreased in the water column from 1 mg L^{-1} to 0.08 mg L^{-1} in 24 hr and remained below the detection limits (0.030 mg L^{-1}) during the rest of the experiment. Thus the removal of the antibacterial agent can reactivate the bacterial division as observed with *C.fucicola* when exposed to 1.5 mg L^{-1} of the NM-300 AgNP type. Even though the recovery was not apparent on the basis of OD (600 nm) measurements, cell cultures were still viable (CFU formed on agar plates free of AgNPs) after 24 hr of exposure. It is known that silver ions can drive the bacterial cell to an active but non-culturable state (ABNC) (Jung *et al.*, 2008) as ionic silver causes DNA condensation impeding cell division (Feng *et al.*, 2000).

2) A loss in the antibacterial activity of AgNPs due to the transformation of nanoparticles into less soluble compounds with lower toxicity or less bioavailable such

as AgCl (AgNPs can be more toxic than AgCl (Choi *et al.*, 2008)), or by binding organic matter (Fabrega *et al.*, 2009a) or/and EPS (Joshi *et al.*, 2012, Kang *et al.*, 2013).

4.5.2.2. Comparison of techniques

The bacterial plate counts and the flow cytometry results were in the same order of magnitude after 24 hr of exposure. Higher counts were expected with flow cytometry as the bacterial plate counts normally represent a small fraction of the total bacterial population, around 1% (Eilers *et al.*, 2000) or even less, 0.1% (Ferguson *et al.*, 1984). However in other microcosm studies it has been observed that the fraction of culturable bacteria can increase up to 26% after 48 and 96 hr in a microcosm study (Lebaron *et al.*, 2001) and 41% after 32 hr in a bottle confinement at 25 ºC (Ferguson *et al.*, 1984). This can explain the similarities in cell numbers observed between the flow cytometry and the plate counts techniques. The bacterial plate counts did not correlate well with the independent-culture techniques, direct microscopy counts and flow cytometry. Only after 24 hr of exposure did the four biological indicators (bacterial plate counts, flow cytometry counts, direct microscopy counts and O_2 uptake rate) showed a statistically significant positive correlation. Between the time points 0 and 24 hr of exposure to AgNPs, the data obtained with microscopy counts (DAPI stain) did not detect changes in the total prokaryotic abundance. In contrast the counts obtained with flow cytometry showed a decrease in the microbial abundance after 24 hr exposure to AgNPs (statistically significant, paired t-test p-value = 0.003). Unexpectedly the abundance analyzed with FC showed that the bacterial abundance in the control (TC) treatment was significantly lower than in the AgNPs (T1) treatment at the beginning of the exposures (t=0 hr), and these differences were not observed with the other techniques (bacterial plate counts and epifluorescence microscopy). Therefore the differences between the control (TC, n=3, one sample lost) and the AgNPs (T1, n=4) treatments might have occurred by chance and the analysis of more samples is advisable.

The results obtained with the bacterial plate counts, FC and the respirometry assay showed a decrease in the bacterial production/activity after 24 hr of exposure to AgNPs. The stain used in FC, Syto9, exhibits affinity for DNA and RNA, whereas DAPI binds DNA. The concentration of RNA in the bacteria exposed to AgNPs (T1) treatment was possibly lower after 24 hr exposure to AgNPs (T1), due to the reduced bacterial metabolic activity as indicated by the O_2 uptake rate. At lower concentrations of RNA, the intensity of the fluorescence emission could also be reduced (Lebaron *et al.*, 2002), and this may explain why the FC counts decreased after 24 hr in the AgNPs

(T1) treatment. The culture independent methods (flow cytometry, direct microscopy counts and the respirometry assay) showed a positive correlation after 24 and 72 hr of exposure and showed that the prokaryotic production and the physiological status were negatively affected after exposure to AgNPs. The bacterial plate counts obtained in the dispersant treatment (T2) was not statistically significantly higher than the counts obtained in the AgNPs (T1) treatment after 72 hr of exposure. In contrast, the results obtained with flow cytometry and microscopy showed that the prokaryotic abundance in the AgNPs (T1) was statistically significantly lower than in the control and dispersant treatments (TC and T2) after 72 hr exposure. The differences between the bacterial plate counts and the culture-independent methods may be caused by the presence of non-culturable groups in the dispersant treatment (T2) that cannot grow in the plates. The unculturable bacterial groups that did not recover after 72 hr of exposure to AgNPs could be identified with molecular techniques based on the analysis of the 16S rDNA sequence or other genes characteristic of a particular bacterial functional group as the ammonia oxidizing bacteria (AOB) as discussed in section (4.5.2.3). After 120 hr of exposure a significant negative correlation between the O_2 uptake rate and the bacterial plate counts was found, which is not meaningful. Respiration levels possibly decreased as a consequence of aerobic groups that entered into stationary phase due to the depletion of nutrients (Navarro Llorens *et al.*, 2010), such as NH_4. Despite the divergences found between the DAPI counts and FC counts after 24 hr of exposure and thereafter, the counts obtained with both techniques correlated positively one with the other. Flow cytometry analysis is a faster technique and less influenced by human biases. For these reasons it would be the most suitable technique to quantify the bacterial abundance in aquatic samples. However complementary techniques such as the bacterial plate counts and the respirometry assay are required to investigate in greater detail the effects of AgNPs on the bacterial community, such as bacterial viability and physiological status, respectively, as this information is valuable when assessing the functioning of the bacterial community as a whole.

4.5.2.3. Effects of AgNPs on ammonia oxidizing bacteria (AOB)

One of the aims of the present research project was to study the effects of AgNPs on the abundance of Ammonia oxidizing bacteria (AOB) with quantitative polymerase chain reaction (qPCR). AOB play a crucial role in the Nitrogen cycle as they oxidize NH_3 (ammonia) to NO_2^- (nitrite) (Sinigalliano *et al.*, 1995). AOB produce the monooxygenase enzyme responsible for the first step in the oxidation of ammonia, converting the ammonia to hydroxylamine which is regulated and encoded by the *amoA*

gene. Previous studies in WWTPs observed that nitrifying bacteria were negatively affected by the ROS production in presence of AgNPs at 0.5-1 mg L^{-1} (Choi *et al.*, 2008, Choi and Hu, 2008). Moreover this functional group plays a crucial role in the nitrification process not only in WWTs but also in estuaries (Bernhard and Bollmann, 2010). In addition, the chemical analysis of the water samples collected from the microcosm established in January 2013 showed that the concentration of ammonia after 24 hr of exposure was significantly higher in the AgNPs treatment (T1) than in the treatments without AgNPs. For this reason it was hypothesized that AOB bacteria that oxidize ammonia to nitrite could have been negatively affected by AgNPs. Recent work investigated the effects of different AgNPs types (different coatings: citrate, PVP, gum arabic (GA)) on the *Nitrosomonas europaea*, a model organism for the species belonging to the AOB groups (Arnaout and Gunsch, 2012). The detrimental effects on the nitrification process were AgNPs type-specific and caused by the release of silver ions and the formation of ROS species. The results obtained with end point PCR indicated the presence of AOB groups in the waters of the Firth of Forth estuary, however, the qPCR performed with SYBR green did not produce satisfactory results as several fluorescent peaks were obtained. One of the factors that can explain the low quality of the standard curves is that the length of the target sequence of the gene or amplicon length was perhaps too long, 491 bp, as the desired length of the amplicon length ranges between 50 and 210 bp (Quellhorst and Rulli, 2008). However there are a few studies that quantified the abundance of the 491 bp sequence with qPCR successfully (Hollibaugh *et al.*, 2011, Caffrey *et al.*, 2007, Cardoso *et al.*, 2013).

One of the alternative techniques that can be applied to quantify the abundance of the AOB groups with qPCR is the use of qPCR with *TaqMan* probes. These probes consist of the sequence of specific oligonucleotides that bind a specific region of the DNA sequence of the *amoA* gene. These probes also incorporate a fluorescent molecule in the 5' end called the reporter and another molecule in the 3' called the quencher that quenches the fluorescent signal from the reporter if no amplification of the *amoA* gene sequence takes place. The use of *TaqMan* probes may increase the specificity of the qPCR and also the sensitivity, as they enhance the detection of the target sequence when the abundance of the gene in the samples is low (Smith and Osborn, 2009). Work with *TaqMan* probes is currently in progress as it has been used successfully to quantify the abundance of AOB groups (Okano *et al.*, 2004, Cavagnaro *et al.*, 2007).

4.5.3. Effects of AgNPs on bacteria inhabiting sediments

In the current study the results obtained with bacterial plate counts and the Biolog EcoPlate™ showed that bacterial cell viability, bacterial growth and metabolic profile of the bacterial communities inhabiting sediments were negatively affected after exposure to the NM-300 AgNPs. On the other hand the PLFAs analysis indicated that AgNPs did not affect the bacterial community structure. The total concentration of silver originating from nanoparticles was below 7 ppm (considering the analysis of sediment samples collected in the microcosms established in August 2012 and January 2013). These values are within the predicted environmental concentrations (PECs) of total silver in river sediments that oscillate between 2 and 14 ppm (Blaser *et al.*, 2008) but could be lower on the basis of the most recent predictions that estimated an accumulation rate of 2.3 ppb per year originating from nanosilver (Sun *et al.*, 2014). There have been no reports of typical levels of PECs in the context of AgNPs in estuarine or coastal sediments. However, they may be of the same order of magnitude due to silver discharges from WWTP and tributary rivers (Flegal *et al.*, 2007).

4.5.3.1. Community level physiological profile (CLPP)

In the presence of AgNPs (T1) the average uptake rate of the carbon substrates included in the Biolog EcoPlate™ was always lower (August 2012 and January 2013) than in the control (TC) following exposure to AgNPs. However differences in the AWCD were observed between the two seasons after 120 hr of exposure. In August 2012 the AWCD decreased between the time points 24 and 120 hr of exposure (in all treatments, control (TC) and AgNPs (T1)) whereas in January 2013 the overall utilization of carbon sources increased in all treatments. These differences in the AWCD between seasons can also be explained by the differences observed at the community level physiological profile (CLPP) showed with the principal component analysis (PCA). The differences at the CLPP observed with the Biolog EcoPlate™ can be due to differences in the bacterial communities in terms of species composition as a result of seasonality (Vishnivetskaya *et al.*, 2011). Interestingly in both microcosms experiments the communities exposed to AgNPs (T1) showed a recovery of the CLPP after 120 hr of exposure. The effects of the NM-300 AgNP type on the community function will be discussed in greater detail on the basis of the experiment carried out in January 2013 as it included the dispersant (T2) treatment that provided valuable information related to the effects of the dispersant on the community function.

4.5.3.1.1. CLPP in January 2013

The overall uptake and number of carbon substrates at the end of the exposure increased in all three treatments. This may be attributed to an increase in the abundance of heterotrophic groups as observed with the bacterial plate counts. However, the increase in the uptake rate of carbon sources in the present study was more remarkable in the dispersant (T2) and AgNPs (T1) treatments, possibly because in these treatments the concentration of ammonium was higher at the beginning of the exposures, and may have enhanced bacterial growth as explained previously in section 4.5.2.1. Perhaps, after a loss in the bacterial activity of AgNPs, bacterial communities exposed to AgNPs were able to take advantage of the extra amendment with NH_4 contained in the dispersant. A priory, based on the literature, starvation would enhance bacterial resistance to antibiotics (Nguyen *et al*., 2011). The natural concentration of ammonia in the water column of the estuary was initially low (0.02 mg L^{-1}), thus the extra amendment of the ammonium nitrate included in the dispersant (increased the concentration in water up to 0.08 mg L^{-1}), that it is known to enhance microbial activity (Aspray *et al.*, 2008), is likely to have increased the bacterial abundance significantly compared to the control treatment (TC). The PCA analysis of the data obtained with the Biolog EcoPlate™ depicted clear patterns of the bacterial metabolic fingerprint, based on the ability of bacteria to use environmentally relevant carbon sources. It revealed that the CLPP of bacterial communities exposed to AgNPs (T1) for 24 hr was different to the communities in the control (TC) and dispersant (T2) treatments, indicating that the bacterial metabolic profile was affected after 24 hr of exposure to AgNPs. At the end of the exposures the three treatments grouped together and (PCA_6 and PCA_{14} of Biolog EcoPlate™) showing that the communities exhibited a similar metabolic fingerprint and suggesting that the bacterial community metabolic function recovered from the exposure to AgNPs.

The shifts in the CLPP patterns observed with PCA_6 and PCA_{14} were similar, although in the PCA_{14} the number of carbon substrates included was higher as more wells exhibited positive growth, possibly due to slow growing bacteria that require longer incubation periods. These results differed from an earlier study in which no significant negative effects on the enzymatic activity were observed (leucine aminopepetidase, phosphatase and sulfatase activity) in microbial communities inhabiting river sediments, even at higher concentrations of AgNPs (Colman *et al.*, 2012). Colman and co-workes (2012) used a different nanoparticle type, although these AgNPs were similar in size and surface charge. Differences in the toxicity of AgNPs

that can also be affected by the environmental conditions (marine in the present study *vs.* freshwater in Colman *et al.*, (2012)) and differences in the bacterial resistance (bacterial community species composition is possibly different) may be the reason for the divergences encountered between both studies. Furthermore, the Biolog EcoPlate™ assay may also be a more sensitive technique to detect the inhibitory effects of AgNPs, and it is regarded as an efficient method for the comparison of functional ability, and suitable for microcosm studies (Preston-Mafham *et al.*, 2002). The Ecoplate has been widely used in ecotoxicological research (Rodrigues *et al.*, 2012, Weber *et al.*, 2008), including investigating the effects of nanoparticles on arctic soil microbial communities. This study indicated that AgNPs exhibited higher toxicity than Cu and SiO_2 NPs (Kumar *et al.*, 2011).

4.5.3.2. Phospholipid fatty acid analysis (PLFAs)

Phospholipid fatty acids (PLFA) are major components of cell membranes, and are rapidly degraded when a cell dies by hydrolytic enzymes. They can therefore be used to estimate the living biomass in soils or sediments (White *et al.*, 1993). PLFAs with a chain length shorter than 20 carbon atoms are predominant in bacterial cells and some of them are specific to certain bacterial groups that can be used as bacterial biomarkers (Frostegard *et al.*, 1993, Zogg *et al.*, 1997). The PLFA analysis is a culture-independent method that was applied in the present study as a tool to quantify the abundance of bacteria in sediments and to assess effects of AgNPs on potential shifts in the bacterial community structure. For this reason even though PLFA analysis is less powerful than molecular techniques in terms of resolution to describe bacterial diversity in sediments, the methodological bias is lower (Kunihiro *et al.*, 2014) and has been used successfully to study the effects of metals in soils (Bååth *et al.*, 1998) and estuarine sediments (Mayor *et al.*, 2013), and also to assess the toxicity of Zn nanoparticles to bacterial communities in soils (Pawlett *et al.*, 2013). The abundance of the Gram positive, Gram negative and total bacteria groups was estimated according to the classification criteria explained in the methodology section.

The abundance of the Gram negative bacteria group, based on specific PLFAs for this group confirmed that the dispersant in which silver nanoparticles were supplied enhanced the growth by up to the 8% for some Gram negative bacteria groups. In the control (TC) treatment the ratio in the abundance between the 16:1ω7c and 16:1ω7t dropped from 0.046 to 0.038 suggesting starvation (Kieft *et al.*, 1997) and supporting the hypothesis that the differences encountered between the control (TC) and dispersant (T2) treatment were due initially to the higher dispersant treatment concentration of

NH_4 in the overlaying water. These findings confirmed the importance of testing the effects of dispersants when conducting ecotoxicological tests of nanomaterials as they can mask the effects of the substance under study. Any conclusions drawn from the abundance of the PLFAs in the AgNPs (T1) treatment should be analyzed cautiously as the turn-over of fatty acids in the community may not have changed at the same rate in all treatments (Frostegård *et al.*, 2011). Furthermore, degradation rates of PLFAs may have been reduced by AgNPs inhibiting enzymatic activity (i.e. the interaction of Ag^+ with thiol groups present in enzymes could disrupt enzymatic activity) in both live and dead bacteria. Another hypothesis to explain the lack of differences between the AgNPs (T1) and the other treatments (TC and T2) is based on the response of bacteria to oxidative stress: the production of fatty acids in the cytoplasmic membrane could have been stimulated in response to damage in the outer envelope as a consequence of ROS production induced by AgNPs, followed by oxidative stress as observed in the Gram negative bacterium *Pseudomonas aeruginosa* after exposure to TiO_2 NPs (Kubacka *et al.*, 2014). The PLFAs analysis showed that there were no differences in the community structure and bacterial abundance between treatments after 24 hr of exposure. However, the results obtained with the Biolog Ecoplate™ and bacterial plate counts showed that AgNPs in sediments had a negative impact on the microbial functioning (functional diversity and bacterial cell viability). The results obtained with the PCA of the PLFAs suggest that overall AgNPs did not affect community structure possibly due to the resilience exhibited by the bacterial communities to this type of nanoparticle. These results agree with a previous study developed by Bradford *et al.*, (2009) using a nested PCR-DGGE approach. They observed that AgNPs did not affect negatively the genetic diversity of natural bacterial assemblages. Although PLFAs can be used to distinguish bacterial groups such as Gram negative and Gram positive bacteria, they are not bacterial species specific biomarkers therefore some shifts in the community composition may not be reflected in the distribution of PLFAs pattern. Molecular techniques based for example on the 16S rRNA gene sequence are needed to determine which bacteria species were the most seriously affected by AgNPs, particularly in terms of reduced abundance or enriched. The presence of more bacterial species with greater resilience to the negative impacts of AgNPs, and bacterial functional redundancy may explain the recovery observed with the Biolog EcoPlate™ assay at the end of the exposures.

4.5.4. Effects of AgNPs on the ecosystem services provided by bacteria: effects on the water quality

Inorganic forms of nitrogen and COD are some of the parameters used to analyse the quality of the water bodies. The analysis of these parameters did not show statistically significant differences between treatments after 120 hr exposure. Therefore it can be concluded that even though a single pulse exposure of the NM-300 AgNPs affected the bacterial uptake of NH_4, the degradation of this compound should not be disrupted in a long term basis as the physiological status of the bacterial community (water and sediments) recovered. On the other hand, the COD analysis showed a similar trend between treatments although the variability within the AgNPs (T1) treatment was high in the experiment developed in January 2013. The concentration of COD exhibited similar trends in August 2012 and January 2013 but the mean value of COD was higher in January 2013, and oscillated between 25 and 75 mg L^{-1}, compared to the COD values obtained in August, COD < 25 mg L^{-1}. There is no time series data relating to COD values for the Firth of Forth estuary for comparison with the results obtained in the present research project. One of the hypotheses is that at a higher temperature (August 2012) the bacterial metabolic activity increased (Arnosti *et al.*, 1998) and as a result of this, the degradation of organic matter could have been enhanced leading to lower values of COD in August 2012 (20/08/2012, 21ºC water temperature when collected from the estuary at 14:30, it was one of the warmest days of the year) than in January 2013 (5.8 ºC, water samples collected at 15:00 on the 14/01/2013).

4.5.5. General remarks and future work

A new question arises related to whether bacterial communities from a more pristine environment would exhibit a similar response when exposed to AgNP. The study location has been subject to high anthropogenic pressure for more than a century, receiving water discharges from a WWTP servicing a highly populated area as well as historical industrial activities associated with the mining and petrochemical industries. For this reason, owing to the continuous exposure to metals from anthropogenic but also geological origin, the bacterial communities in the present study may exhibit higher tolerance to metals (Knapp *et al.*, 2011) including AgNPs. The presence and abundance of metal resistance genes could be investigated with molecular techniques as qPCR. It would also be interesting to establish some microcosm experiments with water and sediment samples collected from a more pristine environment.

To investigate the ecotoxicity of AgNPs in different sediment types as the mudflats (rich in organic matter and silt) of Cramond could be of especial interest as it

could be compared to the work carried with the sediments collected from the sandflats in the same area. Possibly the toxicity of AgNPs in mudflat sediments will be lower due to the higher organic matter content, and the bacterial communities inhabiting these sediments may be also different.

In addition, the effects of AgNPs at (lower salinities, under freshwater/brackish conditions) could be developed by establishing similar microcosm experiments with samples collected from a different section of the estuary, further up, in the areas of Alloa and Stirling. The study of the toxicity of pristine and non-pristine or aged AgNPs (such as aged AgNPs in relevant WWTP media) is also important to achieve a more realistic knowledge about the fate and potential toxicity of AgNPs, and support the development of the ecological risk assessment of these materials in a more efficient way. Toxicity tests could be performed using the minimum and maximum estimated PECs values.

Chapter 5 Conclusion

The present study contributes to reducing knowledge gaps regarding the antibacterial effects of AgNPs in the estuarine and coastal environments, where little research has been done to date, particularly in sediments. In addition the estuarine environment is different to freshwater environments previously studied because the tidal regime creates fluctuations in the salinity of the water column, and under a high concentration of chloride, silver is potentially more mobile than in a fresh water environment. For this reason in the present study estuarine conditions were modelled by establishing a series of microcosms with the aim to characterize the environmental hazard of AgNPs on the functioning of the benthic bacterial community inhabiting marine estuarine sediments.

The work performed in the present research project preceding to the microcosm studies showed that the susceptibility of bacteria to AgNPs depends on the bacterial species and the AgNPs type. Three different AgNPs were examined in the present study, two standard reference materials (Sigma Aldrich AgNPs and the OECD NM-300 AgNPs) and a cleaning product purchased from Mesosilver containing AgNPs. The Mesosilver AgNPs product exhibited the highest antibacterial activity followed by the NM-300 AgNPs. The higher toxicity exhibited by the Mesosilver AgNPs was associated to their smaller particle size and initially higher concentration of silver in ionic form. This study shows that household products containing AgNPs are more toxic than some pristine standard reference materials. Thus these findings highlight the relevance of implementing regulatory measures, for example through legislation, to enforce a comprehensive environmental risks assessment for products containing AgNPs. The use of reference nanomaterials is recommended for comparison across multiple studies. However if AgNPs suspensions are highly unstable, even in Milli-Q water, as observed for the Sigma Aldrich AgNPs, the reference nanomaterial may not be suitable for toxicity studies as produced high variability within treatments. Opposite to the Sigma Aldrich AgNPs, the NM-300 AgNPs working suspensions were stable and produced repeatable results. For this reason the NM-300 AgNP type was used in the microcosm exposures.

Gram negative bacteria exhibited higher resistance to AgNPs than the Gram positive species. The presence of silver resistance genes was not examined but the bacteria production of EPS by the *Pseudoalteromonas* spp. may be crucial as a

protective barrier between the AgNPs (and dissolved forms) and the bacterial cells. The inhibitory concentrations of the NM-300 AgNPs on pure bacterial cultures (wild type) obtained in the present study were in the lower end of the inhibitory concentration range studies to date. For this reason, even though the use of bacterial species models is necessary to understand the antibacterial mechanism of AgNPs, the inhibitory concentrations obtained maybe should not be taken into account in the environmental risk assessment of products containing AgNPs. This is because the protection of more susceptible natural bacterial groups might not be safeguarded. It should be added that at ionic silver was always more toxic than AgNPs.

The microcosm was established with sediments and water samples collected from the Firth of Forth estuary, thus mixed populations of bacterial species were exposed to the NM-300 AgNPs and the associated dispersant. The water column was spiked with a single dose of AgNPs leading to an initial total concentration of silver in the water column of 1 mg L^{-1}. This single pulse caused a reduction in the bacterial cell viability of planktonic heterotrophic bacterial groups analyzed with bacterial plate counts. This is in agreement with the results obtained with culture independent techniques as epifluorescence microscopy and flow cytometry that showed a reduction in the bacterial production after exposure to AgNPs. A recovery of the bacterial numbers at the end of the exposures was possibly due to the removal of the AgNPs in the water column and to the proliferation of more resistant bacterial groups. In presence of NaCl, the most abundant salt in the marine environment, the persistence of the AgNPs (OECD NM-300 AgNPs) in the water column was low as it was initially hypothesized on the basis of previous studies. The concentration of total silver in water decreased significantly with a concomitant increase in sediments during the first 24 hr. Thus, similarly to the water column, the bacterial cell viability was compromised in sediments but and also the metabolic community profile was negatively affected based on the results relating to the use of ecologically relevant carbon sources. The shifts in the metabolic profile of the bacterial community exposed to AgNPs were temporary as the community function recovered after 120 hr. This recovery was possibly feasible due to the community structure (analysed on the basis of PLFAs bacterial biomarkers) was not negatively affected and may be also explained by a number of possible factors, such as the formation of compounds less toxic than AgNPs, or by the complexation of AgNPs with natural organic matter and sediments reducing their bioavailability, or also due to the presence of silver resistance genes or groups of organisms more resistant to silver. The formation of less toxic compounds such as AgCl and complexation with

organic matter has been shown in preliminary experiments with Raman microspectroscopy and also supported by the extensive work published to date relating to the fate of AgNPs in presence of chloride. However the persistence and biological effects of AgNPs (and all ENMs in general) in sediments in a nanoparticle form remains unclear due to the current instrument limitations and nowadays is one of the main topics of research. The presence of silver resistance genes is another piece of work that requires further investigation as may explain the proliferation of more resistant bacterial groups.

Finally future work should focus on the fate and effects of AgNPs in the marine environment taking into account the whole life cycle of the nanoparticles as during the use and waste processes the AgNPs physiochemical properties may be modified. Therefore in future research instead of using pristine AgNPs to assess their effects on the natural bacterial, AgNPs could be aged previously under environmental conditions preceding the estuarine environment as for example WWTP conditions.

Appendices

Appendix I: Procedure for the preparation of AgNPs suspensions

Materials

- Scale precision +0.01 mg
- Sterile Milli-Q water
- Pipettes and disposable sterile tips ranging (100µl to 5000µl)
- Ultrasonic bath (Grant XUB25) with ice
- Disposable Greiner Bio-One tubes (15 and 50 ml)
- Sterile Duran bottles (100 ml) thoroughly clean with detergent Decon 90 and HNO_3
- Lab dancer, test tube shaker
- Micro tubes (1.5- 2 ml)
- Bovine serum albumin (BSA) 10 mg L^{-1} (filter sterilized)

Procedure for the NM-300 AgNPs

- The vial containing AgNPs supplied by the LGC Standards was shaken vigorously for 4 min and ultrasonicated twice for 15 min in an ultrasonic bath containing ice.
- A 15 or 50 ml (depending on the volume of dispersion required) Greiner tube was weighed when empty and this weight registered.
- The AgNPs suspension was pipetted from the vial into the Greiner tube with a 200 or 1000 µl sterile pipette.
- The total weight of AgNPs in the tube was calculated by the difference in weight before and after adding the AgNPs.
- Sterile Milli-Q water was added with a 5000µl pipette up to the desired final concentration of the AgNPs dispersion.

Appendix II: Materials and equipment required for UV-vis spectroscopy

- Disposable standard cuvettes (Sarstedt semi micro cuvettes, ref. 67742 made from polystyrene (PS) and the cuvette with ref. 67740, acrylic (PMMA). Both are suitable for UV-vis spectrum down to the 330 and 300 nm respectively.

- Cuvettes were filled with 1 ml of AgNPs suspensions and the absorbance was measured immediately with a Shimadzu 1650 UV-vis spectrometer.

Appendix III: Analysis of ionic silver in AgNPs suspensions prepared in Milli-Q water

Specific apparatus and reagents

- Lithium Acetate reference (ELIT 003, Nico 2000)
- ISE for silver (ELIT 8211, nico2000)
- Voltmeter
- $AgNO_3$ standard solution
- Dark bottles to preserve the standard solutions

Procedure

Two electrodes were needed, the reference electrode (Lithium Acetate reference ELIT 003, nico2000,) and the ISE for silver (ELIT 8211, Nico 2000) connected separately to a voltmeter with a mono Electrode head. Prior to the measurements, electrodes were preconditioned in 0.01 M (~ 1000ppm) $AgNO_3$ for a minimum period of time of 10 min, until the difference in voltage measured stabilized. The analysis of ionic silver in the AgNP suspensions was carried out with standard and stock suspensions maintained at 4 ºC as the electrodes performed better, and the readings were more stable. The calibration curve was plotted with standards prepared with $AgNO_3$ ranging from 10^{-8} to 10^{-2} M (Figure A1).

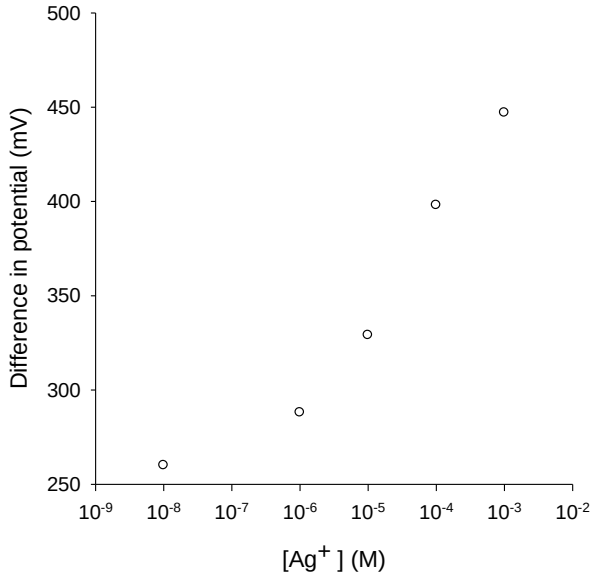

Figure A1 ISE calibration curve plotted with $AgNO_3$ standards

The concentration of silver the standards was plotted against the potential difference measured with the ISE (Figure A2). The linear regression equation was estimated to calculate the concentration of ionic silver in the AgNPs suspensions. To increase the accuracy when estimating the concentration of ionic silver in the AgNPs suspension, the equation of the linear regression can be estimated using exclusively the values bracketing the ionic concentration of interest.

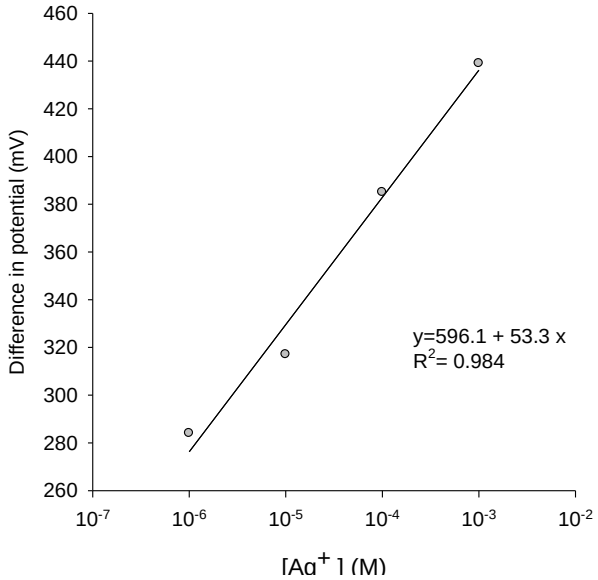

Figure A2 ISE calibration curve used to estimate ionic silver in AgNPs suspensions

Appendix IV: TEM and AFM for particle size analysis

Specific apparatus and reagents for TEM

- Copper grid mesh 400 holey carbon film (Agar scientific)
- Microscope Jeol 1200 TEM

Specific apparatus and reagents for AFM

- Fresh cleaved mica sheet (Agar scientific) 0.25 cm^2
- Steel mounting discs for AFM specimens
- XE-100 Microscope with XEI imaging software

Appendix V: Effects of chloride on the NM-300 AgNPs properties

Materials and equipment

- NaCl
- HEPES (Sigma Aldrich)
- NaOH/ HCl (concentrations 1 M and 0.1 M) to adjust the pH
- Milli-Q water

- 250 ml bottles
- 10 ml dispenser

Procedure

Four different salinities : 0 g L, 10 g L NaCl, 20 g L NaCl, 30 g L NaCl

- Add 200 ml in each bottle
- Label each bottle and to obtain a final concentration of 10, 20 and 30 g L^{-1} of NaCl add 2, 4 and 6 g of NaCl respectively.
- 4 ml of HEPES 1 M solution added into each bottle (4.766 g HEPES in 20 ml milli-Q water).
- Adjust pH to pH 7.5 with NaOH (1M)
- Measure salinity with a YSI 85 probe
- Duran bottles (250 ml)
- Add 40 ml in each experimental flask (50 ml flask) with a dispenser.
- Add 300-NM AgNPs suspension to a final concentration of 1.5 mg L^{-1}.
- Bung the flasks with a foam bung top together with tin foil or parafilm to prevent evaporation.
- Place the flasks in the incubator at room temperature (20 °C) and 125 rpm in the dark.
- Measure the absorbance in the UV-Vis spectrum (300 -700nm) and Z-Average and Zeta-Potential as described in sections 2.2.1 and 2.2.2 respectively.

Appendix VI: Molecular identification based on a partial sequence of the 16S RNA gene

Specific apparatus and reagents

- Thermal cycler (Techne)
- Microwave
- Gelbox apparatus with plates
- Plastic comb
- UV light in Chamber and camera BIO-RAD model Universal Hood II
- Image processor: Image Lab 4.1
- Pipettes and disposable sterile tips ranging (0.2 µl to 1000µl)
- Lab dancer, test tube shaker
- Micro tubes (0.2, 1.5 ml)
- TBE (Tris- Borate-EDTA)

- Ethidium Bromide
- illustraTM PuRe Taq Ready-to-go TM PCR bed (GE Healthcare)
- PureLink® Genomic DNA Mini Kit
- sterile HPLC-grade water (Fisher)
- DNA ladder Hyperlader IV (Bioline)
- Microcentrifuge

i. Agarose gel preparation

The components required for 50ml of 1% agarose gel are the following: 50 ml buffer TBE (Tris- Borate-EDTA) and 0.5 g Agarose (Helena Agarose Bioscience Europe, catalog No 8201-3) specially designed for electrophoresis. The TBE buffer (× 1) was prepared by dissolving in milli-Q water the following reagents in a final volume of 1000 ml: 12.11 g Tris base, 5.16 g Boric acid and 0.37 Ethylenediaminetetraacetic acid (EDTA). It was not necessary to adjust the pH as it was close to pH 8.

Appendix VII: Procedure for the digestion of sediments and water samples *(the chemicals used were analytical reagent grade)*

Water samples adapted from USEPA Protocol (3005A) (USEPA, 1992)

1. Transfer a 50ml aliquot of well-mixed to a beaker.
2. Add 1ml of HNO3 and 2.5ml of HCl.
3. Cover the sample with a ribbed glass.
4. Heat the sample 90- 95°C .
5. Reduced until 7.5- 10 ml.
6. Cool down the sample.
7. Wash the walls with water.
8. Make up volume up to 50ml.

Adapted from USEPA Protocol (3050B) (USEPA, 1996)

1. 1-2 g dry sediments in a Teflon beaker.
2. Add 10ml HNO_3
3. Mix the slurry and cover with a smooth glass.
4. Heat the sample 95°C ± 5°C and reflux for 10 and 15 min without boiling
5. Cool down the sample and add 5 ml HNO_3.
6. Replace the cover and reflux for 30 minutes. Repeat step "5" until not more fumes are generated.
7. Using a ribbed glass evaporated until 5 ml are left.

8. Once the sample has cooled add 2ml of distilled water and 3ml of 30% of H_2O_2.
9. Cover the vessel with a smooth glass and heat to start the peroxide reaction.
10. When effervescence subside cool down the sample.
11. Add aliquots of 1ml of 30% of H_2O_2 until effervescence is minimal. No more than a total of 10ml of H_2O_2.
12. Using a ribbed glass evaporated until 5 ml are left.(95°C ± 5°C without boiling for 2 h)
13. Cool down the sample and add 2.5 ml of HCl and cover with a smooth glass.
14. Heat the sample 95°C ± 5°C and reflux for 10 and 15 min without boiling.
15. Centrifuge the sample and complete the volume distilled water up 50ml.
16. Centrifuge at 3000 rpm for 15 min at 9ºC

Cleaning procedure

Teflon beakers

1. Detergent
2. Tap water
3. HNO3 (2ml)
4. Tap water
5. HCl (1ml)
6. Tap water
7. Milli-Q water

Ribbed and smooth glass

1. Detergent (Decon 90)
2. Rinse with Tap water
3. Rinse with Milli-Q water
4. Dry (to air-drying)

Appendix VIII: Chemical oxygen demand analysis

A mercury-free small scale (2 ml) flask digestion procedure using chromium (III) potassium sulphate and silver nitrate solutions (Environment Agency 2007).

1. Performance characteristics of the methods
   1.1. Range of application Up to 400 mg l^{-1} COD. The range can be extended by pre-dilution of the sample with water.
   1.2. Limit of detection : typically 9 mg l^{-1} (15 degrees of freedom).

1.3. Sensitivity 1 ml of 0.025 M iron(II) ammonium sulphate solution corresponds to 100 mg l^{-1} COD.

2. Reagents

Except where otherwise stated, analytical reagent grade chemicals should be used. Reagents should be stored in glass bottles. All reagents, with the exception of iron (II) ammonium sulphate solution, may be stored at room temperature for up to one month. Commercially available mixtures are obtainable for many of the reagents described. Unacceptable blank values are usually caused by the oxygen demand of the water or sulphuric acid, or the use of dirty apparatus.

2.1. Water.

Water used for blank determinations and preparation of control standards should show negligible interference. Water with conductivity of less than 2 μS cm-1 and total organic carbon content of less than 1 mg l^{-1} has been shown to be satisfactory. Glassware used for the preparation and storage of water should be cleaned with chromic acid solution.

2.2. Concentrated sulphuric acid

2.3. Silver nitrate solution (1200 g l^{-1}).

Dissolve 120 ± 1 g of silver nitrate in approximately 80 ml of water (D2.1). Warm the solution if necessary. Cool and make to 100 ± 1 ml with water (D2.1). Do not cool below about 10 ^{o}C as this solution is saturated at 0 ^{o}C. Stored in the dark in a stoppered glass bottle, this solution may be stored at room temperature for up to an indefinite period.

2.4. Chromium(III) potassium sulphate (250 g l^{-1}). (Sigma-Aldrich - Chromium(III) potassium sulfate dodecahydrate 243361)

Dissolve 25.00 ± 0.01 g of chromium(III) potassium sulphate dodecahydrate ($KCr(SO_4)_2.12H_2O$) in 100 ± 1 ml of hot water i.e. water above 50 ^{o}C. This solution is saturated at 30 ^{o}C. Stored in a glass bottle with a polytetrafluoroethylene stopper, this solution may be stored for up to an indefinite period. When required for use, warm the contents to 50 ^{o}C and stir before use, to re-dissolve any solids.

2.5. 1:10 phenanthroline iron(II) indicator solution (Ferroin indicator solution / 46270 Fluka)

Not more than 2 drops (i.e. 0.1 ml) of indicator solution should be used. Titrations should be made to the same colour end point using equal amounts of indicator solution.

2.6. Iron(II) ammonium sulphate solution (approximately 0.025 M).

To a 1000-ml volumetric flask, add approximately 9.8 g of iron (II) ammonium sulphate hexahydrate to approximately 100 ml of water 2.1. Add 20.0 ± 0.5 ml of sulphuric acid 2.2 and swirl to dissolve the solid. Cool and make to 1000 ml with water 2.1. Stopper and mix well. This solution is not very stable and should be prepared freshly on the day of use, and standardised before use.

Standardise the iron (II) ammonium sulphate solution against 0.02083 M potassium dichromate solution 2.6 using the following procedure. To approximately 60 ml of water 2.1 add 5.00 ± 0.05 ml of 0.02083 M potassium dichromate solution 2.7. Carefully add 15.0 ± 0.5 ml of sulphuric acid 2.2 and cool the solution. Add no more than two drops of indicator solution 2.5 and titrate to the end point with the iron(II) ammonium sulphate solution to be standardised. Towards the end point of the titration, addition of the iron(II) ammonium sulphate solution 2.6 from a narrow-bore burette, in quantities of 0.01 - 0.05 ml, facilitates the detection of the end point. The titre should be approximately 25 ml.

The molarity, M, of the iron(II) ammonium sulphate solution is given by:

$M = 0.625 / V$

where V is the volume (ml) of iron(II) ammonium sulphate solution .

Alternatively, $M = (0.020833 \times 30) / V$ or $M = 5 / (8 \times V)$

2.7. Potassium dichromate solution (0.02083 M, ie M/48).

To a 1000-ml volumetric flask, add 6.129 ± 0.001 g of potassium dichromate (previously dried for one hour at 140 - 150 ^{o}C) in approximately 800 ml of water in. Make to 1000 ml with water, stopper and mix well.

2.8. Silver sulfate-Sulfuric acid solution Sigma Aldrich, product code 34629

3. Apparatus

High blank values may result from the presence of trace amounts of contaminants in the digestion tube, the reflux condenser or on the anti-bumping granules. Apparatus should be cleaned (on repeated occasions) by boiling with fresh dichromate/sulphuric acid/silver sulphate mixture until low and consistent blank values are obtained. Apparatus should be reserved solely for COD determinations. Glassware should have standard ground glass joints where appropriate and grease should not be used. When rinsed with water between use, the digestion apparatus should be drained and dried at 105 ^{o}C. The use of wet apparatus may cause loss of precision. To improve precision, volumetric glassware should be grade B or better.

3.1. Tubes for closed-tube digestion.

Many types of tubes have been shown to be suitable. The main criteria are that the tubes can be heated, cooled, removed from the heater and opened without risk of bursting or spillage. The test data in the tables were obtained using borosilicate-glass culture vials, 125 x 16 mm with plastic screw-cap and polytetrafluoroethylene liner. Tubes with any apparent defect should be discarded. Many commercial systems are available where the tube is used once, and discarded or sent for disposal.

3.2. Heating source.

Thermostatically controlled heating block capable of accommodating the digestion tubes such that the level of the liquid in the tubes is coincident with the surface of the block. The block should be controlled to give a digest temperature of 150 ± 3 ^{o}C. Care should be taken to ensure that the temperature within the block does not rise above 153 ^{o}C. An alternative heating source is a suitable air oven, controlled so as to give a digest temperature of 150 ± 3 ^{o}C.

3.3. Pipettes and burette.

Graduated pipettes capable of dispensing 0.100 ± 0.005 ml and 0.20 ± 0.01 ml, and burette graduated in 0.02 ml divisions.

3.4. Anti-bumping granules.

All anti-bumping granules should be pre-cleaned by using the same digestion procedure.

4. Analytical procedure

4.1. Determination of chloride

Chloride content of the sample is greater than 2000 mg l^{-1}.

4.1.1. Add several anti-bumping granules 3.4 to the boiling tube 3.1 and add 0.20 ± 0.01 ml of silver nitrate solution 2.3 and 2.00 ± 0.02 ml of sample or diluted sample. Swirl the tube to mix the contents. Allow the tube and contents to stand approximately 2 minutes. To the tube add 0.20 ± 0.01 ml of chromium (III) potassium sulphate 2.4 and swirl the tube to mix the contents.

4.1.2. Add 1.00 ± 0.01 ml of potassium dichromate solution 2.7 and 3.00 ± 0.05 ml of silver sulphate-sulphuric acid solution

4.1.3. Close the tube and ensure it is secure. Swirl the tube to mix the contents. Place the tubes in the heating source and reflux for 120 ± 10 minutes. Remove the tubes and allow the contents to cool for approximately 5 minutes under running water to below 20 ^{o}C. Cautiously unseal the digestion tube.

4.1.4. Quantitatively transfer the contents of the tube to a titration flask, rinsing the tube as appropriate with a small amount of water.

4.2. Determination of residual dichromate

4.2.1. Add no more than two drops (0.1 ml) of indicator solution 2.5 to the flask and titrate the residual dichromate with iron(II) ammonium sulphate solution 2.6.After the first addition of iron(II)ammonium sulphate solution, the solution is blue-green in colour. During titration, the flask should be well mixed. The end point of the titration occurs when the colour changes sharply from deep blue to pink. The blue colour may reappear a few moments later but this should be ignored. This is especially common with samples high in chloride.

5. Calculation

The blank value should be the average of at least two determinations. If any blank value differs by more ± 0.5 ml from the average value it should be rejected. In these circumstances, it may be necessary to determine additional blank values.

An acceptable blank determination should require at least 23.5 ml of 0.025 M iron (II) ammonium sulphate solution in the titration. In addition, the difference between a refluxed blank value and an un-refluxed blank value should not exceed 1.5 ml of 0.025 M iron (II) ammonium sulphate solution.

Standard chloride solutions may also need to be analysed to establish potential interference effects especially where samples are analysed and low COD values are determined.

The analysis of AQC samples, for example standard solutions of potassium hydrogen phthalate (D2.10) or other appropriate solutions establishes that correct procedures are being followed.

The COD of the sample is given by

$COD = 4000 \times DF \times M (Vb - Vs)$ mg l^{-1}

where

Vb is the average volume (ml) of iron(II) ammonium sulphate solution used in the titration of blank solutions;

Vs is the volume (ml) of iron(II) ammonium sulphate solution used in the titration of the sample;

DF is the dilution factor, if appropriate;

M is the molarity of standardised iron (II) ammonium sulphate solution

Appendix IX: Influence of the agar media on the bacterial plate counts

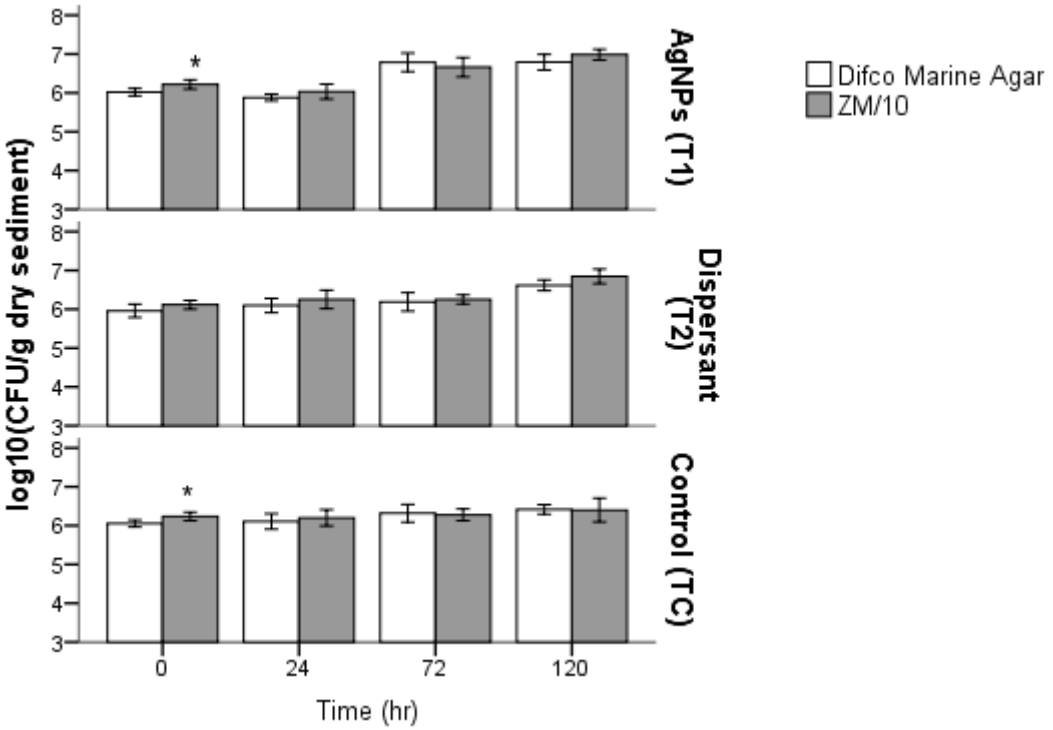

Figure A3 Bacterial abundance in sediments expressed as the mean ± SD of the log 10 (CFU) in different media, Difco Marine Agar (modified) and ZM/10. Independent t-test, $p < 0.05$), * symbolizes statistically significant differences ($p < 0.05$).

Appendix X: PLFAs analysis

Reagents Standards and Quality Control

Citrate buffer (0.15) (need for 20 samples)

Weigh accurately to two decimal places 7.88g anhydrous citric acid dissolved in 250 ml deionized water, and adjust the pH to 4.0 with approximately 1.825g of sodium hydroxide pellets (crushed). Prepare freshly daily.

Extractant: Chloroform: Methanol: Citrate Buffer (1:2:0.8 v/v/v)(Bligh and Dyer, 1959)(11.56ml/sample)

Add 75 ml chloroform to 150 ml methanol to 60 ml citrate buffer for 20 samples. Prepare using fresh citrate buffer.

Methanolic KOH(0.2M)Potassium hydroxide in methanol (1ml/sample)

Weigh accurately to two decimal places 0.28 g potassium hydroxide pellets (crushed) and dissolve in 25 ml of methanol.

Methanol: Toluene (1:1v/v) (1 ml/sample)

Add 50 ml methanol to 50 ml toluene.

Iso-hexane :Chloroform (4:1 v/v)(4.18 ml/sample)

Add 200 ml iso-hexane to 50 ml chloroform

Acetic Acid (1M) (0.3ml/sample)

Add 5.71 ml acetic acid to approximately 100 ml of deionised water. Bring to 100 ml final volume.

Internal Standard C19:0 methyl ester (60µl/sample)

Weigh accurately to 5 decimal places, approximately 6.25 mg of Non-adecanoic acid Methyl Ester ($C_{20}H_{40}O_2$) and dissolve in 250 ml methanol in a volumetric flask. The weight used must be the recorded. Store in cold room at 4ºC, covered in foil or in amber glass bottle for up to 6 months.

Quality control soils (QC)

1500 mg

Equipment and Consumables

- Balance
- Sample concentrator: stainless steel needles
- Vortex mixer
- Water bath
- Bottle dispensers
- Up to 1000µl pipettes and tips
- Centrifuge
- Sample rotator
- Pasteur pipettes
- Glass centrifuge tubes
- CG sample vials with inserts
- Muffle furnace

Procedure

All glassware was muffled at 450 OC overnight to remove any organic C before use.

Extraction of lipids

i. The recommended weight of freeze-dried sediment samples collected in the microcosm is 6 g. This is a high volume of sample thus to ensure an optimum extraction the sample is split in two, 3 g, and combined at the lipid fractioning step.
ii. Weigh out accurately to 4 decimal places 3 g of freeze-dried sediment sample into a 120 mm x 20 mm borosilicate glass centrifuge tube with a black PTFE-lined screw cap.
iii. For every batch of soil samples there must be 2 QC soil samples and 2 blanks included in the PLFAs extractions.
iv. Using a dispenser, add 9.16 ml of single phase Extractant ($CHCl_3$, MeOH, citrate buffer) to each sample. Cap tube.
v. Mix the sample on a vortex mixer. Cover tube rack in foil to keep samples in dark as much as possible. Leave for 2 hr to extract, vortex every 30 min. After 2hr, vortex the samples then spin for 17 min at 15 rpm, 20ºC.
vi. Decant off the supernatant into a clean glass centrifuge tube.

vii. Reset dispenser, add 2.5 ml extractant to the soil residue. Vortex and centrifuge as before. Combine supernatants as before.

viii. Phases are split by adding 3.1 ml $CHCl_3$ and 3.1 ml Citrate Buffer, and vortex. Mix the samples on the sample rotator for 15 min Figure A4.

Figure A4 Sample rotator

ix. Samples are left overnight in the cold room to allow the phases to separate. Both layers should be clear, especially the organic layer at the bottom, indicating that separation has been successful.

----------Stopping point----------

x. Centrifuge as before for 2 min.

xi. Using a clean Pasteur pipette for each sample, transfer the lower organic phase to a clean medium size glass tube. Do not leave any aqueous phase in the sample as water molecules will attack fatty acid double bonds.

xii. In the dark, evaporate the sample to dryness under a gentle stream of nitrogen on the sample concentrator Figure A5. A gentle ripple of solvent surface is sufficient once the sample is completely dry (~2hr) store in the -20ºC freezer.

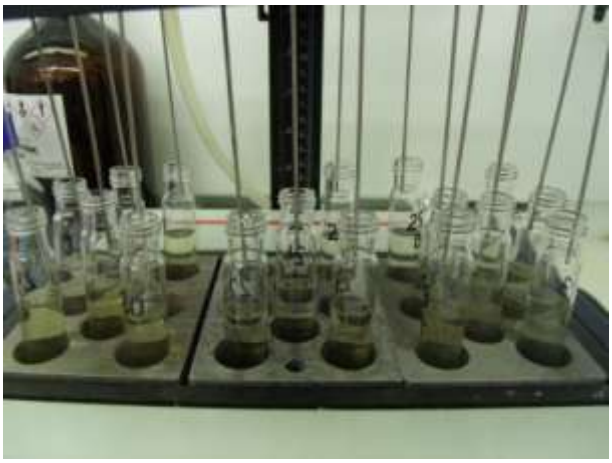

Figure A5 Sample concentrator

----------Optional Stopping point----------

Lipid fractionation

Solid phase extraction uses silica columns Figure A6 with a sorbent mass of 500 mg and a reservoir volume of 6 ml. One-way stopcocks (SPE) are fitted to each column. Each tap must be set so that not only is the drip-rate slow but is the same for all samples. Do not allow the column to dry out during fractionation.

i. Attach taps to columns. Position large size glass test tubes below the columns to collect waste.
ii. Reset dispenser; add 5 ml $CHCl_3$ to each column. Open taps to allow $CHCl_3$ to condition ISOLUTE SI SPE column (BIOTAGE). Close the taps.
iii. With a pipette add 400µl $CHCl_3$ to the sample, vortex twice and using a clean Pasteur pipette, transfer the sample to the centre of the column reservoir.
iv. Wash the vials with 3x 200 µl and transfer the washings to the column.
v. When all column reservoirs filled with samples, open the tap and allow the sample to slowly load onto the column.
vi. With dispenser, add 2x3 ml $CHCl_3$ (at this stage neutral lipids are eluted). Discard the collected $CHCl_3$ into the waste bottle.
vii. With dispenser, add 2x3 ml Acetone (at this stage glycolipids are eluted). Discard the collected Acetone into the waste bottle.
viii. Once the acetone has passed through the column, move the rack forward to clean medium sizes tubes and discard the previous collections into the appropriate waste bottle(s).

ix. With dispenser, add 4 ml and 2 x3 Methanol and collect. The column is allowed to dry out once the methanol has passed through the column (the phospholipids are eluted).

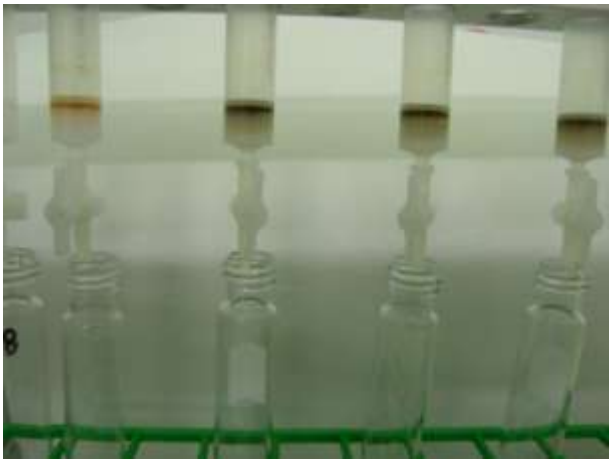

Figure A6 SPE columns

x. Evaporate the methanol eluate to dryness under stream of nitrogen (~4.5 hr). Cap tube with black medium size PTFE lined lids. At this stage the samples can be stored in the – 20ºC freezer.

Mild Alkaline Methanolysis

i. Switch on the water bath, the incubation temperature is 37ºC (±3ºC).
ii. Freshly prepare 0.2 M KOH in methanol.
iii. To each sample, using a pipette add 200µl internal standard.
iv. Using dispenser, add 1 ml MeOH: Toluene (1:1v/v) to each sample and vortex.
v. Using dispenser, add 0.2 M KOH to each sample and vortex.
vi. Place the samples in a rack and incubate at 37ºC in the water bath for 15 min.
vii. After methanolysis, remove the samples from the water bath and allow to cool.
viii. Using a dispenser, add 2 ml iso-hexane: $CHCl_3$ (4:1 v/v), 0.3 ml 1M Acetic Acid and 2 ml deionised water.
ix. Vortex and place the sample on the sample rotator for 10 min.
x. Centrifuge for 2 min at 1500 rpm.
xi. Using a clean Pasteur Pipette transfer the upper organic phase to a clean small glass tube, taking care NOT to take up any of the lower aqueous layer.

xii. Using a dispenser, add a further 2 ml iso-hexane: $CHCl_3$ to the tube containing the lower aqueous layer.

xiii. Vortex and centrifuge as before.

xiv. Again transfer the upper layer using a Pasteur pipette, to the small tube containing the first upper phase, taking care not to take up any of the lower aqueous layer.

xv. Evaporate the sample to dryness under stream of nitrogen (1-2 hr). Once the sample has completely dried it can be stored in the -20ºC freezer.

----------Optional Stopping point----------

Preparation of Phospholipids sample for a gas cromatography flame ionisation detection (GC-FID)

i. Using a pipette add 300µl iso-hexane: $CHCl_3$ to each sample. Mix the transfer to a GC vial using a clean Pasteur pipette.

ii. Evaporate to dryness under nitrogen. Once the sample has completely dried it can be stored in the -20ºC freezer in the dark until required for analysis.

iii. When required for the analysis, defrost samples and add 200µl iso-Hexane.

Suppliers

Citric Acid, and KOH purchased from AnalaR Normapur.

Methanol, Toluene, Chloroform and Acetone purchased from RATHBURN (HPLC grade)

Appendix XI: Epifluorescence microscopy, DAPI counts

Specific apparatus and reagents

Millipore filtration tower

Polycarbonate filters (Nucleopore, white) 0.2 µm pore size

Glass-fibre support filter (GF/C or GF/F) Ø 25 mm (Whatman)

Formaldehyde (38% w/w) BDG product code 284212J

Molecular grade etanol (absolute)

Fluoroshield™ with DAPI (Sigma-Aldrich)

Glass slides/cover slips

Petri dishes

Sterile Milli-Q water

Pencil (marker)

Epifluorescent microscope (Zeiss Axiscope)

Axio digital camera and ZEN 2011 imaging software

Appendix XII: Quantitative polymerase chain reaction (qPCR)

Materials and equipment required

- Thermocycler StepOne (Life technologies)
- UV light in Chamber and camera BIO-RAD model Universal Hood II
- Image processor: Image Lab 4.1
- Thermo Scientific NanoDrop® 2000 spectrophotometer
- 0.2 – 100 µl pipettes
- Water, molecular biology grade, RNAse, DNAse and Protease free Fisher BioReagents
- Pipettor tip SureOne filter sterile rack micropoint tip graduated 0.1 to 10µL (Fisher Scientific)
- Pipettor tip SureOne filter sterile rack micropoint tip graduated 20 to 200µL ((Fisher Scientific)
- Sterile Eppendorf tubes (2 ml)
- MicroAmp® Fast Reaction Tube with Cap, 0.1 ml (Life Technologies) (qPCR reaction)

PCR and qPCR sample preparation

In each tube the following components were added:

- 10µl master mix
- 2 µl of the forward primer
- 2 µl of the reverse primer
- 1 µl of Dimethyl Sulfoxide (DMSO) Sigma Aldrich, final concentration 5% (product number 41639)
- 5 µl of DNA environmental samples
- Negative control: 5 µl of water
- Positive control: 2.5 µl of the *Nm51* cell lysate and 2.5 µl of water

Appendix XIII*:* Media for lithotrophic ammonia-oxidizing bacteria (marine strains) (Courtesy of Dr. Andreas Pommerening-Röser)

Medium IIIa (batch cultures)

NH_4Cl	535.0 mg (10.0 mM)
KH_2PO_4	54.4 mg (0.4 mM)
Cresol red (0.05%)	1 ml
Seawater	750 ml
distilled water	ad 1000 ml

Medium IIIb (stock cultures)

NH_4Cl	535.0 mg (10.0 mM)
KH_2PO_4	54.4 mg (0.4 mM)
$CaCO_3$	5000.0 mg
Cresol red (0.05%)	1 ml
Seawater	750 ml
distilled water	ad 1000 ml

Transfer about 1ml of the cultures to 10-12 ml of new stock culture medium. For stock cultures we use calcium carbonate (5 g per liter) as pH buffer. Initially the colour of the medium is red or light purple. After a couple of days the colour of the medium changes to yellow, which indicates production of nitrous acid (Stock cultures should be transferred to fresh medium after 3-4 month) After one week you can transfer 1 – 2 ml from a well nitrifying stock culture to batch culture medium (150 ml medium / 300 ml Erlenmeyer flasks). In batch cultures, the pH should be adjusted manually by addition of a 10% NaHCO3. Since ammonia is the substrate of AOB, the pH optimum in part depends on the concentration of the added ammonium salt. 10 mM ammonium salts medium (at a pH of about 8.0: light red) can be regarded as good standard for sufficient growth of AOB cultures. Usually after 3 -4 days the colour of the medium changes to yellow and the pH should be adjusted to pH 8 again. Firstly one time per day - thereinafter several times per day (depends on the growth rates). Until approximate one week the AOB have transformed most of ammonia to nitrite and the cells can be harvested.

Appendix XIV:Abundance of the PLFAs

Table A1 Paired t-test of the abundance of individual PLFAs showing statistically significant differences between treatments ($p < 0.05$) after 24 and 120 hr of exposure.

Treatment	PLFAs	p-value (2-tailed)
AgNPs(T1)	**16:1ω11t**	0.032
	18:1ω9	0.025
	10 Me l8:0	0.035
Control(TC)	**15:00**	0.017
	16:1ω7t	0.019
	16:00	0.012
	17:0brb	0.030
	17:0cy	0.042
	17:00	0.006
	12 Me l7:0	0.026
	18:3ω6,8,13	0.015
	18:2ω8,12	0.007
	18:1ω7	0.037
	18:1ω5	0.008
	18:1ω10 or 11	0.050
	10 Me l8:0	0.043
	19:0cy	0.005
	20:4ω 3,6,9,12	0.013
	20:00	0.030

Table A2 Abundance of individual PLFAs in each treatment after 24 and 120 hr of exposure.

PLFAs	Time(hr)	Treatment	Mean (nMol/ g dry sediment)	SD
C12:0	24	AgNPs (T1)	0.00	0.00
		Dispersant (T2)	0.00	0.00
		Control (TC)	0.00	0.00
	120	AgNPs (T1)	0.00	0.00
		Dispersant (T2)	0.00	0.00
		Control (TC)	0.00	0.00
C13:0	24	AgNPs (T1)	0.02	0.04
		Dispersant (T2)	0.00	0.00
		Control (TC)	0.01	0.03
	120	AgNPs (T1)	0.00	0.00
		Dispersant (T2)	0.00	0.00
		Control (TC)	0.00	0.00
C14:0	24	AgNPs (T1)	1.34	0.17
		Dispersant (T2)	1.26	0.51
		Control (TC)	1.56	0.20
	120	AgNPs (T1)	1.19	0.32
		Dispersant (T2)	1.31	0.07
		Control (TC)	1.16	0.21

PLFAs	Time(hr)	Treatment	Mean (nMol/ g dry sediment)	SD
C14:0i	24	AgNPs (T1)	0.22	0.03
		Dispersant (T2)	0.21	0.07
		Control (TC)	0.24	0.05
	120	AgNPs (T1)	0.20	0.06
		Dispersant (T2)	0.21	0.03
		Control (TC)	0.21	0.05
C14:1ω9c	24	AgNPs (T1)	0.08	0.01
		Dispersant (T2)	0.09	0.03
		Control (TC)	0.11	0.01
	120	AgNPs (T1)	0.09	0.01
		Dispersant (T2)	0.08	0.02
		Control (TC)	0.08	0.01
C14:1ω9t	24	AgNPs (T1)	0.04	0.09
		Dispersant (T2)	0.00	0.00
		Control (TC)	0.00	0.00
	120	AgNPs (T1)	0.00	0.00
		Dispersant (T2)	0.00	0.00
		Control (TC)	0.00	0.00
C15:0	24	AgNPs (T1)	0.67	0.08
		Dispersant (T2)	0.62	0.22
		Control (TC)	0.76	0.09
C15:0	120	AgNPs (T1)	0.58	0.10
		Dispersant (T2)	0.60	0.04
		Control (TC)	0.54	0.07
C15:0ai	24	AgNPs (T1)	1.62	0.20
		Dispersant (T2)	1.54	0.37
		Control (TC)	1.63	0.19
	120	AgNPs (T1)	1.40	0.24
		Dispersant (T2)	1.51	0.21
		Control (TC)	1.46	0.13
C15:0i	24	AgNPs (T1)	1.22	0.15
		Dispersant (T2)	1.17	0.28
		Control (TC)	1.26	0.15
	120	AgNPs (T1)	1.11	0.20
		Dispersant (T2)	1.17	0.12
		Control (TC)	1.14	0.11
C16:0	24	AgNPs (T1)	9.20	0.85
		Dispersant (T2)	9.03	2.55
		Control (TC)	10.78	1.07
	120	AgNPs (T1)	8.58	1.24
		Dispersant (T2)	9.41	0.46
		Control (TC)	8.29	0.83
C16:0br	24	AgNPs (T1)	0.09	0.05
		Dispersant (T2)	0.05	0.03
		Control (TC)	0.08	0.02
	120	AgNPs (T1)	0.09	0.02
		Dispersant (T2)	0.06	0.04
		Control (TC)	0.06	0.01
C16:0i	24	AgNPs (T1)	0.32	0.08
		Dispersant (T2)	0.28	0.06
		Control (TC)	0.32	0.06
	120	AgNPs (T1)	0.28	0.04
		Dispersant (T2)	0.29	0.03
		Control (TC)	0.28	0.02
C16:1i	24	AgNPs (T1)	0.08	0.06
		Dispersant (T2)	0.09	0.06
		Control (TC)	0.14	0.03

PLFAs	Time(hr)	Treatment	Mean (nMol/ g dry sediment)	SD
	120	AgNPs (T1)	0.11	0.01
		Dispersant (T2)	0.09	0.06
		Control (TC)	0.10	0.01
C16:1ω11c	24	AgNPs (T1)	0.12	0.23
		Dispersant (T2)	0.03	0.06
		Control (TC)	0.05	0.11
	120	AgNPs (T1)	0.06	0.07
		Dispersant (T2)	0.02	0.04
		Control (TC)	0.03	0.06
C16:1ω11t	24	AgNPs (T1)	0.55	0.09
		Dispersant (T2)	0.73	0.14
		Control (TC)	0.65	0.09
	120	AgNPs (T1)	0.64	0.08
		Dispersant (T2)	0.71	0.12
		Control (TC)	0.70	0.05
C16:1ω5	24	AgNPs (T1)	0.35	0.08
		Dispersant (T2)	0.40	0.06
		Control (TC)	0.35	0.04
	120	AgNPs (T1)	0.32	0.05
		Dispersant (T2)	0.40	0.06
		Control (TC)	0.34	0.03
C16:1ω7c	24	AgNPs (T1)	8.43	1.95
		Dispersant (T2)	9.16	1.73
		Control (TC)	8.49	1.08
	120	AgNPs (T1)	7.93	1.45
		Dispersant (T2)	9.97	1.30
		Control (TC)	7.69	0.64
C16:1ω7t	24	AgNPs (T1)	0.45	0.27
		Dispersant (T2)	0.40	0.08
		Control (TC)	0.39	0.06
	120	AgNPs (T1)	0.40	0.15
		Dispersant (T2)	0.47	0.23
		Control (TC)	0.29	0.03
C17:0	24	AgNPs (T1)	0.43	0.07
		Dispersant (T2)	0.40	0.10
		Control (TC)	0.46	0.02
	120	AgNPs (T1)	0.39	0.04
		Dispersant (T2)	0.39	0.04
		Control (TC)	0.38	0.04
C17:0(10me)	24	AgNPs (T1)	0.05	0.05
		Dispersant (T2)	0.05	0.05
		Control (TC)	0.05	0.01
	120	AgNPs (T1)	0.01	0.03
		Dispersant (T2)	0.04	0.00
		Control (TC)	0.02	0.02
C17:0(12me)	24	AgNPs (T1)	0.02	0.02
		Dispersant (T2)	0.02	0.02
		Control (TC)	0.04	0.01
	120	AgNPs (T1)	0.04	0.03
		Dispersant (T2)	0.03	0.02
		Control (TC)	0.02	0.02
C17:0ai	24	AgNPs (T1)	0.33	0.06
		Dispersant (T2)	0.26	0.07
		Control (TC)	0.31	0.05
	120	AgNPs (T1)	0.27	0.03
		Dispersant (T2)	0.25	0.03
		Control (TC)	0.25	0.02

PLFAs	Time(hr)	Treatment	Mean (nMol/ g dry sediment)	SD
C17:0br	24	AgNPs (T1)	0.01	0.03
		Dispersant (T2)	0.00	0.00
		Control (TC)	0.00	0.00
	120	AgNPs (T1)	0.00	0.00
		Dispersant (T2)	0.00	0.00
		Control (TC)	0.00	0.00
C17:0brb	24	AgNPs (T1)	0.25	0.06
		Dispersant (T2)	0.22	0.04
		Control (TC)	0.23	0.02
	120	AgNPs (T1)	0.22	0.02
		Dispersant (T2)	0.22	0.02
		Control (TC)	0.21	0.01
C17:0cy	24	AgNPs (T1)	0.18	0.04
		Dispersant (T2)	0.16	0.03
		Control (TC)	0.17	0.02
	120	AgNPs (T1)	0.16	0.03
		Dispersant (T2)	0.17	0.02
		Control (TC)	0.15	0.00
C17:0i	24	AgNPs (T1)	0.06	0.01
		Dispersant (T2)	0.03	0.02
		Control (TC)	0.04	0.03
	120	AgNPs (T1)	0.06	0.01
		Dispersant (T2)	0.04	0.03
		Control (TC)	0.03	0.02
C17:1ω7	24	AgNPs (T1)	0.00	0.00
		Dispersant (T2)	0.00	0.00
		Control (TC)	0.00	0.00
	120	AgNPs (T1)	0.00	0.00
		Dispersant (T2)	0.00	0.00
		Control (TC)	0.00	0.00
C17:1ω8c	24	AgNPs (T1)	0.00	0.00
		Dispersant (T2)	0.00	0.00
		Control (TC)	0.00	0.00
	120	AgNPs (T1)	0.00	0.00
		Dispersant (T2)	0.00	0.00
		Control (TC)	0.00	0.00
C17:1ω8t	24	AgNPs (T1)	0.00	0.00
		Dispersant (T2)	0.00	0.00
		Control (TC)	0.00	0.00
	120	AgNPs (T1)	0.00	0.00
		Dispersant (T2)	0.00	0.00
		Control (TC)	0.00	0.00
C18:0	24	AgNPs (T1)	0.74	0.19
		Dispersant (T2)	0.69	0.16
		Control (TC)	0.76	0.11
	120	AgNPs (T1)	0.71	0.09
		Dispersant (T2)	0.71	0.06
		Control (TC)	0.70	0.12
C18:0(10me)	24	AgNPs (T1)	0.06	0.01
		Dispersant (T2)	0.06	0.02
		Control (TC)	0.07	0.01
	120	AgNPs (T1)	0.06	0.01
		Dispersant (T2)	0.06	0.00
		Control (TC)	0.06	0.01
C18:1ω10or11	24	AgNPs (T1)	0.31	0.33
		Dispersant (T2)	0.33	0.14
		Control (TC)	0.16	0.02

PLFAs	Time(hr)	Treatment	Mean (nMol/ g dry sediment)	SD
	120	AgNPs (T1)	0.29	0.12
		Dispersant (T2)	0.38	0.12
		Control (TC)	0.23	0.04
C18:1ω13	24	AgNPs (T1)	0.22	0.04
		Dispersant (T2)	0.23	0.05
		Control (TC)	0.26	0.01
	120	AgNPs (T1)	0.22	0.02
		Dispersant (T2)	0.20	0.05
		Control (TC)	0.22	0.01
C18:1ω7	24	AgNPs (T1)	4.26	0.74
		Dispersant (T2)	4.54	0.71
		Control (TC)	4.23	0.38
	120	AgNPs (T1)	4.03	0.44
		Dispersant (T2)	4.92	0.58
		Control (TC)	4.33	0.34
C18:1ω9	24	AgNPs (T1)	2.01	0.22
		Dispersant (T2)	1.99	0.39
		Control (TC)	1.98	0.24
	120	AgNPs (T1)	1.81	0.21
		Dispersant (T2)	2.01	0.17
		Control (TC)	1.70	0.11
C18:2(4.10or5.10)	24	AgNPs (T1)	0.39	0.14
		Dispersant (T2)	0.30	0.07
		Control (TC)	0.37	0.05
	120	AgNPs (T1)	0.30	0.04
		Dispersant (T2)	0.32	0.05
		Control (TC)	0.27	0.02
C18:2(9.12)	24	AgNPs (T1)	0.28	0.08
		Dispersant (T2)	0.37	0.04
		Control (TC)	0.26	0.02
	120	AgNPs (T1)	0.28	0.05
		Dispersant (T2)	0.35	0.09
		Control (TC)	0.30	0.04
C18:3(5.10.12)	24	AgNPs (T1)	0.33	0.10
		Dispersant (T2)	0.36	0.02
		Control (TC)	0.30	0.02
	120	AgNPs (T1)	0.31	0.04
		Dispersant (T2)	0.41	0.04
		Control (TC)	0.35	0.03
C19:0cy	24	AgNPs (T1)	0.42	0.15
		Dispersant (T2)	0.37	0.08
		Control (TC)	0.43	0.05
	120	AgNPs (T1)	0.34	0.04
		Dispersant (T2)	0.35	0.05
		Control (TC)	0.34	0.03
C19:1ω6	24	AgNPs (T1)	0.16	0.07
		Dispersant (T2)	0.13	0.03
		Control (TC)	0.22	0.12
	120	AgNPs (T1)	0.12	0.01
		Dispersant (T2)	0.12	0.01
		Control (TC)	0.15	0.02
C19:1ω8	24	AgNPs (T1)	0.17	0.05
		Dispersant (T2)	0.14	0.04
		Control (TC)	0.20	0.05
	120	AgNPs (T1)	0.15	0.02
		Dispersant (T2)	0.15	0.02
		Control (TC)	0.15	0.02

PLFAs	Time(hr)	Treatment	Mean (nMol/ g dry sediment)	SD
C20:0	24	AgNPs (T1)	0.08	0.01
		Dispersant (T2)	0.08	0.02
		Control (TC)	0.10	0.01
	120	AgNPs (T1)	0.08	0.01
		Dispersant (T2)	0.09	0.02
		Control (TC)	0.08	0.01
C20:1	24	AgNPs (T1)	0.28	0.21
		Dispersant (T2)	0.10	0.14
		Control (TC)	0.24	0.19
	120	AgNPs (T1)	0.09	0.10
		Dispersant (T2)	0.06	0.07
		Control (TC)	0.15	0.11
C20:1ω9	24	AgNPs (T1)	0.11	0.04
		Dispersant (T2)	0.13	0.02
		Control (TC)	0.25	0.23
	120	AgNPs (T1)	0.25	0.15
		Dispersant (T2)	0.19	0.09
		Control (TC)	0.18	0.13
C20:4(5.8.11.14)	24	AgNPs (T1)	0.00	0.00
		Dispersant (T2)	0.00	0.00
		Control (TC)	0.02	0.02
	120	AgNPs (T1)	0.00	0.00
		Dispersant (T2)	0.01	0.02
		Control (TC)	0.00	0.00
C20:4(6.10.14.18)	24	AgNPs (T1)	0.00	0.00
		Dispersant (T2)	0.00	0.00
		Control (TC)	0.00	0.00
	120	AgNPs (T1)	0.00	0.00
		Dispersant (T2)	0.00	0.00
		Control (TC)	0.00	0.00
C20:4(8.11.14.17)	24	AgNPs (T1)	0.23	0.13
		Dispersant (T2)	0.27	0.24
		Control (TC)	0.22	0.03
	120	AgNPs (T1)	0.11	0.03
		Dispersant (T2)	0.27	0.23
		Control (TC)	0.11	0.03
C20:5ω3	24	AgNPs (T1)	0.85	0.81
		Dispersant (T2)	1.07	0.30
		Control (TC)	0.45	0.12
	120	AgNPs (T1)	0.72	0.21
		Dispersant (T2)	1.06	0.28
		Control (TC)	0.76	0.24
Cphthalate/C16:0(10me)	24	AgNPs (T1)	1.07	0.15
		Dispersant (T2)	1.10	0.17
		Control (TC)	1.08	0.19
	120	AgNPs (T1)	0.93	0.11
		Dispersant (T2)	1.09	0.21
		Control (TC)	0.90	0.08

Table A3 PLFAs showing statistically significant differences (ANOVA, $p < 0.05$) between treatments in terms of abundance

PLFAs	Time(hr) exposure	Sum of Squares		df	Mean Square	F	Sig.
16:17ωc	24	Between Groups	1,32	2	0,66	0,25	0,79
		Within Groups	23,98	9	2,66		
		Total	25,30	11			
	120	Between Groups	12,55	2	6,27	4,50	0,04
		Within Groups	12,55	9	1,39		
		Total	25,10	11			
18:2(9,12)	24	Between Groups	0,03	2	0,01	5,63	0,03
		Within Groups	0,02	9	0,00		
		Total	0,05	11			
	120	Between Groups	0,01	2	0,01	1,48	0,28
		Within Groups	0,04	9	0,00		
		Total	0,05	11			
18:3(5,10,12)	24	Between Groups	0,01	2	0,00	1,17	0,35
		Within Groups	0,03	9	0,00		
		Total	0,04	11			
	120	Between Groups	0,02	2	0,01	7,41	0,01
		Within Groups	0,01	9	0,00		
		Total	0,03	11			
19:1ω6	24	Between Groups	0,01	2	0,01	1,03	0,39
		Within Groups	0,06	9	0,01		
		Total	0,08	11			
	120	Between Groups	0,00	2	0,00	6,54	0,02
		Within Groups	0,00	9	0,00		
		Total	0,01	11			

Table A4 Bonferroni multiple comparisons post-hoc test

PLFAs	Time (hr)	Treatment	vs. Treatment	p-value
C16:1ω7c	24	Control (TC)	Dispersant (T2)	1.00
			AgNPs(T1)	1.00
		Dispersant (T2)	Control (TC)	1.00
			AgNPs(T1)	1.00
		AgNPs(T1)	Control (TC)	1.00
			Dispersant (T2)	1.00
	120	Control (TC)	Dispersant (T2)	0.07
			AgNPs(T1)	1.00
		Dispersant (T2)	Control (TC)	0.07
			AgNPs(T1)	0.11
		AgNPs(T1)	Control (TC)	1.00
			Dispersant (T2)	0.11
C18:2(9.12)	24	Control (TC)	Dispersant (T2)	0.03
			AgNPs(T1)	1.00
		Dispersant (T2)	Control (TC)*	0.03
			AgNPs(T1)	0.10
		AgNPs(T1)	Control (TC)	1.00
			Dispersant (T2)	0.10
	120	Control (TC)	Dispersant (T2)	0.89
			AgNPs(T1)	1.00
		Dispersant (T2)	Control (TC)	0.89
			AgNPs(T1)	0.37
		AgNPs(T1)	Control (TC)	1.00
			Dispersant (T2)	0.37
C18:3(5.10.12)	24	Control (TC)	Dispersant (T2)	0.48
			AgNPs(T1)	1.00
		Dispersant (T2)	Control (TC)	0.48
			AgNPs(T1)	1.00
		AgNPs(T1)	Control (TC)	1.00
			Dispersant (T2)	1.00
	120	Control (TC)	Dispersant (T2)	0.12
			AgNPs(T1)	0.56
		Dispersant (T2)	Control (TC)	0.12
			AgNPs(T1)*	0.01
		AgNPs(T1)	Control (TC)	0.56
			Dispersant (T2)*	0.01
C19:1ω6	24	Control (TC)	Dispersant (T2)	0.57
			AgNPs(T1)	1.00
		Dispersant (T2)	Control (TC)	0.57
			AgNPs(T1)	1.00
		AgNPs(T1)	Control (TC)	1.00
			Dispersant (T2)	1.00
	120	Control (TC)	Dispersant (T2)	0.06
			AgNPs(T1)*	0.03
		Dispersant (T2)	Control (TC)	0.06
			AgNPs(T1)	1.00
		AgNPs(T1)	Control (TC)*	0.03
			Dispersant (T2)	1.00

Output

Papers

Paper 1: Shifts in the metabolic function of a benthic estuarine microbial community following a single pulse exposure to silver nanoparticles

Status (Published)

Elsevier Editorial System(tm) for Environmental Pollution
DOI: doi:10.1016/j.envpol.2015.02.033

Title: Shifts in the metabolic function of a benthic estuarine microbial community following a single pulse exposure to silver nanoparticles
Article Type: Research Paper
Corresponding Author: Dr. Mark Hartl,
Corresponding Author's Institution: Heriot-Watt University
First Author: Virginia Echavarri-Bravo
Order of Authors: Virginia Echavarri-Bravo; Lynn Paterson, PhD; Thomas J Aspray, PhD; Joanne S. S Porter, PhD; Michael K Winson, PhD; Barry Thornton, PhD; Mark G Hartl, PhD

Abstract: The increasing use of silver nanoparticles (AgNPs) as a biocidal agent and their potential accumulation in sediments may threaten non-target natural environmental bacterial communities. In this study a microcosm approach was established to investigate the effects of well characterized OECD AgNPs (NM-300) on the function of the bacterial community inhabiting marine estuarine sediments (salinity 31‰). The results showed that a single pulse of NM-300 AgNPs (1 mg L^{-1}) that led to sediment concentrations below 6 mg Ag kg^{-1} dry weight inhibited the bacterial utilization of environmentally relevant carbon substrates. As a result, the functional diversity changed, but recovered after 120 h under the experimental conditions. This microcosm study suggests that AgNPs under environmentally relevant experimental conditions can negatively affect bacterial function and provides an insight into the understanding of the bacterial community response and resilience to AgNPs exposure, important for informing relevant regulatory measures.

Paper 2: Ecotoxicity and fate of engineered nanomaterials (ENMs) in the marine environment

Status (in preparation)

Topic: Ecotoxicity and fate of engineered nanomaterials (ENMs) in the marine environment
Article Type: Review paper
Journal: Oceanography and Marine Biology: An Annual Review (Taylor & Francis)

Conference presentations

I. SLS PhD conference, Heriot-Watt, Edinburgh, December 2013 (Oral presentation)

Abstract

Effects of silver nanoparticles on the functioning of estuarine bacterial communities

V. Echavarri, L. Paterson, T. J. Aspray and M. G. J. Hartl

Bacterial communities inhabiting estuarine and coastal areas play an important role in biogeochemical processes providing crucial ecosystem services, such as nutrient recycling and bioremediation. The use of silver nanoparticles (AgNPs) has increased in recent years owing to their beneficial antimicrobial properties. However, if these nanoparticles are not efficiently removed from waste water treatment plants (WWTP) they can accumulate in the natural environment. Therefore the present research project aimed to study the effects of AgNPs on bacterial functioning in order to assess whether the ecosystem services provided by these organism could be disrupted. Owing to the existing need for studies that model environmentally relevant conditions, estuarine bacteria were expose to AgNPs in a series of microcosm that were established with sediments and water samples collected from the Firth of Forth estuary. The abundance, viability and metabolic status of the bacterial communities inhabiting the estuary were analyzed with different techniques such as Flow Cytometry, Respirometry and the utilization of ecologically relevant carbon sources. Results obtained revealed that the physiological status of estuarine bacterial communities was negatively affected by a single pulse of acute exposure to AgNPs. However they managed to recover successfully exhibiting strong resilience to these nanoparticles.

II. Marine Alliance for Science and Technology for Scotland (MASTS) annual science meeting, August 2013 (Oral presentation). Awarded with the best talk presentation price.

Effects of silver nanoparticles on the functioning of estuarine bacterial communities.

Virginia Echavarri[1], Lynn Paterson[2], Thomas Aspray[1] & Mark G. J. Hartl[1]

[1)] Centre for Marine Biodiversity and Biotechnology, School of Life Sciences, Heriot-Watt University, Edinburgh, Scotland, UK ve12.@hw.ac.uk

[2)] School of Engineering and Physical Sciences, Heriot-Watt University, Edinburgh, Scotland, UK

Bacterial communities inhabiting estuarine and coastal areas play an important role in biogeochemical processes providing crucial ecosystem services, such as nutrient recycling (Billen *et al.*, 1990) and bioremediation (Head and Swannell, 1999). The use of silver nanoparticles (AgNPs) has increased in recent years owing to their beneficial antimicrobial properties. However, if these nanoparticles are not efficiently removed from wastewater treatment plants (WWTP) they can accumulate in the natural environment(Blaser *et al.*, 2008).For this reason the objective of the present research project aims to study the effects AgNPs on bacterial functioning in order to assess whether the ecosystems services provided by these organism could be disrupted.

To do this a series of microcosm were established with sediments and water samples collected at different times of the year. The physiological status of the microbial communities was analyzed by measuring bacterial abundance, respiration and Community-Level Physiological Profiles (CLPP) based on the utilization different ecologically relevant carbon sources. To assess the effects on the water quality, inorganic nitrogen and chemical oxygen demand (COD) were monitored. The results obtained revealed a significant reduction in the bacterial abundance/viability owing to the exposure to AgNPs which was reflected on the oxygen uptake rate, and also a lower CLPP. AgNPs used exhibited greater toxicity than those used in similar studies(Bradford *et al.*, 2009). This toxicity depends on their physicochemical characteristics, their interactions with the components of the environment in which they were released and the organism targeted (Marambio-Jones and Hoek, 2010). Understanding these aspects is essential for meaningful environmental risk assessment and regulation of an emerging technology. For this reason the AgNPs used in the exposures have been characterized under different salinity gradients as this is one of the environmental parameters responsible for the high variability of the estuarine conditions that in addition significantly influences the persistence and toxicity of AgNPs .We conclude that, even though a negative impact on the bacterial abundance and also in the oxygen uptake was detected, this did not lead to a decrease in the water quality. This approach could enable the investigation of the acute toxicity of similar nanoparticles on estuarine and coastal bacterial communities in a cost-effective way.

Acknowledgements

The authors thank the support and advice provided by the technicians from the School of Life Sciences of Heriot-Watt University (Margaret Stobie, Hugh Barras, Sean McMenamy, Paul Cyphus and Vicky Goodfellow) and the NanoSafety Group. We also would like to thank Strathkelvin Instruments for facilitating the Strathtox Respirometer. This project was financially supported by the Heriot-Watt Environment and Climate Change Theme and NERC FENAC/2012/11/004.

III. 23rd SETAC Europe Annual Meeting in Glasgow, May 2013 (Oral presentation)

"Effects of silver nanoparticles on the functioning of estuarine bacterial communities"

Abstract similar to the one above.

IV. Marine Alliance for Science and Technology for Scotland (MASTS) annual science meeting, August 2012 (Digital Poster presentation)

"A microcosm approach to investigate the fate of silver nanoparticles and effects on bacterial functioning in estuaries"

Authors: Virginia Echavarri Bravo[1], Lynn Patersion[2], Joanne Porter[1], Michael Winson[1] & Mark G J Hartl[1]

[1)] Centre for Marine Biodiversity and Biotechnology, School of Life Sciences, Heriot-Watt University, Edinburgh, Scotland, UK ve12.@hw.ac.uk

[2)] School of Engineering and Physical Sciences, Heriot-Watt University, Edinburgh, Scotland, UK

The rise of nanotechnology has led to an increase in the manufacturing and use of new materials that at nano scale exhibit different characteristics to their respective bulk material. Nano silver is one of those materials, and it is incorporated in a wide variety of applications, such as health and personal care

products owing to their antimicrobial properties. As much of the silver is disposed of through domestic waste water (Blaser et al. 2008), the question arises whether the accumulation in the receiving estuarine environment could negatively affect the functioning of resident bacterial communities that play an important role in biogeochemical processes.

Moreover, the fate and impact on the AgNPs in estuaries, one of the most dynamic environments such, are still unclear. In the present study a microcosm approach was establish in order to model the estuarine conditions to carry out a more realistic study of the effects of AgNPs on bacterial communities.

Previous studies based on a microcosm approach did not detect any significant effect of AgNPs neither on diversity assemblages (Bradford et al, 2009) nor increased antibiotic resistance amongst the natural bacterial population (Mühling et al, 2009). However, in the current study the type of AgNPs used in the exposures exhibited a degree of toxicity at least twenty-five times higher than the nanoparticles used in the studies mentioned above. AgNPs differed in size (Ø 100nm the ones used by Bradford and Mühling, versus Ø 20nm AgNPs used in the current experiment). Smaller particles exhibit higher antimicrobial activity (Morones et al, 2005). In addition, the present project explored the impact on bacteria from a different angle than the studies already discussed, focusing on the bacterial functioning, and their crucial role on nutrient cycling and water quality. To do this, the mineralization of organic matter and nitrogen cycle was explored here by analyzing the impact on bacterial abundance, respiration, chemical oxygen demand (COD) and concentration of inorganic forms of nitrogen. In addition, the effects of salinity, one of the most variable parameters in an estuary during tidal action were studied. Preliminary results suggest that at least in short term exposures (< 10 hr), high salinity (20 - 32 ppt) may decrease the bacterial resistance to silver (Gupta et al. 1998) although particle aggregation was also observed.

Acknowledgements

Thanks to Hugh Barras, Sean McMenamy and Margaret Stobie for their advice and support with the samples collection and chemical analysis and Océane Guillemet for her help with the experimental work.
.

References

Bradford A, Handy RD, Readman JW, Atfield A, Muhling M (2009) Impact of Silver Nanoparticle Contamination on the Genetic Diversity of Natural Bacterial Assemblages in Estuarine Sediments. *Environmental Science & Technology* **43:** 4530-4536

Blaser SA, Scheringer M, Macleod M, Hungerbuhler K (2008) Estimation of cumulative aquatic exposure and risk due to silver: contribution of nano-functionalized plastics and textiles. *Sci Total Environ* **390:** 396-409

Gupta A, Maynes M, Silver S (1998) Effects of Halides on Plasmid-Mediated Silver Resistance in Escherichia coli. *Applied and Environmental Microbiology* **64:** 5042-5045

Morones JR, Elechiguerra JL, Camacho A, Holt K, Kouri JB, Tapia Ramírez J, Yacaman MJ (2005) The bactericidal effect of silver nanoparticles. *Nanotechnology* **16:** 2346–2353

Mühling M, Bradford A, Readman JW, Somerfield PJ, Handy RD (2009) An investigation into the effects of silver nanoparticles on antibiotic resistance of naturally occurring bacteria in an estuarine sediment. *Marine Environmental Research* **68:** 278-283

V. Scottish Toxicology interest group meeting, Heriot Watt, June 2012 (poster presentation) Poster 2

VI. PG conference, Heriot-Watt Edinburgh 2012 (Poster presentation) Poster 2

VII. Marine Alliance for Science and Technology for Scotland (MASTS) annual science meeting, August 2011 (Poster presentation) Best poster price Poster 2
"Impact of silver nanoparticles on estuarine microbial communities"

Authors: Virginia Echavarri Bravo[1], Mike Winston[1], Lynn Patersion[2] & Mark G J Hartl[1]

[1)] Centre for Marine Biodiversity and Biotechnology, School of Life Sciences, Heriot-Watt University, Edinburgh, Scotland, UK

[2)] School of Engineering and Physical Sciences, Heriot-Watt University, Edinburgh, Scotland, UK

The silver ion is a known antibacterial agent, a property that is maintained and possibly enhanced in nanoparticular form. Consequently, the rise of nanotechnology has led to the increased use of silver nanoparticles (Ag-NPs) in a wide variety of applications, such as health and personal care products. As much of the silver (particulate or otherwise) is disposed of with the domestic waste water stream, the question arises whether the accumulation in the receiving estuarine environment could negatively affect the functioning of resident bacterial communities. The importance of the role that these communities play in biogeochemical processes is indisputable. Hence, in this study we highlight the key function they play in estuarine habitats and try to predict whether the natural bacterial communities of estuaries could be negatively impacted by the exposure to wastewater-derived Ag-NPs.

In the present study several bacteria have been isolated at three distinct locations in the Firth of Forth estuary. These isolates have been identified based on phenotypic characteristics and by the sequencing of 16S RNA gene.

The effects of Ag-NPs on the bacterial communities are currently under investigation and preliminary results confirm that these Ag-NPs exhibit antibacterial activity, species-specific in nature. Growth of a marine species belonging to the *Pseudoalteromonas* genus was inhibited by Ag-NPs (10mg/L), concentrations five times lower than for a wild strain of *E. coli* isolated from fresh water. These effects are being quantified through such parameters as bacterial growth, BOD and NH_4 oxidation rate. Furthermore, ecotoxicological biomarkers relevant to microorganisms are being developed.

VIII. World Conference on Marine Biodiversity 2011, Aberdeen, Scotland (Digital poster presentation)
"Impact of silver nanoparticles on estuarine microbial communities"

Authors: Virginia Echavarri Bravo[1], Lynn Patersion[2] & Mark G J Hartl[1]

[1)] Centre for Marine Biodiversity and Biotechnology, School of Life Sciences, Heriot-Watt University, Edinburgh, Scotland, UK

[2)] School of Engineering and Physical Sciences, Heriot-Watt University, Edinburgh, Scotland, UK

The increasing use of silver nano-particles (Ag-NPs) in a wide variety of products such as health and personal care provokes the question whether their accumulation in the natural environment could negatively affect the functioning of bacterial communities. The importance of the role that these communities play in biogeochemical processes is indisputable. Hence, in this study we highlight the key function they play in estuarine habitats and try to predict if the natural bacterial communities of estuaries could be negatively impacted by the exposure to wastewater-derived Ag-NPs.

The bacterial communities of three different sections of the Firth of Forth estuarine have been characterized. In addition the effects of Ag-NPs on these communities are under study and preliminary results showed that these particles exhibit antibacterial activity as expected. Here we outline the topics and techniques being used for current and future research. For the characterisation of bacterial communities, techniques such as Microarrays and nested PCR and are applied. In order to quantify the effects of Ag-NPs, parameters such as bacterial growth, BOD and NH_4 oxidation rate, as well as ecotoxicological biomarkers relevant to microorganisms are being applied.

IX. PG conference, Heriot-Watt Edinburgh 2011 (Poster presentation) Poster 1

Poster 1

Impact of silver nanoparticles on estuarine microbial communities

Virginia Echavarri Bravo[1], Lynn Paterson[2] & Mark G J Hartl[1*]

Introduction and aims

Antimicrobial properties of silver nanoparticles (Ag-NPs) have led to their incorporation in a wide range of products. Consequently, Ag-NPs contained in the treated water or fertilizers could end up in the natural environment if they are not efficiently removed.

Fig. 1 Entry routes of Ag-NPs into the natural environment. Source: www.swedish.com.au/swedish/

This research project will focus on evaluating the impacts of Ag-NPs on the natural estuarine bactena.
Main objectives are as follows:

- Analysis of silver concentration in different estuarine compartments.
- Impact assessment on microbial community structure and identification of potential keystone species.
- Characterisation of Ag-NPs and determination Predicted No Effect Concentration (PNEC).

Location of the study

During the first year the study will take place in different sites of the Firth of Forth (Aliloa, Cramond and Seafield) as the natural conditions of the estuary and also the anthropogenic pressure vary depending on the site.

Fig. 2 Firth of Forth. The red circles represent the sites where sampling surveys are planned.

In future other relevant sites of study are Firth of Tay and Firth of Clyde as examples of highly industrialized and populated areas and then Dornoch Firth as an example of a pristine estuary.

Fig. 3 Beach next to Seafield WWTP

Fig.4 Satellite view of Beach adjacent to the Seafield WWTP

Methodology

Sampling

The first sampling took place in the beach next to Seafield WWTP. Samples were taken from superficial water and 1cm depth of intertidal sediments with sterile Greiner tubes. The water samples for Ag analysis were acidified with HNO_3 just after sampling and kept in the dark once in the lab. The sediment samples for Ag analysis were kept at -20°C. The samples for bacteria isolation were plated immediately once in the lab in ZM/10 and Tryptone media.

Silver - Analysis

Acidic digestion of the samples followed by Flame Atomic absorption (FLAA).

Isolation and culture of natural bacteria

Different species were isolated in ZM/10 media (Green, 2004) and Tryptone (75% sea water, 25% distilled water).

Impact of Ag-NPs on bacterial growth

Study of inhibitory concentrations of Ag-NPs over bacterial growth was carried out with one species (Fig. 5b, E).
Different concentrations of Ag-NPs were added to flasks containing 100ml of ZM/10 (pH 8) and incubated at 25°C.
Evolution of bacterial growth was estimated during a period of 9.5 h ($O.D._{540nm}$).

Current progress

Initial isolates show diverse phenotypes.

Fig 5a. Bacterial colonies (left) after 48 h of incubation on agar plates and bacteria stained (right) using Gram stain isolated from sediments.

Fig. 5b 48h isolates from the surface of the water column (Fig. 5b).

Species "E" (Fig. 5b) was the bacterium utilized to estimate growth inhibition. No bacterial growth was detected at [Ag-NPs] ≥ 12mg/L.

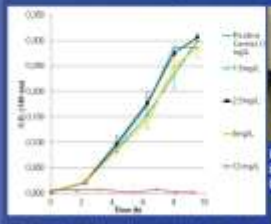

Fig. 6 Bacterial growth expressed as mean O.D (±S.D.). Ag-NP concentrations used were based on Morones et al. 2004 and Bradford et al. 2009. (n=3). For 12 mg/L n=1.

Fig. 7. Broth media with Ag-NPs before bacteria inoculation. Ag-NPs visible in the bottom of the flasks.

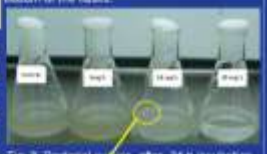

Fig. 8 Bacterial culture after 24 h incubation.

Fig. 9 Ag-NPs attached to the flask.

Bacterial growth was observed at 0 to 5 mg/L but not at 12 mg/L in the first 10 h (Fig.6). After 24h exposure, however, growth did occurred at 12 mg/L (Fig. 8) and Ag-NPs were found attached to the walls of the flask (Fig. 9). This issue was not observed in any other flask.

Discussion

- The O.D. were very similar in all treatments with concentrations ranging between 0 – 5 mg/L. After 8 hours the O.D. of treatment control remained constant whereas it increased in the rest of the treatments. One of the hypotheses is that the Ag-NPs concentration decreased during exposure possibly through adhering to dead bacterial debris and this may have enabled bacterial growth.
- Ag-NPs may inhibit bacterial metabolism but not kill them completely.
- The relatively high inhibitory concentrations are probably a result of Ag-NPs aggregation.
- Although O.D. can be a useful preliminary method for generating rough species-specific effect Ag-NP concentrations, O.D. should not be regarded as the sole parameter for quantifying bacterial growth. In future tests the number of viable cells will be analysed.

Future work

Toxicological studies

During the first year the bacterial growth of different species of bacteria under different concentrations and types of Ag-NPs will be studied. A range of toxicity test will be carried out to study the antibacterial mechanisms of Ag-NPs.

References

Acknowledgements

1) Centre for Marine Biodiversity and Biotechnology, School of Life Sciences, Heriot-Watt University, Edinburgh, Scotland, UK.

2) School of Engineering and Physical Sciences, Heriot-Watt University, Edinburgh, Scotland, UK.

*) www.sls.hw.ac.uk/mark

Poster 2

Impact of silver nanoparticles on estuarine microbial communities

Virginia Echavarri Bravo[1], Michael Winson[1], Joanne S. Porter[1], Lynn Paterson[2] & Mark G J Hartl[1]*

1. Introduction and aims

Every year about 320 tons of silver nanoparticles (AgNPs) are produced.

Use/Application AgNPs are incorporated in a wide range of products, such as cosmetics, detergents and textiles, because of their antimicrobial properties.

Risks associated to AgNPs
If they are not efficiently removed in the waste water treatment process, they could end up in the natural environment.

Main objectives of the present research project

- Study of the effects of AgNPs on natural bacteria from estuaries.
- Evaluation of the impact of AgNPs on microbial ecosystem functioning

2. Exposure of bacteria to AgNPs and challenges when working with metallic nanoparticles

The first approach taken was to study the effects of AgNPs on single species that had been isolated from the Firth of Forth estuary. Bacteria were exposed to different concentrations of AgNPs.

Behaviour of metallic nanoparticles in liquid suspension

Homogeneity in the stock suspension can be difficult to achieve as the nanoparticles (NP) tend to aggregate (Fig.1) and settle quickly.

How to optimize the homogeneity of the AgNPs stock suspensions?

✓ By adding dispersants such as Bovine Serum Albumin (BSA) to avoid aggregation
✓ By reducing the concentration of AgNPs in the solution to minimize sedimentation rate.

Effects of BSA and concentration of AgNPs are depicted in the graph (Fig.2). The concentration of AgNPs was independent of the order of extraction as the sedimentation rate decreased. The recovery of silver increased.

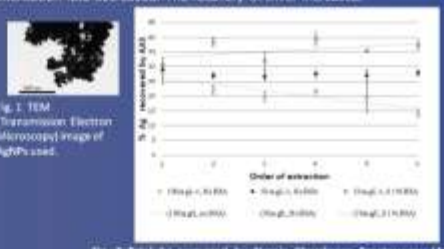

Fig. 1. TEM (Transmission Electron Microscope) image of AgNPs used.

Fig. 2 Total Ag recovered by Atomic Absorbance Spectroscopy (AAS) expressed as mean of % recovered over the nominal concentration(±S.D.) n=6. The three different stock solutions were prepared with AgNPs purchased from Sigma, as nanopowder form, size < 100nm. All the samples were ultrasonicated for 30 min and mixed vigorously in a vortex before the extraction.

Once reproducible amounts of AgNPs were reliably added to each experimental flask (Fig.3 and Fig.4), it was possible to continue with the experiment. However another issue was raised:

How to enhance the dispersion of AgNPs in liquid media?

✓ By inducing a wave motion in the liquid medium (Fig.5)

Fig. 3 AgNPs ended up in the bottom of the flask due to the orbital motion of the incubator.

Fig. 4 AgNPs dispersed thoroughly in the liquid medium in bottles that were placed horizontally in the orbital incubator.

Fig. 5 View from above of the orbital incubator.

References

Moreno, J. R., Rodriguez, J. L., Camacho, A., Hall, K., Noel, J. H., Rankin, L. T., et al. (2015). The bactericidal effect of silver nanoparticles. . Nanotechnology 26 , 239501.

Bradford, A., Handy, R., Readman, J., Rixford, A., & Lead, M. (2009). Impact of Silver Nanoparticles Contamination on the Genetic Diversity of Natural Bacterial Assemblages in Estuarine Sediments. Environ. Sci. Technol. , 4533-4539.

Hannah, I. A. (2015). MSc Dissertation. Investigation of the impact of Ag NPs on waste water treatment bacterial communities. Heriot-Watt University.

Chen et al. 2015. Speciation Analysis of Silver Nanoparticles and Silver Ions in Antibacterial Products and Environmental Waters via Cloud Point Extraction-Based Separation. dx.doi.org/10.1021/ac5038706a [Anal. Chem. XXXX, XXX, 000−000]

3. Isolation of bacteria from the estuary

Heterotrophic bacteria from water and sediments samples were isolated in Tryptone agar media. These species play a crucial role in the nutrient cycling of estuaries as they break down the organic matter releasing nitrogen in a form bioavailable for plants and other microorganisms.

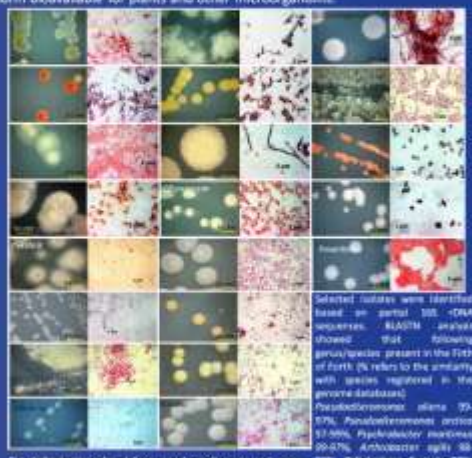

Fig. 6 Bacteria isolated from sandy sediments and water samples in the area of Seafield (Firth of Forth estuary, Fig.11)

Selected isolates were identified based on partial 16S rDNA sequences. BLASTN analysis showed that following genus/species present in the Firth of Forth (% refers to the similarity with species registered in the genome databases): *Pseudoalteromonas atlanta* 99-97%; *Pseudoalteromonas arctica* 97-99%; *Psychrobacter marinimus* 99-97%; *Arthrobacter agilis* 98-98%; *Cellulophaga fucicola* 98%; *Arthrobacter psychrolactophilus* 97%; *Streptomyces hoyangensis* 98%; *Bacillus weihenstephanensis* 98%; *Vibrio sp. Pseudomonas fluorescens*

4. Effects of AgNPs on bacterial growth

Four species were exposed to AgNPs and their growth monitored. *P.arctica* was the least susceptible to AgNPs, no effects observed at 5 mg L^{-1}, whereas *Arthrobacter agilis* was the most sensitive species, showing no growth at AgNPs < 2.5 mg L^{-1}.

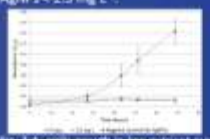

Fig. 7 *A. agilis* growth in low nutrient media expressed as mean $O.D._{540nm}$ (±S.D.).

Fig. 8. *A. agilis* (left) and *B. Weihenstephanensis* (right) colony forming units (CFU) after exposure to AgNPs.

Fig. 10. *S. Aizyangensis* cell culture. Negative control , 0 mg L^{-1} AgNPs (left) and 5mg L^{-1} AgNPs (right). At 5mg L^{-1} growth was affected. Bacteria formed clumps and remained in this life form until the end of the experiment, 46h of duration.

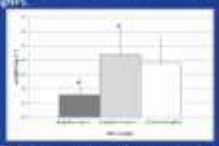

Fig. 9. *S. Aizyangensis* growth expressed in terms in biomass/dry weight,(±S.D.) n=3. The analysis of the variance (ANOVA) showed that there were statistically significantly differences between growth at 5 mg L^{-1} and 2.5 mg L^{-1} ($F = 0.016$, $=0.05$).

Conclusion

✓ Toxicity effects of AgNPs are species-specific.
✓ Bacterial growth was inhibited, however, the viability of cells was not completely suppressed at the AgNPs concentrations tested.

5. Future work

Study of AgNP's antibacterial mechanisms

Within bioassays and advanced microscopy techniques

Study of the impact of AgNPs on the bacterial ecosystem function

- A series of microcosms will be established with sediments collected from different sections of the Firth of Forth estuary. (See fig 11.) The characteristics of the sediments vary depending on the site (table 1) thus the species diversity and their response to AgNPs may differ.
- BOD (Biological Oxygen Demand) and NH_4^+ oxidation rate will be the first parameters to be monitored.

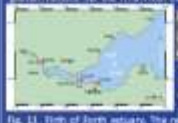

Fig. 11. Firth of Forth estuary. The red circles represent the sites where sampling surveys took place.

Fig. 12. Sandy sediments from Seafield, high content of coal present (right) due to anthropogenic activities.

Table 1. Physicochemical properties analysed

* Very variable depending on the rain and runoff water.

[1] Centre for Marine Biodiversity and Biotechnology, School of Life Sciences, Heriot-Watt University, Edinburgh, Scotland, UK

[2] School of Engineering and Physical Sciences, Heriot-Watt University, Edinburgh, Scotland, UK

Acknowledgements

Thanks to Dawn Austin, Hugh Barras, Paul Cyphus , Vicky Goodfellow, Sean McMenamy, Gina Shepherd, Margaret Stobie and the Nano-Safety Group for their support and advice.

*) http://markhartl.sls.hw.ac.uk/

References

Al-Shaeri, M., Ahmed, D., McCluskey, F., Turner, G., Paterson, L., Dyrynda, E. A. and Hartl, M. G. J. (2013) 'Potentiating toxicological interaction of single-walled carbon nanotubes with dissolved metals', *Environmental Toxicology and Chemistry*, 32(12), 2701-2710.

Al-Subiai, S. N., Arlt, V. M., Frickers, P. E., Readman, J. W., Stolpe, B., Lead, J. R., Moody, A. J. and Jha, A. N. (2012) 'Merging nano-genotoxicology with eco-genotoxicology: An integrated approach to determine interactive genotoxic and sub-lethal toxic effects of C-60 fullerenes and fluoranthene in marine mussels, Mytilus sp', *Mutation Research-Genetic Toxicology and Environmental Mutagenesis*, 745(1-2), 92-103.

Amato, E., Diaz-Fernandez, Y. A., Taglietti, A., Pallavicini, P., Pasotti, L., Cucca, L., Milanese, C., Grisoli, P., Dacarro, C., Fernandez-Hechavarria, J. M. and Necchi, V. (2011) 'Synthesis, characterization and antibacterial activity against Gram positive and Gram negative bacteria of biomimetically coated silver nanoparticles', *Langmuir*, 27(15), 9165-9173.

Anderson, S. A., Sissons, C. H., Coleman, M. J. and Wong, L. (2002) 'Application of carbon source utilization patterns to measure the metabolic similarity of complex dental plaque biofilm microcosms', *Applied and Environmental Microbiology*, 68(11), 5779-5783.

Angel, B. M., Batley, G. E., Jarolimek, C. V. and Rogers, N. J. (2013) 'The impact of size on the fate and toxicity of nanoparticulate silver in aquatic systems', *Chemosphere*, 93(2), 359-365.

Ankireddy, K., Vunnam, S., Kellar, J. and Cross, W. (2013) 'Highly conductive short chain carboxylic acid encapsulated silver nanoparticle based inks for direct write technology applications', *Journal of Materials Chemistry C*, 1(3), 572-579.

Arnaout, C. L. and Gunsch, C. K. (2012) 'Impacts of silver nanoparticle coating on the nitrification potential of *Nitrosomonas europaea*', *Environmental Science & Technology*, 46(10), 5387-5395.

Arnosti, C., Jørgensen, B. B., Sagemann, J. and Thamdrup, B. (1998) 'Temperature dependence of microbial degradation of organic matter in marine sediments: polysaccharide hydrolysis, oxygen consumption, and sulfate reduction', *Marine Ecology Progress Series*, 165, 59-70.

Ashkarran, A. A., Estakhri, S., Nezhad, M. R. H. and Eshghi, S. (2013) 'Controlling the geometry of silver nanostructures for biological applications', *Physics Procedia*, 40(0), 76-83.

Aspray, T., Gluszek, A. and Carvalho, D. (2008) 'Effect of nitrogen amendment on respiration and respiratory quotient (RQ) in three hydrocarbon contaminated soils of different type', *Chemosphere*, 72(6), 947-951.

Aspray, T. J., Carvalho, D. J. C. and Philp, J. C. (2007) 'Application of soil slurry respirometry to optimise and subsequently monitor ex situ bioremediation of hydrocarbon-contaminated soils', *International Biodeterioration & Biodegradation*, 60(4), 279-284.

Bååth, E., Díaz-Raviña, M., Frostegård, Å. and Campbell, C. D. (1998) 'Effect of metal-rich sludge amendments on the soil microbial community', *Applied and Environmental Microbiology*, 64(1), 238-245.

Badawy, A. M. E., Luxton, T. P., Silva, R. G., Scheckel, K. G., Suidan, M. T. and Tolaymat, T. M. (2010) 'Impact of environmental conditions (pH, ionic strength, and electrolyte type) on the surface charge and aggregation of silver nanoparticles suspensions', *Environmental Science & Technology*, 44(4), 1260-1266.

Baker, G. C., Smith, J. J. and Cowan, D. A. (2003) 'Review and re-analysis of domain-specific 16S primers', *Journal of Microbiological Methods*, 55(3), 541-555.

Baker, T. J., Tyler, C. R. and Galloway, T. S. (2014) 'Impacts of metal and metal oxide nanoparticles on marine organisms', *Environmental Pollution*, 186(0), 257-271.

Benn, T. M. and Westerhoff, P. (2008) 'Nanoparticle silver released into water from commercially available sock fabrics', *Environmental Science & Technology*, 42(11), 4133-4139.

Bernhard, A. E. and Bollmann, A. (2010) 'Estuarine nitrifiers: New players, patterns and processes', *Estuarine, Coastal and Shelf Science*, 88(1), 1-11.

Billen, G., Joiris, C., Meyer-Reil, L. and Linderboom, H. (1990) 'Role of bacteria in the North Sea ecosystem', *Netherlands Journal of Sea Research*, 26(2–4), 265-293.

Blaser, S. A., Scheringer, M., MacLeod, M. and Hungerbühler, K. (2008) 'Estimation of cumulative aquatic exposure and risk due to silver: Contribution of nano-functionalized plastics and textiles', *Science of The Total Environment*, 390(2–3), 396-409.

Bligh, E. G. and Dyer, W. J. (1959) 'A rapid method of total lipid extraction and purification', *Canadian Journal of Biochemistry and Physiology*, 37(8), 911-917.

Bolshakova, A. V., Kiselyova, O. I., Filonov, A. S., Frolova, O. Y., Lyubchenko, Y. L. and Yaminsky, I. V. (2001) 'Comparative studies of bacteria with an atomic force microscopy operating in different modes', *Ultramicroscopy*, 86(1–2), 121-128.

Bondarenko, O., Ivask, A., Käkinen, A., Kurvet, I. and Kahru, A. (2013) 'Particle-cell contact enhances antibacterial activity of silver nanoparticles', *PLoS ONE*, 8(5), e64060.

Bradford, A., Handy, R. D., Readman, J. W., Atfield, A. and Mühling, M. (2009) 'Impact of silver nanoparticle contamination on the genetic diversity of natural bacterial assemblages in estuarine sediments', *Environmental Science & Technology*, 43(12), 4530-4536.

Bragg, P. D. and Rainnie, D. J. (1974) 'The effect of silver ions on the respiratory chain of Escherichia coli', *Can J Microbiol*, 20(6), 883-9.

Breznak, J. A. and Costilow, R. N. (1994) 'Physicochemical factors in growth' in Gerhardt, P., Murray, R., Wood, W. and Krieg, N., eds., *Methods for general and molecular bacteriology*, Washington, DC: American Society for Microbiology.

Burchardt, A. D., Carvalho, R. N., Valente, A., Nativo, P., Gilliland, D., Garcìa, C. P., Passarella, R., Pedroni, V., Rossi, F. and Lettieri, T. (2012) 'Effects of silver nanoparticles in diatom *Thalassiosira pseudonana* and Cyanobacterium *Synechococcus* sp', *Environmental Science & Technology*, 46(20), 11336-11344.

Butler, J. L., Williams, M. A., Bottomley, P. J. and Myrold, D. D. (2003) 'Microbial community dynamics associated with rhizosphere carbon flow', *Applied and Environmental Microbiology*, 69(11), 6793-6800.

Caffrey, J. M., Bano, N., Kalanetra, K. and Hollibaugh, J. T. (2007) 'Ammonia oxidation and ammonia-oxidizing bacteria and archaea from estuaries with differing histories of hypoxia', *ISME Journal*, 1(7), 660-662.

Cardoso, J., van Bleijswijk, J. D. L., Witte, H. and van Duyl, F. C. (2013) 'Diversity and abundance of ammonia-oxidizing Archaea and Bacteria in tropical and cold-water coral reef sponges', *Aquatic Microbial Ecology*, 68(3), 215-230.

Carlson, C., Hussain, S. M., Schrand, A. M., K. Braydich-Stolle, L., Hess, K. L., Jones, R. L. and Schlager, J. J. (2008) 'Unique cellular interaction of silver nanoparticles: Size-dependent

generation of reactive oxygen species', *The Journal of Physical Chemistry B,* 112(43), 13608-13619.

Cavagnaro, T. R., Jackson, L. E., Scow, K. M. and Hristova, K. R. (2007) 'Effects of arbuscular mycorrhizas on ammonia oxidizing bacteria in an organic farm soil', *Microbial Ecology,* 54(4), 618-626.

Chao, J.-b., Liu, J.-f., Yu, S.-j., Feng, Y.-d., Tan, Z.-q., Liu, R. and Yin, Y.-g. (2011) 'Speciation analysis of silver nanoparticles and silver ions in antibacterial products and environmental waters via cloud point extraction-based separation', *Analytical Chemistry,* 83(17), 6875-6882.

Chen, K. L. and Bothun, G. D. (2013) 'Nanoparticles meet cell membranes: probing nonspecific interactions using model membranes', *Environmental Science & Technology,* 48(2), 873-880.

Chinnapongse, S. L., MacCuspie, R. I. and Hackley, V. A. (2011) 'Persistence of singly dispersed silver nanoparticles in natural freshwaters, synthetic seawater, and simulated estuarine waters', *Science of The Total Environment,* 409(12), 2443-2450.

Choi, O., Clevenger, T. E., Deng, B., Surampalli, R. Y., Ross Jr, L. and Hu, Z. (2009) 'Role of sulfide and ligand strength in controlling nanosilver toxicity', *Water Research,* 43(7), 1879-1886.

Choi, O., Deng, K. K., Kim, N.-J., Ross Jr, L., Surampalli, R. Y. and Hu, Z. (2008) 'The inhibitory effects of silver nanoparticles, silver ions, and silver chloride colloids on microbial growth', *Water Research,* 42(12), 3066-3074.

Choi, O. and Hu, Z. (2008) 'Size dependent and reactive oxygen species related nanosilver toxicity to nitrifying bacteria', *Environmental Science & Technology,* 42(12), 4583-4588.

Christopher, R. and Raina, M. (2003) 'Issues underlying use of biosensors to measure metal bioavailability', *Ecotoxicology and Environmental Safety 56*, 140–147.

Ciacci, C., Canonico, B., Bilaniĉová, D., Fabbri, R., Cortese, K., Gallo, G., Marcomini, A., Pojana, G. and Canesi, L. (2012) 'Immunomodulation by different yypes of N-Oxides in the hemocytes of the marine bivalve *Mytilus galloprovincialis*.', *PLoS ONE,* 7(5), e36937.

Cleveland, D., Long, S. E., Pennington, P. L., Cooper, E., Fulton, M. H., Scott, G. I., Brewer, T., Davis, J., Petersen, E. J. and Wood, L. (2012) 'Pilot estuarine mesocosm study on the environmental fate of Silver nanomaterials leached from consumer products', *Science of The Total Environment,* 421–422(0), 267-272.

Cohen, Y., Rallo, R., Liu, R. and Liu, H. H. (2012) 'In silico analysis of nanomaterials hazard and risk', *Accounts of Chemical Research,* 46(3), 802-812.

Colman, B., Wang, S.-Y., Auffan, M., Wiesner, M. and Bernhardt, E. (2012) 'Antimicrobial effects of commercial silver nanoparticles are attenuated in natural streamwater and sediment', *Ecotoxicology,* 21(7), 1867-1877.

Colman, B. P., Espinasse, B., Richardson, C. J., Matson, C. W., Lowry, G. V., Hunt, D. E., Wiesner, M. R. and Bernhardt, E. S. (2014) 'Emerging contaminant or an old toxin in disguise? Silver nanoparticle impacts on ecosystems', *Environmental Science & Technology,* 48(9), 5229-5236.

Cox, R. A., Culkin, F. and Riley, J. P. (1967) 'The electrical conductivity/chlorinity relationship in natural sea water', *Deep-Sea Res.*, 14(2), 203-220.

Crémazy, A., Campbell, P. G. C., Fortin, C. (2014) 'In the presence of fluoride, free Sc^{3+} is not a good predictor of Sc bioaccumulation by two unicellular algae: Possible role of fluoro-complexes', *Environmental Science & Technology*. 2014, 48 (16) 9754– 9761

Cronin, M. and Madden, J. (2010) 'In Silico Toxicology—An introduction' in *in silico Toxicology : Principles and Applications* [10.1039/9781849732093], P001-669.

Das, P., Xenopoulos, M. A., Williams, C. J., Hoque, M. E. and Metcalfe, C. D. (2012) 'Effects of silver nanoparticles on bacterial activity in natural waters', *Environmental Toxicology and Chemistry*, 31(1), 122-130.

DeSantis, T. Z., Brodie, E. L., Moberg, J. P., Zubieta, I. X., Piceno, Y. M. and Andersen, G. L. (2007) 'High-density universal 16S rRNA microarray analysis reveals broader diversity than typical clone library when sampling the environment', *Microbial Ecology*, 53(3), 371-83.

Di Giulio, R. T., Benson, W. H., Sanders, B. M. and Van Veld, P. A. (1995) 'Biochemical Mechanisms:Metabolism, Adaptation, and Toxicity' in M.Rand, G., ed. *Fundamentals of aquatic toxicology : effects, environmental fate, and risk assessment* 2ed., Norht Palm Beach, Florida: Taylor & Francis, 523-562.

Dibrov, P., Dzioba, J., Gosink, K. K. and Hase, C. C. (2002) 'Chemiosmotic Mechanism of Antimicrobial Activity of Ag^{+} in *Vibrio cholerae*', *Antimicrobial Agents and Chemotherapy*, 46(8), 2668–2670.

Digital Instruments (2000) *Scanning Probe Microscopy Training Notebook*.

Dobias, J. and Bernier-Latmani, R. (2013) 'Silver release from silver nanoparticles in natural waters', *Environmental Science & Technology*, 47(9), 4140-4146.

Doiron, K., Pelletier, E. and Lemarchand, K. (2012) 'Impact of polymer-coated silver nanoparticles on marine microbial communities: A microcosm study', *Aquatic Toxicology*, 124–125(0), 22-27.

Doolette, C., McLaughlin, M., Kirby, J., Batstone, D., Harris, H., Ge, H. and Cornelis, G. (2013) 'Transformation of PVP coated silver nanoparticles in a simulated wastewater treatment process and the effect on microbial communities', *Chemistry Central Journal*, 7(1), 46.

Downs, B., Robinson, S., Yang, H. and Mooney, P. 'RRUFF Project', [online], available: http://rruff.info/].

Du, Z., Zhang, Z., Miao, T., Wu, J., Lü, G., Yu, J., Xiao, J. and Chen, G. (2011) 'Draft Genome Sequence of the Novel Agar-Digesting Marine Bacterium HQM9', *Journal of Bacteriology*, 193(17), 4557-4558.

Echegoyen, Y. and Nerín, C. (2013) 'Nanoparticle release from nano-silver antimicrobial food containers', *Food and Chemical Toxicology*, 62(0), 16-22.

Eckelman, M. J., Mauter, M. S., Isaacs, J. A. and Elimelech, M. (2012) 'New perspectives on nanomaterial aquatic ecotoxicity: Production impacts exceed direct exposure impacts for carbon nanotoubes', *Environmental Science & Technology*, 46(5), 2902-2910.

Eilers, H., Pernthaler, J., Glöckner, F. O. and Amann, R. (2000) 'Culturability and in situ abundance of pelagic bacteria from the North Sea', *Applied and Environmental Microbiology*, 66(7), 3044-3051.

El Badawy, A. M., Silva, R. G., Morris, B., Scheckel, K. G., Suidan, M. T. and Tolaymat, T. M. (2010) 'Surface charge-dependent toxicity of silver nanoparticles', *Environmental Science & Technology*, 45(1), 283-287.

Environment agency 2007. The determination of oxygen chemical demand in waters and effluents.Methods for the Examination of Waters and Associated Materials. Standing Committee of Analysts (SCA) blue books. https://www.gov.uk/government/uploads/system/uploads/attachment_data/file/316793/COD-215nov.pdf

Epstein, M., Emri, I., Hartemann, P., Hoet, P., Leitgeb, N., Martínez Martínez, L., Proykova, A., Rizzo, L., Rodriguez-Farré, E., Rushton, L., Rydzynski, K., Samaras, T., Testai, E. and Vermeire, T. (2014) 'Nanosilver: safety, health and environmental effects and role in antimicrobial resistance', 1-102.

Fabrega, J., Fawcett, S. R., Renshaw, J. C. and Lead, J. R. (2009a) 'Silver nanoparticle impact on bacterial growth: effect of pH, concentration, and organic matter', *Environmental Science & Technology,* 43(19), 7285-90.

Fabrega, J., Renshaw, J. C. and Lead, J. R. (2009b) 'Interactions of silver nanoparticles with *Pseudomonas putida* biofilms', *Environmental Science & Technology,* 43(23), 9004-9009.

Fairbairn, E. A., Keller, A. A., Mädler, L., Zhou, D., Pokhrel, S. and Cherr, G. N. (2011) 'Metal oxide nanomaterials in seawater: Linking physicochemical characteristics with biological response in sea urchin development', *Journal of Hazardous Materials,* 192(3), 1565-1571.

Farkas, J., Peter, H., Christian, P., Gallego Urrea, J. A., Hassellöv, M., Tuoriniemi, J., Gustafsson, S., Olsson, E., Hylland, K. and Thomas, K. V. (2011) 'Characterization of the effluent from a nanosilver producing washing machine', *Environment International,* 37(6), 1057-1062.

Fayaz, A. M., Balaji, K., Girilal, M., Yadav, R., Kalaichelvan, P. T. and Venketesan, R. (2010) 'Biogenic synthesis of silver nanoparticles and their synergistic effect with antibiotics: a study against gram-positive and gram-negative bacteria', *Nanomedicine: Nanotechnology, Biology and Medicine,* 6(1), 103-109.

Feng, Q. L., Wu, J., Chen, G. Q., Cui, F. Z., Kim, T. N. and Kim, J. O. (2000) 'A mechanistic study of the antibacterial effect of silver ions on Escherichia coli and Staphylococcus aureus', *Journal of Biomedical Materials Research,* 52(4), 662-668.

Ferguson, R. L., Buckley, E. N. and Palumbo, A. V. (1984) 'Response of marine bacterioplankton to differential filtration and confinement', *Applied and Environmental Microbiology,* 47(1), 49-55.

Ferry, J. L., Craig, P., Hexel, C., Sisco, P., Frey, R., Pennington, P. L., Fulton, M. H., Scott, I. G., Decho, A. W., Kashiwada, S., Murphy, C. J. and Shaw, T. J. (2009) 'Transfer of gold nanoparticles from the water column to the estuarine food web', *Nature Nanotechnology,* 4(7), 441-444.

Field, A. (2009) *Discovering Statistics Using SPSS,* SAGE Publications Ltd; Third Edition edition.

Flegal, A. R., Brown, C. L., Squire, S., Ross, J. R. M., Scelfo, G. M. and Hibdon, S. (2007) 'Spatial and temporal variations in silver contamination and toxicity in San Francisco Bay', *Environ. Res.,* 105(1), 34-52.

Flemming, H.-C. (1987) 'Microbial growth on ion exchangers', *Water Research,* 21(7), 745-756.

Frostegård, A. and Bååth, E. (1996) 'The use of phospholipid fatty acid analysis to estimate bacterial and fungal biomass in soil', *Biology and Fertility of Soils,* 22(1-2), 59-65.

Frostegard, A., Tunlid, A. and Baath, E. (1993) 'Phospholipid Fatty Acid composition, biomass, and activity of microbial communities from two soil types experimentally exposed to different heavy metals', *Appl Environ Microbiol,* 59(11), 3605-17.

Frostegård, Å., Tunlid, A. and Bååth, E. (1991) 'Microbial biomass measured as total lipid phosphate in soils of different organic content', *Journal of Microbiological Methods,* 14(3), 151-163.

Frostegård, Å., Tunlid, A. and Bååth, E. (2011) 'Use and misuse of PLFA measurements in soils', *Soil Biol Biochem,* 43(8), 1621-1625.

Gaiser, B. K., Hirn, S., Kermanizadeh, A., Kanase, N., Fytianos, K., Wenk, A., Haberl, N., Brunelli, A., Kreyling, W. G. and Stone, V. (2013) 'Effects of silver nanoparticles on the liver and hepatocytes in vitro', *Toxicological Sciences,* 131(2), 537-547.

Gao, J., Wang, Y., Hovsepyan, A. and Bonzongo, J.-C. J. (2011) 'Effects of engineered nanomaterials on microbial catalyzed biogeochemical processes in sediments', *Journal of Hazardous Materials,* 186(1), 940-945.

García, R. and Pérez, R. (2002) 'Dynamic atomic force microscopy methods', *Surface Science Reports,* 47(6–8), 197-301.

Garland, J. L. (1996) 'Analytical approaches to the characterization of samples of microbial communities using patterns of potential C source utilization', *Soil Biology and Biochemistry,* 28(2), 213-221.

Garland, J. L. and Mills, A. L. (1991) 'Classification and characterization of heterotrophic microbial communities on the basis of patterns of community-level sole-carbon-source utilization', *Applied and Environmental Microbiology,* 57(8), 2351-2359.

Georgiev, P., Bojinova, A., Kostova, B., Momekova, D., Bjornholm, T. and Balashev, K. (2013) 'Implementing atomic force microscopy (AFM) for studying kinetics of gold nanoparticle's growth', *Colloids and Surfaces A: Physicochemical and Engineering Aspects,* 434(0), 154-163.

Gerhardt P, M. R., Wood WA, Krieg NR (eds) (1994) *Methods for general and molecular bacteriology,* Washington, DC: American Society for Microbiology.

Gigault, J. and Hackley, V. A. (2013) 'Differentiation and characterization of isotopically modified silver nanoparticles in aqueous media using asymmetric-flow field flow fractionation coupled to optical detection and mass spectrometry', *Analytica Chimica Acta,* 763(0), 57-66.

Gondikas, A. P., Morris, A., Reinsch, B. C., Marinakos, S. M., Lowry, G. V. and Hsu-Kim, H. (2012) 'Cysteine-induced modifications of zero-valent silver nanomaterials: Implications for particle surface chemistry, aggregation, dissolution, and silver speciation', *Environmental Science & Technology*.

Gottschalk, F., Kost, E. and Nowack, B. (2013) 'Engineered nanomaterials in water and soils: A risk quantification based on probabilistic exposure and effect modeling', *Environmental Toxicology and Chemistry,* 32(6), 1278-1287.

Gottschalk, F., Sonderer, T., Scholz, R. W. and Nowack, B. (2009) 'Modeled environmental concentrations of engineered nanomaterials (TiO2, ZnO, Ag, CNT, Fullerenes) for different regions', *Environmental Science & Technology,* 43(24), 9216-9222.

Green, D. H., Llewellyn, L. E., Negri, A. P., Blackburn, S. I. and Bolch, C. J. S. (2004) 'Phylogenetic and functional diversity of the cultivable bacterial community associated with the paralytic shellfish poisoning dinoflagellate *Gymnodinium catenatum*', *FEMS Microbiology Ecology,* 47(3), 345-357.

Gupta, A., Maynes, M. and Silver, S. (1998) 'Effects of Halides on Plasmid-Mediated Silver Resistance in Escherichia coli', *Applied and Environmental Microbiology,* 64(12), 5042-5045.

Gupta, A., Phung, L. T., Taylor, D. E. and Silver, S. (2001) 'Diversity of silver resistance genes in IncH incompatibility group plasmids', *Microbiology,* 147(12), 3393-3402.

Gutierrez, T., Biller, D., Shimmield, T. and Green, D. (2012) 'Metal binding properties of the EPS produced by *Halomonas* sp. TG39 and its potential in enhancing trace element bioavailability to eukaryotic phytoplankton', *BioMetals,* 25(6), 1185-1194.

Gutierrez, T., Shimmield, T., Haidon, C., Black, K. and Green, D. H. (2008) 'Emulsifying and metal ion binding activity of a glycoprotein exopolymer produced by *Pseudoalteromonas* sp. Strain TG12', *Applied and Environmental Microbiology,* 74(15), 4867-4876.

Händel, N., Schuurmans, J. M., Brul, S. and ter Kuile, B. H. (2013) 'Compensation of the metabolic costs of antibiotic resistance by physiological adaptation in *Escherichia coli*', *Antimicrobial Agents and Chemotherapy,* 57(8), 3752-3762.

Haye, J. M., Santschi, P. H., Roberts, K. A. and Ray, S. (2006) 'Protective role of alginic acid against metal uptake by american oyster (*Crassostrea virginica*)', *Environmental Chemistry,* 3(3), 172-183.

He, D., Dorantes-Aranda, J. J. and Waite, T. D. (2012) 'Silver nanoparticle-algae interactions: oxidative dissolution, reactive oxygen species generation and synergistic toxic effects', *Environmental Science & Technology,* 46(16), 8731-8.

Head, I. M. and Swannell, R. P. J. (1999) 'Bioremediation of petroleum hydrocarbon contaminants in marine habitats', *Current Opinion in Biotechnology,* 10(3), 234-239.

Hendren, C. O., Lowry, M., Grieger, K. D., Money, E. S., Johnston, J. M., Wiesner, M. R. and Beaulieu, S. M. (2013) 'Modeling approaches for characterizing and evaluating environmental exposure to engineered nanomaterials in support of risk-based decision making', *Environmental Science & Technology,* 47(3), 1190-1205.

Hendren, C. O., Mesnard, X., Dröge, J. and Wiesner, M. R. (2011) 'Estimating production data for five engineered nanomaterials as a basis for exposure assessment', *Environmental Science & Technology,* 45(7), 2562-2569.

Hennige, S. J., Wicks, L. C., Kamenos, N. A., Bakker, D. C. E., Findlay, H. S., Dumousseaud, C. and Roberts, J. M. (2014) 'Short-term metabolic and growth responses of the cold-water coral Lophelia pertusa to ocean acidification', *Deep Sea Research Part II: Topical Studies in Oceanography,* 99(0), 27-35.

Hollibaugh, J. T., Gifford, S., Sharma, S., Bano, N. and Moran, M. A. (2011) 'Metatranscriptomic analysis of ammonia-oxidizing organisms in an estuarine bacterioplankton assemblage', *ISME Journal,* 5(5), 866-878.

Holmes, A. J., Costello, A., Lidstrom, M. E. and Murrell, J. C. (1995) 'Evidence that participate methane monooxygenase and ammonia monooxygenase may be evolutionarily related', *FEMS Microbiology Letters,* 132(3), 203-208.

Hornek, R., Pommerening-Röser, A., Koops, H. P., Farnleitner, A. H., Kreuzinger, N., Kirschner, A. and Mach, R. L. (2006) 'Primers containing universal bases reduce multiple amoA gene specific DGGE band patterns when analysing the diversity of beta-ammonia oxidizers in the environment', *Journal of Microbiological Methods,* 66(1), 147-155.

Howard-Jones, M. H., Frischer, M. E. and Verity, P. G. (2001) 'Determining the physiological status of individual bacterial cells' in John, H. P., ed. *Methods in Microbiology*, Academic Press, 175-206.

Impellitteri, C. A., Harmon, S., Silva, R. G., Miller, B. W., Scheckel, K. G., Luxton, T. P., Schupp, D. and Panguluri, S. (2013) 'Transformation of silver nanoparticles in fresh, aged, and incinerated biosolids', *Water Research,* 47(12), 3878-3886.

Ito, T., Saikawa, K., Kim, S., Fujita, K., Ishiwata, A., Kaeothip, S., Arakawa, T., Wakagi, T., Beckham, G. T., Ito, Y. and Fushinobu, S. (2014) 'Crystal structure of glycoside hydrolase family 127 β-l-arabinofuranosidase from *Bifidobacterium longum*', *Biochemical and Biophysical Research Communications,* 447(1), 32-37.

Joshi, N., Ngwenya, B. T. and French, C. E. (2012) 'Enhanced resistance to nanoparticle toxicity is conferred by overproduction of extracellular polymeric substances', *Journal of Hazardous Materials,* 241–242(0), 363-370.

Joshi,N, B.T Bryne T. Ngwenya, I.B. Butler, C. E. French (2015)'Use of bioreporters and deletion mutants reveals ionic silver and ROS to be equally important in silver nanotoxicity', *Journal of Hazardous Materials,* 287, 51-58.

Jung, W. K., Koo, H. C., Kim, K. W., Shin, S., Kim, S. H. and Park, Y. H. (2008) 'Antibacterial activity and mechanism of action of the silver ion in Staphylococcus aureus and Escherichia coli', *Applied and Environmental Microbiology,* 74(7), 2171-8.

Just, J. and Szniolis, A. (1936) 'Germicidal properties of silver in water', *Journal of the American Water Works Association,* 28(4).

Kaegi, R., Voegelin, A., Ort, C., Sinnet, B., Thalmann, B., Krismer, J., Hagendorfer, H., Elumelu, M. and Mueller, E. (2013) 'Fate and transformation of silver nanoparticles in urban wastewater systems', *Water Research,* 47(12), 3866-3877.

Kaegi, R., Voegelin, A., Sinnet, B., Zuleeg, S., Hagendorfer, H., Burkhardt, M. and Siegrist, H. (2011) 'Behavior of metallic silver nanoparticles in a pilot wastewater treatment plant', *Environmental Science & Technology,* 45(9), 3902-3908.

Kah, M. and Hofmann, T. (2014) 'Nanopesticide research: Current trends and future priorities', *Environment International,* 63(0), 224-235.

Kang, F., Alvarez, P. J. and Zhu, D. (2013) 'Microbial extracellular polymeric substances reduce Ag^+ to silver nanoparticles and antagonize bactericidal activity', *Environmental Science & Technology,* 48(1), 316-322.

Keller, A., McFerran, S., Lazareva, A. and Suh, S. (2013) 'Global life cycle releases of engineered nanomaterials', *Journal of Nanoparticle Research,* 15(6), 1-17.

Kent, R. D. and Vikesland, P. J. (2011) 'Controlled evaluation of silver nanoparticle dissolution using Atomic Force Microscopy', *Environmental Science & Technology,* 46(13), 6977-6984.

Kermanizadeh, A., Pojana, G., Gaiser, B. K., Birkedal, R., Bilanicˇová, D., Wallin, H., Jensen, K. A., Sellergren, B., Hutchison, G. R., Marcomini, A. and Stone, V. (2012) 'In vitro assessment of engineered nanomaterials using a hepatocyte cell line: cytotoxicity, pro-inflammatory cytokines and functional markers', *Nanotoxicology,* 7(3), 301-313.

Kieft, T. L., Wilch, E., O'Connor, K., Ringelberg, D. B. and White, D. C. (1997) 'Survival and phospholipid Fatty Acid profiles of surface and subsurface bacteria in natural sediment microcosms', *Applied and Environmental Microbiology,* 63(4), 1531-1542.

Kim, J. S., Kuk, E., Yu, K. N., Kim, J.-H., Park, S. J., Lee, H. J., Kim, S. H., Park, Y. K., Park, Y. H., Hwang, C.-Y., Kim, Y.-K., Lee, Y.-S., Jeong, D. H. and Cho, M.-H. (2007) 'Antimicrobial effects of silver nanoparticles', *Nanomedicine: Nanotechnology, Biology and Medicine,* 3(1), 95-101.

Klein, C., Comero, S., Stahlmecke, B., Romazanov, J., Kuhlbusch, T., van, Doren, E., Wick, P., Locoro, G., Koerdel, W. and Gawlik, B., et al. (2011) 'NM-Series of Representative Manufactured Nanomaterials:NM-300 Silver Characterisation, Stability, Homogeneity'.

Knapp, C. W., McCluskey, S. M., Singh, B. K., Campbell, C. D., Hudson, G. and Graham, D. W. (2011) 'Antibiotic resistance gene abundances correlate with metal and geochemical conditions in archived Scottish soils', *PLoS ONE,* 6(11), e27300.

Korayem, M. H., Ebrahimi, N. and Sotoudegan, M. S. (2011) 'Frequency response of atomic force microscopy microcantilevers oscillating in a viscous liquid: A comparison of various methods', *Scientia Iranica,* 18(5), 1116-1125.

Kubacka, A., Diez, M. S., Rojo, D., Bargiela, R., Ciordia, S., Zapico, I., Albar, J. P., Barbas, C., Martins dos Santos, V. A. P., Fernandez-Garcia, M. and Ferrer, M. (2014) 'Understanding the antimicrobial mechanism of TiO_2-based nanocomposite films in a pathogenic bacterium', *Sci. Rep.*, 4.

Kumar, N., Shah, V. and Walker, V. K. (2011) 'Perturbation of an arctic soil microbial community by metal nanoparticles', *Journal of Hazardous Materials,* 190(1–3), 816-822.

Kunihiro, T., Veuger, B., Vasquez-Cardenas, D., Pozzato, L., Le Guitton, M., Moriya, K., Kuwae, M., Omori, K., Boschker, H. T. S. and van Oevelen, D. (2014) 'Phospholipid-derived Fatty Acids and Quinones as markers for bacterial biomass and community structure in marine sediments', *PLoS ONE,* 9(4), e96219.

Lansdown, A. B. G. (2010) 'A Pharmacological and toxicological profile of silver as an antimicrobial agent in medical devices', *Advances in Pharmacological Sciences,* 2010.

Lebaron, P., Servais, P., Baudoux, A.-C., Bourrain, M., Courties, C. and Parthuisot, N. (2002) 'Variations of bacterial-specific activity with cell size and nucleic acid content assessed by flow cytometry', *Aquatic Microbial Ecology,* 28(2), 131-140.

Lebaron, P., Servais, P., Troussellier, M., Courties, C., Muyzer, G., Bernard, L., Schäfer, H., Pukall, R., Stackebrandt, E., Guindulain, T. and Vives-Rego, J. (2001) 'Microbial community dynamics in Mediterranean nutrient-enriched seawater mesocosms: changes in abundances, activity and composition', *FEMS Microbiology Ecology,* 34(3), 255-266.

Leo, B. F., Chen, S., Kyo, Y., Herpoldt, K.-L., Terrill, N. J., Dunlop, I. E., McPhail, D. S., Shaffer, M. S., Schwander, S., Gow, A., Zhang, J., Chung, K. F., Tetley, T. D., Porter, A. E. and Ryan, M. P. (2013) 'The Stability of silver nanoparticles in a model of pulmonary surfactant', *Environmental Science & Technology,* 47(19), 11232-11240.

Levard, C., Hotze, E. M., Lowry, G. V. and Brown, G. E. (2012) 'Environmental transformations of silver nanoparticles: Impact on stability and toxicity', *Environmental Science & Technology,* 46(13), 6900-6914.

Levard, C., Mitra, S., Yang, T., Jew, A. D., Badireddy, A. R., Lowry, G. V. and Brown, G. E. (2013) 'Effect of chloride on the dissolution rate of silver nanoparticles and toxicity to *E. coli*', *Environmental Science & Technology,* 47(11), 5738-5745.

Li, Y., Zhang, W., Niu, J. and Chen, Y. (2013) 'Surface-coating-dependent dissolution, aggregation, and Reactive Oxygen Species (ROS) generation of silver nanoparticles under different irradiation conditions', *Environmental Science & Technology*, 47(18), 10293-10301.

Lim, J., Yeap, S., Che, H. and Low, S. (2013) 'Characterization of magnetic nanoparticle by dynamic light scattering', *Nanoscale Research Letters,* 8(1), 381.

Lin, P.-C., Lin, S., Wang, P. C. and Sridhar, R. (2014) 'Techniques for physicochemical characterization of nanomaterials', *Biotechnology Advances,* (0).

Lipski, A., Spieck, E., Makolla, A. and Altendorf, K. (2001) 'Fatty Acid Profiles of Nitrite-oxidizing bacteria reflect their phylogenetic heterogeneity', *Syst. Appl. Microbiol.*, 24(3), 377-384.

Liu, H. H. and Cohen, Y. (2014) 'Multimedia environmental distribution of engineered nanomaterials', *Environmental Science & Technology,* 48(6), 3281-3292.

Liu, J. and Hurt, R. H. (2010) 'Ion release kinetics and particle persistence in aqueous nano-silver colloids', *Environmental Science & Technology,* 44(6), 2169-2175.

Liu, J., Pennell, K. G. and Hurt, R. H. (2011) 'Kinetics and mechanisms of nanosilver oxysulfidation', *Environmental Science & Technology,* 45(17), 7345-7353.

Liu, J., Sonshine, D. A., Shervani, S. and Hurt, R. H. (2010) 'Controlled release of biologically active silver from nanosilver surfaces', *ACS Nano,* 4(11), 6903-6913.

Liu, L., Yang, J., Xie, J., Luo, Z., Jiang, J., Yang, Y. Y. and Liu, S. (2013) 'The potent antimicrobial properties of cell penetrating peptide-conjugated silver nanoparticles with excellent selectivity for Gram-positive bacteria over erythrocytes', *Nanoscale,* 5(9), 3834-3840.

Liu, Z.-h., Zhou, Y., Maszenan, A. M., Ng, W. J. and Liu, Y. (2013) 'pH-dependent transformation of Ag nanoparticles in anaerobic processes', *Environmental Science & Technology,* 47(22), 12630-12631.

Lok, C.-N., Ho, C.-M., Chen, R., He, Q.-Y., Yu, W.-Y., Sun, H., Tam, P. K.-H., Chiu, J.-F. and Che, C.-M. (2006) 'Proteomic analysis of the mode of antibacterial action of silver nanoparticles', *Journal of Proteome Research,* 5(4), 916-924.

Lombi, E., Donner, E., Taheri, S., Tavakkoli, E., Jämting, Å. K., McClure, S., Naidu, R., Miller, B. W., Scheckel, K. G. and Vasilev, K. (2013) 'Transformation of four silver/silver chloride nanoparticles during anaerobic treatment of wastewater and post-processing of sewage sludge', *Environmental Pollution,* 176(0), 193-197.

Long, X.-E., Chen, C., Xu, Z. and He, J.-z. (2014) 'Shifts in the abundance and community structure of soil ammonia oxidizers in a wet sclerophyll forest under long-term prescribed burning', *Science of The Total Environment,* 470–471(0), 578-586.

Loosli, F., Le Coustumer, P. and Stoll, S. (2013) 'TiO_2 nanoparticles aggregation and disaggregation in presence of alginate and Suwannee River humic acids. pH and concentration effects on nanoparticle stability', *Water Research,* 47(16), 6052-6063.

López, I., Kalman, J., Vale, C. and Blasco, J. (2010) 'Influence of sediment acidification on the bioaccumulation of metals in *Ruditapes philippinarum*', *Environmental Science and Pollution Research,* 17(9), 1519-1528.

Losasso, C., Belluco, S., Cibin, V., Zavagnin, P., Micetic, I., Gallocchio, F., Zanella, M., Bregoli, L., Biancotto, G. and Ricci, A. (2014) 'Antibacterial activity of silver nanoparticles: Sensitivity of different *Salmonella* serovars. S', *Frontiers in Microbiology,* 5.

Lu, Z., Rong, K., Li, J., Yang, H. and Chen, R. (2013) 'Size-dependent antibacterial activities of silver nanoparticles against oral anaerobic pathogenic bacteria', *Journal of Materials Science: Materials in Medicine,* 24(6), 1465-1471.

Luo, Z., Wang, Z., Li, Q., Pan, Q., Yan, C. and Liu, F. (2011) 'Spatial distribution, electron microscopy analysis of titanium and its correlation to heavy metals: Occurrence and sources of titanium nanomaterials in surface sediments from Xiamen Bay, China', *Journal of Environmental Monitoring,* 13(4), 1046-1052.

Luoma, S. N., Ho, Y. B. and Bryan, G. W. (1995) 'Fate, bioavailability and toxicity of silver in estuarine environments', *Mar. Pollut. Bull.,* 31(1-3), 44-54.

Ma, R., Levard, C., Marinakos, S. M., Cheng, Y., Liu, J., Michel, F. M., Brown, G. E. and Lowry, G. V. (2011) 'Size-controlled dissolution of organic-coated silver nanoparticles', *Environmental Science & Technology,* 46(2), 752-759.

MacCuspie, R. I., Rogers, K., Patra, M., Suo, Z., Allen, A. J., Martin, M. N. and Hackley, V. A. (2011) 'Challenges for physical characterization of silver nanoparticles under pristine and environmentally relevant conditions', *Journal of Environmental Monitoring*, 13(5), 1212-1226.

Macken, A., Byrne, H. J. and Thomas, K. V. (2012) 'Effects of salinity on the toxicity of ionic silver and Ag-PVP nanoparticles to Tisbe battagliai and Ceramium tenuicorne', *Ecotoxicology and Environmental Safety*, 86(0), 101-110.

Maity, S., Downen, L. N., Bochinski, J. R. and Clarke, L. I. (2011) 'Embedded metal nanoparticles as localized heat sources: An alternative processing approach for complex polymeric materials', *Polymer*, 52(7), 1674-1685.

Malvern Instruments Ltd. 2003.Zetasizer Nano Series. User Manual. (MAN0317, Issue 1.1 Feb 2004)

Malvern Instruments 'The accuracy and precision expected from dynamic light scattering measurements',(Version 4 Technical Note).
http://www.malvern.com/en/support/resource-center/technical-notes/TN101104AccuracyPrecisionDLS.aspx

Malvern Instruments (2014a) 'Dynamic light scattering - common terms defined', [online],available:http://www.malvern.com/en/support/resource-center/Whitepapers/WP111214DLSTermsDefined.aspx].

Malvern Instruments (2014b) 'An introduction to DLS microrheology', [online], available:http://www.malvern.com/en/support/resource-center/Whitepapers/WP120917IntroDLSMicro.aspx].

Marambio-Jones, C. and Hoek, E. M. V. (2010) 'A review of the antibacterial effects of silver nanomaterials and potential implications for human health and the environment', *Journal of Nanoparticle Research*, 12(5), 1531-1551.

Marion, G. M., Millero, F. J., Camões, M. F., Spitzer, P., Feistel, R. and Chen, C. T. A. (2011) 'pH of seawater', *Marine Chemistry*, 126(1–4), 89-96.

Martina, I., Wiesinger, R., Jembrih-Simbürger, D. and Schreiner, M. (2012) 'Micro-Raman characterization of silver corrosion products: Instrumental set up and reference database', 9), 1-8.

Maurer, E. I., Sharma, M., Schlager, J. J. and Hussain, S. M. (2013) 'Systematic analysis of silver nanoparticle ionic dissolution by tangential flow filtration: toxicological implications', *Nanotoxicology*, 8(7), 718-727.

Mayor, D. J., Gray, N. B., Elver-Evans, J., Midwood, A. J. and Thornton, B. (2013) 'Metal-macrofauna interactions determine microbial community structure and function in copper contaminated sediments', *PLoS ONE*, 8(5), e64940.

Millero, F. J., Feistel, R., Wright, D. G. and McDougall, T. J. (2008) 'The composition of standard seawater and the definition of the reference-composition salinity scale', *Deep Sea Research Part I: Oceanographic Research Papers*, 55(1), 50-72.

Mitrano, D. M., Ranville, J., Bednar, A., Kazor, K., Hering, A. S. and Higgins, C. (2014) 'Tracking dissolution of silver nanoparticles at environmentally relevant concentrations in laboratory, natural and processed waters using single particle ICP-MS (spICP-MS)', *Environmental Science: Nano*.

Miyoshi, H., Ohno, H., Sakai, K., Okamura, N. and Kourai, H. (2010) 'Characterization and photochemical and antibacterial properties of highly stable silver nanoparticles prepared on montmorillonite clay in n-hexanol', *Journal of Colloid and Interface Science*, 345(2), 433-441.

Mohanty, S., Jena, P., Mehta, R., Pati, R., Banerjee, B., Patil, S. and Sonawane, A. (2013) 'Cationic antimicrobial peptides and biogenic silver nanoparticles kill Mycobacteria without eliciting DNA damage and cytotoxicity in mouse macrophages', *Antimicrobial Agents and Chemotherapy*, 57(8), 3688-3698.

Morones, J. R., Elechiguerra, J. L., Camacho, A., Holt, K., Kouri, J. B., Tapia Ramírez, J. and Yacaman, M. J. (2005) 'The bactericidal effect of silver nanoparticles', *Nanotechnology*, 16(2346), 2346–2353.

Morris B.E.L , Henneberger R., Huber H. , Moissl-Eichinger C. (2013) 'Microbial syntrophy: interaction for the common good', *FEMS Microbiology Reviews*, 37 (3) 384-406.

Mudroch, A., Azcue, J. M. and Mudroch, P. (1996) 'Measurements of physical properties of sediments' in *Manual of Physico-Chemical Analysis of Aquatic Sediments*, CRC Press, 320.

Mühling, M., Bradford, A., Readman, J. W., Somerfield, P. J. and Handy, R. D. (2009) 'An investigation into the effects of silver nanoparticles on antibiotic resistance of naturally occurring bacteria in an estuarine sediment', *Marine Environmental Research*, 68(5), 278-283.

Muyzer, G., Brinkhoff , T., Nübel, U., Santegoeds, C., Schäfer, H. and Waver, C. (1998) 'Denaturing gradient gel electrophoresis (DGGE) in microbial ecology.' in Kowalchuk, G. A., Bruijn, F. J., Head, I. M., Akkermans, A. D. and Elsas, J. D., eds., *Molecular Microbial Ecology Manual*, Springer Netherlands, 1–27.

Navarro Llorens, J. M., Tormo, A. and Martínez-García, E. (2010) 'Stationary phase in gram-negative bacteria', *FEMS Microbiology Reviews*, 34(4), 476-495.

Neidhardt, F. C., Ingraham, J. L. and Schaechter, M. (1990) *Physiology of the bacterial cell : a molecular approach*, Sinauer Associates.

Nguyen D., Joshi-Datar A., Lepine F., Bauerle E., Olakanmi O., Beer K., McKay G., Siehnel R, Schafhauser J., Wang Y., Britigan B.E., and. Singh P.K. (2011) 'Active Starvation Responses Mediate Antibiotic Tolerance in Biofilms and Nutrient-Limited Bacteria' .*Science*, 334 (6058), 982-986.

Nikaido, H. (2003) 'Molecular Basis of Bacterial Outer Membrane Permeability Revisited', *Microbiology and Molecular Biology Reviews*, 67(4), 593-656.

Nordstrom, D. K. and Wilde, F. D. (2005) 'Reduction - Oxidation Potential (Electrode method) (ver.1.2)', *National field manual for the collection of water-quality data*, Chapter A6. Field Measurements

Nowack, B., Ranville, J. F., Diamond, S., Gallego-Urrea, J. A., Metcalfe, C., Rose, J., Horne, N., Koelmans, A. A. and Klaine, S. J. (2012) 'Potential scenarios for nanomaterial release and subsequent alteration in the environment', *Environmental Toxicology and Chemistry*, 31(1), 50-59.

O'Shea, R. and Moser, H. E. (2008) 'Physicochemical properties of antibacterial compounds: Implications for drug discovery', *Journal of Medicinal Chemistry*, 51(10), 2871-2878.

Ojha, A., Forster, S., Kumar, S., Vats, S., Negi, S. and Fischer, I. (2013) 'Synthesis of well-dispersed silver nanorods of different aspect ratios and their antimicrobial properties against gram positive and negative bacterial strains', *Journal of Nanobiotechnology*, 11(1), 42.

Okano, Y., Hristova, K. R., Leutenegger, C. M., Jackson, L. E., Denison, R. F., Gebreyesus, B., Lebauer, D. and Scow, K. M. (2004) 'Application of Real-Time PCR to study effects of ammonium on population size of ammonia-oxidizing bacteria in soil', *Applied and Environmental Microbiology*, 70(2), 1008-1016.

Olsson, P. A., Bååth, E., Jakobsen, I. and Söderström, B. (1995) 'The use of phospholipid and neutral lipid fatty acids to estimate biomass of arbuscular mycorrhizal fungi in soil', *Mycol. Res.*, 99(5), 623-629.

Oukarroum, A., Polchtchikov, S., Perreault, F. and Popovic, R. (2012) 'Temperature influence on silver nanoparticles inhibitory effect on photosystem II photochemistry in two green algae, *Chlorella vulgaris* and *Dunaliella tertiolecta*', *Environ Sci Pollut Res Int*, 19(5), 1755-62.

Pal, S., Tak, Y. K. and Song, J. M. (2007) 'Does the antibacterial activity of silver nanoparticles depend on the shape of the nanoparticle? A study of the Gram-negative bacterium *Escherichia coli*', *Applied and Environmental Microbiology*, 73(6), 1712-1720.

Paniagua, C., Posé, S., Morris, V. J., Kirby, A. R., Quesada, M. A. and Mercado, J. A. (2014) 'Fruit softening and pectin disassembly: an overview of nanostructural pectin modifications assessed by atomic force microscopy', *Annals of Botany*.

Pawlett, M., Ritz, K., Dorey, R., Rocks, S., Ramsden, J. and Harris, J. (2013) 'The impact of zero-valent iron nanoparticles upon soil microbial communities is context dependent', *Environmental Science and Pollution Research*, 20(2), 1041-1049.

Pelletier, D. A., Suresh, A. K., Holton, G. A., McKeown, C. K., Wang, W., Gu, B., Mortensen, N. P., Allison, D. P., Joy, D. C., Allison, M. R., Brown, S. D., Phelps, T. J. and Doktycz, M. J. (2010) 'Effects of engineered Cerium Oxide nanoparticles on bacterial growth and viability', *Applied and Environmental Microbiology*, 76(24), 7981-7989.

Pernthaler, J., Glöckner, F.-O., Schönhuber, W. and Amann, R. (2001) 'Fluorescence in situ hybridization (FISH) with rRNA-targeted oligonucleotide probes' in John, H. P., ed. *Methods in Microbiology*, Academic Press, 207-226.

Porter, K. G. and Feig, Y. S. (1980) 'The use of DAPI for identifying and counting aquatic microflora', *Limnology and Oceanography*, 25(5), 943-948.

Preston-Mafham, J., Boddy, L. and Randerson, P. F. (2002) 'Analysis of microbial community functional diversity using sole-carbon-source utilisation profiles – a critique', *FEMS Microbiology Ecology*, 42(1), 1-14.

PSIA (2002) 'XE-100 User's manual', 86.

Puigdomenech, I. (2004) MEDUSA (Making equilibrium diagrams/using sophisticated algorithms), email to [accessed

Quellhorst, G. and Rulli, S. (2008) *A Systematic Guideline for Developing the Best Real-Time PCR Primers*.

Rand, G. M., Wells, P. G. and McCarty, L. S. (1995) 'Introduction to aquatic toxicology' in Rand, G. M., ed. *Fundamentals of aquatic toxicology : effects, environmental fate, and risk assessment* Norht Palm Beach, Florida: Taylor & Francis, 3-68.

Rauscher, H., Roebben, G., Amenta, V., Sanfeliu, A. B., Calzolai, L., Emons, H., Gaillard, C., Gibson, N., Linsinger, T., Mech, A., Pesudo, L. Q., Rasmussen, K., Sintes, J. R., Sokull-Klüttgen, B. and Stamm, H. (2014) *Towards a review of the EC Recommendation for a definition of the term "nanomaterial"Part 1: Compilation of information concerning the experience with the definition*, Joint Research Centre, Institute for Health and Consumer Protection,European Commission.

Ravindran, A., Singh, A., Raichur, A. M., Chandrasekaran, N. and Mukherjee, A. (2010) 'Studies on interaction of colloidal Ag nanoparticles with Bovine Serum Albumin (BSA)', *Colloids and Surfaces B: Biointerfaces*, 76(1), 32-37.

Ricco, G., Tomei, M. C., Ramadori, R. and Laera, G. (2004) 'Toxicity assessment of common xenobiotic compounds on municipal activated sludge: comparison between respirometry and Microtox®', *Water Research,* 38(8), 2103-2110.

Rodrigues, D. F., Jaisi, D. P. and Elimelech, M. (2012) 'Toxicity of functionalized single-walled carbon nanotubes on soil microbial communities: Implications for nutrient cycling in soil', *Environmental Science & Technology,* 47(1), 625-633.

Rotthauwe, J. H., Witzel, K. P. and Liesack, W. (1997) 'The ammonia monooxygenase structural gene amoA as a functional marker: Molecular fine-scale analysis of natural ammonia-oxidizing populations', *Applied and Environmental Microbiology,* 63(12), 4704-4712.

Sadeghi, B., Garmaroudi, F. S., Hashemi, M., Nezhad, H. R., Nasrollahi, A., Ardalan, S. and Ardalan, S. (2012) 'Comparison of the anti-bacterial activity on the nanosilver shapes: Nanoparticles, nanorods and nanoplates', *Advanced Powder Technology,* 23(1), 22-26.

Safarov, J., Berndt, S., Millero, F., Feistel, R., Heintz, A. and Hassel, E. (2012) '(p,ρ,T) properties of seawater: Extensions to high salinities', *Deep Sea Research Part I: Oceanographic Research Papers,* 65(0), 146-156.

Santos, E. B., de Souza e Silva, J. M. and Mazali, I. O. (2010) 'Raman spectroscopy as a tool for the elucidation of nanoparticles with core–shell structure of TiO2 and MoO3', *Vibrational Spectroscopy,* 54(2), 89-92.

Schreurs, W. J. and Rosenberg, H. (1982) 'Effect of silver ions on transport and retention of phosphate by Escherichia coli', *Journal of Bacteriology,* 152(1), 7-13.

Schulz, G. E. (2002) 'The structure of bacterial outer membrane proteins', *Biochimica et Biophysica Acta (BBA) - Biomembranes,* 1565(2), 308-317.

Schumacher, B. A. (2002) 'Methods for the determination of total organic carbon (TOC) in soils and sediments',

Sekine, R., Khaksar, M., Brunetti, G., Donner, E., Scheckel, K. G., Lombi, E. and Vasilev, K. (2013) 'Surface immobilization of engineered nanomaterials for in situ study of their environmental transformations and fate', *Environmental Science & Technology,* 47(16), 9308-9316.

Selinummi, J., Seppälä, J., Yli-Harja, O. and Puhakka, J. (2005) 'Software for quantification of labeled bacteria from digital microscope images by automated image analysis', *Biotechniques,* 39(6), 859-863.

Šiller, L., Lemloh, M.-L., Piticharoenphun, S., Mendis, B. G., Horrocks, B. R., Brümmer, F. and Medaković, D. (2013) 'Silver nanoparticle toxicity in sea urchin *Paracentrotus lividus*', *Environmental Pollution,* 178(0), 498-502.

Sinigalliano, C. D., Kuhn, D. N. and Jones, R. D. (1995) 'Amplification of the *amoA* gene from diverse species of ammonium-oxidizing bacteria and from an indigenous bacterial population from seawater', *Applied and Environmental Microbiology,* 61(7), 2702-2706.

Smetana, A. B., Klabunde, K. J., Marchin, G. R. and Sorensen, C. M. (2008) 'Biocidal activity of nanocrystalline silver powders and particles', *Langmuir,* 24(14), 7457-7464.

Smith, C. J. and Osborn, A. M. (2009) 'Advantages and limitations of quantitative PCR (Q-PCR)-based approaches in microbial ecology', *FEMS Microbiology Ecology,* 67(1), 6-20.

Sondi, I. and Salopek-Sondi, B. (2004) 'Silver nanoparticles as antimicrobial agent: a case study on *E. coli* as a model for Gram-negative bacteria', *Journal of Colloid and Interface Science,* 275(1), 177-182.

Stefaniak, A. B., Hackley, V. A., Roebben, G., Ehara, K., Hankin, S., Postek, M. T., Lynch, I., Fu, W.-E., Linsinger, T. P. J. and Thünemann, A. F. (2012) 'Nanoscale reference materials for environmental, health and safety measurements: needs, gaps and opportunities', *Nanotoxicology*, 7(8), 1325-1337.

Stolpe, B. and Hassellöv, M. (2007) 'Changes in size distribution of fresh water nanoscale colloidal matter and associated elements on mixing with seawater', *Geochimica et Cosmochimica Acta*, 71(13), 3292-3301.

Stolpe, B. and Hassellöv, M. (2010) 'Title Nanofibrils and other colloidal biopolymers binding trace elements in coastal seawater: Significance for variations in element size distributions', *Journal Limnology and Oceanography*, 55(1), 187-202.

Stone, V., Nowack, B., Baun, A., van den Brink, N., von der Kammer, F., Dusinska, M., Handy, R., Hankin, S., Hassellöv, M., Joner, E. and Fernandes, T. F. (2010) 'Nanomaterials for environmental studies: Classification, reference material issues, and strategies for physico-chemical characterisation', *Science of The Total Environment*, 408(7), 1745-1754.

Stone, V., Pozzi-Mucelli, S., Tran, L., Aschberger, K., Sabella, S., Vogel, U., Poland, C., Balharry, D., Fernandes, T., Gottardo, S., Hankin, S., Hartl, M., Hartmann, N., Hristozov, D., Hund-Rinke, K., Johnston, H., Marcomini, A., Panzer, O., Roncato, D., Saber, A., Wallin, H. and Scott-Fordsmand, J. (2014) 'ITS-NANO - Prioritising nanosafety research to develop a stakeholder driven intelligent testing strategy', *Particle and Fibre Toxicology*, 11(1), 9.

Stukalov, O., Korenevsky, A., Beveridge, T. J. and Dutcher, J. R. (2008) 'Use of Atomic Force Microscopy and Transmission Electron Microscopy for correlative studies of bacterial capsules', *Applied and Environmental Microbiology*, 74(17), 5457-5465.

Su, H.-L., Chou, C.-C., Hung, D.-J., Lin, S.-H., Pao, I. C., Lin, J.-H., Huang, F.-L., Dong, R.-X. and Lin, J.-J. (2009) 'The disruption of bacterial membrane integrity through ROS generation induced by nanohybrids of silver and clay', *Biomaterials*, 30(30), 5979-5987.

Sun, T. Y., Gottschalk, F., Hungerbühler, K. and Nowack, B. (2014) 'Comprehensive probabilistic modelling of environmental emissions of engineered nanomaterials', *Environmental Pollution*, 185(0), 69-76.

Suresh, A. K., Pelletier, D. A., Wang, W., Moon, J.-W., Gu, B., Mortensen, N. P., Allison, D. P., Joy, D. C., Phelps, T. J. and Doktycz, M. J. (2010) 'Silver nanocrystallites: Biofabrication using *Shewanella oneidensis*, and an evaluation of their comparative toxicity on Gram-negative and Gram-positive bacteria', *Environmental Science & Technology*, 44(13), 5210-5215.

Taccari, M., Comitini, F., Casucci, C. and Ciani, M. (2011) 'Toxicity assessment of compounds in soil using a simple respirometric technique', *International Biodeterioration & Biodegradation*, 65(1), 60-64.

Tachon, S., Michelon, D., Chambellon, E., Cantonnet, M., Mezange, C., Henno, L., Cachon, R. and Yvon, M. (2009) 'Experimental conditions affect the site of tetrazolium violet reduction in the electron transport chain of Lactococcus lactis', *Microbiology*, 155(9), 2941-2948.

Taglietti, A., Diaz Fernandez, Y. A., Amato, E., Cucca, L., Dacarro, G., Grisoli, P., Necchi, V., Pallavicini, P., Pasotti, L. and Patrini, M. (2012) 'Antibacterial activity of glutathione-coated silver nanoparticles against Gram positive and Gram negative Bacteria', *Langmuir*, 28(21), 8140-8148.

Tejamaya, M., Römer, I., Merrifield, R. C. and Lead, J. R. (2012) 'Stability of citrate, PVP, and PEG coated silver nanoparticles in ecotoxicology media', *Environmental Science & Technology*, 46(13), 7011-7017.

Teo, W. Z. and Pumera, M. (2014) 'Fate of silver nanoparticles in natural waters; integrative use of conventional and electrochemical analytical techniques', *RSC Advances*, 4(10), 5006-5011.

Thornton, B., Zhang, Z., Mayes, R. W., Högberg, M. N. and Midwood, A. J. (2011) 'Can gas chromatography combustion isotope ratio mass spectrometry be used to quantify organic compound abundance?', *Rapid Communications in Mass Spectrometry*, 25(17), 2433-2438.

Tolaymat, T. M., El Badawy, A. M., Genaidy, A., Scheckel, K. G., Luxton, T. P. and Suidan, M. (2010) 'An evidence-based environmental perspective of manufactured silver nanoparticle in syntheses and applications: A systematic review and critical appraisal of peer-reviewed scientific papers', *Science of The Total Environment*, 408(5), 999-1006.

Tomaszewska, E., Soliwoda, K., Kadziola, K., Tkacz-Szczesna, B., Celichowski, G., Cichomski, M., Szmaja, W. and Grobelny, J. (2013) 'Detection limits of DLS and UV-Vis spectroscopy in characterization of polydisperse nanoparticles colloids', *Journal of Nanomaterials*, 2013, 10.

Tšertova, N., Kisand, A., Baty, F. and Kisand, V. (2013) 'Homogeneous microbial diversity in the upper sediment layers of a shallow lake', *Aquatic Microbial Ecology*, 70(1), 77-85.

Tuoriniemi, J., Cornelis, G. and Hassellöv, M. (2012) 'Size discrimination and detection capabilities of single-particle ICPMS for environmental analysis of silver nanoparticles', *Analytical Chemistry*, 84(9), 3965-3972.

USEPA-3005A, 1992. Acid digestion of waters for total recoverable or dissolved metals for analysis by FLAA or ICP spectroscopy (Method 5000A) Revision 1. United States Environmental Protection Agency.

USEPA-3050B, 1996. Acid digestion of sediments, sludges and soils Method 3050B (Revision 2). United States Environmental Protection Agency.

Van Cauwenberghe, L., Vanreusel, A., Mees, J. and Janssen, C. R. (2013) 'Microplastic pollution in deep-sea sediments', *Environmental Pollution*, 182(0), 495-499.

Villanueva, U., Raposo, J. C., Castro, K., de Diego, A., Arana, G. and Madariaga, J. M. (2008) 'Raman spectroscopy speciation of natural and anthropogenic solid phases in river and estuarine sediments with appreciable amount of clay and organic matter', *Journal of Raman Spectroscopy*, 39(9), 1195-1203.

Vishnivetskaya, T. A., Mosher, J. J., Palumbo, A. V., Yang, Z. K., Podar, M., Brown, S. D., Brooks, S. C., Gu, B., Southworth, G. R., Drake, M. M., Brandt, C. C. and Elias, D. A. (2011) 'Mercury and other heavy metals influence bacterial community structure in contaminated Tennessee streams', *Applied and Environmental Microbiology*, 77(1), 302-311.

von der Kammer, F., Ferguson, P. L., Holden, P. A., Masion, A., Rogers, K. R., Klaine, S. J., Koelmans, A. A., Horne, N. and Unrine, J. M. (2012) 'Analysis of engineered nanomaterials in complex matrices (environment and biota): General considerations and conceptual case studies', *Environmental Toxicology and Chemistry*, 31(1), 32-49.

Wang, C.-B., Deo, G. and Wachs, I. E. (1999) 'Interaction of polycrystalline silver with oxygen, water, carbon dioxide, ethylene, and methanol: In situ Raman and catalytic studies', *The Journal of Physical Chemistry B*, 103(27), 5645-5656.

Wang, Y. and Qian, P.-Y. (2009) 'Conservative fragments in bacterial 16S rRNA genes and primer design for 16S Ribosomal DNA amplicons in metagenomic studies', *PLoS ONE*, 4(10), e7401.

Weber, K. P., Gehder, M. and Legge, R. L. (2008) 'Assessment of changes in the microbial community of constructed wetland mesocosms in response to acid mine drainage exposure', *Water Research,* 42(1–2), 180-188.

White, D. C., Davis, W. M., Nickels, J. S., King, J. D. and Bobbie, R. J. (1979) 'Determination of the sedimentary microbial biomass by extractible lipid phosphate', *Oecologia,* 40(1), 51-62.

White, D. C., Meadows, P., Eglinton, G. and Coleman, M. L. (1993) 'In situ measurement of microbial biomass, community structure and nutritional status', *Phil. Trans. Phys. Sci. Eng.*, 344(1670), 59-67.

Whiteley, C. M., Valle, M. D., Jones, K. C. and Sweetman, A. J. (2013) 'Challenges in assessing release, exposure and fate of silver nanoparticles within the UK environment', *Environmental Science: Processes & Impacts,* 15(11), 2050-2058.

Winkler, D. A., Mombelli, E., Pietroiusti, A., Tran, L., Worth, A., Fadeel, B. and McCall, M. J. (2013) 'Applying quantitative structure–activity relationship approaches to nanotoxicology: Current status and future potential', *Toxicology*, 313(1), 15-23.

Xiu, Z.-m., Zhang, Q.-b., Puppala, H. L., Colvin, V. L. and Alvarez, P. J. J. (2012) 'Negligible particle-specific antibacterial activity of silver nanoparticles', *Nano Letters,* 12(8), 4271-4275.

Xu, H., Qu, F., Xu, H., Lai, W., Andrew Wang, Y., Aguilar, Z. and Wei, H. (2012) 'Role of reactive oxygen species in the antibacterial mechanism of silver nanoparticles on *Escherichia coli* O157:H7', *BioMetals*, 25(1), 45-53.

Yamanaka, M., Hara, K. and Kudo, J. (2005) 'Bactericidal actions of a silver ion solution on *Escherichia coli*, studied by energy-filtering transmission electron microscopy and proteomic analysis', *Applied and Environmental Microbiology*, 71(11), 7589-7593.

Youmans, G. P. (1946) 'A Method for the determination of the culture cycle and the growth rate of virulent human type Tubercle Bacilli', *Journal of Bacteriology*, 51(6), 703-10.

Yu, S.-j., Yin, Y.-g., Chao, J.-b., Shen, M.-h. and Liu, J.-f. (2013) 'Highly dynamic PVP-coated silver nanoparticles in aquatic environments: Chemical and morphology change induced by oxidation of Ag0 and reduction of Ag+', *Environmental Science & Technology*, 48(1), 403-411.

Zhong, Q., Inniss, D., Kjoller, K. and Elings, V. B. (1993) 'Fractured polymer/silica fiber surface studied by tapping mode atomic force microscopy', *Surface Science*, 290(1–2), L688-L692.

Zhou, D., Abdel-Fattah, A. I. and Keller, A. A. (2012) 'Clay particles destabilize engineered nanoparticles in aqueous environments', *Environmental Science & Technology*, 46(14), 7520-7526.

Zogg, G. P., Zak, D. R., Ringelberg, D. B., White, D. C., MacDonald, N. W. and Pregitzer, K. S. (1997) 'Compositional and functional shifts in microbial communities due to soil warming', *Soil Science Society of America Journal,* 61(2), 475-481.

Zook, J. M., Long, S., Cleveland, D., Geronimo, C. and MacCuspie, R. (2011) 'Measuring silver nanoparticle dissolution in complex biological and environmental matrices using UV–visible absorbance', *Analytical and Bioanalytical Chemistry,* 401(6), 1993-2002.

Zweifel, U. L. and Hagstrom, A. (1995) 'Total counts of marine bacteria include a large fraction of non-nucleoid-containing bacteria (ghosts)', *Applied and Environmental Microbiology,* 61(6), 2180-2185.